

CRANFIELD INSTITUTE OF TECHNOLOGY

SCHOOL OF MECHANICAL ENGINEERING

Ph.D THESIS

ACADEMIC YEAR 1987-88

J N MURTHY

GAS TURBINE COMBUSTOR MODELLING
FOR DESIGN

SUPERVISOR : RITI SINGH

FEBRUARY 1988

SUMMARY

The design and development of gas turbine combustors is a crucial but uncertain part of an engine development process. Combustion within a gas turbine is a complex interaction of, among other things, fluid dynamics, heat and mass transfer and chemical kinetics. At present, the design process relies upon a wealth of experimental data and correlations. The proper use of this information requires experienced combustion engineers and even for them the design process is very time consuming.

Some major engine manufacturers have attempted to address the above problem by developing one dimensional computer programs based on the above test and empirical data to assist combustor designers. Such programs are usually proprietary. The present work, based on this approach has yielded DEPTH, a combustor design program. DEPTH (Design and Evaluation of Pressure, Temperature and Heat transfer in combustors) is developed in Fortran-77 to assist in preliminary design and evaluation of conventional gas turbine combustion chambers.

DEPTH can be used to carry out a preliminary design along with prediction of the cooling slots for a given metal temperature limit or to evaluate heat transfer and temperatures for an existing combustion chamber. Analysis of performance parameters such as efficiency, stability and NOX based on stirred reactor theories is also coupled. DEPTH is made sufficiently interactive/user-friendly such that no prior expertise is required as far as computer operation is concerned. The range of variables such as operating conditions, geometry, hardware, fuel type can all be effectively examined and their contribution towards the combustor performance studied. Such comprehensive study should provide ample opportunity for the designer to make the right decisions. It should also be an effective study aid.

Returns in terms of higher thermal efficiencies is an incentive to go for combined cycles and cogeneration. In such cases, opting for higher cycle pressures together with a second or reheat combustor promise higher thermal efficiencies and exhaust temperatures and hence such designs are likely to be of interest. The concepts that are needed for understanding a double or reheat combustor are also addressed using the programme. A specific application of the programme is demonstrated through the design of a double combustor.

ACKNOWLEDGMENTS

I wish to express my deep sense of gratitude to my supervisor, Mr Riti Singh for his continuous guidance and invaluable suggestions during the entire work. I am thankful for his help and continuous encouragement.

I wish to thank my Organization, the Indian Air Force for providing me with this opportunity to further my knowledge.

My thanks are also due to various members of the School of Mechanical Engineering and the Computer Center for providing assistance in relevant specialist topics, especially to Prof. JB Moss for putting up with my nagging discussions and providing the assistance in conceptual understanding of various aspects.

I am grateful to my wife, Subha who has been understanding and supportive throughout my entire period of study. I thank all my family members in contributing in their own respect for the fulfillment of this research work.

CONTENTS

	PAGE NO
SUMMARY	i
ACKNOWLEDGEMENTS	ii
CONTENTS	iii
NOTATION	xi
CHAPTER 1. INTRODUCTION	1
CHAPTER 2. STATUS	3
2.1 BACKGROUND	3
2.2 MODELS	4
2.2.1 EMPIRICAL	4
2.2.2 MODULAR APPROACH	5
2.2.3 FINITE DIFFERENCE APPROACH	9
2.2.4 CLOSURE	25
2.2.5 COMPUTATIONAL CODE	27
2.3 CHOICE OF MODEL	29
2.4 SCOPE	30
CHAPTER 3. PROGRAMME PHILOSOPHY	31
3.1 FOREWORD	31
3.2 STRUCTURED PROGRAMMING	31
3.2.1 LANGUAGE	31
3.2.2 GRAPHICS	31
3.2.3 INTERACTIVE	32
3.2.4 INPUT/OUTPUT	32
3.3 AXIOMS FOR ALGORITHM	32
3.3.1 MAJOR ASSUMPTIONS	32
3.3.2 GRIDDING	33
3.3.3 PROGRAMME HIERARCHY	34
CHAPTER 4. PRELIMINARY DESIGN	35
4.1 INTRODUCTION	35

4.2	BASIC DESIGN FEATURE	35
4.3	COMBUSTOR REQUIREMENTS	37
4.4	COMBUSTOR TYPES	38
4.5	SELECTION	39
4.6	REFERENCE CONDITIONS	40
4.6.1	THETA PARAMETER APPROACH	40
4.6.2	PRESSURE LOSS APPROACH	41
4.7	DIFFUSER	42
4.8	SIZING	45
4.8.1	LINER CROSS SECTIONAL AREA	45
4.8.2	LINER LENGTH	46
4.8.3	EQUIVALENCE RATIO	48
4.8.4	FLAME TEMPERATURE	49
4.8.5	EXIT TEMPERATURE PROFILE	52
4.8.6	FLAME STABILIZATION	53
4.9	SWIRLER	57
4.10	FUEL INJECTION	57
4.10.1	NUMBER OF FUEL INJECTORS	60
CHAPTER 5.	FLOW EVALUATION	61
5.1	FLOW CONDITIONS	61
5.1.1	PRECONDITIONS	61
5.2	PROPERTIES	61
5.2.1	SPECIES CONCENTRATION	62
5.2.2	THERMODYNAMIC PROPERTIES	63
5.2.3	TRANSPORT PROPERTIES	64
5.2.4	EFFECT OF PRESSURE	68
5.2.5	STATE	69
5.3	DIFFUSER	69
5.4	LINER EVALUATION	72
5.4.1	LINER HOLES	74
5.4.1.1	DOMES HOLES	74
5.4.1.2	SECONDARY HOLES	74
5.4.1.3	DILUTION HOLES	76
5.4.1.4	COEFFICIENT OF DISCHARGE	76

5.4.2	LINER PRESSURE DROP	78
5.4.3	COMBUSTION	80
5.4.4	COLD FLOW	81
5.4.5	LINER ANALYSIS	81
5.4.6	SUDDEN EXPANSION LOSSES	82
5.4.7	MASS BALANCE	83
5.4.8	CONTROL VOLUME	84
5.5	PATTERN FACTOR	84
CHAPTER 6.	HEAT TRANSFER	85
6.1	INTRODUCTION	85
6.2	RADIATION	86
6.2.1	NON-LUMINOUS RADIATION	86
6.2.2	LUMINOUS RADIATION	86
6.2.3	RADIATION MODELS	87
6.2.4	SCOPE	90
6.3	HEAT BALANCE	91
6.3.1	METHOD OF SOLUTION	92
6.3.2	INTERNAL RADIATION	93
6.3.3	ANNULAR RADIATION	96
6.3.4	INTERNAL CONVECTION	96
6.3.5	EXTERNAL CONVECTION	111
6.3.6	WALL CONDUCTION	112
6.3.7	ADDITIONAL MEASURES	112
6.3.8	PROPERTIES	113
CHAPTER 7.	EFFICIENCY AND STABILITY	115
7.1	REQUIREMENT	115
7.2	BACKGROUND	115
7.2.1	COMBUSTION CHAMBER	115
7.2.2	EFFICIENCY	116
7.2.2.1	CLOSURE	121
7.2.3	STABILITY	121
7.2.2.1	CLOSURE	123
7.3	REQUIREMENT	124
7.3.1	EFFICIENCY CORRELATION	124
7.3.2	KINETIC TIME APPROACH	129
7.3.3	STABILITY RELATION	133
CHAPTER 8.	EMISSIONS	138
8.1	SCOPE	138

8.2 NO _x - BURNING ZONE	139
8.2.1 CHOICE OF KINETIC REACTION SCHEME	142
8.3 NO _x - MIXING ZONE	144
CHAPTER 9. DOUBLE COMBUSTOR	146
9.1 WHY REHEAT ?	146
9.2 STATE-OF-ART	146
9.2.1 ANALYSIS	147
9.2.2 CONCLUSIONS	148
9.2.3 RELEVANT COMBUSTOR FEATURES	149
9.3 DESIGN CONCEPTS OF SECOND COMBUSTOR	150
9.3.1 PROPERTIES	150
9.3.2 COMBUSTION	150
9.3.2.1 AFRS	151
9.3.2.2 ADIABATIC FLAME TEMPERATURE	151
9.3.2.3 COMBUSTION EFFICIENCY	152
9.3.2.4 FLAMMABILITY LIMITS	152
9.3.3 HEAT TRANSFER	153
9.3.4 NO _x	153
9.3.5 SIZING CRITERIA	156
9.3.6 STARTING	156
CHAPTER 10. PROGRAMME DESCRIPTION	157
10.1 FOREWORD	157
10.2 INPUT	157
10.2.1 INTERACTIVE	157
10.2.2 NEW DESIGN	157
10.2.3 CONTINUATION FROM LAST TERMINATION	163
10.3 OUTPUT	163
10.3.1 TABULAR	163
10.3.2 GRAPHICAL	163
10.4 PC ADAPTABILITY	164
CHAPTER 11. CASE STUDIES AND DISCUSSION	165
11.1 VALIDATION	165

11.2 DISCUSSION	165
11.3 CLOSURE	172
CHAPTER 12. CONCLUSIONS	174
REFERENCES	176
LIST OF APPENDICES	
APPENDIX A : STOICHIOMETRIC AIR-FUEL RATIO EVALUATION	188
APPENDIX B : REFERENCE AREA EVALUATION	189
APPENDIX C : SIMPLE METHOD TO EVALUATE FLAME TEMPERATURE	191
APPENDIX D : PROCEDURE TO ESTIMATE THE NUMBER OF FUEL INJECTORS	203
APPENDIX E : COEFFICIENTS FOR THERMODYNAMIC PROPERTIES	204
APPENDIX F : COLLISION DIAMETERS AND LENNARD-JONES POTENTIAL PARAMETERS	206
APPENDIX G : COEFFICIENTS FOR SPECIES VISCOSITY DATA	207
APPENDIX H : ISOENTROPIC PROPERTY EVALUATION	208
APPENDIX I : RAYLEIGH EQUATION SOLUTION	209
APPENDIX J : ONE DIMENSIONAL STEADY FLOW EVALUATION	210
APPENDIX K : NAG LIBRARY FOR HEAT TRANSFER SOLUTION	217
APPENDIX L : HEAT TRANSFER SOLUTION	220
APPENDIX M : FLOW AREA - WIGGLE STRIP	224
APPENDIX N : MATERIAL PROPERTIES	225
APPENDIX O : CONVERSION FOR TRACE SPECIES	226
APPENDIX P : INTEGRATION TECHNIQUE FOR NO _x EQUATIONS	228
APPENDIX Q : FLOW CHARTS	230
APPENDIX R : RESULTS OF CASE STUDIES	232

LIST OF FIGURES

Fig 2.1	Schematic of Modular Model of Swithenbank et al. (1973)	7
2.2	Stream tube model of Mosier & Roberts	8
2.3	Exhaust Emission for the P&W JT9D combustor	9
2.4	Comparison of one equation model prediction for center velocity decay, reacting H ₂ -air jet	13
2.5	NO _x model of Fletcher & Heywood (1971)	20
2.6	NO _x model of Hung (1975)	21
2.7	Types of recirculation zones	24
2.8	Summary of the accuracy of prediction of the various regions of the flow field	25
Fig 3.1	Stairstep Coordinate System	33
3.2	Programme Hierarchy	34
Fig 4.1	Stages in evolution of a conventional Gas Turbine combustor	36
4.2	Main components of a Gas Turbine combustor	37
4.3	Various tyoes of straight flow combustors	39
4.4	Design curves for conventional combustors	41
4.5	Types of Diffusers	43
4.6	Influence of diffuser angle on pressure loss	43
4.7	Flow pattern downstream of prediffuser	44
4.8	Liner in its modular form	46
4.9	Primary zone airflow patterns	54
Fig 5.1	Effect of pressure on transport properties	68
5.2	Energy conversion in diffuser	69
5.3	Simulation of velocity profile with equivalent rectangular profile	70
5.4	Sudden expansion in a duct	71
5.5	Outline of flow evaluation	73
5.6	Jet in cross flow	75
5.7	Flow through a liner hole	76
5.8	Correlations by Adkins & Gueroui (1986)	77
5.9	Curvature corrections	78
5.10	Electrical analogy for a flow through a hole	79
5.11	Electrical analogy for thr front end	79
5.12	Sudden Expansion in the anulus	82
Fig 6.1	Intensity of Radiation	87
6.2	Basic Heat Transfer Processes	91
6.3	Heat Balance Configurations	92
6.4	Effect of Fuel C/H ratio on flame luminosity	95
6.5	Trends in amount of cooling air employed	98
6.6	Cross section of liner cooling devices	99
6.7	Elastci buckling geometry relationship Sturgess (1980)	100
6.8	Schematic of film wooling process	101
6.9	Basic impingement model geometry and nomenclature	107

6.10	Impingement injection type	107
6.11	Typical convective channel arrangement	108
6.12	Heat transfer characteristics of artificially roughened surfaces	110
6.13	Flow area fractions	111
6.14	Heat transfer by conduction	112
6.15	Effect of Coating on wall temperatures	113
Fig 7.1	Simplified schematic of various primary zones	119
7.2	Schematic diagram of the relation of mixing layer to the primary zone and exhaust efficiency	120
7.3	The adiabatic stirred reactor heat balance	122
7.4	Combustion efficiency- Moonlight project	125
7.5	AFRS & Tadiabatic under vitiation	126
7.6	Efficiency under vitiation- Modified Theta Parameter	128
7.7	Variation of activation energy for methane	131
7.8	Stability curves- Moonlight combustor for E/R = 16000 K	134
7.9	Stability curves- Moonlight combustor for E/R = 20000 K	135
7.10	Conceptual representation of combustion volume	136
Fig 8.1	Schematic representation of stirred reactors	140
Fig 9.1	Reheat Gas turbine schematic diagram	147
9.2	Intercooled reheat Gas Turbine schematic	148
9.3	Specific humidity versus vitiation	151
9.4	AFRS & Tadiabatic under vitiation	151
9.5	Effect of vitiation on weak extinction in a double combustor	152
9.6	NOx under vitiation	154
9.7	Schematic representation of NOx production in a a system with a double combustor	155
Fig 10.1	Combustor Geometry	159
10.2	Slot Specification	162
Fig 11.1	Mass flow splits CASE 3	166
11.2	Basic configuration of Reheat Combustor (Mori (1983))	168
11.3	Air Distribution of RC (Mori (1983))	170
11.4	Air Distribution of RC by DEPTH	170
Fig B.1	Combustor Geometry	189
C.1	Adiabatic flame temperature comparision	202
D.1	Schematic of fuel spary pattern	203
I.1	Rayleigh curve for simple T change	209
J.1	Control surfaces defined for several methods of gas injection and liquid evaporation	210
PLATE R-1	TEST LINER (CASE 3) RUN WITH THERMAL PAINT	285
R-2	TEST LINER (CASE 3) IN WATER FLOW VISUALISATION	286

LIST OF TABLES

Table 2.1	Extended C-H-O chemical kinetic reaction mechanism	15
2.2	Models for Gas Turbine Combustors Mellor(1979)	25
2.3	Finite Difference Model comparisons in recirculating flow	26
4.1	An overview of Gas turbine combustors	38
4.2	Relative merits of various chamber types	40
4.3	Relative merits of various diffuser types	44
4.4	Relative zonal lengths	47
4.5	Influence of various primary zone mixture strengths	48
4.6	Relative merits of fuel injectors	58
5.1	Dry air composition	62
6.1	Constants for correlation for impingement cooling	107
6.2	Nusselt number comparison for parallel plates and pipe analogy	109
7.1	Characteristic Time Scales (Mellor(1976))	120
7.2	Combustor air/fuel flow distribution Moonlight Project	125
7.3	Kinetic times for Moonlight combustors	133
7.4	Blow Out values for M1 combustor	135
8.1	NOx Reaction Mechanism	143
8.2	NOx mass fractions for different mixedness	145
9.1	Concepts - Double Combustor	150
10.1	Input for Preliminary design	158
10.2	Input for flow Evaluation	160
Table F.1	Collision diameter and Lennard_Jones Potential parameters	206
F.2	Value of KT/ϵ and $\Omega(2,2)^*$	206
J.1	Influence Coefficients	214
N.1	Representative Properties of typical materials	225
N.2	Coefficients for temperature dependent Emissivity Ubhi(1987)	225
P.1	Values for 6 point Gaussian quadrature	229

NOTATION

A	Area (m^2)
AR	Area Ratio
AFRS	Stoichiometric Air fuel ratio
B	Mass Transfer Number, Blockage Factor
C_1 to 6	Convective Flux (W/m^2)
C_α	Mass fraction of species α
C_p	Mixture specific heat at constant pressure ($J/kg\ K$)
C_{p_i}	Specific heat at constant pressure of species i
D_{ij}	Coefficient of diffusion (m^2/s)
D_0	Sauter Mean Diameter (m)
DDL	Diffuser to dome length (m)
Dft	Flame tube diameter (m)
DZL	Dilution Zone length (m)
E	Activation Energy ($J/kg\text{-mol}$)
	Emissive power of a radiating body (W/m^2)
E_b	Emissive power of a black body (W/m^2)
E_λ	monochromatic Emissive power ($W/m^2\ m$)
f	fraction of total combustor airflow
F/A	Fuel to air mass ratio
FLCV	Fuel lower calorific value (J/kg)
g_i	Gravitational acceleration vector
G_c	Slot crossflow mass velocity based on slot cross sectional area $(\rho U)_{slot}$
G_j	Jet mass velocity based on hole area $(\rho U)_{jet}$
h	Mixture specific enthalpy (J/kg)
h_i	Enthalpy of species i
Hd	Hydraulic diameter (m)
I	Intensity of radiation per unit solid angle (W/sr)
K_{1-2}	Heat conducted through the wall 1-2 (Watts)
Le	Lewis Number α/D
LL()	Liner Length (Zone) (m)
m	mass velocity ratio $(\rho U)_c/(\rho U)_g$
\dot{m}	Mass Flow (kg/s)
Mn	Mach Number

Mw _α	Molecular Weight of species α
NS	Number of Species
Nu	Nusselt Number hl/λ
p	Static Pressure (N/m^2)
P	Total Pressure (N/m^2)
PF	Pattern Factor
PFR	Plug Flow Reactor
PHI()	Equivalence ratio (Zone)
Pr	Prandtl Number $C_p\mu/\lambda$
PSR	Perfectly Stirred Reactor
PZL	Primary Zone length
q	dynamic head $(1/2 \rho \bar{U}^2)$
f	Net formation rate of α per unit mass
R	Universal gas constant 8314.3 (J/kg-mol K)
R _a	Gas constant for air (J/kg K)
R ₁ to 6	Radiative Flux (W/m^2)
Re	Reynold Number $\rho U l/\mu$
s	depth of film cooling slot (m)
S _α ()	Source term in scalar conservation equation
Sc	Schmidt Number ν/D
sphum	specific humidity (kg of water/kg of air)
St	Stanton Number $Nu/Re Pr$
SZL	Secondary Zone length (m)
t	Static Temperature (K)
	Slot lip thickness (m)
T	Total temperature (K)
TT()	Total temperature (Zone) (K)
T _{w1} to 6	Liner wall temperature (K)
U	Velocity (m/s)
V	volume (m^3)
WSR	Well Stirred Reactor
x	Distance downstream of slot (m)
	Length of control volume (m)
ZNL	Nozzle length (m)

Greek Symbols

α	Thermal diffusivity
δ_{ij}	Kronecker delta
$\epsilon_{ij}^{K_{LJ}}$	Lennard-Jones Constant
ϵ	Emissivity, Turbulent Kinetic energy dissipation rate
ϵ_w	Emissivity of wall or Coating (if used)
λ	Thermal Conductivity (W/m K)
λ_{eff}	Evaporation Constant (m^2/s)
μ	Dynamic Viscosity (kg/m s)
ρ	Density (kg/m^3)
γ	Ratio of Specific Heats
τ	Characteristic time s
σ	Stefan_Boltzman Constant $5.67 \times 10^{-8} \text{ W/m}^2 \text{ K}^4$
σ_j	Mole number of species j
σ_{jj}	Collision diameter of the molecule in angstroms
$\Omega_{\mu j}^{(2,2)*}$	Thermal conductivity collision integral
ϕ	Equivalence Ratio
χ	Winter Parameter
η	Combustion Efficiency, Cooling Effectiveness

Subscripts

2	entry to combustor
4	exit to combustor (8 in the programme)
a	air
at	atomiser
b	burning zone (combustion)
c	coolant, combustion
CO	carbon monoxide
dh	dome holes
diff	diffuser
eb	droplet evaporation and combustion
f	fuel

F	flame
ft	flame tube
l	liquid (fuel)
L	liner
NO	nitric oxide
pz	primary zone
ref	reference
sl	shear layer
sw	swirler
sz	secondary zone
w	Wall

Superscripts

'	Reynolds fluctuating component
"	Favre fluctuating component
—	Time average or ensemble average
~	Favre average

CHAPTER 1

INTRODUCTION

"Combustor design is an art not a science" is still an accepted statement within the gas turbine industry. During the past four decades the gas turbine combustor technology has developed gradually and continuously, exhibiting high combustion efficiency over the normal working range, in spite of ever increasing operating conditions- higher pressures, temperatures and velocities. However, new concepts and technology are still needed to satisfy current and projected pollutant emissions regulations and to respond to the growing emphasis on engines that can utilize a much broader range of fuels.

Gas turbine combustors involve complex simultaneous processes of three-dimensional flow, droplet evaporation, gas phase mixing, radiation and chemical kinetics. The complexity of these interacting processes is such that most current gas turbine combustor designs depend largely on empirical correlations. The design of combustion chambers and prediction of performance, however, still owes, in most instances, as much to art and past experience as it does to science. It has long been recognized the need for understanding the various processes on a common basis and also the difficulty of unifying the common fundamentals in a general and practically useful theory. General theories apparently were not useful, and useful theories were not general. In recent years, thanks to the rapid development of computers and concurrent research into fundamentals of the various aspects of combustion and turbulent flow, mathematical models of a fundamental nature have started to emerge. Although not yet sufficiently reliable design tools, these models have proven to be very effective in analyzing existing designs and it is likely that they will progressively replace the cut-and-try approach to combustor design. The approach is potentially capable of substantially reducing development time as well as cost at the same time improving combustor performance.

Performance parameters concerning fluid dynamics, heat fluxes, efficiency, stability, ignition characteristics, altitude behaviour are all important in qualifying a combustor. The advantage of a model lies in the fact that it is able to predict any performance parameter for a given design. However, the biggest reward is when the model is able to optimally design for the given performance specifications at a reasonable confidence level such that it grossly reduces the need for expensive experimental work. The choice of any model greatly depends on as to what is required, while cost and time limit its complexities.

Major gas turbine manufacturers and design organizations are continuously developing powerful programmes such as PACE, CONCERT, PHOENICS etc., over the years based on their immense wealth of practical and research experience. But the complexities of the field will also demand simpler, but effective procedures. Even to use the existing wealth of information, it is time consuming to carry out a design.

The present work consists of developing a design programme for a straight flow combustor through modelling. The programme will be able to carry out a preliminary design and to evaluate its performance. A one-dimensional model based on basic assumptions and existing correlations is ventured here, to join the multitude of codes which are increasingly getting complicated in terms of coding or coordinate system or colour output. Considering the nature of approach, it may be hard for the model to find its rung on the existing ladder of modelling techniques; but the intention is to produce a useful design and study tool. Parametric study of performance variation due to a range of variables such as operating conditions, geometry, hardware or fuel, can be effectively carried out. This should provide ample scope for the designer to make the right design decisions.

A specific application of the programme is demonstrated through the design of a double combustor. Breaking away from traditional concepts will be beneficial in either substantiating or improving the present returns. Cogeneration or combined cycle technology promises higher returns in terms of thermal efficiency. Reheat combustor or double combustor appears to be a promising feature to be used in conjunction with this technology. Thermal efficiencies well over 50% appear to be round the corner. Though the philosophy is viable, the conceptual understanding and practicability of reheat combustor are still desired. The model is used to cover these areas as well. Though, premature, these ideas could well be the concepts of future technology.

CHAPTER 2

STATUS

2.1 BACKGROUND

Combustor modelling is an attempt to provide a mathematical framework as a foundation for increasing understanding of reacting flow phenomena and to provide a means for the prediction of the performance of combustion systems. Combustor models also provide the means for the analysis and interpretation of experimental data, as well as the scaling necessary to apply laboratory results to full-scale systems.

Most of this recent development work has involved hardware and thus considerable expense; the alternative, some sort of quantitative model of the combustion process, is not generally available because of the complexity of the combustion process in a gas turbine combustor. The need to understand the fundamental process and be able to effectively model it to predict accurately, grew with

- 1) cost of new development and the pressing demands to get the design right at the first attempt.
- 2) alternative use of gas turbines from the traditional aviation field to ground and marine transportation as well as stationary applications.
- 3) growing awareness of atmospheric pollution and the consequent increasingly stringent measures to control it.
- 4) the depleting high-grade crudes and the need to use broad specification and alternate fuels.

An incentive to this impetus is the explosive growth in the computer technology. Ideally, a model should allow prediction, in terms of combustor geometry, inlet conditions, and fuel and injector properties, of several performance parameters including gaseous and particulate emissions, combustion efficiency, heat transfer flux to the liner and metal temperatures (information necessary to estimate the stress and life), rich and weak combustion stability limits, pattern factor, ignitability and altitude relight.

The advantage of a model lies in the fact that it should be able to predict the value for a given design. However, the biggest reward is when the model is able to optimally design for the given performance specifications at a reasonable confidence level that it should grossly reduce the need for expensive experimental work. However, the present day art is striving to fulfill this.

The information relating to combustor technology and combustor modelling is very vast ranging from simple correlations to sophisticated finite difference techniques. The present model is at an intermediary level, drawing substantial advantages from the low level models using correlations but also deriving the benefits from the high level models using finite difference techniques. Hence the thesis is intended to present the information which should provide a typical background to the state-of-art and also serve as a starting point for the expansion of the present work, if desired in future. However, a specific mention is made, wherever applicable as to which information is actually used in the present work.

2.2 MODELS

The various models can broadly be classified as

- 1) Empirical
- 2) Modular
- 3) Finite Difference Approach

2.2.1 EMPIRICAL CORRELATION

Gross features are described by correlations of experimental data based on dimensional arguments, extensive testing and precedent. Studies naturally focus on gross properties - expressions for combustion efficiency, for example, in terms of airflow rate, pressure drop, global temperature and geometry. Correlations may be inter-related, permitting a modular treatment of the combustor and its aerodynamic environment. Such modelling is sustained by a blend of intuition, dimensional reasoning and experience. Interpolation can be performed with more confidence than extrapolation. The approach and the wealth of empirical observation supporting it is described by Lefebvre (1983).

Perfectly Stirred Reactor (PSR) approach of Longwell and Weiss (1955), through the experiments on the well known 'Longwell Bomb', had provided more productive data for 'global reaction' than the individual ones. This approach may not be directly applicable to practical systems where mixing processes are equally predominant. Using similar approach the Theta parameter relation developed by Greenhough and Lefebvre (1957) has found wide application.

As an example to correlative approach, an expression for fuel/air ratio at lean blow out derived by Lefebvre (1987) is reproduced.

$$q_{LBO} = A \left[\frac{f_{pz}}{V_{pz}} \right] \left[\frac{\dot{m}_a}{P_2^{1.3} \exp(T_2/300)} \right] \left[\frac{D_o^2}{\lambda_{eff} \text{ FLCV}} \right] \quad \dots(2.1)$$

where

A depends on the geometry and mixing characteristics of combustion zone and needs to be derived experimentally. A=0.54 for F101 combustor,

Thus, first term is a function of combustor design, second term represents combustion operating conditions, while the third embodies the relevant fuel dependent properties.

Following are the typical approaches for emission estimation. Mellor et al (1983) have correlated the pollutant data of existing combustion chambers using semi empirical scaling approach. They have suggested a characteristic time model for gaseous pollutant emissions from conventional gas turbines :

$$\text{NOx EI} = 4.5 \tau_{sl,NO} / \tau_{NO} \quad (\text{g NO}_2/\text{Kg of fuel}) \quad \dots(2.2)$$

$$\text{CO EI} = 35 \tau_{CO} / \tau_{sl,CO} \quad (\text{g CO/Kg of fuel}) \quad \dots(2.3)$$

Leonard et al.(1983) extended the model to relate to the combustion inefficiency, as

$$(1 - \eta_c) = 2.15 (\tau_{\eta} / \tau_{sl}) [1 + 0.12 (\tau_{eb} / \tau_{sl})] \quad \dots(2.4)$$

This attempt to include evaporation, mixing as well as kinetic processes will again depend on the prior knowledge or assumptions of individual characteristic time models and their dependence on fuel type, injection, quenching .

Though successful designs have resulted out of such empirical relations, the growing importance of emissions and need for the knowledge of detailed picture of the local variations have evolved more elaborate techniques.

2.2.2 MODULAR APPROACH

In order to achieve overall picture of the combustion chamber, single stage stirred reactor models of Longwell and Weisse must be combined in series to include staged air addition, or in parallel to include recirculation flows. Modular concept enables one to depart from PSR concept to Well Stirred Reactor (WSR) where limitation can be mixing or reaction or both. Here the combustion chamber is divided into convenient number of discrete zones, characterized by a

limited number of global parameters e.g. air-fuel ratio, residence time, degree of 'unmixedness' etc. The basic interest in the application of approximate techniques is to avoid the complexities inherent in a direct calculation of an elliptic flow field by making suitable assumptions that allow the flow to be computed using simpler approaches. Clearly the simplest possible procedure is to assume that the flow field is one dimensional, thus avoiding any necessity for definition or calculation of velocity or species profile effects. A somewhat more sophisticated approach is to assume that the combustor flow field can be broken down to separate zones, each of which can be calculated individually in some detail and then coupled together in some fashion to obtain an overall computational analog of the combustor flow.

An excellent model was proposed by Hottel et al. (1958) to include combustion in the recirculation flow. This was extended to include air staging by Hammond and Mellor (1970).

Individual zones are further divided to include possible downstream combustion and unmixedness by Swithenbank (1973). As shown in Fig 2.1, the primary zone is represented by three modules, a pair of WSR's coupled by a PFR. The volumes are calculated from jet entrainment theory, the total volume of the primary zone having been assessed previously by some independent method. The volumes of the various reactors are estimated on the assumption of uniform gas density; the swirler and recirculation volumes are ratioed according to their mass flows; that of the primary is considered to be symmetrical about the primary orifices. The secondary zone has two modules, a WSR followed by a PFR. The volume of the WSR is obtained by the assumption that it is symmetrical about the secondary zone holes, with its upstream boundary abutting the primary zone. The dilution stirred reactor is supposed symmetrical about the dilution holes, and of a volume which is ratioed in proportion of its mass flow to that of the secondary zone. Between the secondary WSR and the dilution WSR the resultant volume is taken as being the secondary PFR. The plug flow module of the dilution zone is taken as that between the downstream end of the dilution WSR and the exit of the combustor. Thus, for each module, the mass flow, volume and residence time have been defined, and this may be used to predict the composition leaving each module using a suitable reaction scheme. The output of one module becomes the input of the next, although within the primary zone an iterative calculation must be used since there is recirculation from one zone to another. Though, extensive testing has not been attempted, this method offers valuable performance as well as emission information.

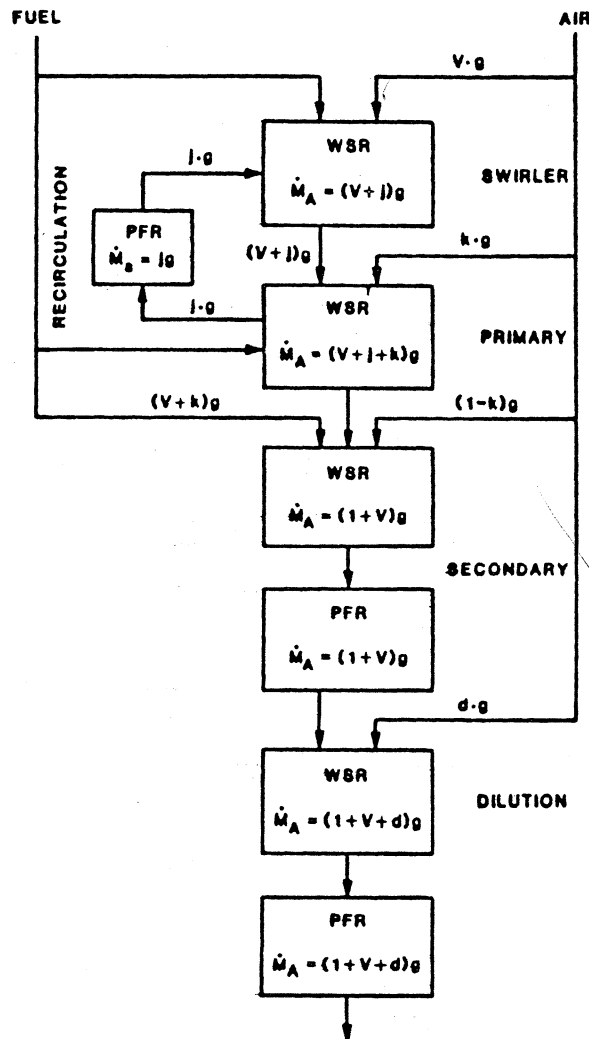
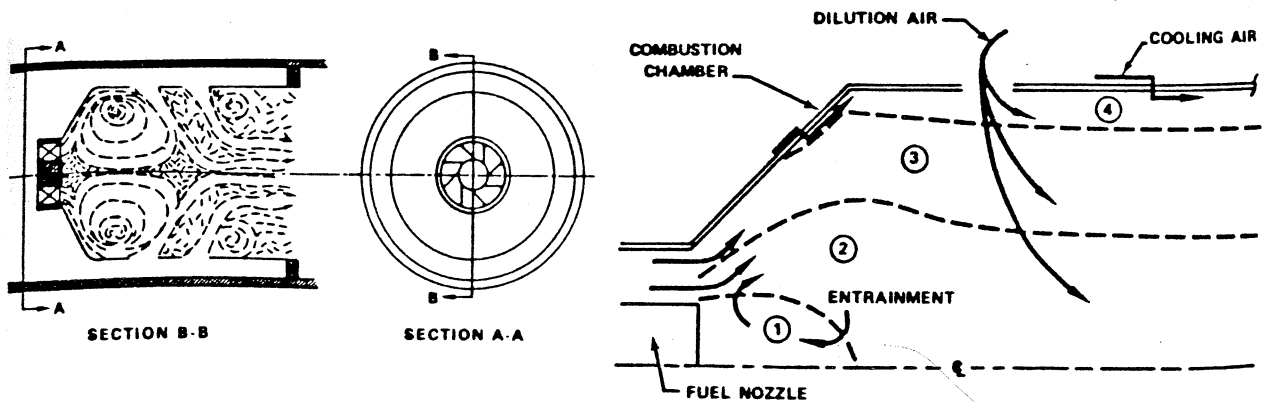


Fig 2.1 Schematic of Modular model of Swithenbank et al. (1973)

So far all these models examined have assumed that the influence of fuel droplets is negligible. It is obvious that a more complete analysis could be made if the fuel droplet size and distribution were incorporated together with evaporative effects.

More sophisticated modular formulation is that by Mosier and Roberts (1973) in which the combustor flowfield is described by radial array of one dimensional, coannular stream tubes (4 for tubular and 7 for annular) symmetric about geometric combustor axis (Fig 2.2).



a) Primary zone flow pattern

b) Internal flow field

Fig 2.2 Stream_tube model of Mosier and Roberts (1973)

The model includes physical description of fuel droplet burning and equilibrium or kinetic limited hydrocarbon-air thermochemistry. Initial values of mean droplet size and injection velocity are determined from Separate droplet vaporization equations are written for each stream tube. All fuel that enters the recirculation zone is assumed to be fully vaporized and mixed with the region (1) airflow. Quasi-global kinetic model is used for gas phase chemistry. The applicability of the programme can be seen from its sample result given as Fig 2.3. The correlations are described by Mellor (1978) as quite suitable.

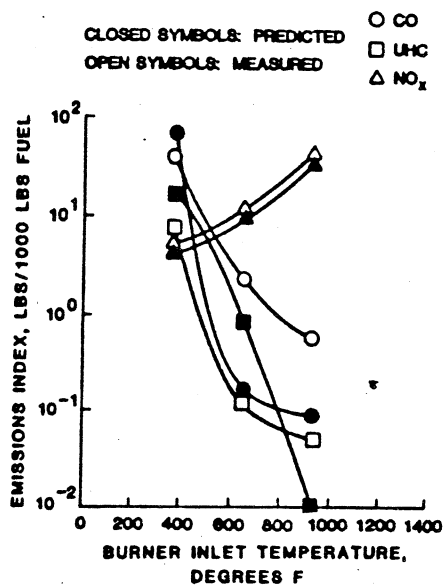


Fig 2.3 Exhaust emissions for the P&W JT9D combustor

Modular models are by nature correlative rather than predictive, some details of the flow field configuration must be known before a calculation can commence. Apart from experimental data obtained from a geometrically similar combustor, finite difference techniques can provide flow fields.

2.2.3 FINITE DIFFERENCE APPROACH

Progress in computational techniques has diverted present day research activity towards analyzing flowfields using finite difference techniques. Considering the fact that the governing equations of heat, mass, momentum and other processes taking place in a combustor are partial difference equations, finite difference techniques are more suitable to arrive at solutions. It is worth reviewing the basic process and the governing equations at this stage.

GOVERNING EQUATIONS

For gas-fuelled flames, in the absence of radiation, the instantaneous values of velocity, concentration of chemical species and enthalpy can be represented by the following conservation equations in cartesian tensor notation.

. Continuity

$$\frac{\partial \rho}{\partial t} + \frac{\partial \rho U_i}{\partial x_i} = 0 \quad \dots(2.5)$$

. Momentum

$$\rho \frac{\partial U_i}{\partial t} + \rho U_j \frac{\partial U_i}{\partial x_j} = - \frac{\partial p}{\partial x_i} + \frac{\partial}{\partial x_j} \left\{ \mu \left(\frac{\partial U_i}{\partial x_j} + \frac{\partial U_j}{\partial x_i} - \frac{2}{3} \delta_{ij} \frac{\partial U_k}{\partial x_k} \right) \right\} + \rho g_i \quad \dots(2.6)$$

. Chemical Species

$$\rho \frac{\partial C_\alpha}{\partial t} + \rho U_j \frac{\partial C_\alpha}{\partial x_j} = \frac{\partial}{\partial x_j} \left\{ \frac{\mu}{Sc} \frac{\partial C_\alpha}{\partial x_j} \right\} + \rho r_\alpha \quad \alpha = 1, NS \quad \dots(2.7)$$

. Enthalpy

$$\rho \frac{\partial h}{\partial t} + \rho U_j \frac{\partial h}{\partial x_j} = \frac{\partial p}{\partial t} + \frac{\partial}{\partial x_j} \left\{ \frac{\mu}{Pr} \frac{\partial h}{\partial x_j} + \frac{\mu}{Pr} \left(\frac{Pr}{Sc} - 1 \right) \sum_{\alpha=1}^{NS} h_\alpha \frac{\partial C_\alpha}{\partial x_j} \right\} \quad \dots(2.8)$$

. Equation of state

$$p = \frac{P}{RT \sum_{\alpha=1}^{NS} (C_{\alpha}/Mw_{\alpha})} \quad \dots(2.9)$$

. Auxiliary thermodynamic data

$$h = h_{\alpha}(T) \quad \dots(2.10)$$

$$h = \sum_{\alpha=1}^{NS} C_{\alpha} h_{\alpha} \quad \dots(2.11)$$

The reaction mechanism and associated rate constants must be known to obtain the formation rate per unit volume. For example, in the idealized irreversible reaction where species A and B combine to form species C, i.e



the forward rate constant is, typically, $k_f = a \exp(-E/RT)$ and the net formation rates, which appear in the species mass fraction equations, are

$$\dot{r}_A = - \frac{p}{Mw_B} k_f C_A C_B \quad \dots(2.12)$$

$$\dot{r}_B = - \frac{p}{Mw_A} k_f C_A C_B \quad \dots(2.13)$$

$$\dot{r}_C = + \frac{p}{Mw_A Mw_B} k_f C_A C_B \quad \dots(2.14)$$

These complete the formulations to evaluate local velocity, pressure, density, temperature, concentration of species and other dependent variables (of course, with the need of some reasonable assumptions). However, when these have to be extended to practical combustors, a variety of difficulties arise due to the complexity of the process.

COMBUSTION PROCESS :

In the process of combustion in a gas turbine, liquid fuel is usually injected into a region of flow reversal, and combustion is initiated after a time interval during which partial or complete evaporation is achieved. The primary purpose is to raise the temperature of the airflow by

efficient burning of the fuel. The various processes taking place in the combustion chamber are extremely complex. They involve fuel atomization and evaporation and subsequent mixing with air and combustion products, all occurring simultaneously with chemical reaction and heat transfer. The problem is less severe if the fuel is prevaporised and premixed or the initial state of the fuel is gaseous. Progress in isolating individual process and its detailed theoretical treatment is inevitably very slow. The simplified processes treated individually are amplified below:

TURBULENCE

The flow in practical combustion systems is invariably turbulent and the temporal and spatial variations in the dependent variables encompass such a wide range of time and length scales so as to preclude the direct numerical solution of the governing equations. The computer storage and time requirements are well beyond the capacity of any existing or planned computer.

As a consequence, the dependent variables are decomposed into mean and fluctuating components, and the resulting equations averaged to convert them into statistical equations describing the evolution of mean quantities. In general, the averaging process should involve ensemble averaging but for the stationary flows considered here this is indistinguishable from time averaging. As a consequence of the non-linearity of the equations, averaging results in a loss of information so that the equations are no longer closed and closure assumptions are necessary before solution is possible.

Reynolds Decomposition	Favre Averaging
$\phi = \bar{\phi} + \phi'$	$\phi = \tilde{\phi} + \phi''$
$\bar{\phi} = \frac{1}{\Delta t} \int_0^{\Delta t} \phi dt$	$\tilde{\phi} = \frac{1}{\bar{\rho} \Delta t} \int_0^{\Delta t} \rho \phi dt$
$\bar{\phi}' = 0$	$\overline{\rho \phi''} = 0; \text{ but } \overline{\phi''} \neq 0$
convective term $\rho U_i U_j$	
$\bar{\rho} \bar{U}_i \bar{U}_j + \bar{\rho} \overline{U'_i U'_j} + \bar{U}_i \overline{\rho' U'_j}$ $+ \bar{U}_j \overline{\rho' U'_i} + \overline{\rho' U'_i U'_j}$	$\bar{\rho} \tilde{U}_i \tilde{U}_j + \bar{\rho} \overline{U''_i U''_j}$

The introduction of Favre averaging (Favre(1969)) simplifies the closure problems in that it reduces the number of terms to be modelled, as an example, the convective term $\rho U_i U_j$ is shown above. This is also known as density weighted averaging. With this, the equations of continuity, conservation of momentum and a scalar may be written as

$$\frac{\partial}{\partial x_i} (\bar{\rho} \tilde{U}_i) = 0 \quad \dots(2.15)$$

$$\frac{\partial}{\partial x_j} (\bar{\rho} \tilde{U}_i \tilde{U}_j) = \bar{\rho} g_i - \frac{\partial \bar{p}}{\partial x_i} - \frac{\partial}{\partial x_j} (\bar{\rho} \widetilde{U_i'' U_j''}) \quad \dots(2.16)$$

$$\frac{\partial}{\partial x_i} (\bar{\rho} \tilde{U}_i \tilde{\phi}_\alpha) = - \frac{\partial}{\partial x_i} (\bar{\rho} \widetilde{U_i'' \phi_\alpha''}) + \bar{\rho} \widetilde{S_\alpha}(\phi) \quad \dots(2.17)$$

Considerable progress has been made in devising 'models' which allow the calculation of the Reynolds stress $\bar{\rho} \widetilde{U_i'' U_j''}$ ($\bar{\rho} \widetilde{U_i' U_j'}$ for unweighted) and turbulent flux $\bar{\rho} \widetilde{U_i'' \phi_\alpha''}$ ($\bar{\rho} \widetilde{U_i' \phi_\alpha'}$ for unweighted). Launder and Spalding (1972) summarized an array of models with increasing number of equations ranging from zero to as many as 28 equations. Depending on the complexities one might wish to enter, and the computing time available, any model can be chosen. However, simple algebraic eddy viscosity models found wider application due to their simplicity.

Mosier and Roberts (1973) have assumed turbulent mixing between adjacent streamtubes. The eddy viscosity model is of the form

$$\mu_t = \rho k b | U_{\max} - U_{\min} | \quad \dots(2.18)$$

where k is empirical constant fitted to experimental mixing data for two-dimensional turbulent jets

b is proportional to the width of the mixing region

Edleman and Harsha (1978) compared the one equation and two equation models, and sample results are given as Fig 2.4. It is pointed out that accuracy can be improved in both the models by better prescription of mean Prandtl and Lewis numbers.

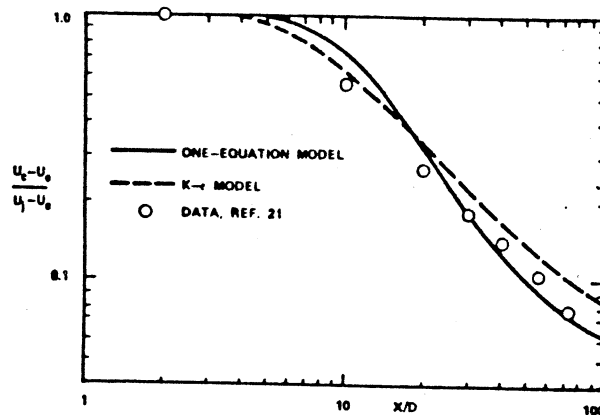


Fig 2.4 Comparison of one equation model prediction for center velocity decay, reacting H_2 -air jet

However better predictive accuracy is anticipated when two equation turbulence models are invoked: the most commonly used dependent variables are the turbulence kinetic energy k and energy dissipation rate ϵ , which are modelled with differential equations (Jones (1979), for example).

CHEMICAL KINETICS

The combustion model in essence must provide a method of evaluating the mean formation rate of each species present, and in addition allow the calculation of mean fluid temperature and the density of the mixture. With reasonable assumptions, the instantaneous thermochemical state of the gas is determinable as a nonlinear function of a single strictly conserved (i.e. zero source) scalar variable. All the relevant strictly conserved scalar variables are linearly related, so the actual one to be used becomes a matter of taste. Typical choices are the normalised mixture fraction, ζ , defined as the mass fraction of fuel both burnt and unburnt, the elemental mass fraction of any element present, and the enthalpy or any composite variable made up of these quantities. If the mixture fraction ζ will be taken as the scalar variable to be used, all other conserved quantities can then be obtained from :

$$\begin{aligned}
 h &= (h_{fu} - h_a)\zeta + h_a \\
 Y_\alpha &= (Y_{\alpha_{fu}} - Y_{\alpha_a})\zeta + Y_{\alpha_a}
 \end{aligned}
 \quad \dots(2.19)$$

where Y_α is the mass fraction of element α and where subscripts 'fu' and 'a' refer to the values appropriate to the fuel and air streams respectively. The instantaneous composition, temperature and density must now be related to the instantaneous value of ζ .

EQUILIBRIUM

The simplest approach is to assume instantaneous reaction to equilibrium at the equivalence ratio dictated by the local mixing. With this assumption it is not necessary to specify a precise reaction mechanism and the equilibrium state including composition, temperature and density can be obtained by minimizing the free energy. A well tested and reliable computer programme based on this technique is described by Gordon and McBride (1971).

ONE STEP

Another simple method is to assume single step irreversible reaction of the form



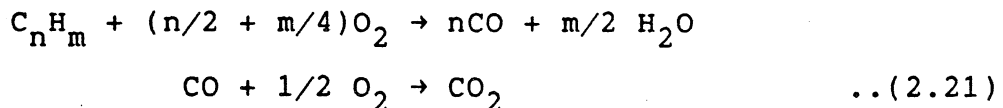
The fast reaction assumption then implies that the mixture (at any instant) consists of either fuel plus products or oxidant plus products, i.e. fuel and oxidant cannot coexist on an instantaneous basis. A knowledge of mixture fraction is then sufficient to determine the (instantaneous) fuel, oxidant and product mass fractions and with the adiabatic flow assumption the temperature may also be calculated.

In so far as major species and temperature are concerned both for the H₂/air system and lean hydrocarbon/air mixtures there is little to choose between the single step irreversible reaction (with accurate thermodynamic data) and the full equilibrium calculation.

However for hydrocarbon/air mixtures richer than stoichiometric where large amounts of carbon monoxide may be formed differences between the two methods becomes significant: the single step reaction model which allows no carbon monoxide to be formed may generate temperatures upto 200 K higher than equilibrium temperatures.

MULTI STEP

It is well recognized that typical hydrocarbons burn in a sequential manner. That is, the fuel is partially oxidized to CO and H₂, which are not appreciably consumed until all of the hydrocarbon species have disappeared. Dryer and Glassmen (1973) used this observation, to construct a two-reaction model for methane oxidation in a turbulent flow reactor which can be generalized for application to arbitrary fuels



With optimal rate reaction rate parameters, the two-step reaction mechanism performs as well as the single-step mechanism, but also provides information about CO concentration with the adiabatic flame temperature much closer to the correct value. Thus the two-step model will provide more accurate NOx production rate predictions.

Another reaction can be added to account for the H₂ - H₂O equilibrium in the burned gas region. For each reaction added another species equilibrium concentration can be estimated. The logical limit of this process is the quasi-global reaction mechanism of Edelman Fortune (1969),

Reaction	A		Forward b	E/R	
	Long Chain	Cyclic		Long Chain	Cyclic
1) $C_n H_m + \frac{n}{2} O_2 + \frac{m}{2} H_2 + n CO$ ^a	6.0×10^4	2.08×10^7	1	12.2×10^3	19.65×10^3
2) $CO + OH = H + CO_2$	5.6×10^{11}		0	0.543×10^3	
3) $CO + O_2 = CO_2 + O$	3.0×10^{12}		0	25.0×10^3	
4) $CO + O + M = CO_2 + M$	1.8×10^{19}		-1	2.0×10^3	
5) $H_2 + O_2 = OH + OH$	1.7×10^{13}		0	24.7×10^3	
6) $OH + H_2 = H_2O + H$	2.19×10^{13}		0	2.59×10^3	
7) $OH + OH = O + H_2O$	5.75×10^{12}		0	0.393×10^3	
8) $O + H_2 = H + OH$	1.74×10^{13}		0	4.75×10^3	
9) $H + O_2 = O + OH$	2.24×10^{14}		0	8.45×10^3	
10) $M + O + H = OH + M$	1.0×10^{16}		0	0	
11) $M + O + O = O_2 + M$	9.38×10^{14}		0	0	
12) $M + H + H = H_2 + M$	5.0×10^{15}		0	0	
13) $M + H + OH = H_2O + M$	1.0×10^{17}		0	0	
14) $O + N_2 = N + NO$	1.36×10^{14}		0	3.775×10^4	
15) $N_2 + O_2 = N + NO_2$	2.7×10^{14}		-1.0	6.66×10^4	
16) $N_2 + O_2 = NO + NO$	9.1×10^{24}		-2.5	6.46×10^4	
17) $NO + NO = N + NO_2$	1.0×10^{10}		0	4.43×10^4	
18) $NO + O = O_2 + N$	1.55×10^9		1.0	1.945×10^4	
19) $M + NO = O + N + M$	2.27×10^{17}		-0.5	7.49×10^4	
20) $M + NO_2 = O + NO + M$	1.1×10^{16}		0	3.30×10^4	
21) $M + NO_2 = O_2 + N + M$	6.0×10^{14}		-1.5	5.26×10^4	
22) $NO + O_2 = NO_2 + O$	1.0×10^{12}		0	2.29×10^4	
23) $N + OH = NO + H$	4.0×10^{13}		0	0	
24) $H + NO_2 = NO + OH$	3.0×10^{13}		0	0	
25) $CO_2 + N = CO + NO$	2.0×10^{11}		-0.5	4.0×10^3	
26) $CO + NO_2 = CO_2 + NO$	2.0×10^{11}		-0.5	2.5×10^3	

$$^a \frac{dC_{n H_m}}{dt} = -A T^b P^{0.3} C_{n H_m}^{1/2} C_{O_2}^{1/2} \exp\left(-\frac{E}{RT}\right); [C] = \frac{\mu\text{m moles}}{\text{cc}}, [T] = \text{OK}, [P] = \text{atm.}, [E] = \frac{\text{k cal}}{\text{mole}}$$

Table 2.1 Extended C-H-O Chemical Kinetic Reaction Mechanism
 $K_f = AT^D \exp(-E/RT)$

which combines a single reaction of fuel and oxygen to form CO and H₂, together with a detailed reaction mechanism for CO and H₂ oxidation, given as Table 2.1. Since all of the important elementary reactions and species in the CO-H₂-O₂ system can be included, this approach can provide accurate values for adiabatic flame temperature and the equilibrium post-flame composition. Because thermal NO_x production in flames depends on burned gas properties, the extended Zeldovich mechanism reactions can be added to the quasi-global reactions to give an estimate of NO_x formation rates. Radical levels in the flame zone as per Dryer and Westbrook (1979) itself are not predicted well by the quasi-global model, so NO_x production due to radical overshoot will not be predicted correctly.

The computational costs of a given reaction mechanism depend primarily on the number of chemical species included, rather than on the number of reactions. Conventional numerical solution techniques indicate that the computer time requirements are roughly proportional to N², where N is the number of species (Westbrook and Dryer (1981)).

Single step	5	(including Nitrogen)
Two step	6	
CO-H ₂ -O ₂	10	(H, O, H ₂ , O ₂ , OH, H ₂ O, N ₂ , CO, CO ₂ , FUEL)

Increasingly elaborate mechanisms for hydrocarbons consisting of several hundreds of reactions are being investigated. (238 reactions with 47 species for n-butane by Pitz, Westbrook (1984), for example).

Interaction with Turbulence

When finite rate chemistry is coupled with flow calculations, caution is to be exercised when turbulence is considered. The importance of fluctuations in turbulent flows is well known and must be represented in the evaluation of mean formation rates, density and temperature. Thus the reaction rate for the one-step reaction in equation 2.12 can not be accurately evaluated in terms of mean quantities and, for example, the equation

$$\bar{r}_A \neq -\bar{\rho} k (\bar{T}) \bar{C}_A \bar{C}_B \quad \dots(2.22)$$

will lead to errors upto three orders of magnitude. The most convenient way to represent the necessary scalar fluctuations is with a probability density function (PDF).

PROBABILITY DENSITY FUNCTIONS

Considering the stochastic nature of turbulence, it is logical to rely on probability theory to arrive at averaging. A Probability Density Function $P(U_i)$, is defined so that $P(U_i)dU_i$ is the probability that the i th component of velocity will lie in a small range dU_i about the value U_i at particular, fixed values of x_i and t .

$$\begin{aligned} \int_{-\infty}^{\infty} P(U_i)dU_i &= 1 \\ \int_{-\infty}^{\infty} U_i P(U_i)dU_i &= \overline{U_i} \\ \int_{-\infty}^{\infty} U_i^2 P(U_i)dU_i &= \overline{U_i^2} = \overline{U_i}^2 + \overline{U_i'^2} \end{aligned} \quad \dots(2.23)$$

There are joint probability density functions, such as $P(\rho, U_i)$, having $P(\rho, U_i)d\rho dU_i$ equal to the probability that fluid density lies in a small range $d\rho$ about ρ and the i th component of velocity lies in a small range dU_i about U_i .

Thus by knowing the PDF of the variable, its mean value can be evaluated. Various methods are being evolved to specify or construct or generate from its transport equation.

Different forms of PDFs are being investigated to suit the variable. Velocity components do not involve sharp bounds, but by their nature the mass fractions, mixture fraction are restricted to the range of zero to unity. A consequence of these different behaviours as well as programming technique, is that for some variables Gaussian distributions, while for others clipped Gaussian or Beta Function, or Gaussian bounded by Delta functions (Lockwood and Naguib (1975)) are being tried out.

Chemical prescription and its incorporation into a turbulent flowfield calculations are being approached using laminar flamelet concept (Liew, Bray, Moss (1981,1984)). Burning within the turbulent flame is assumed to occur locally in laminar-like flamelets, the scalar structure of which is substantially invariant when expressed in mixture fraction space. The Laminar flame experiments of Mitchel et al (1980) confirm that composition measurements at different flame positions can be collapsed into common profiles against local equivalence ratio (or mixture fraction ζ) since fuel-air mass ratio

$$\text{FAR} = \frac{\zeta}{(1-\zeta)} \quad \dots(2.24)$$

Given knowledge of the mixture fraction in the turbulent flame, the accompanying scalar description can be simply inferred from the flamelet relationship. Then evaluating the probability density of the mixture fraction (in a beta function form), all the other variables are evaluated from this scalar variable and its distribution function :

for e.g. mean concentration

$$\bar{C}_\alpha = \int_0^1 C_\alpha(\zeta) \tilde{P}(\zeta) d\zeta \quad \dots(2.25)$$

However, at this development stage of the concept, the applicability of the existing data for reaction rates etc, often generated under turbulent conditions, to laminar flamelets is a matter of concern.

Single step global reaction (2.20) is made use of in the present programme to evaluate the species concentration and product temperature.

NOx

The oxides of Nitrogen of which the predominant compound at high emission levels is Nitric Oxide, can be produced by three different mechanisms

- 1) Thermal NO is produced by oxidation of atmospheric nitrogen in the post flame gases.
- 2) Prompt NO is produced by high-speed reactions at flame front. Under certain circumstance and especially in low temperature fuel rich flames NO is found very early in the flame region. The intermediates including CN- and HCN-type species may play a role in the "early" formation of NO (Fenimore (1971)). Prompt NO levels cannot be predicted with any degree of precision. However, it is likely their contribution in the modern gas turbine engines could be of the order 0-30 ppmv, with low values occurring at high temperature lean combustion and high levels at low temperature rich conditions.
- 3) Fuel NO is produced by oxidation of Nitrogen contained in the fuel. Its importance increases with the increase in availability of nitrogen containing fuels.

The present work discusses in detail the estimation of Thermal NO.

Nitric Oxide is normally present in trace quantities and has negligible influence on the reactions associated with heat

release, the thermodynamic state of the gas of the flow. It is generally accepted- at least under fuel lean and near stoichiometric conditions- that formation of NO is described by the extended Zeldovich mechanism :



With consideration of superequilibrium O atom, models for gas turbines with lean primary zones, can expect reasonable predictive ability.

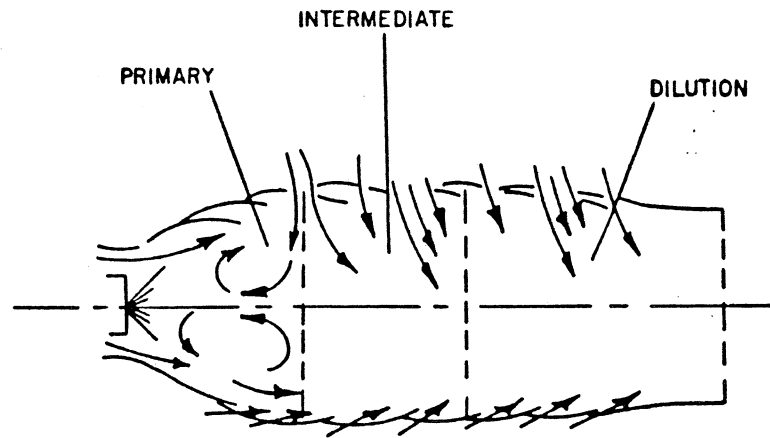
Reasonable predictions are possible by simple expressions correlating the operating conditions, mixing characteristics etc.. Mellor's (1983) characteristic model indicated as Eqn. 2.1 is one such example. Lefebvre (1987) has proposed of the form

$$\text{NOx} = \frac{9 \times 10^{-8} P_2^{1.25} V_c \exp(0.01 T_{st})}{\dot{m}_a T_{pz}} \quad \text{g/Kg} \quad \dots(2.29)$$

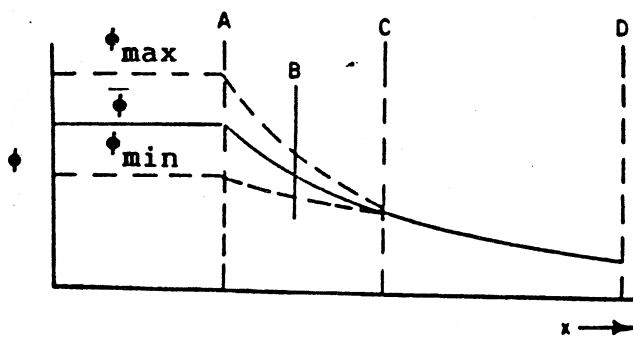
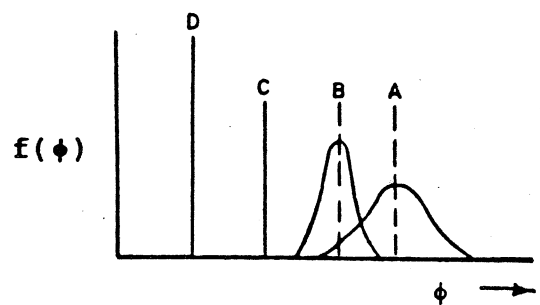
where T_{st} = Primary zone stoichiometric flame temperature

V_c = combustion volume

Fletcher and Heywood (1971) developed a NOx model applying the well-stirred reactor concepts to primary zone, accounting for the unmixedness through a normal distribution of equivalence ratio about an assumed mean value (Fig 2.5) and a residence time distribution about a mean value.



a) combustor flow distribution pattern

b) variation of ϕ along the liner length

c) equivalence ratio distribution along the liner

Fig 2.5 NO_x model of Fletcher and Heywood (1971)

Qualitative predictive ability is achieved, with a priori knowledge of a number of performance parameters.

Better predictive ability is demonstrated (Fig 2.3) by Mosier, Roberts (1974). As NO_x heavily depends on the local values of temperature and stoichiometry of the flow, better flow field calculations are the contributing factors. As explained previously the combustor flow is evaluated by assuming a number of stream tubes.

Following similar philosophy, Hung (1975) approached the problem dividing the combustor into five regions, as shown in Fig 2.6.

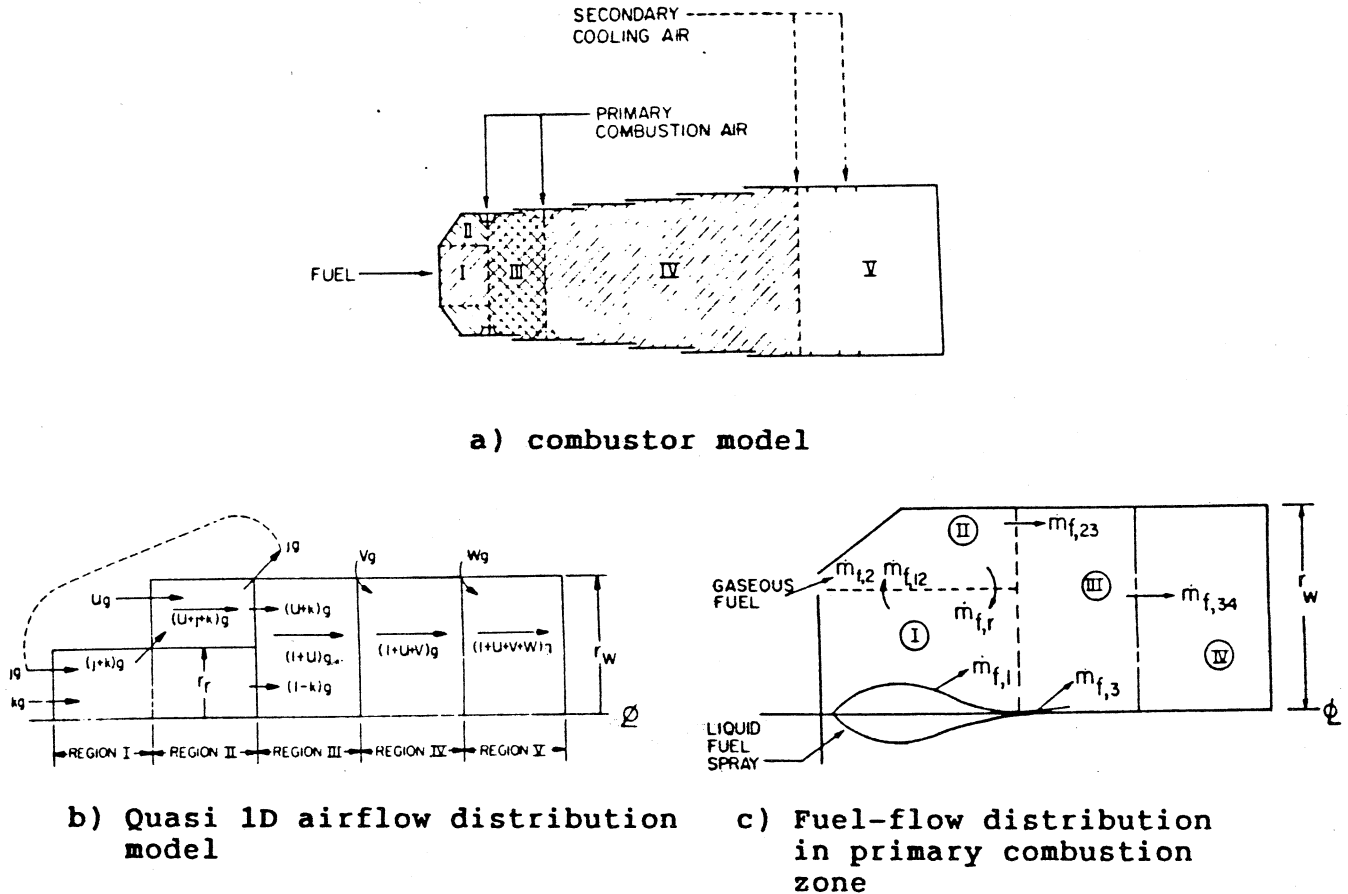


Fig 2.6 NO_x Model of Hung (1975)

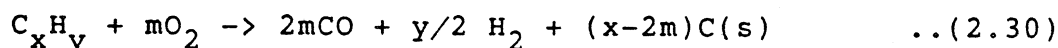
Though, prior knowledge of flow proportions is required, this model demonstrated reasonable accordance with the test results. Steps are included to account for the effect of humidity and water injection. Hung (1975b) had extended the model to NO_x due to fuel bound Nitrogen, by assuming that chemically bound Nitrogen in fuel is 100% reacted to form nitric oxide and post combustion nitric oxide formation is through Zeldovich mechanism, as is the case in his original model.

It is common to distinguish between combustion reactions involving the exothermic formation of CO₂ and H₂O, and the NO_x formation reactions. In practice, however, these two processes cannot be distinguished, and they are coupled. For example, Edelman and Harsha (1977) treated combustion and NO_x formation mechanisms within the framework of a unified scheme, considering the assumption that O is at its equilibrium level is not entirely valid. However, the present work adopted the approach of Fletcher and Heywood (1971) and treated NO_x formation as a post flame phenomenon

SOOT

Soot formation and oxidation involve complex physico-chemical processes. The generation of soot in hydrocarbon flames represents a potential source of several problems. Soot is combustible, and therefore if it is not consumed in the flame it represents a contribution to combustion inefficiency. Soot also can be the primary source of thermal radiation. Finally, its impact on the environment as undesirable emissions also needs to be considered. These problems will become more apparent as alternate sources of hydrocarbon fuels are developed.

The processes governing the rates of formation and subsequent oxidation of soot are highly complex and quantitative models to describe these processes are not yet fully developed. However, the main controlling factors are much better understood. For the pressures and temperatures prevailing in gas turbine combustors, equilibrium considerations suggest that solid carbon appears when there is insufficient oxygen to oxidize the fuel to CO and H₂.



According to the above reaction (Haynes and Wagner (1981)), the formation of soot should start when x becomes equal to or larger than 2m, i.e. when the C/O atomic ratio exceeds unity. However, since soot formation is essentially a non-equilibrium phenomenon, soot is reported to be observed at C/O ratios much less than unity for temperatures less than 2000 K.

The amount of soot produced is generally too small to influence the rate of heat release and, in principle, its rate of formation can be calculated from a knowledge of hydrocarbon and oxygen concentrations if an approximate correlation equation is known. In general, soot concentration is given by

$$\frac{dC}{dt} = \frac{dC_f}{dt} - \frac{dC_{oxid}}{dt} \quad ..(2.31)$$

f : formation, oxid : oxidisation

A simple representative correlation based on test data proposed by Lefebvre (1985) is of the form:

$$S_f - S_{oxid} = (18-H)^{1.5} P_2^{2.0} \left[\frac{F/A}{f \dot{m}_a 2T} \right]_{pz} \left[C_5 - C_6 \left(\frac{e^{0.0011T}}{F/A} \right)_{sz} \right] \quad ..(2.32)$$

C₅ and C₆ are experimentally evaluated for each combustor

Investigations typically relating the global soot formation rates to the experimental results include Najjar (1986) on gas turbine combustors, , Mullins et al. (1987) on shock tube experiments. Though numerous correlations and models exist, more work is required to effectively predict soot at this stage of development. Hence, soot estimation is not included in the present work.

FUEL SPRAY

So far, the discussions described the models for homogeneous gas phase turbulent diffusion flames. However many flow fields of technological interest involve multiphase reacting flows, for example, problems involving coal combustion, droplet and spray combustion phenomena associated with liquid hydrocarbon fuels, and slurry and metal particle combustion. In these areas combustion modelling approaches are not nearly as well-developed. Here the discussion is limited to only droplet and spray combustion. Even though this aspect is not included in the present programme the typical approach and governing equations are presented below.

A detailed model for fuel spray penetration and evaporation requires the introduction of a species conservation equation for each size classification of the droplets, and similar momentum equations including drag effects and energy equations for droplet temperature histories.

Normally the size distribution of the fuel droplet is adequately described by a single value of Sauter Mean Diameter (SMD).

$$\text{SMD} = \frac{\sum n D^3}{\sum n D^2} \quad \text{where } n \text{ number of drops} \quad \dots(2.33)$$

One typical Lagrangian formulation (Wild et al.(1987)) for the droplet motion is given as

$$\frac{dU_{id}}{dt} = - \frac{18}{\rho_d D_d^2} \frac{C_D \text{Re}}{24} (u_{id} - U_i) \quad \dots(2.34)$$

where u_{id} denotes the component of droplet velocity, D_d is the droplet dia, ρ_d is its density. The droplet Reynolds no Re is defined as

$$\text{Re} = \frac{\rho_d D_d}{\mu} | u_d - U | \quad \dots(2.35)$$

C_D is Reynold's number dependent drag coefficient

Droplet evaporation is described by

$$\frac{dD_d}{dt} = \frac{8\lambda}{2 \rho_d C_p D_d} \ln \left[1 + \frac{C_p}{L} (T - T_d) \right] \left[1 + 0.23 Re^{1/2} \right] \dots (2.36)$$

SWIRL- RECIRCULATION

Another complication of the practical combusting systems is that they are swirling with recirculation. Typical recirculation regions are shown as Fig 2.7 (Edleman & Harsha (1977)). However, considering its nature, this aspect cannot be included in the present work, which is only one dimensional in nature.

Lilley (1986) presented the results of a series of work on turbulent flows with swirl in 2D axisymmetric geometries under low speed and non-reacting conditions. He highlights the need for better models, reminding that the accuracy of currently available prediction codes for swirling recirculating confined flows is in doubt, because of questionable turbulence models and lack of suitable experimental data base.

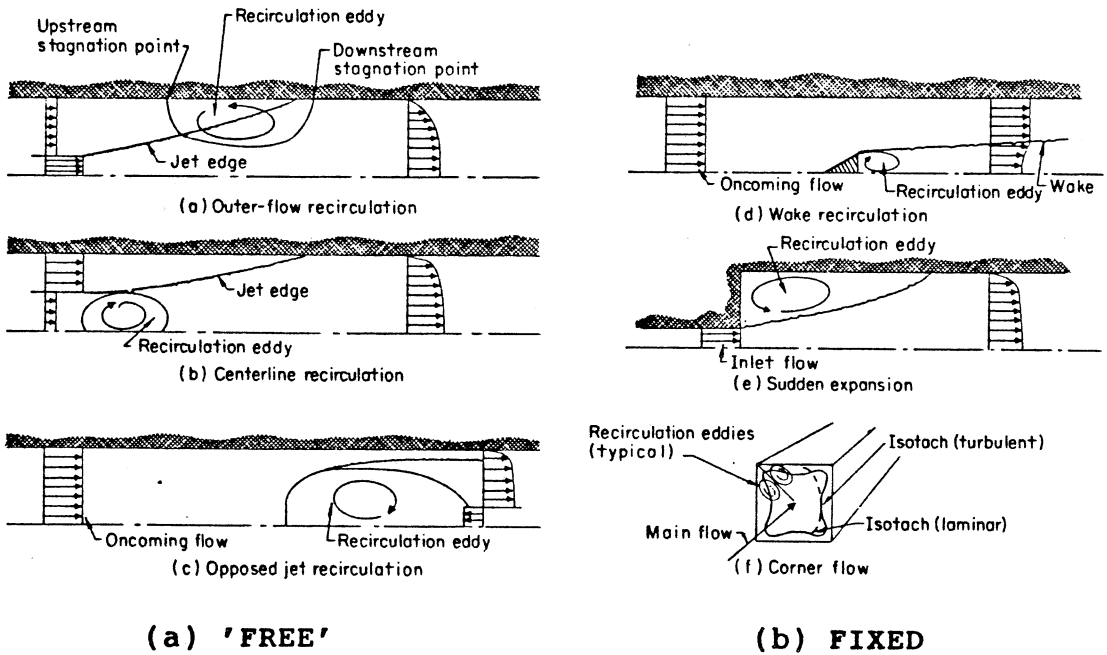


Fig 2.7 Types of Recirculation zones

Lilley (1977) summarises that while good results can be achieved for swirling jets, for reacting flows in combustion geometries which include recirculation zones, it is difficult to achieve reasonable level of quantitative

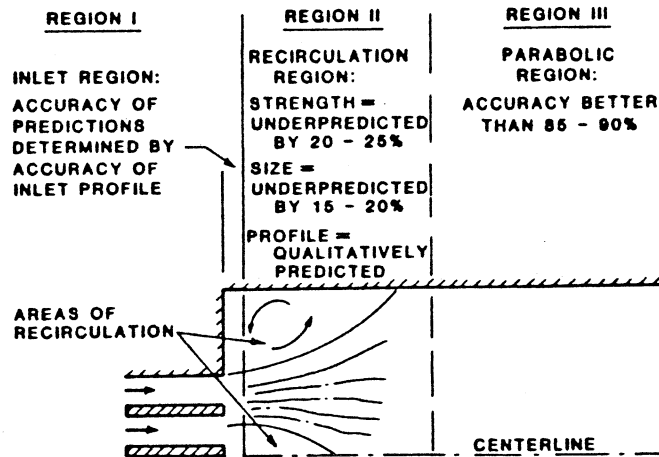


Fig 2.8 Summary of the accuracy of predictions in the various regions of the flow field

agreement with experiment. Syed and Sturgess (1980) describe the present status of predictive capability of swirling and recirculating flow as shown in Fig 2.8.

2.2.4 CLOSURE

The treatment of above processes and coupling of submodels is gradually growing. However, the empirical approach, to date has arguably been the more influential in determining the design.

The Existing models of the gas turbine combustion are itemized in Table 2.2 and 2.3. (Mellor (1979)) interms of whether they are modular (MO) or finite difference (FD) .

Reference	^a FD or MO	Submodel Chemistry	Complexity Turbulence	(extra PDE's) fuel spray	Submodel Interactions	Comments
Hammond & Mellor (1971)	MO	^b n	WSR ^c	NA ^d	None	Poor trend predictions; can't fit both NO and CO
Fletcher, Heywood (1971)	MO	0 + NO	PSR ^e	NA	None	Can't fir NO over entire engine operating range
Mosier Roberts et al (1973)	MO	n	WSR's ^f PFR's ^f	1	None	Good agreement
Anasoulis et al (1974)	FD	0 + NO	0	n	None	Very poor agreemnt
Reynolds et al (1977)	FD	2	2	unknown	EBU ^g	Predicted HC and CO too high; no NO predictions
Serag-Eldin Spalding (1978)	FD	0	2	NA	PDF ^h	Limited agreement for T
Edleman et al (1972)	Parabolic FD + WSR	n	0	n	None	No comparision with experiment
Felton et al (1977)	FD and MO	2 n	2 PSR's	unknown n	EBU None	MOs sized from FD analysis, no MO results compared with gas turbines yet

a FD = finite difference, MO = modular;

b number of steps see text

c WSR = well stirred reactor

d not appropriate

* see Mellor (1979) for references

e PSR = partially stirred reactor

f PFR = plug flow reactor

g EBU = eddy break up model

h PDF = probability function

Table 2.2 Models for Gas Turbine Combustors (Mellor(1979))

Reference	Experiment	Submodel chemistry	Complexity Turbulence	(extra PDE's) fuel spray	Submodel Interactions	Comments
Lockwood et al. (1974)	Axi-symmetric furnace	0	0	NA	None	Local mixing can be calculated
Bradley et al (1977)	WSR	2	2	NA	EBU	No k's match both T and composition
Wormeck and Pratt (1977)	WSR	n	2	NA	None	NO predictions poor
Peck and Samuelsen (1977)	Opposed jet reactor	2 + NO	0 or 2	NA	None	Predicted η_c too high, cold flow off
Wuerer and Samuelsen (1977)	Opposed jet reactor	NA	0 or 2	NA	NA	cold flow only
Schefer and Sawyer (1977)	Opposed jet reactor	2 + NO	0	NA	None	Predicted η_c and NO too high
Gibling et al (1975)	3D model combustor	1 + NO	0	n	None	very poor agreement for T and NO
Gibeling et al (1976)	3D model combustor	1 + NO	2	n	None	same as above
McDonald and Buggeln (1977)	Axisymmetric model Combustor	1 + NO	2	NA	None	very poor agreement for T
Altenkirch & Mellor (1975)	Quasi-axisymmetric burner	n	0	NA	None	Very poor agreement for NO and CO
Boyson and Swithenbank (1977)	Axisymmetric burner	NA	2	n	None	No comparison with experiment

* see Mellor (1979) for references

Table 2.3 Finite Difference Model comparisons in recirculating flow

A cursory glance of the comments offered by Mellor (1979) do highlight the gap between the prediction and the practical situation and hence, the formidability of the task. Observations, so far are made with no reference to the complications involving the computing technique used in these methods.

2.2.5 COMPUTATIONAL CODES

The essential difference between the various available computer codes include the following: the complexity of the

equations set for the simulation of the physical processes, the storage requirements, the location of variables in the grid space system, the method of deriving the finite-difference equations that are incorporated and the solution technique. Problems are classed according to the degree of realism and refinement, as represented by their dimensionality (the number of independent variables from three space dimensions and time) and type (parabolic and elliptic). The flow classification of parabolic (possessing one coordinate direction with first- but without second order derivatives-boundary layer type with prominent direction(s)) or elliptic (possessing second order derivatives in all coordinate directions- recirculating type with upstream influence) governs the type of boundary conditions required and the solution method. Marching methods are appropriate for the former, relaxation methods for the later.

Wide range of readily available large codes are:

- . Parabolic : GENMIX
- . Elliptic : CHAMPION, TEACH, PACE, SIMPLE, FLUENT, CONCERT, PHOENICS etc.

In recent times the finite difference approach has gained rapidly in popularity since it can resolve details of the flow and temperature fields which are important to the turbine designer. Nevertheless there are significant features of combustor operation, such as the prediction of the rich and weak combustion stability limits as a function of pressure, temperature and flow, which are both difficult and expensive to compute via the finite difference procedure. Fortunately, the reactor network approach is well suited to this latter task and the two approaches should be regarded as complementary rather than as competing alternatives (Evan et al. (1984)). The difficulty in using finite difference modelling procedures for calculating the stability limits arises partly from the form of the differential equations. These are stiff non-linear equations and their use in searching for the flame blow-off loop conditions not only involves long computation times but is also complicated by the need to distinguish against numerical instabilities when computing close to a real flame instability. The stirred reactor model is therefore potentially more suitable for the accurate prediction of chemical kinetic effects on combustion efficiency and pollution, maximum throughput and stability limits. However it requires additional measures to consider mixing effects.

The model described by Jones and Pridden (1979) provides a representative example in computing three-dimensional combustor flowfields. The governing equations for this model are written in Favre averaged form and a two-equation $k-\epsilon$

turbulence model is used. Fast chemical reaction is assumed so that the species concentrations can be determined from a single normalized concentration variable; a scalar probability density function model is used to take into account fluctuations in scalar properties. For the case of a liquid fueled combustor, dynamic equilibrium (for both mean and rms velocities) is assumed and the fuel temperature is assumed constant; a d^2 law is used for droplet evaporation and the droplet concentration field is described by a scalar probability density function for droplet size. The NO formation process is described by an overall irreversible rate expression, based on instantaneous concentrations and temperatures; the average production rate for NO is also obtained from the scalar probability density function

2.3 CHOICE OF MODEL

In deciding on and justifying the use of a particular procedure, one has some deliberation:

- 1) Does it predict with sufficient accuracy?
- 2) How much time is needed to obtain solution?
- 3) How easy is it to understand the result and its implications?
- 4) What is the cost?

Until a clear understanding of all the complex processes and their interaction are well understood, the gas turbine combustor field will continue to use correlations based on experimental results and cautiously utilize the results of modular and finite difference approaches to supplement the wealth of experience.

Spalding once stressed the importance of a balance of complexity in mathematical models, pointing out the absurdity of a highly sophisticated reaction scheme in a primitive flow model. There is no point in including a factor that will have a tenth order of magnitude influence on the result when all factors responsible for fourth to ninth order of magnitude effects, in that particular context, have been omitted (and a factor important in one combustor configuration may be totally irrelevant in another). The answer does not therefore (necessarily) lie in construction of a "kitchen sink" theory in which all conceivable and many inconceivable factors have been included. The answer can lie in selection of parameters such that all are in balance in complexity, and the "accuracy" of the answer does not grossly exceed the accuracy of experimental determination and test.

One example of need of different degrees of complexity are the grid size for flow calculations, radiation calculations and the emission calculations.

2.4 SCOPE

Keeping in mind the adequacy of prediction technique depends largely on the detail required, it is decided to take the following steps:

- 1) Major emphasis should be on a comprehensive design procedure.
- 2) One dimensional parabolic flow analysis with a constant property assumption radially, for flow evaluation.
- 3) Simple kinetic model based on a single step global reaction to evaluate temperatures. Soot is neglected.
- 4) Heat transfer analysis such that metal temperature and related heat transfer data can be obtained. Also a design procedure to estimate the cooling configuration for a given maximum metal temperature.
- 4) Modular approach with stirred reactor concept, to estimate NO_x, based on Zeldovich reaction mechanism as a post flame phenomenon.

The expected advantages are :

- 1) Savings on computing time and storage
- 2) An effective design tool at a preliminary stage to compare the various design options qualitatively and quantitatively on relative basis

The demand for better efficiency and the potential co-generation and combined cycles, are sufficiently tempting to attract Gas Turbine technology towards reheat combustor. Though conceptually not a new topic, practical usage would be novel. Possibility of exploring the concepts and design approach for a double combustor using the developed programme, will also be considered.

Though the initial aim was to evolve a programme, as described above, in order to improve the utility of the programme, it was subsequently decided to enter into stability and efficiency estimation. This attempt will be described in the subsequent chapters.

CHAPTER 3

PROGRAMME PHILOSOPHY

3.1 FOREWORD

Combustion technology, being much experimented, but less documented, will be approached with less certainty from the software point of view. However, computers enhance the utility of the existing information if suitably structured in an algorithm. Design oriented software for combustors, apart from satisfying the norms of software engineering interms of highest reliability, least number of bugs, would be more beneficial if it is interactive or user friendly. Its utility will invariably rest both on

- 1) Design or Evaluation Approach
- 2) Computing Technique

3.2 STRUCTURED PROGRAMMING

The computing technique will decide the time and storage requirement. Both obviously, have to be minimized. Any development work should be structured in such a way that evolution or continuation in future is an easy process. Modular approach is the best technique considering the interactive complex individual phenomena in a combustor. Thus partitioning the system as per process and defining the problem in a modular fashion should enhance the modifiability of the software.

3.2.1 LANGUAGE

It is decided to write the programme in Fortran-77, a widely accepted engineering language using the available VAX computers.

3.2.2 GRAPHICS

The available GINO libraries lend themselves to be easily programmable with Fortran-77 language. Though systems like UNIRAS or GKS (Graphical Kernel System) could have been a better choice if future standards and portability between systems are considered. However, considering the short time span available, and also the need for the programme to be used as a study tool in the School, it is decided to adhere to the available GINO libraries.

NOTE : The inevitable did happen much sooner than expected. Just before this thesis went for a print, it was announced that existing GINO libraries will be phased out by Sep 88.

UNIRAS would be the next choice. Change over should not be a problem as the output is already stored in a convenient tabular form.

3.2.3 INTERACTIVE

Maximum benefit can be accrued from any design programme, which is intended to be a study aid too, when the programme is interactive or so called 'user-friendly'. Any combustor design process involves a variety of design decisions which largely depend on past experience or design environment (in short there is no one single standard design code). Hence providing a choice with all the options offers an opportunity for a user to investigate the implication of any option on the overall design.

Interactive exercise can be enhanced by a variety of ways. Facilities like Forms Management, Screen Management or Screen Graphics provide the desired effect of windowing the screen and displaying maximum information on the same screen at different locations. The only disadvantage is that they are highly system oriented. Portability between systems is impossible. However a version with the available Forms Management System on the VAX will be produced.

3.2.4 INPUT/ OUTPUT

The input information, the user is required to provide should be made as simple as possible. File and/or interactive input will be made possible. Interactive input will be assisted with the possible range of each variable, so that the input process will be reduced to a matter of judgment in majority of the cases. Graphical output is more effective as opposed to a tabular output. Considering the nature of variation of variables such as temperature, pressure etc., interactive graphics enhance the utility of the package. However, for the present study, both the graphical and the tabular output will be provided with an option to choose a range of variables for plotting. If any session is discontinued, for any reason, programme should be able to store all the intermediate values, so that continuation is an easy process.

3.3 AXIOMS FOR ALGORITHM

3.3.1 MAJOR ASSUMPTIONS

- 1) One dimensional analysis
- 2) Primary aim is to be an effective design tool and a study aid.

- 3) All the steps would be based on available correlations and experimental results
- 4) It should cover all the essential features of design and performance in terms of fluid dynamics, metal temperatures, efficiency, stability and emissions.
- 5) It should be interactive.

3.3.2 GRIDDING

By and large conventional combustors are axisymmetric or approximated to axisymmetric shapes. Though cylindrical polar coordinates easily represent the system, cartesian coordinates are preferred as they lend themselves for easy understanding. However, for multi-dimensional systems, the above representation is not preferable due to nonconformity to a complicated geometry with a coarse grid or long computational times with a fine grid. In such cases, 3D body fitted coordinates should be a preferred system. Kenworthy et. al. (1984) have demonstrated the disadvantages of a stairstep coordinate system as compared to a body fitted coordinate system. For analyzing combustors with contoured walls, 3D body fitted coordinate system would be an automatic choice for the future finite difference codes. For the present work, stairstep system, is a natural choice. The X-direction spacing would decide how closely the boundary conforms to the contour of the combustor.

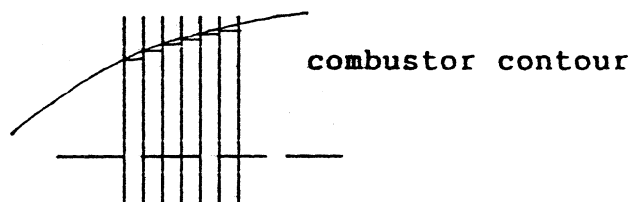


Fig 3.1 Stairstep Coordinate System

3.3.3 PROGRAMME HIERARCHY

True to the title 'DEPTH', programme is intended to be able to probe sufficiently deep into both the aspects of design as well as evaluation. Accordingly it is divided into two parts as represented below.

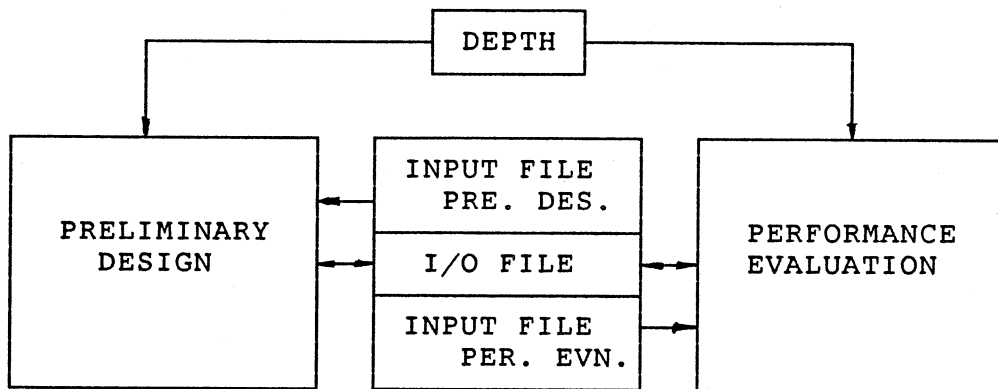


Fig 3.2 Programme Hierarchy

'DEPTH' consists of two primary blocks, one Preliminary Design and the other Performance Evaluation. The Evaluation phase further comprises of

- . Flow Evaluation
- . Heat Transfer Calculations
- . Efficiency and Stability Evaluations
- . Emission Estimation

User will have an option to enter any block giving the necessary input.

CHAPTER 4

PRELIMINARY DESIGN

4.1 INTRODUCTION

"Combustion Chamber design is an art not a science". The reminder to this statement, however, is not to take cover under the magnitude of the problem, but to highlight the inadequacy of a start-to-finish design procedure. As design is a process with a lot of feedbacks, it would be difficult to draw out a simple order of events. Also design is always a logical extension to the past experience. Combustor technology has always been following this consistently over the past few decades. Many types of combustors, differing widely in size, concept and method of fuel injection have been designed. However close inspection reveals that many aerodynamic features are common to all systems.

4.2 BASIC DESIGN FEATURE

In order to define the essential components needed to carry out the primary functions of a combustion chamber, the process needs to be defined briefly.

Figure 4.1(a) shows the simplest possible form of combustion chamber- a straight-walled duct connecting the compressor to the turbine. Unfortunately, this simple arrangement is impractical because the pressure loss incurred would be excessive. The fundamental pressure loss due to combustion is proportional to the square of the air velocity, and for compressor outlet velocities of the order of 150 m/s this loss could amount to about a quarter of the pressure rise achieved in the compressor. To reduce this pressure loss to an acceptable level, a diffuser is used to lower the air velocity by a factor of usually about 5, as shown in fig 4.1(b).

However, even with a diffuser, a flow reversal must be created to provide a low-velocity region in which the flame can be sheltered and sustained. Fig 4.1(c) shows how this may be accomplished with a plain baffle. The only remaining defect in this arrangement is that, to produce the desired temperature rise, the overall chamber air/fuel ratio must normally be around 50, which is well outside the limits of flammability for air-hydrocarbon mixtures. Ideally, the equivalence ratio in the primary combustion zone should be around 0.8, although lower values (around 0.6) are sometimes preferred if low emission of nitric oxides is a prime consideration. To solve this problem the simple baffle is replaced with a perforated liner, as illustrated in

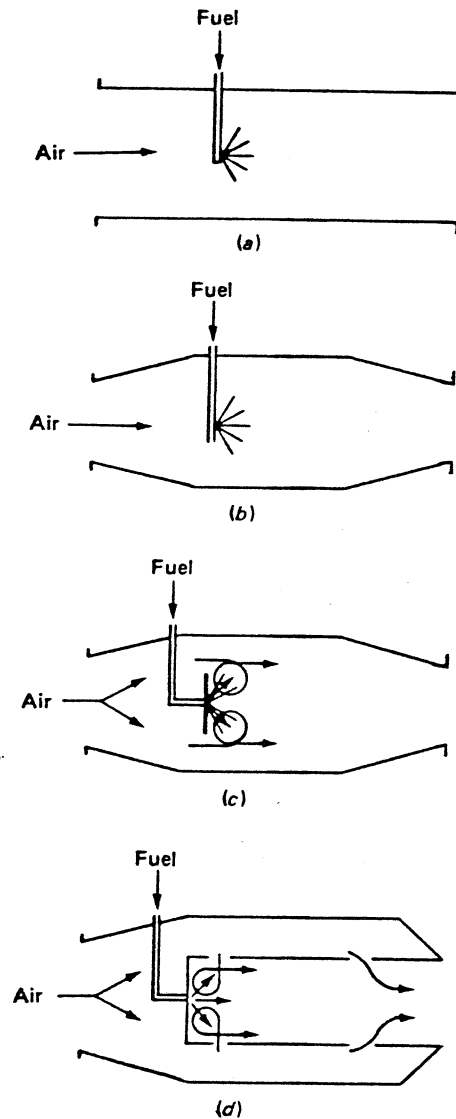


Fig 4.1 Stages in evolution of a conventional Gas Turbine Combustor (Lefebvre (1983))

fig 4.1(d). The function of the liner is to provide a region of low velocity in which combustion is sustained by a recirculatory flow of burned products that provide a continuous source of ignition for the incoming fuel-air mixture. The air not required for combustion is admitted downstream of the combustion zone to mix with the hot burned products and thereby reduce their temperature to a value that is acceptable to the turbine. In Practice it is customary to insert, between the primary and dilution zones, a so-called "intermediate" zone whose purpose is to recover losses due to chemical dissociation of the primary combustion products. This is done via the addition of small discrete amounts of air.

Fig 4.1 thus illustrates the logical development of the conventional gas turbine combustion chamber in its most widely used form. As would be expected there are many variations on the basic pattern shown in Fig 4.1 (d) but, in general, all chambers incorporate, as key components, an air casing, diffuser, liner and fuel injector- as shown below:

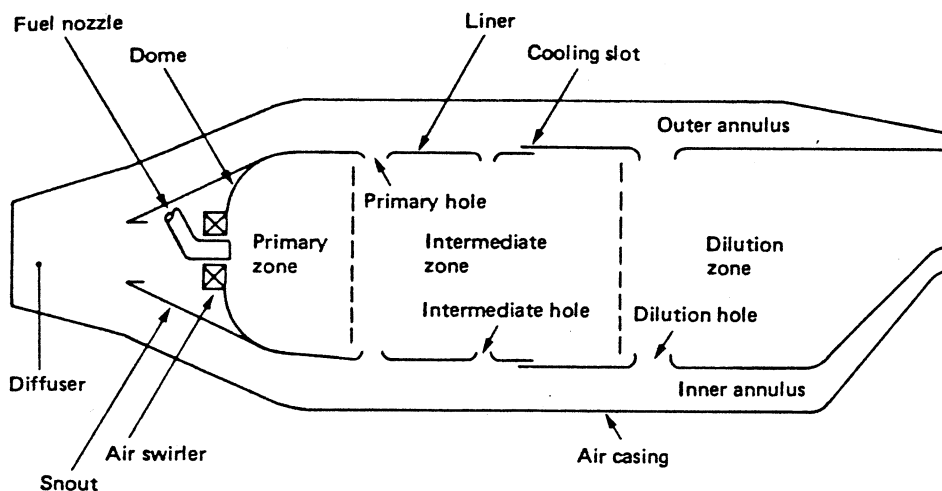


Fig 4.2 Main Components of a Gas Turbine Combustor

The choice of a particular type and layout of combustion chamber is determined largely by engine specifications but is also strongly influenced by the desirability of using the available space as effectively as possible.

4.3 COMBUSTOR REQUIREMENTS

A gas turbine must satisfy a wide range of requirements whose relative importance varies among engine types. However, the basic requirements of all combustors may be listed as follows:

- 1) High combustion efficiency (i.e., the fuel should be completely burned so that all its chemical energy is liberated as heat)
- 2) Reliable and smooth ignition, both on the ground (especially at very low ambient temperatures) and, in the case of aircraft engines, after a flameout at high altitude
- 3) Wide stability limits (i.e., the flame should stay alight over wide ranges of pressure, velocity, and air/fuel ratio)

- 4) Freedom from pressure pulsations and other manifestations of combustion-induced instability
- 5) Low pressure loss
- 6) An outlet temperature distribution (pattern factor) that is tailored to maximize the life of the turbine blades and nozzle guide vanes
- 7) Low emissions of smoke, unburnt fuel, and gaseous pollutant species
- 8) Design for minimum cost and ease of maintenance
- 9) Size and shape compatible with engine envelope
- 10) Durability
- 11) Multifuel capability

4.4 COMBUSTOR TYPES

A broad classification of the many different kinds of combustion chamber is given as Table 4.1.

TYPE	SIZE	GEOMETRY	FUEL SYSTEM
Air borne high altitude low altitude	Large	Straight flow	Premix
Ground Industrial Marine Road transport	Small	Annular Tubular Tuboannular	Partial Mix air blast atomiser airassist atomiser
		Reverse flow	Liquid droplets simplex, duplex
			Vaporiser

Table 4.1 An Overview of Gas Turbine Combustors

As straight flow combustors are only considered, no information regarding reverse flow would appear henceforth. A schematic description of the different combustors are given as Fig 4.3.

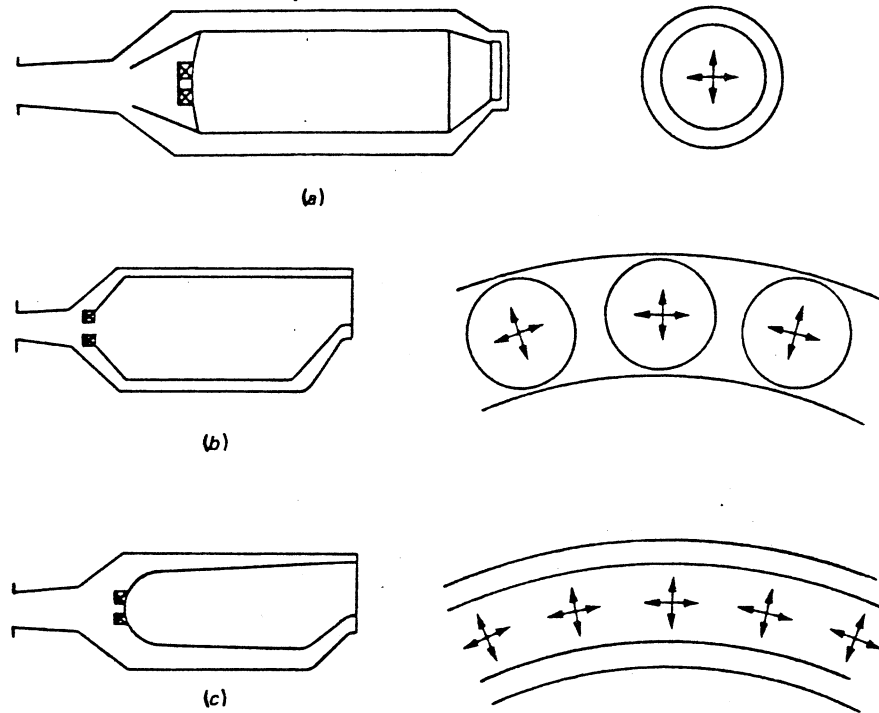


Fig 4.3 Various Types Straight-flow Combustors
 (a) Tubular (b) Tuboannular (c) Annular.

4.5 SELECTION

This must be one of the prime tasks to conclude at the beginning of any project. However, treating the combustor as a black box between compressor and turbine, the initial norms are set aside by the overall system requirements. Overall cycle considerations decide the inlet massflow, temperature and pressures and the required exit combustor conditions interms of temperature rise, accepted pressure loss for the given operating environment and requirement. This would have considered the ambient conditions, type of fuel etc. The overall dimensions for this black box to fit within, would be the next major input. All these factors, as they have external dependency, are grouped and would required to be opted for before the design phase begins.

The type of fuel and oxidant medium would have known at this stage. Oxidant medium is mentioned as opposed to air for the simple reason for reheat combustors the medium would be burned products and even for conventional combustors if water/steam could be added for emission control. Stoichiometric air fuel ratio is calculated using oxidation potential, the procedure outlined in Appendix A. AFRS is useful parameter to judge the amount of medium required as well as the maximum temperature that can be obtained which

is the adiabatic equilibrium value.

Though the selection as to the type of combustor largely may depend on past experience and the environment of the engine. However for completeness, the relative advantages and disadvantages are listed below as Table 4.2.

Chamber type	Advantages	Disadvantages
Tubular	<ol style="list-style-type: none"> 1. Mechanically robust 2. Fuel-flow and airflow patterns are easily matched 3. Rig testing necessitates only small fraction of total engine air mass flow 	<ol style="list-style-type: none"> 1. Bulky and heavy 2. High pressure loss 3. Requires interconnectors 4. Incurs problem of light-round
Annular	<ol style="list-style-type: none"> 1. Minimum length and weight 2. Minimum engine frontal area 3. Minimum pressure loss 4. Easy light-round 	<ol style="list-style-type: none"> 1. Serious buckling problem on outer liner 2. Rig testing necessitates full engine air mass flow 3. Difficult to match fuel-flow and airflow patterns 4. Difficult to maintain stable outlet temperature traverse
Tuboannular	<ol style="list-style-type: none"> 1. Mechanically robust 2. Fuel-flow and airflow patterns are easily matched 3. Rig testing necessitates only small fraction of total engine air mass flow 4. Low pressure loss 5. Shorter and lighter than tubular chambers 	<ol style="list-style-type: none"> 1. Less compact than annular 2. Requires connectors 3. Incurs problem of light-round

TABLE 4.2 Relative Merits of Various Chamber Types (Lefebvre (1983))

4.6 REFERENCE CONDITIONS

Knowing the inlet conditions, the combustor requires to be sized. The parameters which facilitate this would be the reference velocity U_{ref} , which is the mean velocity across the maximum cross sectional area of the casing in the absence of a liner i.e.

$$U_{ref} = \frac{\dot{m}_2}{\rho_2 A_{ref}} \quad \dots(4.1)$$

In order to quantify A_{ref} at this stage, two approaches are possible.

4.6.1 THETA PARAMETER APPROACH

Knowing the variation of the Θ parameter (which will be described in chapter 7), A_{ref} can be estimated as per the

required efficiency level. Lefebvre (1966) indicates the variation of θ parameter for the various types of combustors, given as Fig 4.4. As performance in terms of efficiency is linked with the geometry and operating conditions

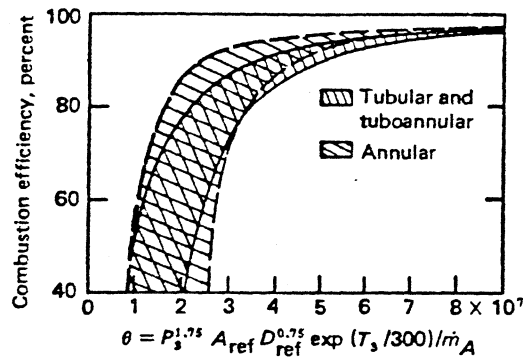


Fig 4.4 Design Curves for Conventional Combustors (Lefebvre (1966))

this empirical relation is an useful design tool. However, prior knowledge of Theta parameter variation is essential for this approach. The proprietary nature of information makes it difficult to obtain the exact relation, but in the absence of better information Fig 4.4 may be used. This, evaluation option is incorporated in the programme. In the case of combustor for airborne applications, altitude relighting is a major criterion for the sizing. If the operating conditions for the relight can be quantified, Theta parameter provides what should be the minimum size to achieve the expected efficiency level.

The general procedure involves, in specifying the efficiency level acceptable in the operating envelope, which in turn decides the level of Theta parameter. Knowing the operating conditions, A_{ref} can be evaluated

4.6.2 PRESSURE LOSS APPROACH

An alternative solution is to resort to two dimensionless pressure loss parameters

OPL (Overall Pressure Loss) $(P_2 - P_4)/P_2$: often quoted as a percentage ranging from 4 to 10 %. Smaller the value more is the energy to the turbine and lower is the specific fuel consumption.

PLF (Pressure Loss Factor) $(P_2 - P_4)/q_{ref}$: It is a measure of flow resistance introduced into the airstream between compressor outlet and turbine inlet. Unlike the OPL, which

depends on operating condition, the pressure loss factor is a fixed property of the combustion chamber. It represents the sum of two separate sources of pressure losses.

$$\frac{P_2 - P_4}{q_{ref}} = \frac{\Delta P_{diff}}{q_{ref}} + \frac{\Delta PL}{q_{ref}} \quad \dots(4.2)$$

The ΔP_{diff} should be kept as minimum as possible as this does not contribute in anyway to combustion. It is equally important to minimize the later part, although higher it is, better is combustion and dilution process due to high level of turbulence better penetration which promote good mixing and can result in shorter liner. Hence optimization is required. The values range from 17 to 50, for annular to tubular types.

The two parameters are related by the equation (the derivation is given as Appendix B)

$$A_{ref} = \left[\frac{R_a}{2} \left[\frac{m_2^2 T_2}{P_2^2 A_{ref}^2} \right] \left[1 + \frac{\gamma - 1}{2} Mn_2^2 \right]^{1/(\gamma-1)} \right]^{1/2} \quad \dots(4.3)$$

Similar expression (Lefebvre (1983)) does not contain the mach number term, probably for ease of calculation. In order to use this approach, judgment is still required in guessing the value for PLF.

The combustor reference size is taken as the larger value from the above two approaches.

4.7 DIFFUSER

The exit area of the compressor is required to be joined to the above reference area by means of a diffuser. The result would be to reduce the air velocity at the exit of compressor to a level where combustion is possible, which is decided by the reference velocity. An ideal diffuser is one that achieves the required velocity reduction in the shortest possible length, with minimum loss in total pressure and with uniform and stable flow conditions at its outlet. The various types are as shown as Fig 4.5.

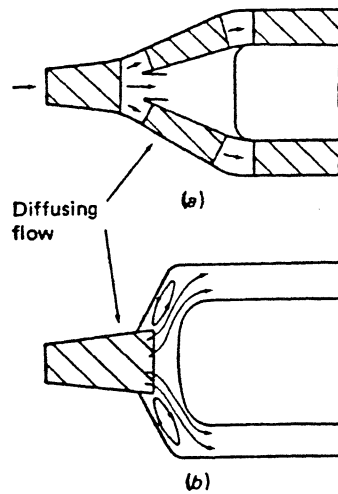


Fig 4.5 Types of Diffusers (a) Aerodynamic (b) Dump

No real design procedure is offered except following the principles of geometry and the basic fluid dynamics. The latter indicates the typical dependence of losses in the diffuser on the included angle (Fig 4.6). They are optimized around

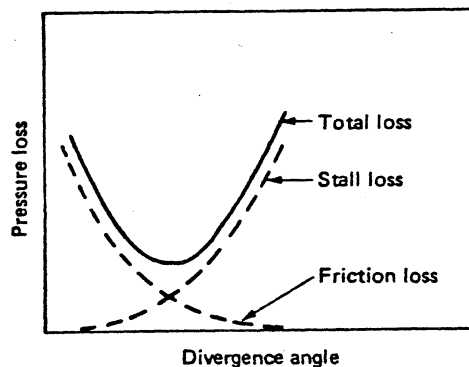


Fig 4.6 Influence of diffuser angle on Pressure Loss

11 degrees, to the left more friction losses due to very long diffuser and to the right separation losses due to very steep expansion. However, in annular diffusers the included angle can go up to 20-22 degrees.

The relative merits of different diffusers are given as a reminder. As the design procedure is not fully established for the later two types of diffusers, they are not considered for the present study.

If the diffuser included angle is specified, using inlet geometry and area ratio, diffuser length can be calculated

from simple geometrical relations.

Diffuser type	Merits	Drawbacks
Aerodynamic or faired	1. Low pressure loss	1. Relatively long 2. Performance susceptible to thermal distortion and manufacturing tolerances 3. Performance and stability sensitive to variations in inlet velocity profile
Dump	1. Relatively short 2. Insensitive to variations in inlet flow conditions	1. Pressure loss about 50% higher than for faired type
Vortex-controlled	1. High performance 2. Short length 3. Low pressure loss	1. Requires minimum of 4% air bleed 2. Design procedures not fully established
Hybrid	1. High performance 2. Short length 3. Low pressure loss	1. Design procedures not fully established

Table 4.3 Relative Merits of various Diffuser Types (Lefebvre (1983))

Dump Diffuser : Following Fishenden et al. (1977), the optimum area ratio for the conventional part of the diffuser is assumed to be 1.8 and the rest is dumped. It is joined at 90 degrees to the reference area.

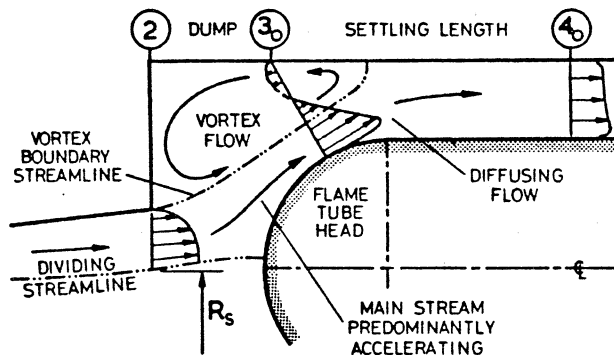


Fig 4.7 Flow pattern down stream of prediffuser

They have summarized that the principal factors determining the losses in dump and settling length regions are 1) the amount of diffusion being attempted and 2) the radius of curvature of the flow which determined by the size and shape of the flame tube head and the dump gap. As generalization is difficult, a good design practice appears to be when the diffuser to dome length is chosen such that:

$$\frac{DDL}{HT3} \geq 1.2 \quad \dots(4.4)$$

where HT3 is the prediffuser exit height

Adkins (1983) suggested a diffuser design based on G parameter. This technique is presented for designing annular diffusers which give the optimum configuration for producing maximum pressure recovery with a stipulated length (ie. Cp* diffusers). An empirical relationship has been used for the parameter :

$$G^* = \left[0.915 (AR)^{1.424} - 1 \right]^{-0.5} \quad \dots(4.5)$$

The G* parameter, if held constant along the diffuser, should yield the maximum Cp for a given length. Thus knowing the profile of one diffuser wall and the overall area ratio, the shape of the other wall can be optimized.

This method was experimented. However, considering the level of sophistication of the overall program, this method was considered superfluous and hence discontinued.

4.8 SIZING

4.8.1 LINER CROSS SECTIONAL AREA

For any given casing area higher liner area results in lower velocities and higher residence times which are good for ignition, stability and combustion efficiency. At the same time, this results in a smaller annulus which raises annulus velocity and hence lowers its static pressure causing inadequate penetration and mixing. Hence an optimum value is required. Lefebvre and Norster (1969) have derived, considering the primary zone considerations, relations for optimum value for area ratio between liner and casing.

$$\left[\frac{A_L}{A_{ref}} \right]_{opt} = 1 - \left[\frac{(1 - m_{sn})^2 - \lambda}{\Delta P_{2-4}/q_{ref} - \lambda (A_{ref}/A_2)^2} \right]^{1/3} \quad \dots(4.6)$$

where

msn = frontend massflow as a fraction of total mass flow

λ = diffuser pressure loss coefficient

However, for PLF between 25 to 50, the optimum value is fairly constant. Hence it is decided to leave the option to the user, to choose the ratio of liner width to casing width, the range being 0.65 to 0.85.

4.8.2 LINER LENGTH

From analytical view point, it is convenient to consider the liner as comprising two main zones, Burning and Mixing zone.

Burning Zone : Primary requirement is to achieve the maximum combustion efficiency. It is further divided into two parts namely Primary and Secondary (also known as intermediary). THE majority of the combustion should take place in the primary. In the secondary, a small amount of air is injected into the hot gases emanating from the primary zone to lower the temperature and thereby encourage the completion of the combustion process. However certain conditions like altitude or very rich primary zone combustion could carry on into secondary due to slow reaction kinetics or insufficient time in the primary zone. A secondary zone may not exist for engines like lift engines where weight is the main criteria.

Mixing Zone : Here the balance of air is added to dilute or reduce the exit temperature to the level of turbine. This zone may further be divided as dilution and nozzle. Dilution is where bulk of the mixing takes place. Nozzle is the transition piece between combustor to the turbine inlet guide vanes. Thus the final form of modular liner, is as shown in Fig 4.8

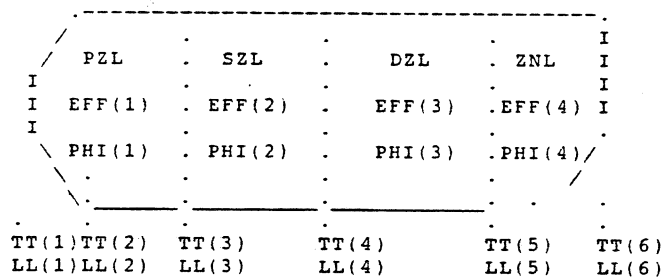


Fig 4.8 Liner in its modular form

The individual zonal lengths are signified by PZL to ZNL and the cumulative by LL(1) to LL(6). The efficiency and the equivalence ratios are represented by EFF() and PHI() respectively. TT(1) to TT(6) stand for the total temperature at that location.

NOTE: It is worth highlighting a point of deviation from standard zonal division and the present model. In majority of the works the primary zone is the area between dome head

to the plane passing through the centerline of primary/secondary holes and similarly secondary zone is the area between former plane and the plane passing through the dilution hole centerline. It is found that when preliminary design and evaluation are interlinked, exact size of the holes are not determined till the evaluation reaches the location of the hole. Zonal end values are used as reference values for evaluation as well as geometry calculations. Also evaluation requires the beginning of the hole location. Hence it is decided to choose the zonal end planes as those at the beginning of primary/secondary or dilution holes. Similar strategy is applied to any mixing hole that its specification with respect to the dome head is given upto the beginning of the hole and not the centerline distance.

The relative lengths and amount of airflow split will be based on the relative importance of combustion efficiency, emissions, turbine inlet temperature pattern and stability.

Based on experience L/D ratio of each zone can be guessed depending on the engine role airborne, industrial etc. and operating conditions like altitude, range etc. Typical values being 0.5 to 1.0 for the primary zone, 0 to 1.5 for secondary, 1.0 to 1.5 for the dilution and 0.4 to 0.6 for the nozzle zones. The following are the default values incorporated in the programme.

	P	S	D	N
Ground	0.8	0.4	1.4	0.6
Airborne > 10 km	0.5	1.0	0.7	0.6
Airborne ≤ 10 km	0.55	0.85	0.9	0.4

Table 4.4 Relative Zonal Lengths

The guesses are generally proven to be as good as any possible generalized analytical reasoning. However, for the burning zone stirred reactor concept is used to ensure that adequate burning volume is available to arrive at a desired level of efficiency.

Herbert's (1962) combustor loading parameter is used to deduce the relation for the minimum combustion volume:

for $\phi \leq 1.0$

$$V_{\min} = 6.403E-5 \frac{m_{pz} T_{pz} e^{1.5 (21200/T_{pz})} \eta (1+\phi\eta/AFRS)^2}{P_2^2 (1-\eta)(1-\phi\eta)} \quad \dots(4.7)$$

for $\phi > 1.0$

$$V_{\min} = 6.403E-5 \frac{m_{pz} T_{pz} e^{1.5 (21200/T_{pz})} \eta (1+\phi/AFRS)^2}{P_2^2 (1-\eta)(\phi-\eta)} \quad \dots(4.8)$$

4.8.3 EQUIVALENCE RATIO

Apart from the manner in which air is distributed throughout the primary zone, another major design variable is the actual quantity supplied. As the fuel flow rate is determined by the overall combustors fuel/air ratio, the only independent control that can be exercised over the primary zone fuel/air ratio is via the amount of air employed in primary combustion. It is the primary zone fuel/air ratio that, more than any other single factor, governs the nature of the combustion process and overall chamber characterization. Considering the importance, the relative merits of stoichiometric, fuel-rich and weak primary zones are listed as Table 4.5, which forms the basis for selection. The future designs, considering the stringent

Primary-zone mixture strength	Advantages	Disadvantages
Stoichiometric	<ol style="list-style-type: none"> 1. Maximum heat-release rate 2. Low-luminosity flame 3. Little exhaust smoke 4. No carbon deposits 	<ol style="list-style-type: none"> 1. High rate of heat transfer to liner walls 2. Requires intermediate zone 3. High nitric oxide emissions
Fuel-rich	<ol style="list-style-type: none"> 1. Low recirculation velocity gives good "weak-extinction" point and easy ignition 2. High combustion efficiency at low power conditions 	<ol style="list-style-type: none"> 1. Low volumetric heat-release rate 2. High-luminosity flame 3. Copious exhaust smoke 4. Coke deposition on walls 5. Liner wall temperature varies with fuel type 6. Requires long intermediate zone
Fuel-weak	<ol style="list-style-type: none"> 1. Clean, blue flame 2. No exhaust smoke 3. No carbon deposits 4. Cool liner walls 5. Requires no intermediate zone 6. Good exit temperature distribution 	<ol style="list-style-type: none"> 1. High recirculation velocity adversely affects stability and ignition performance

Table 4.5 Influence of Various Primary-Zone Mixture Strengths (Lefebvre (1983))

emission regulations would be designing well below the stoichiometric value. Suitable values are guessed accordingly for the equivalence ratios for each zone. However, for a preliminary design, some basic guidelines observed are:

- 1) The lower limit for fuel weak mixture is considered as 0.6 and upper limit for fuel rich as 1.2. The reasons are as indicated in Table 4.5.
- 2) If atomizer is used, the atomization quality drops when air/liquid mass ratio falls below 4, based on the experimental investigation by El-Sshanawany et al (1980).

4.8.4 FLAME TEMPERATURE

Evaluation of flame temperature is an involving and complex process that itself can form a major research topic. As the processes involved are chemical kinetics in multiphase with heat losses through radiation and convection, superimposed with the problems of evaporation, mixing and recirculation, the system renders itself a formidable task to programme within the available resources. However, flame temperature and its distribution temporal and spatial is essential for flow as well as metal temperature calculations. The basic one dimensional approach of DEPTH simplifies the problems associated with spatial distribution. But the basic problem remains as to the evaluation of flame temperature at each axial location of combustor.

Time dependent kinetic reactions, one step or multi step accounting for the heat loss and coupled with the flow calculations is what is desired in any combustor analysis. However, simple analysis usually relies on isobaric, adiabatic equilibrium temperatures corrected by an extent of reaction at that instant which could be based on experience or empiricism. These values are reasonably accurate for any initial design step. Heat losses are usually neglected as they constitute only to a maximum of 3%, with standard current fuels and established injection techniques.

Equilibrium calculations by programs such as Gordon and McBride (1969) is widely accepted and used as a reference in many design and development works. A quicker way to achieve the results is to use charts which are prepared for standard fuels such as kerosene or diesel giving combustion temperature rise versus fuel air ratio for given inlet temperature. Even simpler methods are available in equation form which grossly represent these charts with fair accuracy which make them obvious choices for any computer algorithms. Some such examples are

Harman's (1981) correlations for fuels which are very close to kerosene

$$\text{AFR} = \frac{\text{FLCV } \eta}{1.1 (1 + T_2/3250) (\Delta T - 50)} \quad 400 \leq \Delta T \leq 900 \quad \dots(4.9)$$

$$\text{AFR} = \frac{\text{FLCV } \eta}{0.99 (1 + T_2/3250) (\Delta T - 10)} \quad 200 \leq \Delta T < 400 \quad \dots(4.10)$$

Another useful correlation presented in the work by Candelier et al.(1987):

$$\text{AFR} = \frac{(15580+T_2) (3923-T_2)}{1632.5 \Delta T - 102212 - 14.5T_2 - 0.067 T_2^2} \quad \dots(4.11)$$

These again fall short of the needs if the fuels are changed or inlet oxidant medium changed, say by water injection or by precombustion. However these can be easily accommodated in programs such as Gordon and Mcbride (1969).

Flame temperature estimation of conventional and future jet fuels by Gulder (1986) is good correlation for adiabatic flame temperature accounting for pressure, temperature, equivalence ratio, and carbon to hydrogen ratio and yielding the result within a maximum error of 0.8%. Initial development of the program did make use of these expressions, however, the need for individual species concentrations for the purpose of transport and thermodynamic property evaluations, has rendered this approach inadequate.

Next comes the issue of converting this adiabatic equilibrium temperature to actual, as the reaction will rarely be 100% complete, heat is lost due to radiation and convection, the diffusion due to temperature and concentration gradients and the effects of turbulence.

Combustion Efficiency:

The extent of reaction is usually accounted for by way of efficiency of combustion.

$$\text{based on temperature } \eta = \frac{\text{actual } \Delta T}{\text{theoretical } \Delta T}$$

$$\text{based on fuel air ratio } \eta = \frac{\text{theoretical FAR for given } \Delta T}{\text{actual FAR for given } \Delta T}$$

However, neither definitions are quite the same as the

fundamental definition based on the ratio of actual energy released to the theoretical quantity obtainable. The difference between all the definitions is negligible when η is very high. However, efficiency is an important factor, but uncertain to quantify analytically. Past experience had been the major input. Considering the experimental nature of the information, assuming the efficiency variation across the combustor is as good a guess as to predict using any equation at a preliminary stage. Stirred reactor concepts indicate that the efficiency at the end of primary zone is rarely over 90% and should reach the maximum at the end of burning zone. Hence these values are assumed at the end of each zone.

Heat Loss:

Heat lost due to radiation is around 3% maximum, hence not specifically accounted for in simple analyses. However, if analysis do require the effect of future fuels or injection techniques, it may be worth including the heat losses into the coding, however, empirical it may sound. This loss, in practice, will effect the primary zone temperature, but this is not lost from the system as this is carried away by the annulus air which reenters the liner. The actual heat loss from the casing to surroundings, in reality is quite insignificant.

Diffusion Process :

The temperature and concentration gradients are ignored due to constant property assumption. Turbulence effects reduce the mean value, however, neglected for coding simplicity. This would possibly mean, the temperature could at least be 50 K higher near stoichiometric region, giving corresponding errors in the evaluation of metal temperatures and NOx estimation. However, preliminary designs should tolerate this crude approach.

Based on the η and equivalence ratio, flame temperature should be able to be evaluated. Empirical equations with an accuracy quoted at ± 100 K are forwarded by Odgers (1980). They appear in the following form

Primary Zone

$$\begin{aligned}
 T_r &= T_a + \eta_r \Delta T_{\phi=1} \\
 \eta_r &= 0.56 + 0.44 \tanh [1.5475 \times 10^{-3} (T_a + 108 \ln P_a - 1863)] \\
 T_{pz} &= T_a + 0.5 \eta_{pz} (\Delta T_{\phi=1} + \Delta T_{pz}) \\
 \eta_{pz} &= 0.72 + 0.29 \tanh [1.5475 \times 10^{-3} (T_a + 108 \ln P_a - 1863)] \\
 T_{out\ pz} &= T_a + \eta_{pz} \Delta T_{pz} \quad \dots(4.12)
 \end{aligned}$$

Secondary Zone

$$\begin{aligned}
T_{in_{sz}} &= T_{out_{pz}} \\
T_{out_{sz}} &= T_2 + \eta_{sz} \Delta T_{\phi=pz} \\
T_{mean_{sz}} &= 0.5(T_{in} + T_{out}) \quad \dots(4.13)
\end{aligned}$$

Dilution Zone

$$\begin{aligned}
T_{in_{dz}} &= T_{out_{sz}} \\
T_{out_{dz}} &= T_2 + \eta_{dz} \Delta T_{\phi=pz} \\
T_{mean_{dz}} &= 0.5(T_{in} + T_{out}) \quad \dots(4.14)
\end{aligned}$$

Disregarding the uncertainty over the evaluation of the efficiency, the approach is based on simple assumptions. However, the evaluation of temperature rise again requires a temperature, curve/chart or some other computer programme, the problem as discussed before.

In view of the above it is decided to adopt a strategy such that the analysis

- 1) is a simple method interms of coding complexity and computing time, at the same time within reasonable accuracy.
- 2) is fairly general that it accounts for any inlet conditions interms of medium (oxidant or fuel), or conditions such as temperature or pressure.
- 3) accounts for completeness of reaction and heat loss.
- 4) is able to provide flame temperature along with the concentrations of combustion products.

The procedure is developed and described in Appendix C. Comparison shows that the results are within the accuracy level in commensurate with the present work's sophistication.

4.8.5 EXIT TEMPERATURE PROFILE

Radial and circumferential distribution of exit temperature largely decides the life and durability of hot end components namely, nozzle guide vanes and turbine blades. The most important parameters to represent the temperature traverse quality are

$$\text{Pattern Factor} = \frac{T_{\max} - T_4}{T_4 - T_2}$$

where T_{\max} = maximum recorded temperature at the exit plane

T_2 = mean inlet temperature

T_4 = Mean exit temperature

These values should ideally be less than 30 %. The desired average radial distribution at combustor exit is usually has a profile that peaks above mid-height of blade. Ideally design should aim to achieve this. One dimensional uniform property assumption in the present programme does not permit no real design or evaluation based on traverse analysis. However, existing correlations are used to ensure this. The relation that is incorporated in the programme is by Lefebvre (1983), who correlated the existing combustor data to

$$\frac{T_{\max} - T_4}{T_4 - T_2} = 1 - \exp \left[-C_1 \frac{L_1}{D_1} \frac{\Delta P_1}{q_{\text{ref}}} \right]^{-1} \quad \dots(4.15)$$

where $C_1 = 0.07$ for tubular and tuboannular
 0.05 for annular

L_1 = combustor length

D_1 = liner height or dia

4.8.6 FLAME STABILIZATION

The primary zone airflow pattern is of prime importance to flame stability. Many different types of airflow patterns are employed (Fig 4.9), but one feature common to all is the creation of toroidal flow reversal that entrains and recirculates a portion of the hot combustion products to mix with incoming air and fuel. These vortices are continually refreshed by air admitted through primary/secondary holes supplemented in most cases by air flowing through swirlers and flare cooling slots and sometimes by air supply through atomization. Hence at this stage there is a need to decide whether atomizer, swirler, domeholes all/or some are employed or not. Here once again the choice is a matter of experience. At the present time, accurate information is lacking on air-massflow recirculation ratios for primary

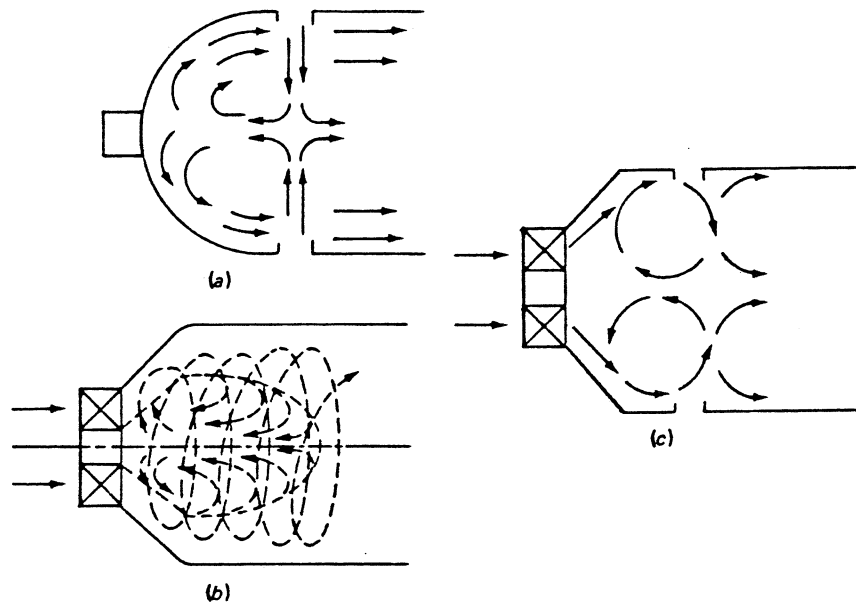


Fig 4.9 Primary Zone airflow patterns. (a) Opposed jet (b) Swirl-stabilized (c) Combined swirl and opposed jet

zones that utilize a combination of swirler and opposed primary jets, supplemented by wall cooling air and atomizing air. However, an empirical approach is incorporated in the program based on the parameters that would influence the amount air that would take part in the combustion

- 1) Distance of the cooling slot/ mixing hole from the injector head
- 2) Depth of penetration
- 3) Angle of the jet
- 4) Spray angle
- 5) Swirl strength (normally indicated by the swirl number)

The empirical approach to evaluate the fraction is outlined.

Cooling Slot : \dot{m}_{comb} represents the actual amount of air taking part in the combustion from the available cooling air \dot{m}_{cool} through the slot:

$$\dot{m}_{comb} = \dot{m}_{cool} * \text{FRACTION} \quad \dots(4.16)$$

$$\text{where FRACTION} = 1 \quad \text{if } \Delta l / 0.5D_{ft} \leq 1/3$$

$$= 3(\Delta l / 0.5D_{ft}) \quad > 1/3$$

Δl is the distance between the cooling slot beginning to the end of the burning zone

Mixing Hole : from the available mixing air \dot{m}_{mix} ,

$$\dot{m}_{comb} = \dot{m}_{mix} * \text{FRACTION} \quad \dots(4.17)$$

where FRACTION = $F_{1d} * F_{1p} * F_{1q}$

$$F_{1d} = 1.0 \quad \text{if } (Y_{max}/D_{ft}) * F_{1s} \geq 0.9$$

$$= (Y_{max}/D_{ft}) * F_{1s} / 0.9 \quad \text{else}$$

$$F_{1s} = 1.0 \text{ for staggered hole} \quad \left| \begin{array}{l} \text{only for annular} \\ \text{combustors, depends} \\ \text{on the relative} \\ \text{position of holes} \\ \text{on outer \& inner} \\ \text{annuli in an} \\ \text{opposing row.} \end{array} \right.$$

$$= 2.0 \text{ for inline holes}$$

$$F_{1p} = 1.0 \text{ for plunged holes}$$

$$= 0.95 \text{ for plain holes}$$

$$F_{1q} = 0.5 \quad \text{if } \phi/180 \geq 0.5$$

$$= \phi/180 \quad > 0.3$$

$$= (\phi/180)/0.3 \quad \text{otherwise}$$

Swirl strength should be used to find the length of the burning zone. Empirical relations such as the one by Kerr and Fraser (1965), as shown below

$$\frac{\dot{m}_e}{\dot{m}_{sw}} = (0.35 + 1.4S_N) \frac{x}{d_{eff}} \quad \dots(4.18)$$

where \dot{m}_e = entrained mass flow rate

$$d_{eff} = (D_{sw}^2 - D_{hub}^2)^{0.5}$$

x = downstream distance

The length of the recirculation zone can be approximately indicated, by assuming the value of entrained fraction as 0.5. However, experimental evidence through water flow visualisation or temperature measurements through thermal paint etc. should indicate the burning zone length in a more positive way. However, the above equation is incorporated, due to inadequate procedures to represent the complex 3D phenomena- swirl and recirculation. User, however, can choose the location where peak temperature would exist, to represent the burning zone.

For the above approach flow conditions are needed to estimate these numbers. Hence for the preliminary design, the following expression for the amount of air involved in primary combustion is sufficiently accurate.

$$\dot{m}_{pz} = \dot{m}_{sw} + \dot{m}_{at} + \dot{m}_{fc} + 0.5 (\dot{m}_{lc} + \dot{m}_s) \quad \dots(4.19)$$

where

- \dot{m}_{pz} = total primary air
- \dot{m}_{sw} = swirler air
- \dot{m}_{at} = atomizer air
- \dot{m}_{fc} = flare cooling air
- \dot{m}_{lc} = liner cooling air
- \dot{m}_s = total air flow through the secondary holes

Once again apportioning suitable values to the individual flows, front end and the primary zone cooling and mixing flows can be estimated.

NOTE : Wherever the term suitable values appear, default values are stored in the program from the available combustor data. User will have the option to change them to suit individual requirement.

Similarly from the equivalence ratios at the end of each zone appropriate mass flow for the dilution holes is estimated.

NUMBER OF CANS :

The choice of number of cans in tuboannular combustor is once again a matter of experience. There are designs with 12 cans. But there is no available literature to suggest a procedure to choose the exact number. One interesting suggestion is to choose a prime number like 7, 11 or 13, so that any possible resonance can be avoided due to low order multiple frequencies. There is no proof to support it or disprove this supposition. However, one analytical reasoning is proposed by the author, based on the non-dimensional mach number in the burning zone, leading to

$$\dot{m}_{can} = \frac{1.0e^{-5} \times D_{ft}^2 \times P_3 \times (100. - OPL)}{\sqrt{Tpz}} \quad \dots(4.20)$$

$$\text{Number of cans} = \dot{m}_{pz} / \dot{m}_{can}$$

Reasonable preliminary estimates can be obtained.

4.9 SWIRLER

A comprehensive literature search brought to light virtually no work on which such a sound theoretical swirler design method could be based. The method used is therefore based on an examination of swirler designs that have been previously been used on combustors mainly of the tubular type. Although the range of Dft does not cover the values normally encountered in annular combustors, the following relation obtained from Northern Research Engineering (1974), may be used until more information on swirler is available.

$$D_{sw} = \text{Outer Dia} = 0.225 D_{ft} + 0.01905 \quad \text{m} \quad \dots(4.21)$$

$$D_{hub} = \text{Inner Dia} = 0.100 D_{ft} + 6.35 \times 10^{-3} \quad \text{m} \quad \dots(4.22)$$

Beer and Chigier (1972) provided a non-dimensional criterion to characterize the amount of rotation imparted to the axial flow

$$S_N = \frac{2 G_m}{D_{sw} G_t} \quad \dots(4.23)$$

where G_m = axial flux of angular momentum

G_t = axial thrust

and derived the same as

$$S_N = \frac{2}{3} \frac{1 - (D_{hub}/D_{sw})^3}{1 - (D_{hub}/D_{sw})^2} \tan \theta \quad \dots(4.24)$$

Swirl is classified strong when $S_N \geq 0.6$ and weak otherwise.

θ , the vane angle is generally between 45 to 60 degrees.

The other factors which influence the swirl are the number of blades and type. The number of blades are usually between 8 to 16. The curved blades show better performance than flat blades.

4.10 FUEL INJECTION

A major design decision in combustor is the choice of type of fuel injection. Its importance is growing as the future combustors are subjected to an increasingly severe emissions regulation and are called upon to burn a larger proportion of heavy distillate and synthetic fuels. The injectors can be broadly classified as pressure atomizer, twin-fluid atomizer and vaporizer- the relative merits are listed in Table 4.6.

Type	Description	Advantages	Drawbacks	Applications
Pressure atomizer	Plain orifice	1. Simple, cheap 2. Rugged	1. Narrow spray angle 2. Solid spray cone	Afterburners, torch igniters
	Simplex	1. Simple, cheap 2. Wide spray angle (up to 300°)	1. Needs high fuel-pump pressures 2. Excessive soot formation at high combustion pressures 3. Fuel distribution, and hence exit pattern factor, varies with fuel flow rate	Engines of low fuel flow range (not greater than 7 to 1)
	Duplex	Same as simplex, plus good atomization over a very wide range of fuel flows	Same as simplex	Engines of low to medium pressure ratio
	Duple or dual orifice	1. Good atomization over a very wide range of fuel flows 2. Wide burning range 3. Mechanically robust 4. Easily modified to facilitate combustor development	1. Same as simplex, plus complexity 2. High cost of manufacture 3. Susceptibility of small passages to blockage by contaminants and fuel gumming	Wide range of aircraft and industrial gas turbines; cannot be used on high-pressure-ratio engines owing to excessive exhaust smoke
	Spill return	1. Simple construction 2. Large holes and flow passages obviate risk of blockage	1. Spray angle varies with fuel flow 2. Fuel-pump power requirements can be excessive	Good potential applications for "dirty" fuels and fuels of low thermal stability
Rotary atomizer	Slinger system	1. Simplicity 2. Low cost 3. Needs only low-pressure fuel pump	1. Atomization relatively poor at high-altitude reflight condition 2. Slow response to changes in fuel flow rate	Small engines of low compression ratio
Twin-fluid atomizer	Plain-jet airblast	1. Operates satisfactorily with low fuel pressures 2. Simple, cheap 3. Low susceptibility to blockage	1. Narrow spray angle 2. Atomizing performance inferior to prefilming airblast	Few, to date
	Prefilming airblast	1. Operates satisfactorily with low fuel pressures 2. Low soot formation 3. Exit pattern factor fairly insensitive to changes in fuel flow rate 4. Mechanically robust 5. Atomizing performance is superior to all forms of pressure atomizer, especially at high combustion pressure	1. Narrow burning range 2. Atomization quality is low for low combustor velocities, such as occur at start-up	Wide range of modern high-performance, high-pressure-ratio engines
	Piloted or hybrid	Same as prefilming airblast, plus 1. Wide burning range 2. Easy engine start-up	1. Needs pilot nozzle	General application to all types of engines
	Air assist	Good atomization	1. Needs external source of high-pressure air or steam	Industrial engines
Vaporizer	Conventional vaporizer (walking stick, T, mushroom, etc.)	1. Operates satisfactorily with low fuel pressures 2. Reduced soot formation due to pre-mixing of fuel and air 3. Pattern factor fairly insensitive to fuel flow rate	1. Requires auxiliary fuel jet for starting 2. Difficult to develop 3. Mechanically suspect, especially at high pressures 4. Fairly narrow burning range 5. Unsuitable for heavy distillate fuels owing to coke deposition	Used on several early aircraft engines of medium pressure ratio
	Lean premix prevaporizer	1. Very low NO _x emissions 2. No exhaust smoke 3. Very low flame radiation 4. Constant pattern factor	1. Susceptible to autoignition, flashback, and flame blowout 2. Requires sophisticated control system	All types of engines where ultralow pollutant emissions is prime requirement

Table 4.6 Relative merits of fuel injectors (Lefebvre (1983)).

The choice once again is the result of confidence from past experience. However, fuel properties notably viscosity, density, surface tension, mass transfer number will play a major role on the selection and so are the atomizing characteristics of the given injector. No design procedure is incorporated. However, the influence of fuel type and given injector on the atomization quality (through SMD), combustion efficiency and radiation, can be examined empirically. The approach and the equations incorporated in the programme are amplified in the subsequent paragraphs.

Following Lefebvre (1983), if fuel evaporation is considered as rate_limiting process, the efficiency is given by-

$$\eta_{ce} = \frac{8(\lambda/Cp)_g \ln(1+B)(1+0.25Re_D^{0.5})t_{res}}{\rho_f D^2} \dots(4.25)$$

where

B = mass transfer number

$$= \frac{Cp_g(T_{amb}-T_1)}{L + Cp_l(T_1-T_o)} \dots(4.26)$$

several assumptions are required to evaluate these, following Leonard and Mellor (1983)

L = heat of evaporation J/kg

$$= \frac{360. - 0.39 T_f}{\rho_f} 10^3 \text{ J/kg} \dots(4.27)$$

$$Cp_l = \frac{760. + 3.35 T_f}{\rho_f^{0.5}} \text{ J/kg K} \dots(4.28)$$

$T_{amb} = 1000 \text{ K}$

$T_1 = 50\%$ boiling point of the fuel

$T_o =$ inlet fuel temperature

$$Re_D = \frac{\rho_g U D_0}{\mu_g}$$

$D_0 =$ Drop size in SMD

U = main stream velocity

$t_{res} =$ residence time

on a qualitative basis, when comparing two fuels a and b this reduces to

$$\frac{1-\eta_b}{1-\eta_a} = \frac{\rho_{fb} D_b^2 \ln(1+B_a)}{\rho_{fa} D_a^2 \ln(1+B_b)} \dots(4.29)$$

Droplet size is commonly expressed as SMD (Sauter Mean Diameter)(eqn 2.33). A great deal of work has gone into

deriving empirical relations between SMD and fuel properties, the type of injector, its geometry and operating conditions. It is not practicable to code all of them as generalization is not easy. However, SMD generally varies as:

$$\text{SMD} = K_1 \sigma^a \mu^b (\Delta P)^c m_L^d \rho_a^e (1+m_L/m_a)^f + K_2 \quad \dots(4.30)$$

where σ = surface tension

$K_1, a, b, c, d, e, f, K_2$ are the coefficients, to be experimentally derived for each type.

for a typical pressure atomizer

$$\begin{aligned} a &= 0.16 \text{ to } 0.19 & ; b &= 0.16 \text{ to } 0.3 & ; c &= -0.275 \text{ to } -0.5 \\ d &= 0.25 & ; e &= -0.1 \text{ to } -0.25 \end{aligned}$$

f and K_2 are applicable to airblast atomizers.

However, the dominating term being viscosity μ , the effect of fuel variation can be effectively evaluated by a simpler efficiency relation

$$\frac{1-\eta_b}{1-\eta_a} = \frac{\rho_{fb} \mu_{fb}^{0.5} \ln(1+B_a)}{\rho_{fa} \mu_{fa}^{0.5} \ln(1+B_b)} \quad \dots(4.31)$$

This relation is incorporated into the programme.

4.10.1 NUMBER OF FUEL INJECTORS

In order to provide a rough estimation of number of nozzles at preliminary stage the following empirical relation is derived.

$$\text{Number of injectors} = \pi/\theta \quad \dots(4.32)$$

where $\sin \theta = 0.5 \text{ PZL} / R_{ref}$

The complete derivation is described as Appendix D.

CHAPTER 5

FLOW EVALUATION

5.1 FLOW CONDITIONS

The processes in the combustion chamber are complex and interdependent. It may be hard to justify in certain cases to isolate a process for evaluation. However flow evaluation is the first step to understand the aerodynamics of the combustor and provide the major input for other performance parameters. Following the flow as it enters the combustor is the starting point.

5.1.1 PRECONDITIONS

Inlet conditions are defined at this stage. The overall geometry of the combustor has been established either through the preliminary design or as an input by the user. When it is a new design, initial estimates of mass flows are available based on which, cooling and mixing configurations will be sized at the appropriate zonal positions.

5.2 PROPERTIES:

Before attempting further evaluation there is a need to address to one of the most important areas, namely, thermodynamic and transport properties. As combustors are involved with flows which are reacting, it is difficult to choose a model which is accurate as well as simple in terms of computing time and storage. The uncertainty of knowledge of exact composition and consequent temperature at each point inside the combustor is simplified to an extent by the basic assumption of uniform properties/composition at each axial location i.e., circumferential variations are neglected. Literature concerning the thermodynamic or transport properties of combustion products, will not be universal in nature due to the complexity and generality involved.

The initial phase of the work involved with the feasibility of overall programme's technique. Hence property evaluation was simplified by using the best available algebraic expressions representing the properties of air and combustion products. The initial phase itself occupied nearly 10 months, a major portion of the total effort. Once the basic algorithm was proven, clearing most of the bugs, the attention was shifted to use the program to analyze a double combustor which would be described in chapter 9. Then there was a greater need for a generalized method to evaluate properties as opposed to few experimental curve fits.

Literature availability is rather poor when it comes to reheat combustor where vitiated air would be the oxidant medium. Barr and Mullins (1947) as well as Odgers and Kretschmer (1980) did carry out experiments with vitiated medium and presented results. But their work did not contain any information on the properties. Powell (1985) developed polynomials for thermodynamic and transport properties for vitiated test medium based on composition. Though the procedure is broadly outlined, the final form of polynomials is not published. Individual species data is available in Reid et al (1977), Reklaitis (1983), National Engineering Laboratories (1972,1973). However, either the temperature range or number of species for which data is presented is a limitation to use any one data completely.

Hence it is decided to fall back on the fundamental approach to derive the relevant properties of any mixture from its constituent pure gas values knowing its fractional content in the mixture. Now the uncertainty is shifted to the type of model used to convert pure gas values to the mixture value and also on to the accuracy of estimation of exact content of each constituent in the mixture. However, attempt is made to use the current models, which are generally used in any large finite difference codes.

5.2.1 SPECIES CONCENTRATION

Evaluation of exact species concentrations and hence the mixture properties sounds noble and may be considered the best approach. For dry or wet air or for fuel alone the method is straight forward.

For dry atmospheric air, the mole fractions are

	mole fraction
N ₂	0.7809
O ₂	0.2095
Ar	0.0093
CO ₂	0.0003

Table 5.1 Dry air composition

For wet air the % of H₂O is also to be included. For hydrocarbon fuel, the major constituents are expressed in some approximate formula like C_xH_y. Traces of N,O,S can also be considered.

Combustion Products : Following zonal division, equivalence ratio is already estimated as indicated in para 4.8.3. From the equivalence ratio, the simple method coded by the author as described in Appendix C solves for the temperature based on the single global reaction. This yields the concentration of individual species which represent the products at that plane. Hence for any intermediary plane inside the zone, the average values are based on the equivalence ratio at the exit of the zone. However properties inside the zone are evaluated based on the concentrations at the end of the zone, but at the appropriate temperature at that location.

$$\text{Mean Molecular Weight } M_w = \sum_j^{NS} \sigma_j M_{w_j} \quad \dots(5.1)$$

5.2.2 THERMODYNAMIC PROPERTIES

Thermodynamic Properties (heat capacities and enthalpies) are computed from JANAF Thermochemical tables (Stull and Prophet (1971)), which are expressed as polynomials in temperature by Gordon and McBride (1971)

$$\frac{C_{p_j}}{R} = z_1 + z_2 T + z_3 T^2 + z_4 T^3 + z_5 T^4 \quad \dots(5.2)$$

$$\frac{h_j}{RT} = z_1 + \frac{z_2 T}{2} + \frac{z_3 T^2}{3} + \frac{z_4 T^3}{4} + \frac{z_5 T^4}{5} + \frac{z_6}{T} \quad \dots(5.3)$$

There are six coefficients z_1 to z_6 corresponding to each species for each of the temperature range 300 K to 1000 K and 1000 K to 5000 K. The coefficients for the 10 species are tabulated in Appendix E. The enthalpy equation (5.3) consists of the sensible enthalpy and the standard enthalpy of formation.

THERMODYNAMIC PROPERTIES OF A MIXTURE

The mixture enthalpy is given by :

$$h = \sum_j^{NS} \sigma_j h_j \quad \dots(5.4)$$

The specific heat capacity of a mixture is given by :

$$C_p = \sum_j^{NS} \sigma_j C_{p_j} \quad \dots(5.5)$$

5.2.3 TRANSPORT PROPERTIES

Transport properties (absolute viscosity and thermal conductivity) for individual species are calculated from the appropriate Enskog-Chapman expressions (Fristrom and Westenberg, 1965) using the Lennard-Jones Potentials.

NOTE : In practice, the molecular transport properties have insignificant effect on the flow, as real flows in the combustion chambers are highly turbulent and the corresponding turbulent values dominate these molecular properties. However, the present work does not consider turbulence. But, laminar viscosity is required to calculate the flow Reynolds number and the viscous effects near the wall. This value is also needed in determining the thermal conductivity of the medium which is required in the convective flux calculations. Hence the need exists for the evaluation these transport properties.

VISCOSITY

The absolute viscosity for all species except H_2O , μ_j , and the viscosity of the species H_2O , μ_{H_2O} (Croom and Leyhe 1966), are respectively given as:

$$\mu_j = \frac{2.6693 \times 10^{-6} (Mw_j T)^{1/2}}{\sigma_{jj} \Omega_{\mu j}^{(2,2)*}} \quad (\text{kg/m/s}) \quad \dots(5.6)$$

where $j \neq H_2O$

$$\mu_{H_2O} = \begin{cases} \frac{2.5639 T^{1/2}}{1 + \frac{1371}{T} \times 10^{-37.4/T}} \times 10^{-6} & ; T \leq 1300 \text{ K} \\ \frac{1.498 T^{1/2}}{1 + \frac{24.51 \times 10^4}{T^2}} \times 10^{-6} & ; T > 1300 \text{ K} \end{cases} \quad \dots(5.7)$$

where

σ_{jj} collision diameter of the molecule in angstroms.

(2,2)*

$\Omega_{\mu j}$ the thermal conductivity collision integral;

(this is a function of ϵ_{ij}/K_{LJ} , the Lennard-Jones constant in degree kelvin) (Hirschfelder et al. 1967)

The Lennard-Jones constants and the collision diameters, are listed in Appendix F for the species of interest in this study.

The viscosities of individual species at any temperature between 300 K and 2500 K, could be evaluated using the above equations. This vast data of temperature dependent viscosities for each species is reduced to a form of AT^B , using the least-square linear regression analysis. In order to optimize the error, effort and storage space, the range is divided into three regions. 300-800, 800-1300 and 1300-2500 degrees kelvin. The maximum deviation is within 1.75%. The coefficients A and B for each species are listed as Appendix G.

THERMAL CONDUCTIVITY

The monatomic thermal conductivity is obtained from the viscosity, through the kinetic theory (Hirschfelder et al. 1967):

$$\lambda_j^o = \frac{15 R \mu_j}{4 M w_j} \quad \dots(5.8)$$

The thermal conductivity, λ of any polyatomic nonpolar gas can be arrived at with the aid of the Eucken correction, (Fristrom and Westenberg, 1965) :

$$\frac{\lambda_j}{\lambda_j^o} = 1 - \delta_f + \frac{2}{5} \delta_f C_{p_j} \quad \dots(5.9)$$

where δ_f is dimensionless parameter given an average value of 0.885 (Hirschfelder et al. 1967)

It has been observed (Fristrom and Westenberg 1965) that it is usually sufficient to follow the same treatment for a polar gas such as H₂O, which is present in considerable amounts in the combustion gases.

TRANSPORT PROPERTIES OF A MIXTURE

The mixture viscosity is given by (Tam, 1981) :

$$\mu = \frac{0.301875 \sum_i^{NS} \sigma_i \mu_i + 0.92925 \sum_i^{NS} \frac{Cp_i}{R} \sigma_i \mu_i}{\sum_i^{NS} \frac{Cp_i}{R} \sigma_i} \quad \dots(5.10)$$

Though the basis for this formula is not clear, its accuracy reasonably agrees with any standard mixture relation. It compares well the following expression

$$\mu = \frac{\sum_i^{NS} \frac{\sigma_i^2}{\mu_i} + 1.385 \sum_{\substack{j=1 \\ j \neq i}}^{NS} \frac{\sigma_i \sigma_j}{pMw_i [D_{ij}]}}{\sum_i^{NS} \frac{\sigma_i^2}{\mu_i} + 1.385 \sum_{\substack{j=1 \\ j \neq i}}^{NS} \frac{\sigma_i \sigma_j}{pMw_i [D_{ij}]}} \quad \dots(5.11)$$

where

$[D_{ij}]$ = diffusion coefficient for specie i through specie j

$$= \frac{1.86 \times 10^{-7} \sqrt{T^3 (Mw_i + Mw_j) / Mw_i Mw_j}}{p \sigma_{ij}^2 \Omega_{D_{ij}}^{(1,1)*}} \quad \dots(5.12)$$

The evaluation is as outlined in Hirschfelder et al. (1954).

Eqn. (5.10) is also compared with the empirical relation of the form given as eqn. (5.14), which is true for any property of a mixture. The difference is within $\pm 5\%$.

Considering the uncertainty of the composition or the exact value due to scarce experimental data, the approximate eqn. (5.10) is considered adequate, as the other two methods involve evaluation of additional parameters such as diffusion coefficient. Hence this equation is used in the programme to evaluate the mixture viscosity.

The empirical relation proposed by Wassiljewa (1937) is used to evaluate the mixture thermal conductivity.

$$\lambda = \frac{\sum_i^{NS} C_i \lambda_i}{\sum_j^{NS} C_j A_{ij}} \quad \dots(5.13)$$

where A_{ij} is a function as proposed by Mason and Saxena (1958)

$$A_{ij} = k \frac{[1 + (\lambda_i^\circ/\lambda_j^\circ)^{1/2} (Mw_i/Mw_j)^{1/4}]^2}{[8(1 + Mw_i/Mw_j)]^{1/2}} \quad \dots(5.14)$$

with k , a numerical constant given as unity.

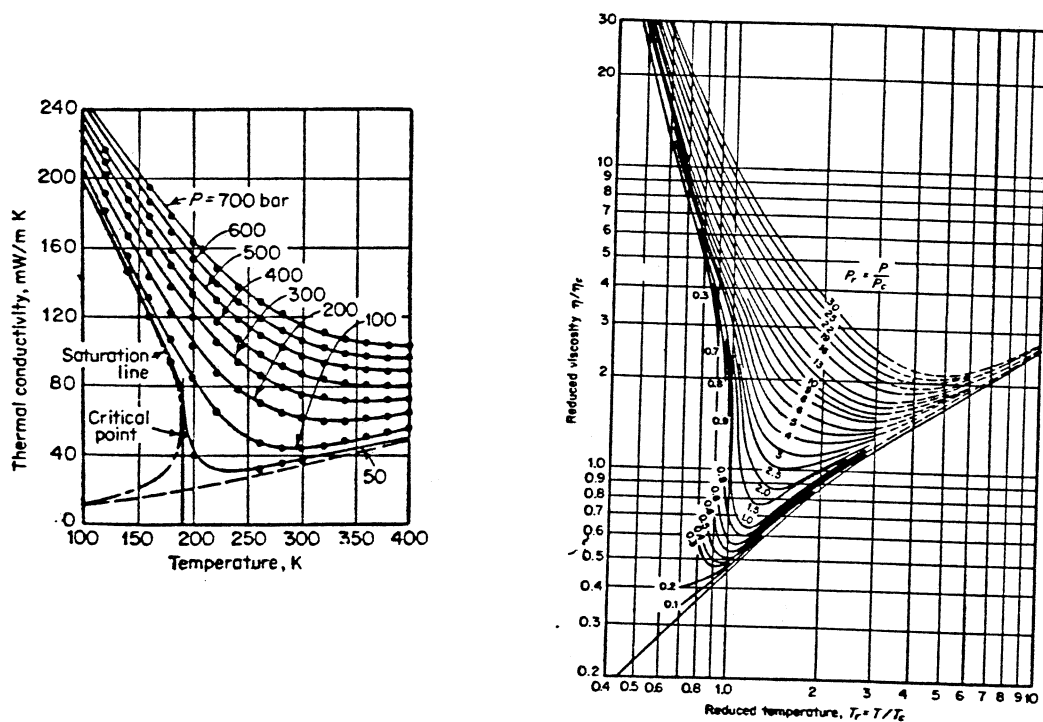
Though the conductivity of the gas mixture as obtained using the above semiempirical formula (Reid et al., 1977) has an error rarely exceeding 5%, this method is chosen due to its simplicity and independence from any extra parameters or coefficients.

The mixture conductivity can however be simplified if Prandtl number, Pr , is assumed to be unity, however this approach is not resorted to.

$$Pr = \frac{Cp_i \mu_i}{\lambda_i} \quad \dots(5.15)$$

5.2.4 EFFECT OF PRESSURE

It can be seen from Fig 5.1, the values do not appreciably change upto moderate pressures. However, very few experimental data is available. At this stage of development of this work it is felt better not to correct for pressures. It may be necessary to approach this problem at a later stage, considering the fact that the usual pressures when double combustors are utilized are around 50 atm.



a) Thermal Conductivity of Methane

b) Generalized reduced Viscosities

Fig 5.1 Effect of Pressure on Transport Properties

5.2.5 STATE

Knowing the properties and total or static condition and/ or geometry at any location, isentropic relations are used to fully define the state. The exact evaluation procedure is given as Appendix H. Thus the values describing the state, thermodynamic and transport properties of the medium would be estimated at any axial plane.

5.3 DIFFUSER

In order to estimate the diffuser performance the following terms are defined (Fig 5.2)

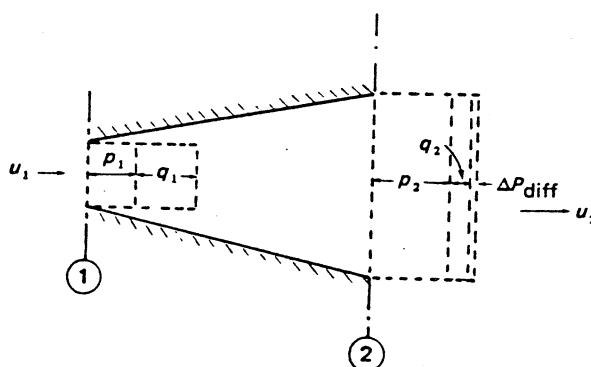


Fig 5.2 Energy conversion in a Diffuser

$$\text{Mean Velocity } \bar{U}_1 = \frac{\dot{m}}{A_1} \quad \dots(5.16)$$

$$\text{Inlet dynamic pressure } \bar{q}_1 = P_1 - p_1 \quad \dots(5.17)$$

$$\text{Pressure loss } \Delta P_{\text{diff}} = P_1 - P_2 \quad \dots(5.18)$$

$$\text{Pressure loss coefficient } \lambda = \Delta P_{\text{diff}} / \bar{q}_1 \quad \dots(5.19)$$

One Dimensional approach

$$P_1 + \bar{q}_1 = P_2 + \bar{q}_2 + \Delta P_{\text{diff}} \quad \dots(5.20)$$

$$\text{Pressure recovery coefficient } C_p = \frac{P_2 - p_1}{q_1} \quad \dots(5.21)$$

Using blockage concept developed by Sovran and Klomp (1967), the diffusers equivalent flow can be defined as shown

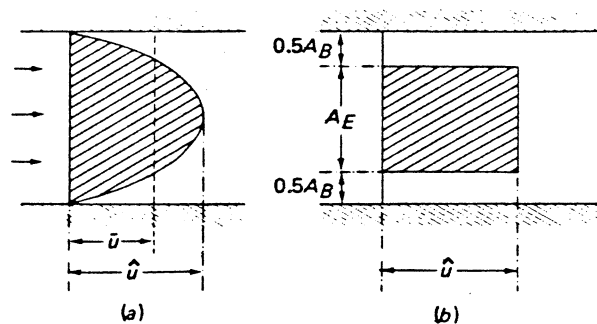


Fig 5.3 Simulation of velocity profile with an equivalent rectangular profile (a) real profile (b) equivalent profile

$$\text{Blockage factor } B = \frac{A - A_E}{A} = 1 - \frac{\bar{U}}{U} \quad \dots(5.22)$$

Tyler and Williamson (1968) empirically related the inlet and exit blockage factor to the geometry as

$$\text{for } B_1 \leq 0.16; \quad B_2 = 0.8 (AR)^{0.07} (B_1)^{1/[2(AR)-1]} \quad \dots(5.23)$$

$$\text{for } B_1 > 0.16; \quad B_2 = 1.044 - 1.13 (1-B_1) AR^{-0.69} \quad \dots(5.24)$$

The value of C_p can then be calculated by assuming that the flow is one dimensional between the effective areas at diffuser inlet and exit. It is given as

$$C_p = \frac{1}{(1-B_1)^2} - \frac{1}{(1-B_2)^2 AR^2} \quad \dots(5.25)$$

Realistic Approach

Kinetic coefficient is applied to account for the discrepancy between realistic profile and the one-dimensional approach, where

$$\text{Kinetic Flux Coefficient } \alpha = \frac{\int \frac{1}{2} U^2 \rho U \, dA}{\frac{1}{2} \bar{U}^2 \cdot m} \quad \dots(5.26)$$

Equation 5.20, when accounted for α , transforms to

$$p_1 + \alpha_1 \bar{q}_1 = p_2 + \alpha_2 \bar{q}_2 + \Delta P_{\text{diff}} \quad \dots(5.27)$$

$$C_p = \frac{p_2 - p_1}{\alpha_1 \bar{q}_1} \quad \dots(5.28)$$

$$\begin{aligned} \lambda &= \frac{\Delta P_{\text{diff}}}{\alpha_1 \bar{q}_1} \\ &= 1 - C_p - \frac{\alpha_2}{\alpha_1 AR^2} \quad \dots(5.29) \end{aligned}$$

In the case of dump diffuser, it is treated as sudden expansion in a duct. As shown in Fig 5.4

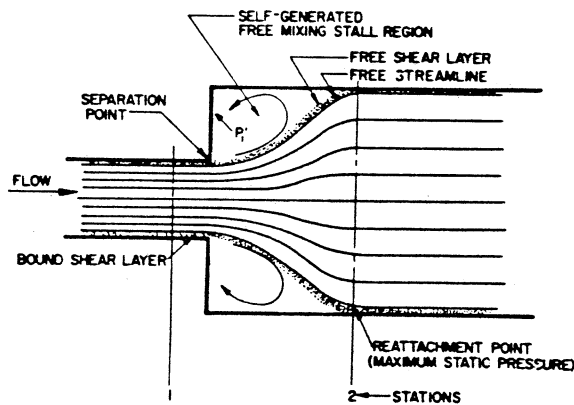


Fig 5.4 Sudden Expansion in a duct

$$\lambda = \left[1 - \frac{1}{AR} \right]^2 \quad \dots(5.30)$$

For the total loss, the coefficient for conventional diffuser given by eqn (5.32) and that for sudden expansion by eqn (5.33) are simply added.

$$\Delta P_{\text{diff}} = (\lambda_{\text{conv}} + \lambda_{\text{sudden}}) \alpha_1 \bar{q}_1 \quad \dots(5.31)$$

Thus p_2 , P_2 are evaluated by assuming B_1 , α_1 and α_2 , typical values being 0.03, 1.1 and 1.2 respectively. These are not far from realistic values observed in typical combustors. The properties are assumed to be constant at the exit of diffuser.

5.4 LINER EVALUATION

Preliminary design sized the liner as a broad five zone container. If it is a new design, the liner hole size and number as well as cooling configuration need to be optimized based on metal temperatures. But for an existing design, as these are already known only pressure drops, coolant/mixing flows, metal temperatures need to be evaluated. Hence for the former case heat transfer calculations need to be simultaneously performed along with the flow calculations. As the selection of any of above variables depends on one or more of the rest, the process may require a number of iterations and suitable selection. However for an existing design these complications do not arise and flow evaluation can be done independently. The following are the steps through which the combustor is evaluated, the same is shown as Fig 5.5.

- 1) Combustor, through the preliminary design or through initial input for an existing combustor, has been divided into five zones, namely, recirculation, primary, secondary, dilution and nozzle. Equivalence ratio, efficiency and gas temperature are known at the exit of each zone and hence the composition of the media is also known at those planes. The variation of any variable between the zones is based on the end zone values.
- 2) In case of a new design, based on initial estimates cooling/mixing flows, cooling and liner hole configurations are sized at the appropriate location using simple standard design practices. This step will not be needed for an existing design.
- 3) An initial guess is made for the front end flow. Balance would be going to the annulus. In case of Annular combustors a second guess is also required as to the flow split between inner and outer annuli.
- 4) Liner front end pressure drop is calculated from the mass flow, area and discharge coefficient. Discharge coefficients are either predefined or evaluated appropriate to the flow conditions and geometry.
- 5) Assuming an instantaneous combustion of the front end air which entered the liner and attributing an arbitrary temperature rise (150 degree Kelvin in this case), exit conditions are evaluated, with the help of Rayleigh's equations.
- 6) One dimensional steady flow analysis is used to evaluate the flow in the streamwise direction in the liner and in annuli using appropriate state properties. This is done over a control volume of infinitesimal length. This value varies but generally taken as 1 mm.

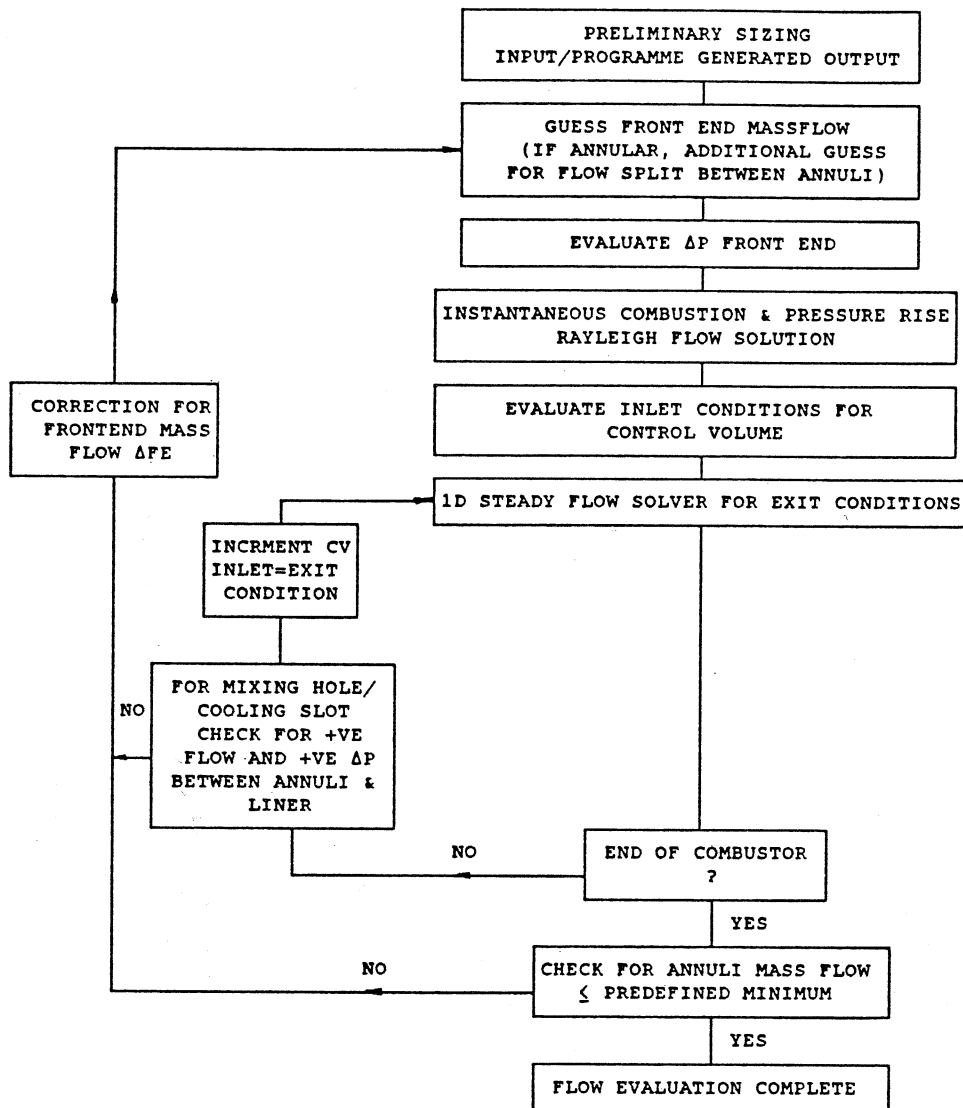


Fig 5.5 Outline of Flow Evaluation.

- 7) At the end of any cooling/mixing configuration conditions are checked for positive mass flow in the annuli and also positive static pressure difference across the annulus and the liner. If either condition is not satisfied these calculations are repeated from the beginning of the liner with suitable corrections to the initial guesses.
- 8) The calculations are performed in a marching fashion till the end of combustor is reached. At the end of combustor, the mass flows remaining in the annuli should be as negligible as the accuracy demands. It is assumed that 0.05% of total mass flow can be considered negligible. If this condition is not satisfied, with suitable corrections to the initial guesses, calculations are repeated from step 4. Thus steps 4 through 8 are carried out till the left over massflow condition is satisfied.

Assumptions and appropriate evaluation procedure are described in the subsequent paragraphs.

NOTE : Contrary to the above approach of starting from the liner beginning and marching forward, it is possible to evolve a procedure of starting from the exit of the combustor and marching backwards. The latter method is considered to lead to faster convergence. However, this routine is not suited for the present work as evaluation phase is coupled with preliminary design of slot geometry. Hence this approach is not considered.

5.4.1 LINER HOLES

Liner holes have to be estimated in terms of size and number only when it is a new design. The basic equation for flow through a hole may be expressed as

$$\dot{m}_h = C_d A_h \text{ geom} \sqrt{2 \rho_3 (P_2 - P_j)} \quad \dots(5.32)$$

where $A_h \text{ geom} = \text{geometric area } 1/4 \pi d_h^2 n$

n = number of holes

P_2 = total pressure upstream of hole

P_j = static pressure downstream of hole

C_d = coefficient of discharge which requires to be estimated depending on the type of hole, location and flow conditions. The evaluation procedure is outlined in the subsequent paragraphs.

Preliminary design evaluates $A_h \text{ geom}$ based on the massflow estimates. The total area, the diameter and the number are evaluated based on standard combustor design practices.

5.4.1.1 DOME HOLES

If employed, normally same number as the number of injectors for the annular and 2 or 4 in case of tubular. A_h effective is estimated from the guessed dome flow and pressure drop Δp .

$$\Delta p = 0.9 (100 \times \text{OPL} \times P_2 - \Delta P_{\text{diff}}) \quad \dots(5.33)$$

5.4.1.2 SECONDARY HOLES

The choice is based on the depth of penetration of the jet. Lefebvre (1983) has described Norester's (1964) equations for round air jets into a tubular liner as

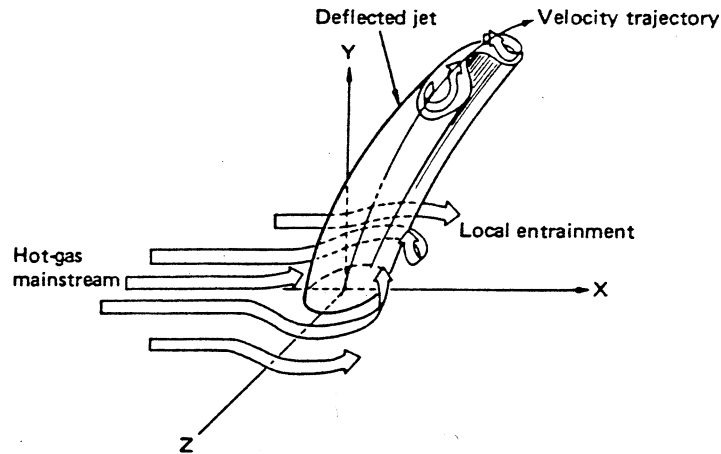


Fig 5.6 Jet in cross flow

$$\frac{y_{\max}}{d_j} = 1.25 J^{0.5} \frac{\dot{m}_g}{\dot{m}_g + \dot{m}_j} \quad \dots(5.34)$$

$$\text{where } J = \frac{\rho_j U_j^2}{\rho_g U_g^2} = \frac{P_{an} - p_L}{P_L - p_L}$$

g denotes gas in the liner

j denotes jet

$$\dot{m}_j = \frac{1}{4} \pi d_j^2 n \rho_3 U_j \quad \dots(5.35)$$

$$\text{where } U_j = \left[\frac{2 (P_{an} - p_L)}{\rho_3} \right]^{0.5}$$

$$d_j^2 = Cd d_h^2$$

Specifying y_{\max} , d_h and n can be evaluated. Here the procedure is iterative as depth of penetration also depends on the amount of jet flow. However, n for each liner can be guessed as double the number of injectors in case of annular and six or eight in the case of tubular combustors.

5.4.1.3 DILUTION HOLES

Similar argument applies to the dilution holes, except that the depth of penetration is to a much lesser extent— 0.25 to 0.4 of the flame tube width. The total number being same as the number of injectors in case of annular or six or eight in case of tubular.

5.4.1.4 COEFFICIENT OF DISCHARGE

For most liner holes the upstream flow direction is parallel to the plane of the holes as illustrated in fig 5.7

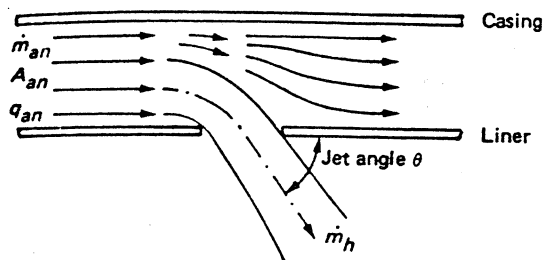


Fig 5.7 Flow through a liner hole

$$\text{where } K = \frac{\text{jet dynamic pressure}}{\text{annulus dynamic pressure}} = \frac{P_{an} - p_L}{P_{an} - p_{an}}$$

$$\alpha = \frac{\dot{m}_h}{\dot{m}_{an}}$$

Kaddah(1964) satisfactorily correlated C_d for plain circular, oval and rectangular holes by

$$C_d = \frac{A (K-1)}{[4K - K(2-\alpha)]^{0.5}} \quad \dots(5.36)$$

where A is found to be 1.25

Freeman (1965) extended the correlation to plunged holes by increasing the constant A to 1.65 from 1.25.

Adkins and Gueroui (1986) suggested an alternate method to evaluate flow and C_d for plain circular holes. It avoids the iterative technique to be followed with eqn (5.36), where in

α contains the term hole massflow. The method has evolved expression for the hole massflow and C_d through a parameter ingestion ratio, based on flow characteristics and geometry considering the curvature and contraction effects.

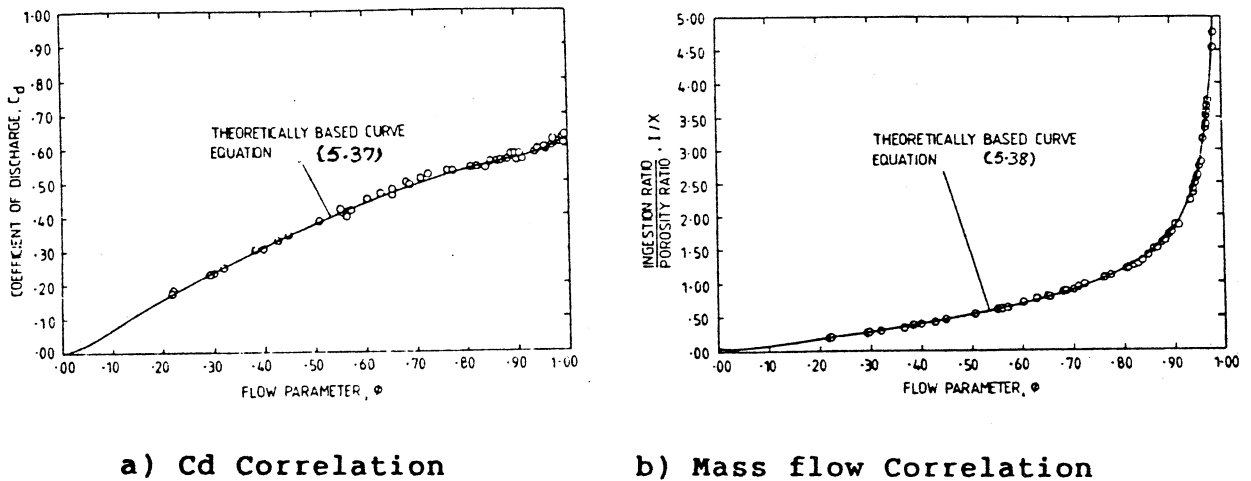


Fig 5.8 Correlations by Adkins and Gueroui (1986)

Coefficient of Discharge :

$$C_d = f \sqrt{C_{fc}^2 - 1 + \phi} \quad \dots(5.37)$$

where

$$\phi = \frac{P_{an} - P_L}{P_{an} - P_L}$$

$$C_{fc} = \left[1 - \exp(-1) + \exp\{-1/\sqrt{(1-\phi)}\} \right]$$

$$f = \frac{\text{circumferential surface area}}{\text{circular plain area}}$$

Correction f , is conceptually shown as Fig 5.9, but calculated using the correlation of the form

$$f = 0.14(d/D)^2 - 0.03(d/D) + 1.0$$

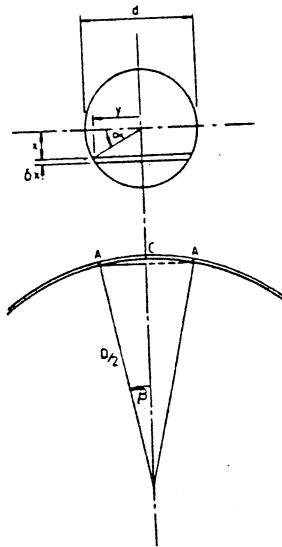


Fig 5.9 Curvature corrections

Mass flow:

$$\frac{I}{X} = f \sqrt{\frac{Cfc^2 - 1 + \phi}{1 - \phi}} \quad \dots(5.38)$$

where

$$I = \text{Ingestion Ratio} = \dot{m}_h / \dot{m}_{an}$$

$$X = \text{Porosity Ratio} = A_h / A_{an}$$

The results are comparable for plain holes. This procedure, however is not adopted in the program as it is not derived for plunged or other shapes of holes. However, it is incorporated in the programme as a cross check to the values generated by eqn (5.36) and also for a possible inclusion into the programme in future, considering its non-iterative approach.

The discharge coefficients for the dome holes are assumed to be 0.8 as the plane of the hole is nearly perpendicular to the flow direction.

5.4.2 LINER PRESSURE DROP

There is no published literature to describe the pressure drop when all the three configurations namely, swirler, atomizer and dome holes are employed.

The author taking analogy from electrical circuits developed a simple formula to combine the effects of all.

Flow through a hole can be represented as

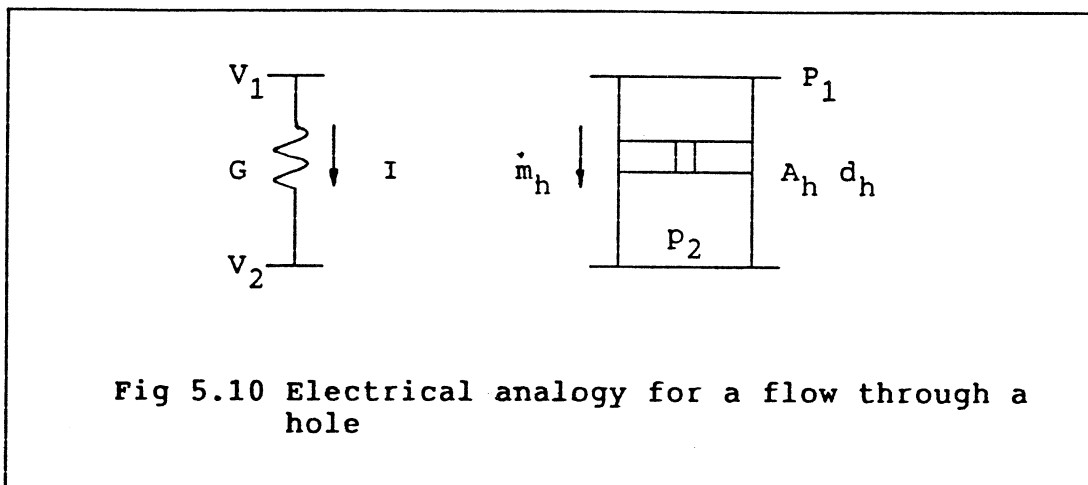


Fig 5.10 Electrical analogy for a flow through a hole

$$I = G \Delta V$$

$$\dot{m}_h = A_h C_d \sqrt{2\rho(P_1 - P_2)}$$

where

- I current - massflow \dot{m}_h
- ΔV potential difference - f (pressure drop) $\sqrt{2\rho\Delta P}$
- G conductance - effective area $A_h C_d$

...(5.39)

Higher the conductance higher is the current for the same potential difference.

When all the three devices are present, the combined circuit will be as shown in Fig 5.11

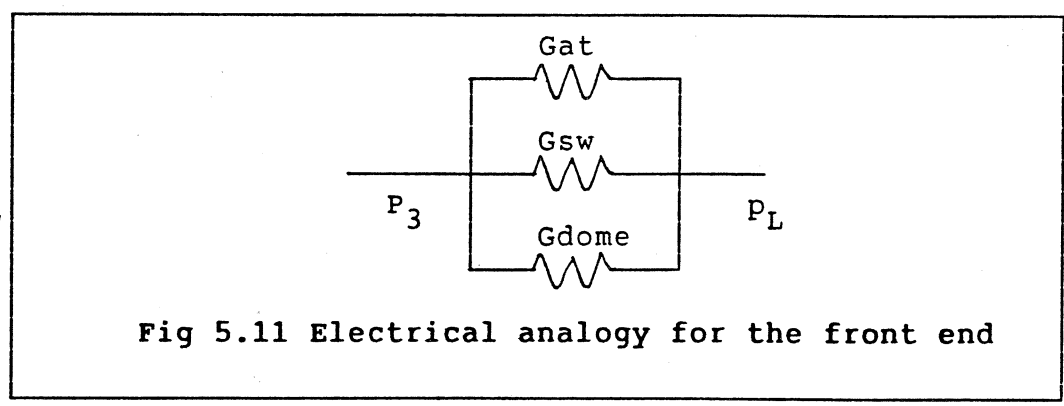


Fig 5.11 Electrical analogy for the front end

$$\text{then } \Delta V = \frac{I}{G}$$

$$\text{where } \Delta V = \sqrt{2 \rho_3 (P_3 - P_L)}$$

$$I = \text{total mass flow} = \dot{m}_{at} + \dot{m}_{sw} + \dot{m}_{dome}$$

$$G = \text{total conductance} = G_{at} + G_{sw} + G_{dome}$$

$$G_{at} = A_{at} C_{d_{at}} \quad 1$$

$$G_{sw} = \frac{1}{\left[K_{sw} \left[\frac{1}{\cos \theta A_{sw}} \right]^2 - \frac{1}{A_L^2} \right]^{0.5}}$$

$$G_{dome} = A_{dh} C_{d_{dh}} \quad \dots(5.40)$$

The G_{sw} is derived from the expression proposed by Knight and Walker (1957) for the pressure loss of thin vaned axial swirlers

$$\Delta P_{sw} = K_{sw} q_{ref} \left[\left(\frac{A_{ref}}{A_{sw}} \right)^2 \sec^2 \theta - \left(\frac{A_{ref}}{A_L} \right)^2 \right] \left[\frac{\dot{m}_{sw}}{\dot{m}_3} \right]^2 \quad \dots(5.41)$$

where $K_{sw} = 1.3$ for flat vanes
 1.15 for curved vanes

$\Delta P_{sw} =$ total pressure drop due to swirler

$A_{sw} =$ frontal area of swirler

$\theta =$ vane angle

Conductance of any feature would obviously be zero if it doesnot exist. When pressure atomizer is used, G_{at} would be zero.

Thus knowing the mass flow and geometry, the pressure drop can be estimated.

5.4.3 COMBUSTION

The front end air after entering the liner will mix with fresh fuel and the recirculated burnt products and will take part in combustion. Considering the chemical kinetics and

recirculation, mixing pattern and fuel droplet chemistry, it is impossible to model in the one dimensional sense. In order to grossly represent, an instantaneous combustion is assumed and an arbitrary value of 150 degree Kelvin temperature rise is assigned for the state after combustion. Using Rayleigh flow relations, properties after combustion are evaluated. The method of evaluation is outlined in Appendix I.

5.4.4 COLD FLOW

Generally in the case of new designs, analysing cold flow or combustionless aerodynamics is a very useful study to understand the flow characteristics of the combustor. It is well established that the flow pattern with and without combustion is by and large similar. In practice, water flow visualisation is an accepted and most widely used technique to represent the flow pattern inside a combustor. In order to simulate this situation, cold flow analysis is facilitated where in temperature rise is assumed to be zero, ie. exit temperature is same as the inlet. This study helps to identify the mean equivalence ratios in each zone, based on which liner gas temperature profile can be reasonably predicted which could be used for the flow evaluation with combustion. Case 3 in the Chapter 11 amplifies this point.

5.4.5 LINER ANALYSIS

As the analysis is one dimensional the combustion chamber is divided into control volumes by vertical planes at each axial location which can be varied as per convenience. As the system is treated parabolic, the exit condition of the control volume is solved knowing the inlet condition accounting for

- 1) Area change
- 2) Wall friction
- 3) Mixing of gases which are injected into the main stream
- 4) Change in molecular weight and specific heat occasioned by combustion, gas injection

The unknowns, pressure, temperature, density and velocity are evaluated by solving equations of conservation of mass, momentum, energy and that of state. These finite differential equations can be solved by several methods. Here, the flow in the down stream direction x is obtained by using one dimensional steady flow analysis, outlined by Shapiro (1953). The assumptions are as follows

- 1) The flow is one-dimensional and steady
- 2) Changes in stream properties are continuous
- 3) The gas is semi-perfect i.e., it obeys Boyle's and Charles' laws and has a specific heat which varies only with temperature and composition.
- 4) Recirculation is not considered
- 5) Heat exchange is neglected. (However the radiation exchange is grossly accounted for while evaluating the flame temperature value.)

The differentials are converted to finite difference and using method of influence coefficients the exit state of the control volume is evaluated. The exact procedure is outlined as Appendix J.

5.4.6 SUDDEN EXPANSION LOSSES

In the annulus, when the air is removed from the cooling

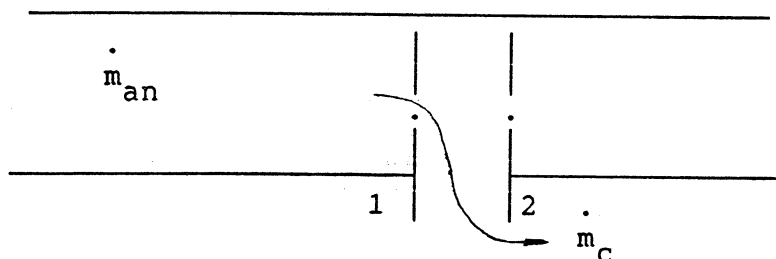


Fig 5.12 Sudden expansion in the annulus

slots or mixing holes, the remaining air suddenly expands to fill the area, for which the losses are calculated by the empirical relation (Northern Research Engg (1974)).

$$P_1 - P_2 = 1.85 \frac{\rho_1 V_1^2}{2} \left(\frac{\dot{m}_c}{1.36 \dot{m}_{an}} \right)^{1/B} \quad \dots (5.42)$$

$$\text{where } B = 0.5 + 0.242 (Mn_1)^{2.22}$$

Though this relation is valid when the air is removed

through static ports only, they are used for total head devices also, due to lack of literature at this stage.

5.4.7 MASS BALANCE

When the calculations reach the end of the combustion chamber the left over mass in the annuli should be less than 0.05% of total air, or any user defined value. If not, the initial guess of mass flow splits is corrected and evaluation repeated from the front end of liner. Similar correction is also required if the massflow left in annuli is negative or static pressure in annuli is lower than liner at any cooling slot/mixing hole.

Tubular

- 1) At the end of combustor, if flow is left over, the front end flow is increased in the ratio of front end opening to total effective opening area on the mass left over in the annulus.
- 2) If the static pressure is less in the annulus then front end flow correction is doubled from the previous value.
- 3) If massflow is negative then front flow correction is halved.
- 4) If the previous front end correction is zero for case 2 or 3, then the correction is taken as 0.1 of frontend flow.

Annular

- 1) If the remaining mass flows in the annuli are of the opposite signs, then the annuli flow split guess correction is changed by half for the +ve side of annulus. If zero it is taken as half of the mass flow left on the +ve side. Front end flow remains the same.
- 2) If the remaining mass flows in the annuli are of the same sign, then the front end correction is changed by half in the same direction. If it is zero it is taken in the ratio of frontend opening to the total opening on the amount left over in the annuli.
- 3) At any cooling/ mixing configuration, when one of the static pressure is less than that of liner, similar correction as step 1) is done, but in the opposite direction. Front end remains the same.

- 4) To avoid oscillations and to hasten convergence, a maximum number of 11 sub-iterations are allowed where steps like 1) or 3) can occur for a front end flow, which is held constant for these sub-iterations. Then front end flow is changed accordingly and sub-iteration counter renews.

An iteration is one in which the calculations successfully reach the end of the combustion chamber. In case the massflow or static pressure difference change sign before the end of the combustion chamber, it is counted as sub-iteration. After a predefined number of iterations, evaluation can be stopped or continued with an option for detailed output for closer examination of the variables or flow evaluation can be stopped, but continuing with the remaining performance evaluation with existing mass flow splits.

5.4.8 CONTROL VOLUME

This value should be as small as possible considering the finite difference method used to solve the differential equations. It has been observed that the procedure explained as Appendix J fails to converge, for certain large area ratios or mass flow ratios across the control volume. To avoid that 1mm is assumed as the control volume length, though it may be viewed as too fine a grid to attempt for a gross evaluation procedure. This value, however is not constant, it increases to the diameter of the mixing hole or reduces to the balance of the distance between control volume and end of a zone, if the distance is less than the control volume's length. Also the beginning of cooling slot is evaluated for 0.5 mm for the same reason of sudden area change.

5.5 PATTERN FACTOR

Uniform property across a plane precludes any calculation to evaluate the temperature traverse quality. However, comparative figures are obtained by using the correlations as stated in 4.8.5. However, it is possible to generate realistic analysis by dividing the combustor into convenient concentric tubes and extending the present one dimensional concept to each of them, with a suitable interaction between the tubes.

CHAPTER 6

HEAT TRANSFER

6.1 INTRODUCTION

Liner durability essentially depends upon the thermal stresses they are subjected to under the severe pressure conditions inside any combustion chamber. A major operating cost of aircraft turbine engines is the replacement of combustor liners after relatively short periods of use. One of the primary aims of the design is to avoid this. Damage is usually in the form of cracks, which develop at discontinuities in the wall such as cooling slots and air admission holes or at locations where manufacturing processes leave severe residual stresses. A liner is a complex structure, so the calculation of thermal stresses and the prediction of liner life present formidable problems. In general, combustor failures are known to result from operation under conditions that subject the liner to a combination of high temperatures and high temperature gradients. Cracks are caused by low-cycle fatigue due to transient excursions in the liner wall temperature. These usually peak during acceleration and take-off from sea level which is when buckling loads across the liner are also at a maximum. Temperatures and temperature gradients must therefore be kept down to ensure a satisfactory liner life. Hence one of the primary intentions of heat transfer analysis has been to predict metal temperature over the years. The need for the accurate predictions will continue to grow due to the continuous growth in severity of system variables like pressure, turbine inlet temperature or need to use wide-cut fuels. An additional incentive for establishing methods for prediction stems from their potential contribution to the control and reduction of pollutant emissions. To optimize the performance and liner durability, a better understanding of the heat transfer process is necessary.

For the purpose of analysis a liner may be regarded as a container of hot flowing gases surrounded by a casing. Between the container and the casing flows relatively cool air. The liner is heated by radiation and convection from the hot gas-soot mixture inside it and is cooled by radiation to the outer casing and by convection to the annulus air. The relative proportions of the radiation and convection components depend upon the geometry and operating conditions of the engine; however, typically radiation accounts for 30 to 50% of the overall heat flux to the walls of present-day engines. As fuels of an increasingly soot-forming nature are used, the radiative contribution may reach up to 80% of the total wall heat flux.

Of the four heat transfer processes that govern liner wall

temperature, two (external convection and external radiation) can be calculated with reasonable accuracy. However, it is quite difficult to model with the same level of accuracy, the internal radiation, due to the multi-dimensionality of the radiative field. Internal convection also poses a problem due to the introduction of various film cooling devices. The nature of interaction between cooling film and the main flow is again not a multi-dimensional phenomenon. Thus, in the design of combustion chambers for high-pressure gas turbines, only rough estimates of liner wall temperature, and hence liner durability can be made.

6.2 RADIATION

Considering its importance, it is appropriate to review the field of radiation first. It is now well established that in gas turbine combustion chambers a large proportion of the total heat flux to the liner walls is by radiation from the flame. For the combustion gases generated by gas turbine fuels the total emitted radiation has two components (1) the "non-luminous" radiation that emanates from certain hetero-polar gases notably carbon dioxide and water vapour (2) "luminous" radiation that depends on the number and size of the solid particles (mainly soot) in the flame.

6.2.1 NON-LUMINOUS RADIATION

The non-luminous component of radiation is due to the combustion products. A characteristic of gas radiation is that it occurs in the form of banded spectra (Tourin (1966)). In non-luminous flames the banded spectra from H₂O and CO₂ are the most prominent feature at temperatures upto about 3000° K. The strongest emission bands for H₂O are centered at 1.4, 1.9, 2.7, 6.3 and 21 μm. CO₂ radiates strongly around 2.7, 4.3 and 15 μm. At higher temperature H₂O and CO₂ are depleted by dissociation, but radiation from diatomic molecules, notably CO, is increased. Although CO can contribute significantly to the emission and attenuation of radiation within flames, its contribution is localized and is of secondary importance in evaluating radiative fluxes. The contributions of SO₂ and NO_x can be neglected because of their low concentrations. Moreover, gases with symmetrical molecules, such as H₂, O₂ and N₂, give no appreciable radiation, even at the highest temperatures.

6.2.2 LUMINOUS RADIATION

In the primary combustion zone most of the radiation emanates from soot particles produced in fuel-rich regions of the flame. Soot may be generated in any part of the combustion zone where fuel/air ratios are high and mixing of fuel and air is inadequate, but the main soot-forming region lies inside the fuel spray at the center of the liner. In

this region local pockets of fuel and fuel vapour are enveloped in oxygen-deficient burned products at high temperatures thereby creating conditions that are highly conducive to soot formation.

At low pressures the presence of soot particles may give rise to a luminous flame, but usually they are too small in number to significantly affect the level of radiation. However, at the high levels of pressures encountered in modern gas turbines, the soot particles attain sufficient concentration to radiate as black bodies in the infrared region. It is under these conditions that radiant heating is most severe and pose serious problems in regard to liner durability. Due to lack of complete understanding of the mechanism at this stage development, technical problems connected with soot formation in combustion at elevated pressures still have to be handled on a trial and error basis (Wagner (1987)).

6.2.3 RADIATION MODELS

The field of radiation modelling has been fairly active and is growing in importance. A variety of methods of varying complexity are available, though a simple prediction procedure for the ultimate user is still much wanted. A review of the status by Viskanta (1984) and Lefebvre (1984) bring out the relative complexities, inadequacies, and the problems in areas such as soot modelling or availability of experimental data. However, an over view of some of the techniques is worthwhile.

The problems coupling of radiation calculations with flow field calculations, can be better judged, by cursory look at the type of equations which represent the radiative field.

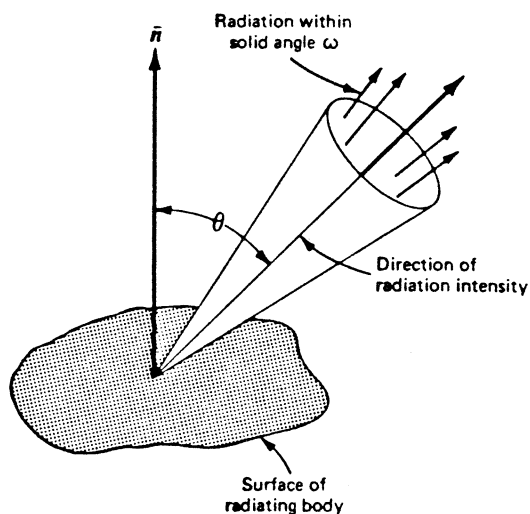


Fig 6.1 Intensity of Radiation

The intensity of radiation I is a function of angle, wavelength and distance (fig 6.1). For a monochromatic radiation it is given by Bouguer-Lambert law as

$$\frac{dI_{\lambda}}{ds} = k \left[\frac{E_{b\lambda}}{\pi} - I_{\lambda} \right] \quad \dots(6.1)$$

where $E_{b\lambda}$ is the monochromatic black body radiation given by Planck's Law as

$$E_{b\lambda} = \frac{C_1 T^5}{\lambda^5 \left[e^{C_2/\lambda T} - 1 \right]} \quad \dots(6.2)$$

where C_1 and C_2 are Planck's constants

k absorption coefficient- this is the sum k for both gas and soot particles.

The total rate of radiation emission is obtained by integrating eqn (6.1) over the entire path length, then over the entire spectrum of wavelengths and over the solid angle Ω , as

$$q = \int_{\Omega} \int_0^{\infty} I_{\lambda} d\lambda d\Omega \quad \dots(6.3)$$

Computing time is enormous, if the above integrations have to be performed over the entire domains of integration and more so if the grid size is small and the geometry is complex. All the models try to achieve to solve these with various assumptions to reduce computing time to an acceptable accuracy.

'ZONE' METHOD : Described by many as an elegant and for many several years ahead of its time, the method developed by Hottel and COHEN (1958), perhaps, is the most widely used. Application of the method requires the whole gas volume to be divided into a number of smaller volumes, each with uniform properties such as temperature, composition, emissivity and transmissivity. The radiation from each volume to the liner wall can then be calculated, provided their relative geometrical orientation is known. The method requires only the solution of a set of simultaneous algebraic equations; however, the computer time involved may be so lengthy as to seriously restrict the number of zones

into which the total combustion volume is divided. In addition to limiting the accuracy of the method, this could also lead to incompatibility between the coarse grid used for radiative transfer calculations and the finer grids required for associated fluid-mechanics calculations. It is also complex to calculate and store exchange coefficients for complex geometries.

MONTE-CARLO METHOD : The Monte-Carlo method is also based on the solution of the simultaneous algebraic equations of 3-D heat transfer, but the calculations are greatly simplified by treating the radiative exchange between gases and/or surfaces in a probabilistic manner. This allows the number of zones into which the combustion volume is subdivided to be greatly increased. The total energy emitted by each zone is divided into several beams each of which is emitted with equal energy in a random direction from a random location in the zone. As each beam travels through the gas its attenuation is described by Beer's law. If its energy is not totally absorbed by the combustion gases before it reaches a wall surface, the remaining energy is reflected back into the combustion volume in a random direction. The calculation continues until the beam energy is completely absorbed (Siegel and Howell (1981)). Its main advantage lies in its flexibility and its ability to be applied to complex geometries. But its principal drawback is that it is time consuming.

FLUX METHOD : These methods are based on the use of simplifying assumptions of the angular variation of radiant intensity in space. These allow the exact integro-differential radiation transport equation to be reduced to a system of approximate partial differential equations, which may be solved in parallel with the flow equations. Two flux to multflux methods are being investigated (Siddal (1972)). The reasons for inaccuracies are a) the radiant flux is divided into too few directions (2,4 or 6 being small for many applications) and b) the fluxes in the different directions are unrealistically independent of each other.

SPHERICAL HARMONIC METHOD : Here the intensity is represented by a series of spherical harmonics (P_N). This method is attractive in that it has a strong mathematical basis and allows the possibility of replacing the integro-differential equation for radiative transfer by a set of partial differential equations. Retention of terms through the first ($N=1$), third ($N=3$) or fifth ($N=5$) results in P_1 , P_3 , P_5 approximations respectively. However reasonable agreement is reported using P_3 approximation (Menguc et. al (1985)).

DISCRETE METHOD : This method proposed by Lockwood and Shah (1980) is similar to the Monte-Carlo method in that it is based on the solution of representatively-directed beams of radiation within the combustor. However, in this method the ray directions are not random but are specified in advance, and are solved only between two boundary walls. The method is economical, easy to apply and has potential for high accuracy.

6.2.4 SCOPE

In order to interface with the existing programming style simple correlations are required. Taking cover under basic assumption of uniform properties at any axial plane and one dimensional approach, we fall back on the currently available method (Lefebvre and Herbret (1960)) which is based on mean beam length.

The basis is that the gas would be considered gray. Hence k would be a constant, independent of wavelength. Integration of eqn(6.1) over a mean path length l , characteristic of the given combustor geometry, leads to

$$I = (1 - e^{-kl}) \frac{E_b}{\pi} \quad \dots(6.4)$$

If the surface is assumed to radiate diffusely, then

$$E = \pi I \quad \dots(6.5)$$

Hence,

$$E = (1 - e^{-kl}) E_b \quad \dots(6.6)$$

$$\begin{aligned} \text{where } E_b &= \sigma T^4 \\ \epsilon &= \text{emissivity} \\ &= 1 - e^{-kl} \end{aligned}$$

Thus radiation emission, is evaluated based on emissivity, which is empirically correlated using the mean beam length, and other operating conditions.

This is the simplest of the available techniques. However, this can only predict average radiation heat flux; radial non-uniformities of radiative properties are not accounted for.

6.3 HEAT BALANCE

Representing the various heat fluxes of the liner as shown in Fig 6.1, heat balance can be attempted. Under equilibrium conditions the liner temperature is such that the internal and external heat fluxes at any point are just equal. Loss of heat by conduction along the liner wall is comparatively small and is neglected for ease of calculations.

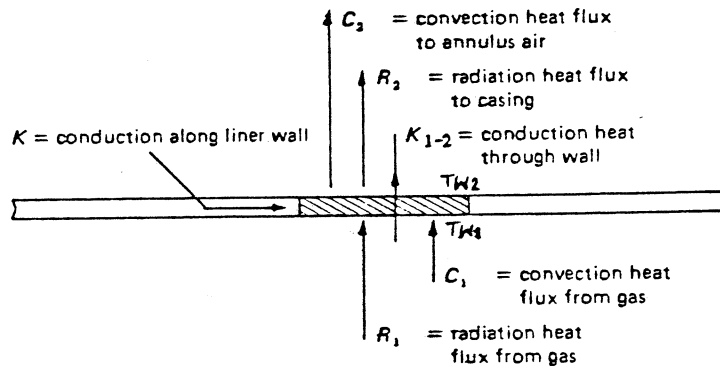


Fig 6.2 Basic Heat Transfer Processes.

The heat transfer model shown as Fig 6.2, includes only the axial variation of properties. Under steady-state conditions, the rate of heat transfer into a wall element must be balanced by the rate of heat transfer out. Therefore, an element with inside surface area ΔA_{w1}

$$(R_1 + C_1) \Delta A_{w1} = (R_2 + C_2) \Delta A_{w2} = K_{1-2} \quad \dots(6.7)$$

Evaluation of individual terms and subsequent balance yields the liner wall temperature for any operating condition.

However, the above simple balancing procedure soon gets complicated when cooling channels (single or double) are introduced. The number of equations will be 5 and 8 respectively (as shown in Fig 6.3).

NOTE: The notation in Fig 6.3 is different in that, R_1 is represented by $RR1$, C_1 by $CC1$, and K_{1-2} by $KK12$. Similarly for the other skins also this changed notation holds good.

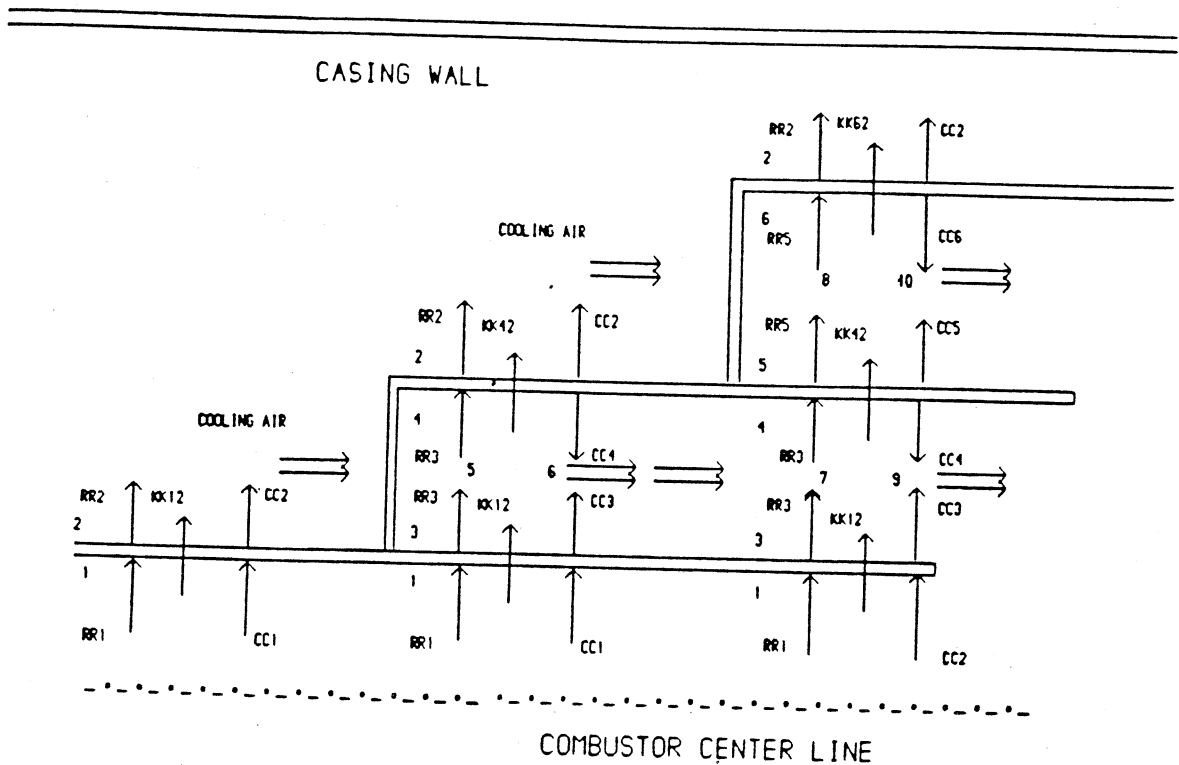


Fig 6.3 Heat Balance Configurations

6.3.1 METHOD OF SOLUTION

The solution of these non-linear equations is carried out using NAG subroutine C05NCF (detailed information is attached as Appendix L).

At the development stage of the program this NAG library has been made use of. Obvious advantages are simple to use and no need for additional coding. In order to improve the programme's stand alone capability, use of external libraries need to be avoided. Hence recourse is taken to account for this. The solution of these non-linear equations is carried out using modified Newton Raphson method with Gaussian elimination technique, which is explained as Appendix M.

The choice of correlations for coefficients will largely depend on the past experience and availability. However, every effort is made to locate the best available expressions representative of all the configurations that are intended to be analyzed. It is worthwhile to highlight the advantage of modular structure programmes where the user defined correlations can be very easily introduced into the programme.

6.3.2 INTERNAL RADIATION :

The radiative interchange rate at a black bounding surface at uniform temperature is given by Hottel(1967) as:

$$R_1 = \sigma (\epsilon_g T_g^4 - \alpha_g T_{w1}^4) \quad \dots(6.8)$$

When gray walls of emissivity ϵ_w are considered, partial absorption occurs leading to multiple reflections and absorptions. The resulting sum is the gas to wall flux, which must be smaller than for a black walled system by a factor lying between ϵ_w and 1. If the emissivity is high, ($\epsilon > 0.8$), the use of the factor $0.5(\epsilon_w + 1)$ as a multiplier to eqn (6.8) cannot lead to much error. Thus,

$$R_1 = \sigma \left(\frac{\epsilon_w + 1}{2} \right) (\epsilon_g T_g^4 - \alpha_g T_{w1}^4) \quad \dots(6.9)$$

This is adopted by Lefebvre and Herbert (1960). They further approximated the above expression with

$$\left(\frac{\alpha_g}{\epsilon_g} \right) = \left(\frac{T_g}{T_{w1}} \right)^{0.5} \quad \dots(6.10)$$

leading to

$$R_1 = \sigma \left(\frac{\epsilon_w + 1}{2} \right) \epsilon_g T_g^{1.5} (T_g^{2.5} - T_{w1}^{2.5}) \quad \dots(6.11)$$

However, considering the need to incorporate coatings and materials of low emissivities, a more rigorous approach is followed where allowance for non gray radiation is also included. This leads to (Hottel (1967))

$$R_1 = \sigma \epsilon_w \left(\frac{\epsilon_g T_g^4}{\epsilon_g + \epsilon_w - \epsilon_g \epsilon_w} - \frac{\alpha_g T_{w1}^4}{\alpha_g + \epsilon_w - \epsilon_w \alpha_g} \right) \quad \dots(6.12)$$

FLAME EMISSIVITY :

Reeves (1956) correlated Hottel's graphical data of flame emissivities of water vapour and carbon-dioxide at various temperatures and pressures and developed expression for emissivities of non-luminous flames given fuel/air ratio and

operating conditions. These are corrected for luminosity by multiplying with luminosity factor.

for distillate fuel $\sim \text{CH}_2$:

$$\epsilon_f = 1 - \exp(-0.286 L P (fl)^{0.5} T_g^{-1.5}) \quad \dots(6.13)$$

for distillate fuel $\sim \text{CH}_{1.5}$:

$$\epsilon_f = 1 - \exp(-6.378 L P^{0.75} (fl)^{0.5} T_g^{-1.5}) \quad \dots(6.14)$$

where L = luminosity factor

l = mean beam length

f = fuel air ratio

LUMINOSITY FACTOR

The uncertainty of evaluating exactly the soot forming and consumption processes is lumped in one fiddle factor. The fidelity of the approach yielded many correlations of which, the expression by Kretschmer and Odgers (1978) is chosen considering it is the best fit of available data, and it is accepted that carbon hydrogen ratio is a fair measure of luminosity.

$$L = 0.0691 (C/H - 1.82)^{2.71} \quad \dots(6.15)$$

where C/H = carbon, hydrogen mass ratio

The above expression is limited to fuels having molecular weight of 44 or above, provided that

- 1) the fuel is a saturated hydrocarbon
- 2) it is commercial liquid fuel ranging from gasoline to fuel oils

The estimated accuracy is $\pm 25\%$ and range of variation is as shown in the Fig 6.4.

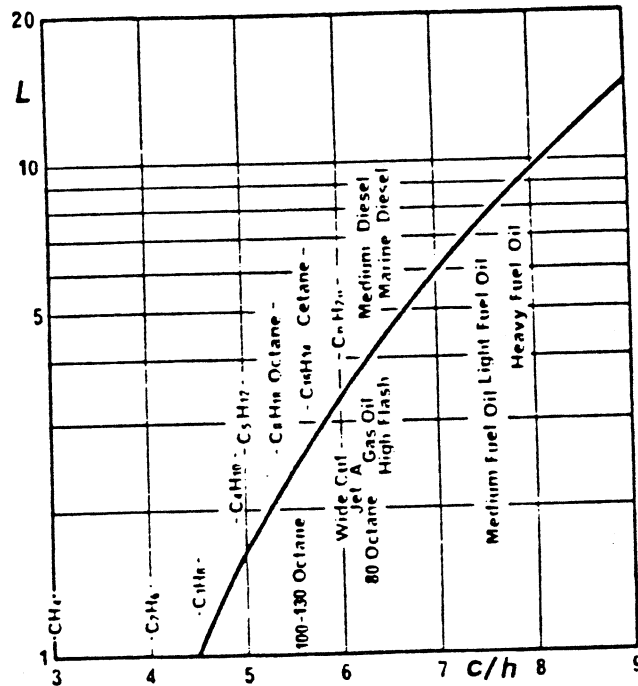


Fig 6.4 Effect of fuel carbon/hydrogen on flame luminosity

MEAN BEAM LENGTH

The beam length is determined by the size and shape of the gas volume. For most practical purposes it is given with sufficient accuracy by the expression

$$l = 3.4 \frac{\text{volume}}{\text{surface area}} \quad \dots(6.16)$$

However, in the programme the following are made use of,

Tubular

$$l = 1.2 \text{ Rad} \quad \dots(6.17)$$

Annular

$$l = 1.14 (\text{Rad}_o - \text{Rad}_i) \quad \dots(6.18)$$

where

Rad denotes radius, with o and i signifying the outer and inner respectively)

FLAME ABSORPTIVITY :

Using Kirchhoff's radiation law which states in essence that the monochromatic emittance is equal to the monochromatic absorptance for any surface. ie.

$$\epsilon_{\lambda}(\lambda, T) = \alpha_{\lambda}(\lambda, T) \quad \dots(6.19)$$

Hence absorptivity is evaluated using similar expression as for emissivity but evaluated at wall temperature.

6.3.3 ANNULAR RADIATION :

The heat transferred by radiation from the flame tube to the casing is generally small compared to the external convective heat transfer. Its significance, however increases with the flame tube wall temperature due to its quartic nature (Lefebvre (1983)). It is reasonable to assume that the casing wall temperature is identical to that of the compressor delivery temperature. The following expression by Hottel and Sarofim (1981) reasonably represents the radiation across the annular space :

$$R_2 = \sigma \frac{\epsilon_w \epsilon_c}{\epsilon_c + \epsilon_w (1 - \epsilon_c) (A_w / A_c)} (T_{w2}^4 - T_{in}^4) \quad \dots(6.20)$$

6.3.4 INTERNAL CONVECTION**UNCOOLED SECTION :**

The uncooled section is that which does not employ film cooling. Following relation is accepted as the best available, considering the process involving gases which are at high temperature and undergoing rapid physical and chemical change. As the flame tube can be reasonably be assumed to be a straight pipe, the appropriate classical heat transfer for extreme turbulence, as proposed by Lefebvre and Herbert (1960) is used.

$$St = 0.0283 Re^{-0.02} \quad \dots(6.21)$$

$$C_1 = 0.02 \frac{\lambda}{Hd^{0.2}} \left(\frac{\dot{m}}{A_L \mu_g} \right)^{0.8} (T_g - T_{w1}) \quad \dots(6.22)$$

However, the constant in the above equation is changed to 0.017 for the primary zone calculations in order to account

for various other factors like recirculation, temperature profile etc.

The following uncertainties, though highlighted at the time of proposing, do remain till date.

- 1) Though the analogy is taken from fully developed turbulent pipe flow, the conditions in the primary zone contains by design a reversal of flow so that only in a region adjacent to walls does the direction of flow correspond to that of the assumed pipe analogy. It is difficult to precisely allocate a value of (m/A_L) , however, no allowance is made for such discrepancy.
- 2) The average heat transfer over the length of a pipe from its entrance is known to depend and vary quite considerably with length/diameter ratio, so called thermal entry effects. However, considering the extreme turbulence, it is reasonable to assume that the value derived closely represents the stirred flow in the combustor.
- 3) The question of which temperature to be used for evaluating the properties is another major one. Here we have a situation of gas temperature having both radial and circumferential variation, whose bulk static temperature is used for radiation calculation. Another assumption is that considering the low mach numbers, the total and bulk temperatures are indistinguishable. The gas temperature T_g for convection calculations will obviously be between the bulk static and the wall temperature T_w . Variety of approaches are being followed. Either, end temperatures ie. bulk or wall temperature or a mean between the bulk and wall temperatures, at which all the properties could be evaluated. When bulk temperature is used, it is normally corrected by $(T_g/T_w)^m$ where $m=0$ to 0.5 for high to low Reynolds number. In the present study, however, the bulk mean total temperature itself is used.

COOLED SECTION :

In order to supplement the removal of heat from the liner by external radiation and convection, a film cooling air on the inside of liner wall may be used. Essentially it makes use of a number of annular slots through which air is injected axially along the inside wall of the liner, to provide a protective film of cooling air between the wall and hot combustion gases. The cooling film is gradually destroyed by turbulent mixing with the hot gas stream, so that a

succession of slots at about 4 to 8 centimeter intervals along the length of the liner may be provided. A basic limitation of the method is that it does not allow a uniform wall temperature. The heat sink potential of the cooling air is not effectively utilized since the wall adjacent to the slot is inevitably overcooled. Advanced cooling materials such as porous surfaces are the ideal, and technology is striving to overcome limitations such as structural weakness and clogging. Till the ideal is available, the existing techniques have to be made use of effectively. The following film cooling devices are being examined.

The cooling devices that are being used are shown conceptually below. They appear in the decreasing order of amount of cooling air required

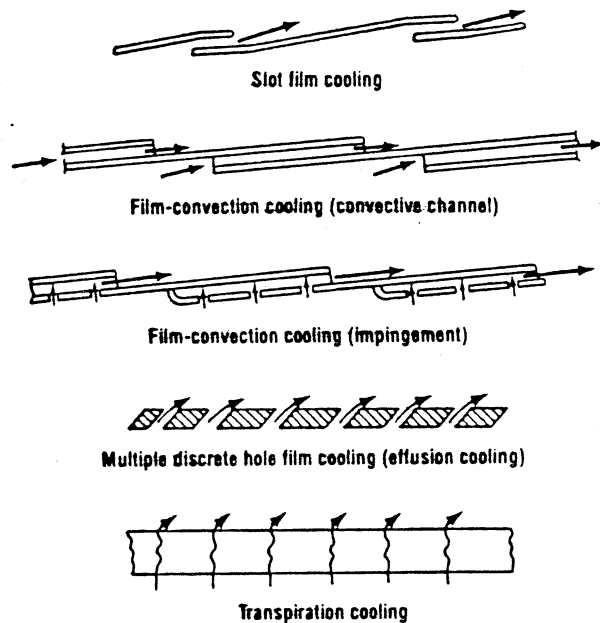


Fig 6.5 Trends in amount of cooling air employed

The simple slot film cooling has traditionally received the most attention both in terms of application and fundamental studies. Some of the variations of the simple slot are presented as fig 6.6.

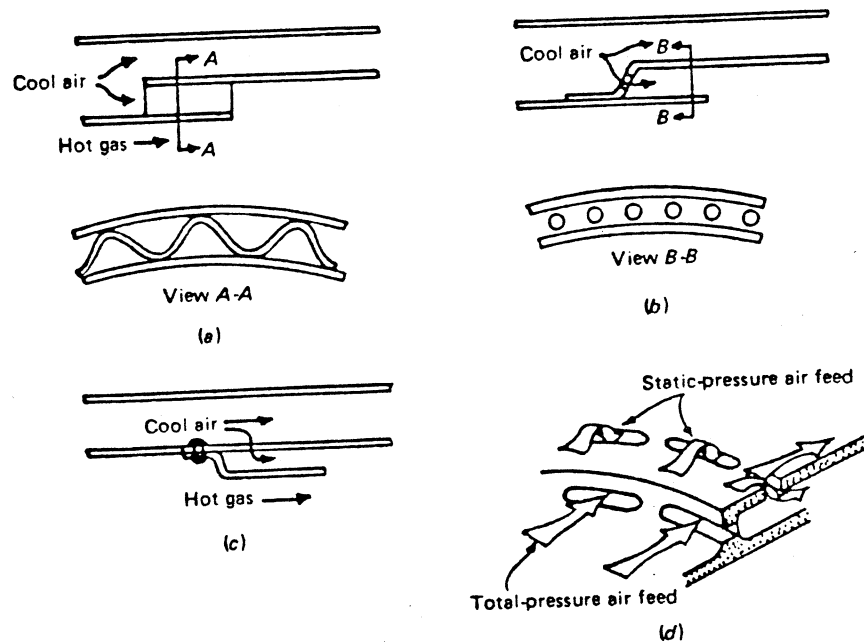


Fig 6.6 Cross section of film cooling devices. a) wiggle strip. b) stacked ring c) splash cooling d) machined ring

However, the present study has limited to the following devices.

- 1) Unobstructed Gap
- 2) Wiggle Strip Slot
- 3) Splash Cooled Type
- 4) Impingement cooling
- 5) Convective channel (double walled cooling)

NOTE : The notation followed to differentiate splash from impingement cooling is that splash has just one row of holes and hence one row of impingement jets, whereas impingement cooling has several rows of jets. In other words, impingement cooling is an extension of splash cooling along the axial length.

DESIGN

Sturgess (1985) established MIX grouping to describe the performance of a machined ring. But for the other types, no such published information is available. Hence, broad design guide rules interms of lip length selection or cooling flow

estimation are incorporated for guidance. The temperature results and effectiveness decay should provide adequate feedback for improved designs.

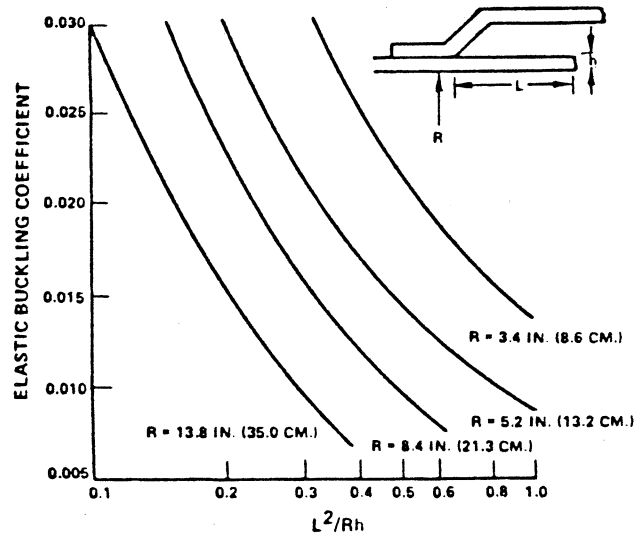


Fig 6.7 Elastic buckling geometry relationship (Sturgess (1980))

The lip lengths are normally less than 2 cm. Experience suggests that for a large diameter combustor, L^2/Rh should have a value less than 0.1 to avoid lip buckling.

FILM COOLING CORRELATING PARAMETER

When a wall is film cooled by injecting a stream of air between the surface and the hot main stream flow, three separate flow regions may be identified as shown as fig 6.8 (Stollery and El-Ehwany (1965)).

The first flow region comprises a potential core, in which the wall temperature remains close to the coolant-air temperature. This is followed by a zone where the velocity profile is similar to that of a wall jet. Further downstream, the flow conditions approximate to those in a turbulent boundary layer. The relative lengths of the three regions are governed mainly by the velocity ratio U_c/U_g . For $U_c < U_g$, the second zone is nonexistent, and a turbulent boundary-layer model is appropriate for regions downstream of the potential core. In some practical devices, there is a rapid mixing at the entry region, raising the coolant inlet temperature.

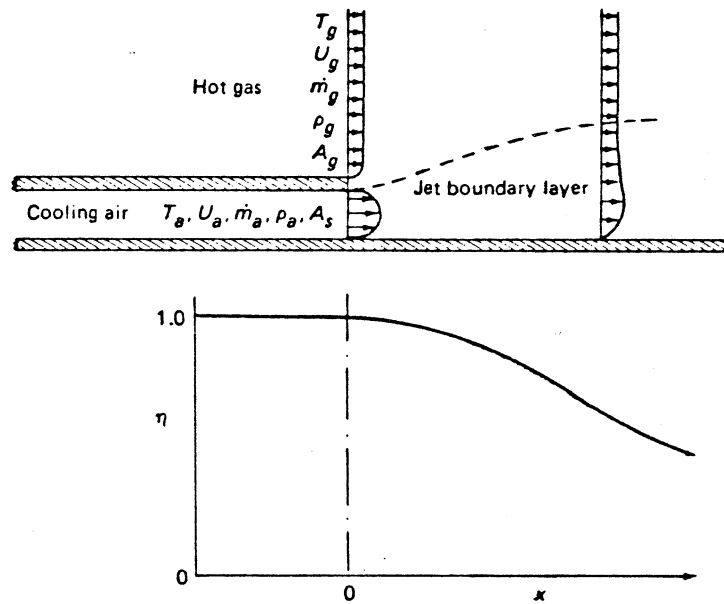


FIG 6.8 Schematic of film cooling process.

The concept of well known film cooling effectiveness defined as

$$\eta = (T_g - T_{wad}) / (T_g - T_c) \quad \dots(6.23)$$

is accepted as a practical means relating the performance of any cooling device. A variety of expressions (Stollery et. al. (1965)) exist to describe the wall adiabatic temperature variation with the distance. The form of parameter chosen for the present work is that of Winter (1963), for the following reasons:

- . it is very effective at correlating a wide variety of test data
- . it has yielded acceptable wall temperature predictions for a variety of combustors
- . according to Schofield, Moore (1963), this gives less scatter than others when tested over a wide range of conditions.

WINTER PARAMETER :

$$\chi = k \left(\frac{\dot{m}_g A_c}{\dot{m}_c A_g} \right)^{0.8} \left(\frac{T_g}{T_c} \right)^{0.6} \left(\frac{x}{s} \right)^{0.8} \quad \dots(6.24)$$

where $k = 1.0$ when $U_g/U_c > 0.8$
 $k = (U_g/U_c + 0.2)^{-1.25}$ when $U_g/U_c \leq 0.8$

Programme makes use of effectiveness variation with Winter parameter χ

$$\eta = f(\chi) \quad \dots(6.25)$$

The correlations employed are the best from the available literature. It may be highlighted that they may not be universal. User will have the option to change any of the correlations to one in which he has better confidence. However, the form that are included in the programme are (Bergquist (1975)):

Unobstructed Gap:

$$\eta = 1.0 - 0.00204 \chi^{1.34} \quad \dots(6.26)$$

Splash Cooled:

$$\eta = 1.0 - 3.032E-2 * \left(\ln(0.6953 \chi) \right)^{2.178} \quad \dots(6.27)$$

Wiggle Strip:

$$\eta = 1.0 - 4.84E-4 * \exp\left(2.77 \chi^{0.236}\right) \quad \dots(6.28)$$

For any clean 2D slot the following after Ballal and Lefebvre(1973) is also included

for $x/ms < 8$:

$$= 1.0$$

for $8 < x/ms < 11$:

$$= \left(0.6 + 0.05 \frac{x}{ms} \right)^{-1}$$

for $x/ms > 11$:

$$= 0.7 \left(\frac{x}{s} \right)^{-0.3} \left(\text{Re}_s \frac{\mu_c}{\mu_g} \right)^{0.15} m^{-0.2} \quad \dots(6.29)$$

$$\text{where } m = (\rho U)_c / (\rho U)_g$$

These equations can be applied to near slot regions provided the thickness of the slot lip is small in relation to slot

height. However, for mechanical integrity, the lip is sometimes made quite thick. In those circumstances, the following correction (Lefebvre(1972)) is applied, to account for the slot lip thickness, t .

$$\text{Correction Factor} = 1.83 \left(\frac{x}{s}\right)^{0.1} \left(\frac{t}{ms}\right)^{-0.2} (Re_s)^{-0.15} \quad \dots(6.30)$$

No specific correlation could be obtained for impingement or convective channel cooling configurations. It is assumed that the effectiveness variation for impingement type is the same as that of splash cooled and for the convective channel that of wiggle strip. This assumption appears reasonable considering the similarities in the downstream flow in both pairs.

The adiabatic wall temperature thus obtained is used to calculate the heat convected using appropriate film coefficient relations of the form

$$Nu = f (Re_s, x, s)$$

FILM HEAT TRANSFER COEFFICIENT

As suggested by Ballal and Lefebvre (1972), the flow field at the injection point becomes a significant variable for the definition of heat transfer coefficient.

$$m = \text{mass velocity ratio} = \frac{(\rho U)_c}{(\rho U)_g} \quad \dots(6.31)$$

Their analysis revealed that when the mass flow ratio m is less than 1.3, the near slot region ($x/s < 50$) can be described by a boundary layer model while for higher mass flow rates it represents a wall jet model.

BOUNDARY LAYER MODEL ($m < 1.3$)

The model yields

$$Nu = 0.069 \left(Re_s \frac{x}{s}\right)^{0.7} (T_{wad} - T_{w1}) \quad \dots(6.32)$$

$$C_1 = 0.069 \frac{\lambda}{x} \left(Re_s \frac{x}{s}\right)^{0.7} (T_{wad} - T_{w1}) \quad \dots(6.33)$$

WALL JET MODEL ($m > 1.3$)

The model yields

$$Nu = 0.10 Re_s^{0.8} \left(\frac{x}{s} \right)^{0.44} (T_{wad} - T_{w1}) \quad \dots(6.34)$$

$$C_1 = 0.10 \frac{\lambda}{x} Re_s^{0.8} \left(\frac{x}{s} \right)^{0.44} (T_{wad} - T_{w1}) \quad \dots(6.35)$$

Here all the property evaluation is done at the T_{wad}

IMPINGEMENT COOLING

Higher heat transfer coefficients can be achieved on the external forced convection by means of impingement cooling. The impingement cooling review by Beccko (1976) for the turbine blade cooling provides useful relations that are available currently. For one line of round jets on a plane wall, Gardon and Cobonpue (1962) obtained the following expression:

$$\begin{aligned} \overline{Nu}_{d(0-x/d)} &= 0.247 Re_d^{0.625} Pr^{0.33} \left(\frac{d}{x} \right)^{0.375} && \text{for } z/d < 6.63 \\ &= 0.806 Re_d^{0.625} Pr^{0.33} \left(\frac{d}{x} \right)^{0.375} \left(\frac{d}{z} \right)^{0.625} && \text{for } z/d > 6.63 \end{aligned} \quad \dots(6.36)$$

where d = dia of the hole
 x = downstream distance
 z = jet to plate distance

The effect of transversal flow added along the wall was investigated by Metzger and Korstad (1972), who suggested a new parameter M^* , where

$$M^* = \frac{m_t}{m_j}$$

when m_t and m_j are respectively the total flow rate along the wall and the flow rate only due to the jets. However, they found a weak dependence of M^* as:

$$Nu_{dav} = 0.065 Re_d^{0.662} Pr^{0.333} M^{*-0.049} \quad \dots(6.37)$$

This correlation is appropriate to use for splash cooling slots, where there is one row of impingement hole. As the evaluation is in a discrete control volume in a marching fashion, there is a need to differentiate between average to instantaneous value. However, it is beyond the scope of analytical work to derive exact solutions for a turbulent field. The best way to utilize the available information is, to treat the maximum heat transfer coefficient right under the impingement jet with $d/x=2$. Then the value reduces with d/x , as x increases from $d/2$.

The beginning of the slot, upstream of the hole, though small in length, poses computational problem. It does not know what lays ahead and also how much of air impinged recirculates back. For the present an average value is assumed for this initial region, till a better scheme is devised in future, where in temperature calculation is done in an iterative manner. Instead of assuming a minimum value of Nusselt number for a typical splash cooled configuration, (which is around 30 to 60), it is felt better to assume a minimum mass flow which is 2% of the total flow for annular and 3% for of the total flow for the tubular. Corresponding heat transfer coefficients are evaluated based on pipe flow.

Gardon and Akfirat (1966) have extended the previous single row to two dimensional array of jets. But the average heat transfer coefficients were correlated by the equation

$$Nu_{av} = 0.36 Re_{av}^{0.62} \quad \dots(6.38)$$

$$\text{and } Re_{av} = \frac{U_a x_N \rho}{\mu} \quad \dots(6.39)$$

$$\begin{aligned} U_a &= \text{arrival velocity} \\ &= U_e \quad (\text{for } z_n/B \leq 7) \\ &= U_e \sqrt{\frac{7B}{z_n}} \quad (\text{for } z_n/B > 7) \end{aligned}$$

where U_e = jet velocity
 x_n = spacing between centers of nozzles
 z_n = nozzle to plate distance
 B^n = width of slot nozzle
 d = diameter of the nozzle

The departure from standard notation, according to the authors, is justified by the utility of the resulting

correlations. It is interesting to note that the combustor field has to rely on the above equations which are actually developed for the annealing of non-ferrous metals and the tempering of glass.

One major difference in the cooling configuration, in deriving the above equations, is that the jets are not confined i.e. after impinging they do not have a predominant way to escape. A more tried out relation is by Singh(1972), which is an extension to the above, correlating the existing data. The final form is as given :

$$\log_{10}(S) = C_1 \log_{10}(x_n/z_n) + C_2 \quad \dots(6.40)$$

$$\text{where } C_1 = -0.8950468$$

$$C_2 = -0.8085483$$

$$\text{where } S = St_{av}^{1/3} Re_{av}^{2/3} Pr^{1/5} (z_n/d) \quad \dots(6.41)$$

$$Re_{av} = \frac{U_{av} x_n \rho}{\mu}$$

The arrival velocity is calculated, using the expression as suggested by Gardon and Cobonpue (1962), which is of the form

$$U_{av} = \frac{6.63 d U_e}{z_n} \quad \dots(6.42)$$

The present work has incorporated these correlations.

However, even the above equations are more appropriate to use for an average value over an array of impingement holes. The above derivation is strictly for a square matrix, in the sense equal separation of jets in the x and y directions, ie. along the axis and circumference respectively. When the spacing along the axial length greatly differs from that of circumferential spacing, it is difficult to attribute a value to X_n .

Better predictive ability appears to be obtained from the correlations of Florschnetz, Truman and Metager (1981). Their investigation covers a two-dimensional array of circular jets of air impinging, with the air, after impingement is constrained to exit by the surface in single direction along the channel formed by the surface and the jet plate, as shown :

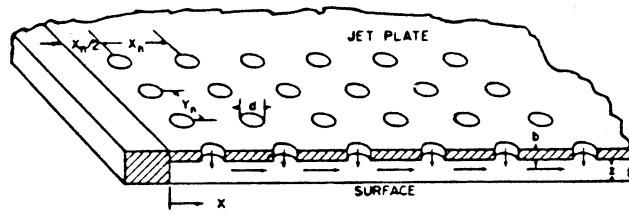
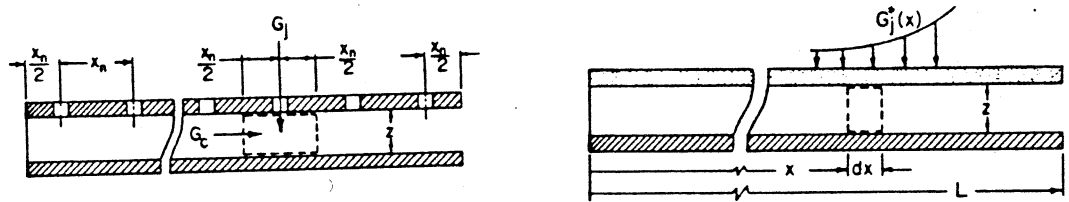


Fig 6.9 Basic model geometry and nomenclature

The advantage is that it could be used for any horizontal spacing, including a continuous injection (theoretically).



a) Discrete hole injection b) Continuous injection model

Fig 6.10 Impingement injection type

The final correlation is of the form

$$Nu = A Re_j^m [1 - B\{(z_n/d)(G_c/G_j)\}^n] Pr^{1/3} \quad \dots(6.43)$$

where

$$A, m, B, n = C (x_n/d)^x (y_n/d)^y (z_n/d)^z \quad \dots(6.44)$$

with the following coefficients

	Inline Pattern				Staggered Pattern			
	C	n_x	n_y	n_z	C	n_x	n_y	n_z
A	1.18	-0.944	-0.642	0.169	1.87	-0.771	-0.999	-0.257
m	0.612	0.059	0.032	-0.022	0.571	0.028	0.092	0.039
B	0.437	-0.095	-0.219	0.275	1.03	-0.243	-0.307	0.059
n	0.092	-0.005	0.599	1.04	0.442	0.098	-0.003	0.304

Table 6.1 Constants for Impingement Correlation

The model is derived for the following range of variables

Re_j	2.5×10^3	to 7×10^4
G_c/G_j	0	to 0.8
x_n/d	5 to 15	for inline
	5 to 10	for staggered
y_n/d	4	to 8
z_n/d	1	to 3

Using the correlations beyond these values is questionable. However, the range appear to be within typical values found in combustion chambers.

This yields comparable results with that of Eqn 6.40. Both the equations are, however, incorporated in the programme.

CONVECTIVE CHANNEL

This class of cooling technique appear to be referred to by a variety of names. Combined film cooling and augmented external convection (Lefebvre (1983)), film/convection cooling (Sjoblom (1984)), convective channel (Nealey et al. (1985)) or simply double walled cooling (author) are all synonyms for this alternate technique, which is sure to find wider application. The convective channel arrangement (Nealey (1985)), as shown, relies largely on the axial

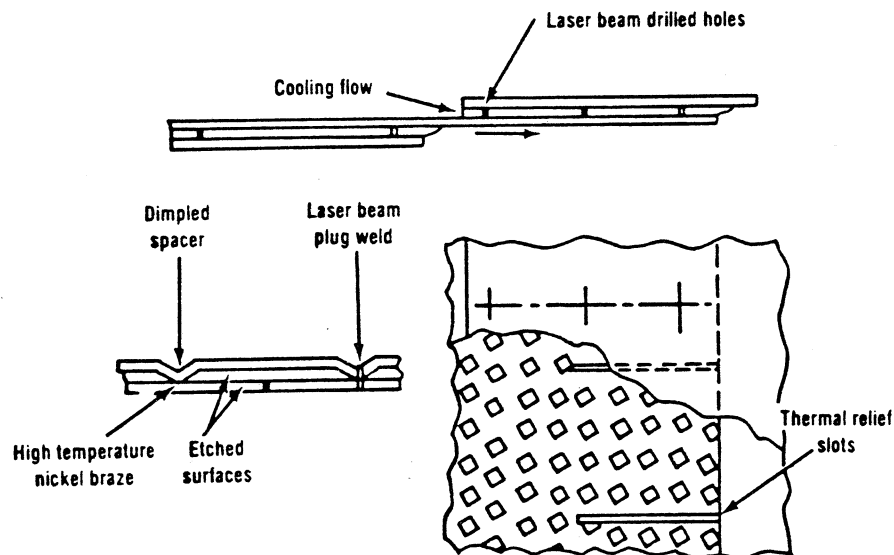


Fig 6.11 Typical Convective channel arrangement

velocity of the coolant through the double wall channel region to achieve cooling of the liner inner surface prior

to tangential injection of the air film.

No specific correlations are put forward in the available literature. Sjoblom (1984) treats the channel as pipe flow, the same analogy drawn for the entire combustor. However, it may raise skepticism due to the narrow height of the channel, in relation to the diameter of the combustor. For a typical 30 cm reference diameter with 2 mm slot height amounts to a ratio $d/h = 150$. In such high ratios, it may appear better to consider the system as parallel plates. However, the available literature does not give simple equations for them either. Kays (1966) presented the Nusselt number data for infinitely long parallel plates. Comparison of that with the pipe analogy leads to

Pr = 0.7 Re		4 10	4 3x10	5 10	5 3x10	6 10
1	Nu parallel plates	27.8	61.2	155	378	1030
2	0.8 0.02Re	31.7	76.3	200	482	1262
3	0.785 0.02Re	27.6	65.4	168	399	1026

Table 6.2 Nusselt No comparison for parallel plate and pipe analogies

The last two rows show the results by assuming the pipe analogy (eqn 6.21) with standard constants and the second due to a possible new correlation. No doubt, the second correlation gives closer result, but no attempts or claims are being made due to insufficient experimental data. Also the difference in values and the uncertainty in the parallel plate assumption are of the same order. Hence the evaluation procedure for the convective channel is same as the external convective heat transfer coefficient, except that when heat balance is being made an additional wall is considered.

SURFACE ROUGHNESS

The above cooling rates can be enhanced by artificially roughening one or both of the coolant side channel surfaces. The order of increase is qualitatively shown as (Nealey (1985))

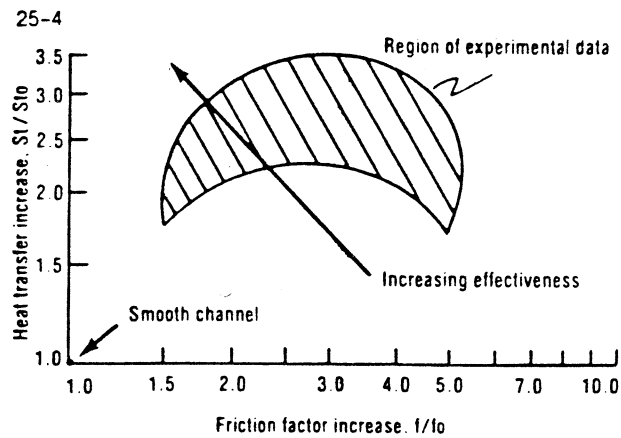


Fig 6.12 Heat Transfer characteristics of artificially roughened surfaces

Kays (1966) semiempirically related the Nusselt number increase, for air at $Pr=0.7$, through friction coefficient as

$$\frac{Nu}{Nu_{smooth}} = \left(\frac{f}{f_{smooth}} \right)^{0.5} \quad \dots(6.45)$$

The empirical data is based on values corresponding to pipes. But, this seem to reasonably represent the above data (fig 6.12). The increase could be due to the proximity of both the surfaces in a convective channel. However, this relation will be introduced into the programme as a qualitative measure.

It has also been observed by Nealey (1985), that channels with only one roughened surface exhibited about half the pressure drop (at a given flow rate) of comparable channel with both surfaces roughened. However, the configurations with only roughened surface exhibited almost the same heat transfer coefficient level as the channel with both surfaces roughened. Apparently, the induced turbulence and extended surface area of the heated wall alone control the overall heat transfer rates to a significant extent.

EFFECTIVE FLOW AREA

When film cooling is employed the effective geometrical area, including the effects of blockage need to be evaluated. It is felt easier to express this as a fraction of the available slot area, which is calculated based on liner radius and the height of the slot. However, only a fraction of the above area would be utilised for the actual

flow, due to the blockage of stiffeners, supports or wiggles. The guidelines to evaluate the fraction are as follows:

- 1) Unobstructed Gap: It is assumed to be fairly high (0.8).
- 2) Wiggle Strip : The wiggles are approximated to triangular strips and blockage is accordingly calculated, as per the method devised Appendix M.
- 3) Stacked Ring : The total hole area is calculated which is actually the flow area. Hence the fraction here simply the ratio of this area and the slot area.

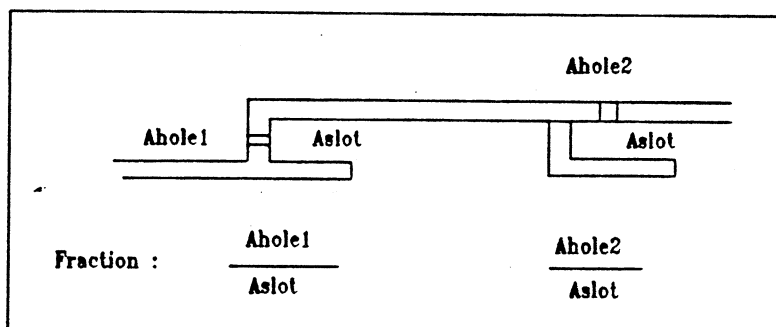


Fig 6.13 Flow Area Fractions

Then discharge coefficient is applied on this fraction to arrive at the effective flow area.

$$\text{Effective Area} = \text{Aslot} \times \text{Fraction} \times C_d$$

There is no published procedure available to evaluate their C_d s. However, being total head devices, in most cases it can be assumed to be very high between 0.75 and 0.8. However, C_d s for the impingement or splash holes will be lower, being evaluated on the lines of a mixing hole.

6.3.5 EXTERNAL CONVECTION :

This component is estimated by making the same assumptions of pipe flow as was done for the internal convection in the uncooled section. The Reynolds number in this case, however, is based on the hydraulic mean diameter of the annulus. The fluid properties are evaluated at the bulk annulus air temperature, same as the combustor inlet temperature. In practice, the cooling air temperature will increase during

its passage downstream, but its increase is neglected due to its small effect.

$$C_1 = 0.02 \frac{\lambda}{Hd^{0.2}} \left(\frac{\dot{m}_{an}}{A_{an}\mu} \right)^{0.8} (T_{w2} - T_{in}) \quad \dots(6.46)$$

6.3.6 WALL CONDUCTION :

The heat flow through the liner wall is calculated by assuming the liner as multi-layered cylinder (Kreith(1976)). This becomes true if there is a coating on the inside of the liner wall, otherwise only the thickness of the liner wall need to be considered.

$$\frac{K_{1-2}}{x} = 2 \pi \frac{(T_{w1} - T_{w3})}{\frac{\ln(r_2/r_1)}{\lambda_1} + \frac{\ln(r_3/r_2)}{\lambda_2}} \quad \dots(6.47)$$

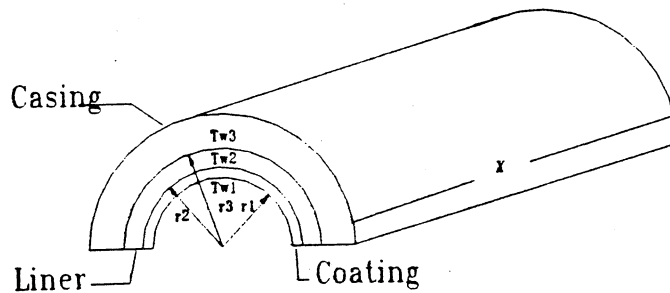


Fig 6.14 Heat Transfer by Conduction

6.3.7 ADDITIONAL MEASURES

A good maximum design temperature for commercial life requirements with materials (Nickel and Cobalt based alloys such as Nimonic 75 and Hastelloy X, and C 263 and Haynes 188) is 925-975 K. In order to combat higher liner temperatures, additional methods such as a thin coating of thermal barrier may be required. Though stability of coatings is still much desired, they offer the immediate advantages till alternate

materials developed. Liner wall coatings can reach thicknesses upto 0.5 mm. Typical materials and their properties are described in subsequent paragraphs. The Parametric study of wall temperature variation with and without coating for Case 2 (rest of the details are described in Chapter 11) is shown as Fig 6.15 to indicate the benefits.

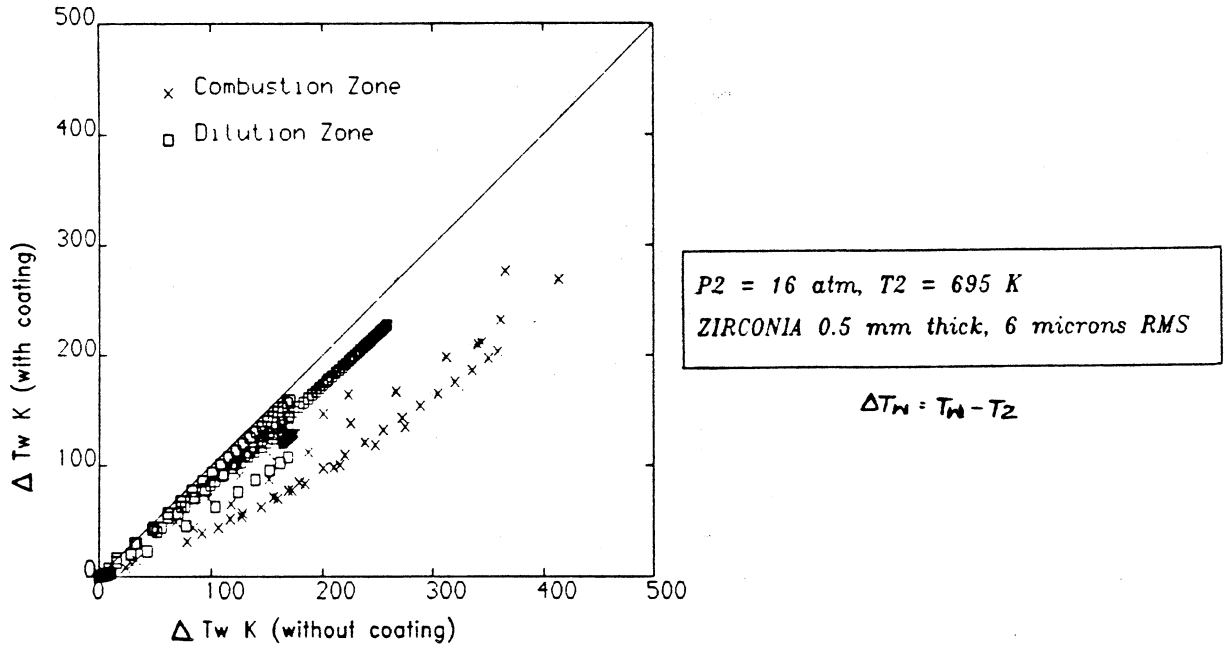


Fig 6.15 Effect of Coating on Wall Temperatures (Case 2)

6.3.8 PROPERTIES

TRANSPORT

The transport properties, λ and μ are mainly required for the film cooling air and hence the function correlated by Kretschmer and Odgers (1978) is made use of during the initial development

$$\frac{\lambda}{\mu^{0.8}} = 74.811 + 1.674 T^{0.75} - 0.0081599 T^{1.5} + 2.2539E-5 T^{2.25} - 2.5287E-8 T^3$$

..(6.48)

However subsequently the properties generated by the programme explained in the chapter 5 is made use of.

MATERIALS

The properties emissivity and conductivity for typical liner and coating materials are stored as data, though not exhaustive at this stage. These values are known to be temperature dependent. But obtaining information as a function of temperature is time consuming. The mean values are quoted as Appendix N.

It has been experimentally correlated by Ubhi (1987), the effect of temperature along with thickness and surface roughness of coating, on emissivity. According to his study, the emissivity of a coating can be expressed as:

$$= f(\text{Thickness, Surface Temperature, Roughness}) \\ = A(1) + A(2)\exp(-C T/100) \quad \dots(6.49)$$

where

$$A(J) = X(1,J) + X(2,J) t + X(3,J) R + X(4,J) tR \quad J=1,2$$

$$t = (\text{thickness of coating in m}) \times 1000,$$

$$R = (\text{RMS of surface roughness in } \mu\text{m}) \times 10^5,$$

(! The constants 1000 and 10^5 are introduced to size the coefficients $X(i,j)$ to appreciable figures)

$$T = \text{surface temperature in } ^\circ\text{C}$$

$$C = \text{a constant}$$

The range of applicability is 0.1mm to 1mm for the thickness and 2 to 10 μm for the surface roughness value). The coefficients for alumina and zirconia are listed as Appendix 'N'.

This data is also made use of, though limited for few materials at this stage. Such detailed, approach may sound superfluous for the present model. But the emphasis is on the utility of the present programme in comparing these sub-models relatively easily. These results are presented as case 4C and 4D, in Chapter 11.

CHAPTER 7

COMBUSTION EFFICIENCY AND FLAME STABILITY

7.1 REQUIREMENT

Two of the primary design goals of any combustor are to attain the highest possible combustion efficiencies whilst providing the largest possible stability limits within the operating environment. So far, designers are able to achieve these criteria with quite a reasonable confidence level. However, a critical review of the available information indicate the absence of quantitative expressions for efficiency and stability limits that can be applied to any gas turbine combustor in general. The reason, quite obviously, is due to the fact that there is no one single rate limiting process. This can vary from system to system and in a system from situation to situation. However, extensive work, was undertaken between 1950-70, which, laid out a good foundation for the combustor design field, however, empirical or qualitative they may appear. Though, the underlying mechanism at a macro level is very clear and understood, the microlevel quantification is a bit involving and doesnot permit itself to be generalized in few simple relations.

With the interest of laying down the rules for double combustor, it is necessary to reopen the investigation chapter for these two criteria. Hence the need for qualitative as well as quantitative generalization of combustion efficiency and stability limits, when the combustor has to work with vitiated oxidant medium.

7.2 BACKGROUND

7.2.1 COMBUSTION CHAMBER

A broad classification of the many different kinds of combustion chamber is given as Table 4.1. The existing multitude of combinations can even be doubled since there are two well-defined philosophies by which air is added to the chamber; the first being small and frequent additions, otherwise commonly known as pepperpot configuration, and the second with large and infrequent additions. These combinations can even be complicated by the way in which fuel is added, upstream or downstream or staged injection. It is not the purpose here, to argue the merits and demerits of the various systems, but merely to use their existence as an indication of the improbability of a "universal correlation" for all types of practical units.

Despite the large number of design differences, all gas turbine combustion chambers have three features which may be identified: (a) a recirculation zone, (b) a burning zone which includes the recirculation zone and which extends to the dilution region, and (c) a dilution region. The function of the recirculation zone is to evaporate, partly burn, and prepare the fuel for rapid combustion within the remainder of the burning zone. At the end of the burning zone, ideally all fuel should be burnt so that the function of the dilution zone is solely to mix the hot gas with the dilution air such that the mixture leaving the chamber has a temperature and velocity distribution which is acceptable to the guide vanes and the turbine. Generally the addition of dilution air is so abrupt that if combustion is not complete at the end of the burning zone, then chilling occurs which prevents further completion. However, there is evidence within some chambers that if the burning zone is run overrich, some combustion does occur within the dilution region.

Based upon the above assumption, it would appear logical to treat the combustion chamber as (a) a partially stirred reactor within the recirculation zone, followed by (b) a plug flow reactor to the the end of the burning zone, followed by (c) a zone of negligible reaction but intense mixing. Hence, theories based on stirred reactor should yield reasonable qualitative picture for efficiency and stability. Also, with suitable experimental support, they could even be extended for qualitative analysis.

7.2.2 EFFICIENCY

Combustion efficiency is an important parameter, but uncertain to quantify analytically. Past experience has been the major input. In combustion, efficiency relates to the extent to which fuel supplied releases its heat energy. Quantification in terms of measurable parameters is a matter of choice. Oxygen content unutilised, carbon monoxide and or unburnt hydrocarbons left over in the exhaust stream are all a measure of inefficiency or the amount of unconverted energy and temperature rise is a direct measure of efficiency. Thus, gas analysis or pyrometry are the two measuring techniques for the efficiency. Now, expressing the same in analytical expressions in terms of operating conditions is even more involved process.

Progress in isolating and evaluating the component processes under representative environmental conditions is inevitably slow and, until more detailed knowledge is available, suitable parameters relating combustion performance to combustor dimensions and operating conditions can only be derived using simplified models.

Lefebvre (1966) suggested one such model based on the widely accepted notion that the total time required to burn a liquid fuel is the sum of the times required for fuel evaporation, mixing of fuel vapour with air and combustion products, and chemical reaction. The time available for combustion is inversely proportional to the air flow rate. Thus, combustion efficiency may be expressed as:

$$\eta_c = f(\text{airflow rate})^{-1} \left[\frac{1}{\text{evaporation rate}} + \frac{1}{\text{mixing rate}} + \frac{1}{\text{reaction rate}} \right]^{-1} \quad \dots(7.1)$$

In practical combustion systems, the maximum rate of heat release at any operating condition may be governed either by evaporation, mixing or chemical reaction, but rarely by all three at the same time. Lefebvre's (1966) Θ parameter is still widely known and used

$$\eta_c = f(\Theta)$$

$$\text{where } \Theta = P_2^{1.75} A_{\text{ref}}^{0.75} D_{\text{ref}} \exp\left[\frac{T_2}{300}\right] / \dot{m}_a \quad \dots(7.2)$$

This model presumes that primary zone energy release kinetics are limiting to combustor performance. Combustors may be sized to achieve some acceptable minimum efficiency by choosing Θ sufficiently large at some point in the combustor operating envelope. For high efficiency ($\eta > 90\%$) this model is not strictly valid because primary zone kinetics are no longer limiting to overall combustor performance. Rather it is secondary zone performance which controls emissions and efficiency. Even at high efficiency, however, Θ remains a useful parameter for comparing the performance of different combustors and fuels. However, prior knowledge of the Θ parameter for a particular combustion chamber for a given equivalence ratio is a prerequisite. Due to the proprietary nature of these experimentally generated information, this type of input to the computer program is rather difficult to obtain.

The importance of evaporation can also be included as proposed by Lefebvre (1987) as:

$$\eta_c = \eta_{c\Theta} \eta_{ce} \quad \dots(7.3)$$

$$\eta_{c\theta} = 1 - \exp \left[\frac{-0.022 P_2^{1.3} V_c \exp(T_c/400)}{f_c \dot{m}_a} \right] \quad \dots(7.4)$$

$$\eta_{ce} = 1 - \exp \left[\frac{-36 P_2 V_c \lambda_{eff}}{T_c D_0^2 f_c \dot{m}_a} \right] \quad \dots(7.5)$$

where

$\eta_{c\theta}$ = reaction rate efficiency

η_{ce} = evaporation rate efficiency

f_c = combustion air fraction

λ_{eff} = effective value of evaporative constant m^2/s

It may be noted that as opposed to the global values of overall operating conditions representing the earlier proposed θ parameter (eqn 7.2), the parameters in the latest (eqn 7.4) represent the combustion zone directly. This brings it closer to the stirred reactor concept. Hence these should be better representative of the efficiencies.

A more complicated model formulation for the primary zone is that of Swithenbank et al. (1973), similar to the following expression:

$$\eta_{pz} = \frac{1}{1 + \frac{t_K}{t_R} + \frac{t_D}{t_R} + \frac{t_E}{t_R}} \quad \dots(7.6)$$

and the relative time scales are proposed as -

t_R/t_K , reaction kinetic time scales, based on Arrhenius expression a function of $\exp(E/RT)$

t_R/t_D = turbulent mixing scale

$$= 50(\xi/3)^{1/2} \quad \dots(7.7)$$

where $\xi = \Delta P/q$

In case of droplet systems, a total mixing time is defined as

$$t_D = (t_D'^2 + t_E^2)^{1/2} \quad \dots(7.8)$$

where t_D' is only due to turbulent mixing same as (7.7)

t_E is droplet evaporation time.

Mellor (1976) has extended the model through characteristic times, to define efficiencies of the entire combustor accounting for the various operating environments. When the regions are schematically represented considering the flow pattern, we can identify the different mixing zones, in the

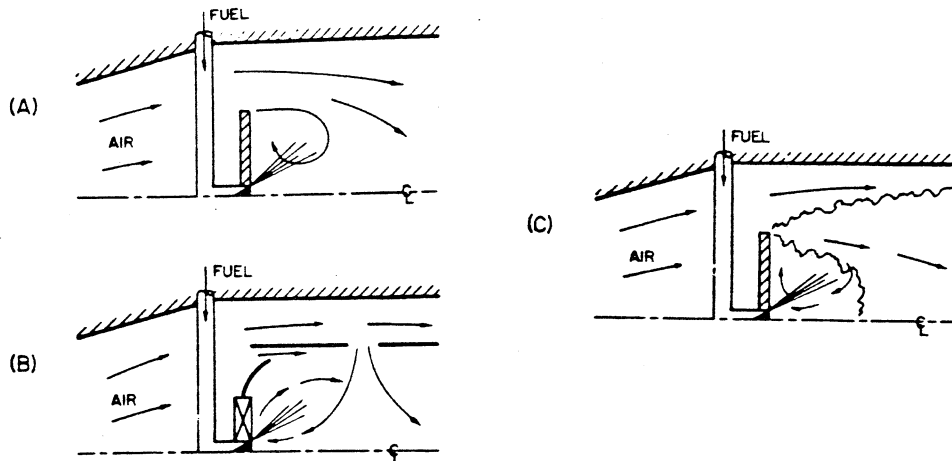


Fig 7.1 Simplified schematics of various primary zones (Mellor (1976)).

primary section. The two important mixing processes in this schematic representation of the primary zone (Fig 7.1); one involves the mixing of the fuel vapor eddies with the hot recirculating burned gases, and the other that of the resulting fuel-burned gas mixture with the fresh air in the shear layer. Characteristic times for these two mixing processes can be thought of as turbulent eddy dissipation times or lifetimes. The various characteristic times are indicated as Table 7.1.

TIME	SYMBOL	PHYSICAL/CHEMICAL PROCESS
Fuel, droplet lifetime	τ_{eb}	Droplet evaporation and/or combustion
Eddy dissipation time for injected fuel	τ_{fi}	Small scale turbulent mixing near the fuel injector in the recirculation zone
Eddy dissipation time in the shear layer	τ_{sl}	Large scale turbulent mixing between fresh air and the recirculating burnt products
Fuel ignition delay and burning time	τ_{hc}	Homogeneous combustion of the fuel to CO_2
Conversion Kinetic time	τ_{η}	Conversion times for the CO and UHC in the shear layer

Table 7.1 Characteristic Time Scales (Mellor (1976)).

if,

$$\frac{t_K}{t_R} + \frac{t_D}{t_R} + \frac{t_E}{t_R} = X$$

$1/(1 + X) \approx 1 - X$ (expanding through Taylor's series & neglecting higher powers of X, if X is small; as is the case when the primary zone inefficiency is low.)

Hence the primary zone inefficiency becomes, from eqn 7.6

$$(1-\eta)_{pz} = \frac{t_K}{t_R} + \frac{t_D}{t_R} + \frac{t_E}{t_R} \quad \dots(7.7)$$

Leonard and Mellor (1983), using the above concept have correlated the combustor efficiencies which included fuel type and atomization effects. The model is shown as fig 7.2.

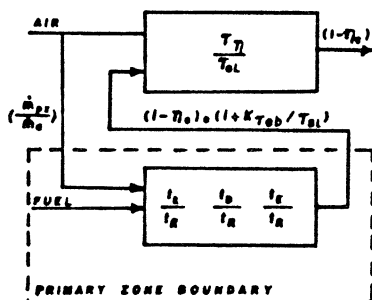


Fig 7.2 Schematic diagram of the relation of the mixing layer to the primary zone and exhaust efficiency (Mellor (1983)).

where

$(1-\eta)_0$ = reference efficiency considering negligible kinetic and evaporation rates, constant for a combustor configuration and operating cycle design.

$$\tau_{\eta} = 10^{-2} \exp(4500/RT_{\eta})$$

$$T_{\eta} = 0.9 T_2 + 0.1 T_4$$

$$\tau_{sl CO} = l_{CO} / V_{ref}$$

$$l_{CO} = [l_q^{-1} + d_{ft}^{-1}]^{-1}$$

The model reproduces the primary empirical observations reasonably. The time scale approach should provide useful guidance to designers.

Another approach is that by Odgers and Carrier (1973) who have correlated efficiency for weak primary zones based on experimental observations as,

$$\Pi = A \log \psi + B \phi_{pz} + C \quad \dots(7.8)$$

Where Π = parameter $\log \log (100/\eta)$

η = combustion efficiency

ψ = fuel loading $\dot{m}_f / V_c P^n$

n = reaction order

A, B, C, for fuel loading in $\text{lb}/(\text{s ft}^3 \text{ atm}^n)$, were derived as 0.911, -1.1, 0.557

Constant C is dependent on the chamber and has to be evaluated experimentally for each case.

7.2.2.1 CLOSURE

Considering above, the approach of Leonard, Mellor(1983) based on time scales appears to have a potential to cover all aspects that influence efficiency and also amenable for easy coding in a computing programme. This possibility is explored as explained in the subsequent paragraphs.

7.2.3 STABILITY

Stable combustion during erratic fuel or oxidant medium supply to the combustor is a prerequisite of any gas turbine

combustion chamber.

One theory to explain the stability phenomenon stems from stirred reactors. Longwell et al (1955), Herbert (1962) have derived stability criteria based on the postulation that if the mean gas residence time in the recirculation zone exceeds the requisite fuel burning time there, then a stable flame will spread into the free stream.

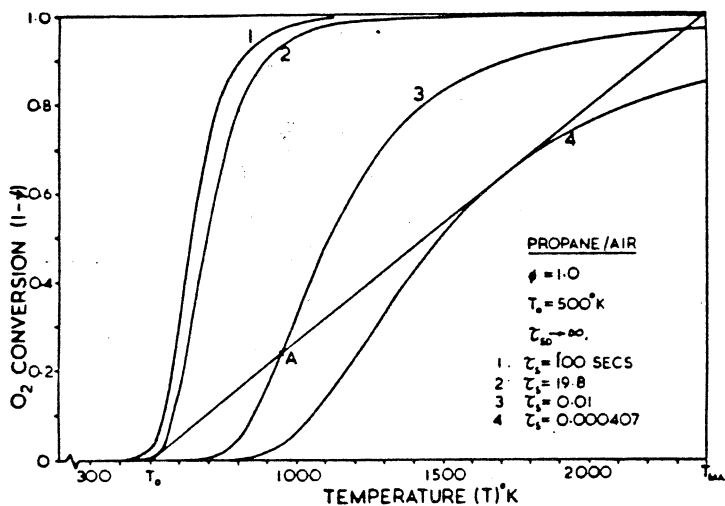
For a stirred reactor the analysis (Swithenbank (1973)) reduces to a zero-dimensional system. In a steady state operation:

$$\begin{array}{ccc} \text{Heat liberated by} & & \text{Heat removed from} \\ \text{chemical reaction} & = & \text{reactor volume} \\ \text{I} & & \text{II} \end{array} \quad \dots(7.9)$$

each side when represented in a non-dimensional form with respect to fraction of oxygen conversion (ψ)

$$\text{I} \quad (1-\psi)_I = \frac{t_K}{t_R} + \frac{t_D}{t_R} + \frac{t_E}{t_R} \quad \dots(7.10)$$

$$\text{II} \quad (1-\psi)_{II} = v (T - T_0) \quad \text{where } v \text{ is the slope of the heat removal line} \quad \dots(7.11)$$



$$\psi = \frac{\text{final oxygen conc.}}{\text{initial oxygen conc.}}$$

$$v = 1/(T_{\max} - T_0)$$

$$\tau_s = \text{residence time}$$

0 represents initial conditions

Fig 7.3 The adiabatic Stirred reactor heat balance (Swithenbank (1973))

Expressing the solution graphically, as shown in Fig 7.3

- 1) Point A on curve 3 is meta stable w.r.to small changes of inlet parameters (τ_s, ϕ, T_o)
- 2) Thermal ignition-stay time is achieved as curve 2
- 3) Blow-off occurs at the stay time given by curve 4

Lean blow-off limit is signified by that critical condition where heat removed just equals to the heat liberated at that operating condition. Any change in condition to increase heat removal rate, quickly gets into the unstable condition of extinguishing the flame.

Kretschmer and Odgers (1972) had derived an empirical equation for stability in terms of air loading parameter as shown below

$$\frac{N}{VP^{2\phi}} = \frac{1.29 \times 10^{10} (m+1)[5(1-Y\epsilon)]^{\phi} [\phi - Y\epsilon]^{\phi} e^{-C/(T_i + \epsilon\Delta T)}}{0.08206^{2\phi} Y\epsilon[5(m+1) + \phi + Y\epsilon]^{2\phi} [T_i + \epsilon\Delta T]^{2\phi - 0.5}} \quad \dots(7.12)$$

where

- N = gas massflow into a reactor gmol/s
- V = volume lit
- P = pressure atm
- m = ratio of inerts/oxygen by volume in mixture
- Y = ϕ for $\phi \leq 1$ and 1 for $\phi > 1$
- ΔT = undissociated adiabatic temperature rise in K
- ϵ = oxygen consumption efficiency

Zukowski and Marble (1956) have associated stability with the shear layer, such that stable combustion is achieved if the fluid residence time is greater than the burning time in the shear layer. An extension of the same is that of Leonard and Mellor (1983) which states that for a heterogeneous systems the criterion for blow off is that the mixing time available in the shear layer surrounding the flameholding recirculating zone must be sufficient to both evaporate the fuel and ignite the mixture.

$$(T_2/T_{\phi=1})\tau_{sl} \sim \tau_{hc} + k\tau_{eb} \quad \dots(7.13)$$

The temperature ratio is required to account for the velocity difference between the liner and outer regions of the shear layer.

7.2.3.1 CLOSURE

The approach (eqn 7.12)) of Kretschmer and Odgers (1972) appears to be the simplest to be incorporated into the

program which accounts for a wide range of operating conditions and commensurate with the accuracy needed. Hence similar strategy is adopted for the present work by deriving a loading parameter expression to account for the various inlet media, which is explained in the subsequent paragraphs.

7.3 REQUIREMENT

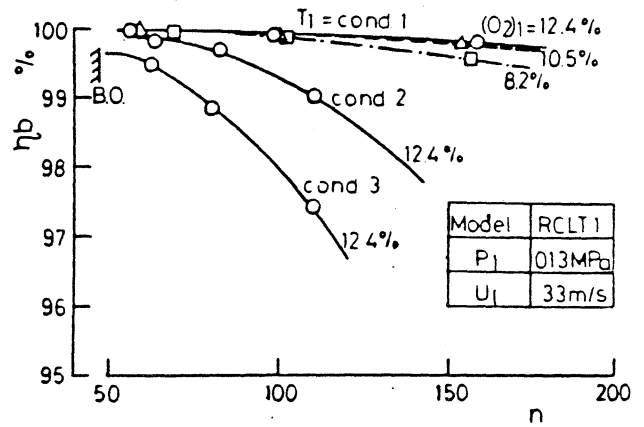
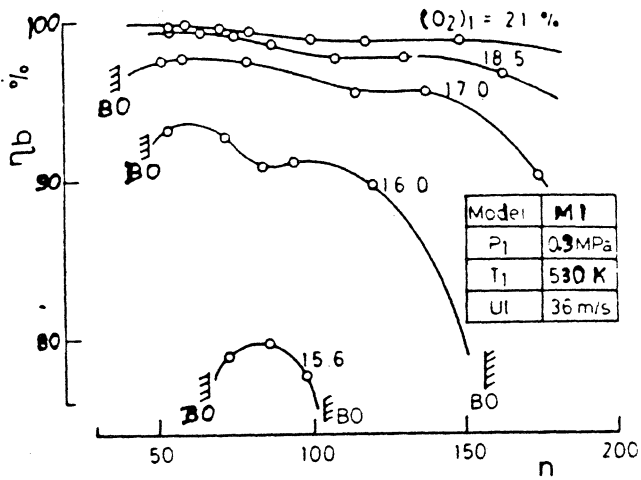
The regime of interest would be, how do efficiency and stability vary with medium change viz.

- 1) **FUEL** : fuel type may be varied due to deliberate blends or due to inevitable shortage crisis.
- 2) **OXIDANT** : this medium may be changed from air to vitiated medium either by precombustion in the case of rigs or reheat combustors or through water/steam injection for emission control.

The effect of fuel medium change is being vigorously investigated since a decade and reasonable empirical and semi-empirical guidelines have been formulated quantifying efficiency or stability changes, by relating evaporation times or drop life times to the fuel properties. Leonard & Mellor(1983), Gleason & Bahr(1980), Ballal & Lefebvre (1979) are some of representative work. The efficiency variation based on evaporation as rate limiting process had already been discussed as 4.10. Though much has been done for the later medium, the interest was mainly to relate the rig results to the actual combustors, as invariably some form of vitiation was undertaken to simulate the inlet temperatures or pressures. Barr & Mullins (1949), Greenhough & Lefebvre (1957), represent some of earlier published work on vitiation. Odgers & Kretschmer (1980) have recommended to avoid vitiated preheating for test analyses, considering the differences observed in pollutant formations and radiation values from vitiated to unvitiated atmospheres. For a gas turbine combustor, no model is currently available in the literature that has been published, which would relate vitiated preheating results to an unvitiated performance with sufficient accuracy. With the interest in reheat combustor or double combustor concept as opposed to simple gutters in the reheat duct of any afterburner engine, it is decided to probe deeper as to the possibility of correlation, between vitiated and unvitiated performances.

7.3.1 EFFICIENCY CORRELATION

The data available from the Moonlight Project, however limited, should provide the starting point for this exercise. Mori et al (1982) have investigated vitiation effects, whose results are quoted subsequently.



a) M1 Combustor (Main)

b) RLC1 Combustor (Reheat)

Fig 7.4 Combustion Efficiency - Moonlight Project (1982)

Main combustor : combustion air : 23.6%

AFR overall	50	60	70	80	90	100	125	150	175	
sphum O2% AFRS	equivalence ratio									
.000 20.95 14.73	.294	.245	.210	.184	.164	.147	.118	.098	.08	
.082 18.50 15.94	.319	.266	.228	.199	.177	.159	.128	.106	.09	
.145 17.00 16.85	.337	.281	.241	.211	.187	.169	.135	.112	.09	
.193 16.00 17.56	.351	.293	.251	.219	.195	.176	.140	.117	.10	
.213 15.60 17.87	.357	.298	.255	.223	.199	.179	.143	.119	.10	

Reheat combustor : combustion air : 35.9%

n (AFR overall)	50	60	70	80	90	100	125	150	175	
sphum O2% AFRS	equivalence ratio									
.143 12.40 23.11	.462	.385	.330	.289	.257	.231	.185	.154	.13	
.281 10.50 25.90	.518	.432	.370	.324	.288	.259	.207	.173	.14	
.534 8.20 31.03	.620	.517	.443	.388	.345	.310	.248	.207	.17	

Table 7.2 Combustors air/fuel flow distribution- Moonlight Project

n = overall air fuel ratio

sphum = specific humidity kg of water/ kg of air

The Tables 7.2 are generated from the limited data presented by the MOONLIGHT project by Mori et al. (1981). Investigation of vitiation effects on AFRS and adiabatic temperature is carried out using the simplified technique to find the temperature rise as indicated in Appendix C. For the same oxygen volumetric percentage reduction, the two methods, water addition or precombustion, yield different AFRS and also different adiabatic temperatures (Fig 7.5).

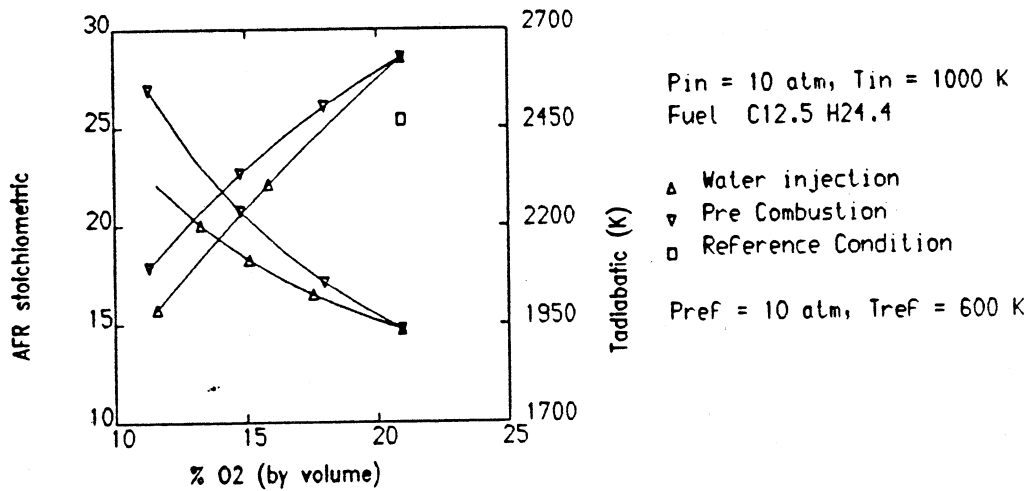


Fig 7.5 AFRS and T_{ad} under vitiation

The adiabatic temperature is roughly lowered by 50 degrees for each 1% reduction in oxygen volumetric percentage. Hence vitiation of the medium can be represented by any two of the variables O2 %, AFRS, water content (specific humidity). It is proposed that the widely accepted θ parameter (eqn. 7.2) may be modified to account for vitiation in the following manner.

$$\text{Modified } \theta \text{ parameter} = C_1 \frac{A_{ref}^{0.75} D_{ref}^{1.75} P_2}{\dot{m}} \exp(T_2/C_2) \quad \dots(7.14)$$

C_1 is introduced considering the fact that collision frequency should reduce as number of inerts to oxygen increases, in other words as vitiation increases.

$$C_1 = f(\phi_{pz}, \text{AFRS}, \text{sp humidity})$$

$$= (\phi_{pz})^a \left[\frac{\text{AFRSr} \times (1 + \text{sphumr})}{\text{AFRS} \times (1 + \text{sphum})} \right]^b \quad \dots(7.15)$$

C_2 is introduced as maximum adiabatic temperature falls with vitiation. It also depends on how vitiation is achieved.

Hence, the proposed form of C_2 is

$$C_2 = B [0.0679 \text{ AFRS} (1 + \text{sphum})]^c \quad \dots(7.16)$$

where AFRSr | for a reference condition
 sphumr | say, with the fuel without vitiation
 B = 300, coefficient assumed as in original Θ
 a,b,c require to be evaluated experimentally

The final form of the correlation is

$$\eta = f(\text{modified } \Theta)$$

For the Moonlight combustor they worked out to be as

$$a = 0.14 ; b = 2.0 ; c = 1.3$$

These appear to correlate the limited data reasonably, as the correlation coefficient $r = 0.9689$ (closer to unity better is the fit). The final form of relation is

$$\eta = A_0 + A_1 X + A_2 X^2 + A_3 X^3 + A_4 X^4 + A_5 X^5 \quad \dots(7.17)$$

where

$$X = (\Theta_{\text{mod}})^{0.25}$$

$$A_0 = -1925294.039322875, \quad A_1 = 129741.0127543312,$$

$$A_2 = -3492.133076386518, \quad A_3 = 46.93142351950109,$$

$$A_4 = -0.314914209478934, \quad A_5 = 8.4404338915763207E-04$$

However, the range of applicability of the above equation is narrow due to the nature of high degree of polynomial. In order to avoid an ill-conditioned solution (wherein the solution is very sensitive to small changes in independent

variable; this arises due to high order of the polynomial), double precision is used in the least square curve fitting routine. Consequently the coefficients appear in such lengthy form. It may be impractical to use them. Also efficiency values above 100 and may be below 50 have to be approximated to the respective limiting values. In order to circumvent this, a simplified representation is done by splitting the region. The same is represented graphically as Fig 7.6.

$$\text{for } \theta \leq 2.02E7 \quad \eta = A_0 + A_1 \theta^{0.25} \quad \text{where } A_0 = -543.6047$$

$$A_1 = 9.5194$$

$$r = 0.9045$$

$$\text{for } \theta > 2.02E7 \quad \eta = A_0 + A_1/\theta \quad \text{where } A_0 = 104.1648$$

$$A_1 = -1.85041E8$$

$$r = 0.9035$$

$$\text{for } \theta > 4.45E7 \quad \eta = 99.999$$

r is the correlating coefficient

..(7.18)

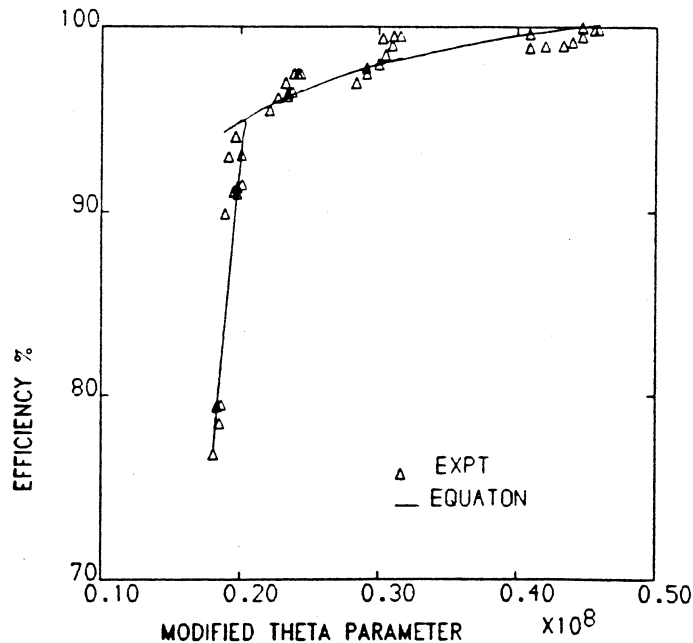


Fig 7.6 Efficiency under vitiation- Modified theta parameter

7.3.2 KINETIC TIME APPROACH

In order to arrive at the correlation analytically an attempt is made to bring in the effect of vitiation through kinetic time. Following the characteristic time model, as described earlier (fig 7.2), with the assumptions that mixing times and evaporation times are not rate limiting, the inefficiency can be deduced as

$$(1 - \eta_c) = C_1 \frac{\tau_h}{\tau_{s1}} (1 - \eta_c)_0 \left[C_2 + C_3 \frac{\tau_K}{\tau_R} \right] \quad \dots(7.19)$$

All the terms have the same definition as described earlier in fig 7.2 except $(1 - \eta_c)_0$ would be a constant for a combustor representing the reference condition inefficiency due to mixing and evaporation, which is assumed to be constant even when the oxidant medium is changed. C_1, C_2, C_3 are the constants to be evaluated later. C_2 representing the combined effect of the mixing and evaporation. Now there is a need to evaluate the kinetic reaction time τ_K .

A review to evaluate the kinetic time, has yielded the following correlation after Odgers

$$t_K \text{ (ms)} = 1.281 \times 10^{-7} \left(\frac{T_{pz}}{P^{1.25}} \right)^{0.25} \times \left(\frac{[1 + \phi_{pz}(1 + \eta)/23.8]^{1.75}}{[\phi_{pz}(1 - \eta)]^{0.75} [1 - \eta\phi_{pz}]} \right) \exp(E/R T_{pz}) \quad \dots(7.20)$$

However, due to paucity of complete information about the applicability of the equation, it is decided to evaluate the times through material consumption equations.

KINETIC REACTION

According to the collision theory for a bimolecular reaction, material consumption rate is given by

$$-\frac{dm}{dt} = V k \sqrt{T} \left(\frac{P}{RT} \right)^n X_{\text{comb}}^f X_{\text{oxi}}^{n-f} e^{-(E/RT)} \quad \dots (7.21)$$

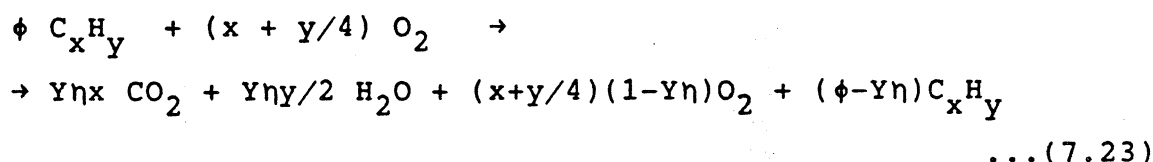
which for a gas flowing into a perfectly stirred reactor vessel becomes

$$\frac{NY\eta}{(1+m)} = v k \sqrt{T} \left(\frac{P}{RT} \right)^n X_{\text{comb}}^f X_{\text{oxi}}^{n-f} e^{-(E/RT)} \quad \dots (7.22)$$

where X=mole fraction
 η oxygen consumption efficiency
 the other terms are as defined for
 eqn 7.12

The constants k, f, n, E are all derived using "best-fit" values to the experimental data. Hence there is this uncertainty in extending the results to the other cases. However, for carbon/hydrogen/oxygen/nitrogen containing fuel-oxidant media, the qualitative agreement can be reasonably expected.

The mass balance for any hydrocarbon fuel burning in air can be represented on a global rate reaction basis thus:



$$X_{\text{comb}} = \frac{(\phi-Y\eta)}{(x+y/4)+\phi+Y\eta(y/4-1)} \quad \dots(7.24)$$

$$X_{\text{oxi}} = \frac{(x+y/4)(1-Y\eta)}{(x+y/4)+\phi+Y\eta(y/4-1)} \quad \dots(7.25)$$

The individual proportions will be different if all the assumptions introduced in Appendix c, are superimposed considering dissociation. The above ratios are listed to illustrate the approach.

The best fit value for k , the collision frequency factor, varies from $1.29E10$ for propane (Kretschmer & Odgers (1973)) to $1.2E12$ for n-heptane (Longwell & Wise (1955)). As most of the data derived is in the presence of air and hence extending it to vitiated medium is dubious. However, it can be argued, that k , the collision frequency should decrease in the same proportion as more vitiation or number of inerts increase. As stoichiometric air-fuel ratio between the two media is also a measure of the increase in inerts with

respect to a reference value, it is proposed that

$$k = 1.29 \text{ E}10 \left[\frac{\text{AFRSr}(1+\text{sphumr})}{\text{AFRS}(1+\text{sphum})} \right]^b \quad \text{where } b \text{ is } 2.0$$

$$\text{lit} / (\text{g.mole})^{n-1} \text{K}^{1/2} \text{s}$$

...(7.26)

This has yielded reasonable correlation for the Moonlight data, though more experiments may be needed for confirmation or improvement.

Similarly the activation energy E , varies from 24 Mj/kg mole to 88 Mj/kg mole. Even for propane Kretschmer & Odgers (1972) have indicated a scatter ranging from 69771 to 28037 cal/g mol (Fig 7.7). For Kerosene 88 Mj/kg mole is being used by a large number of correlators and hence this value is presently being adopted.

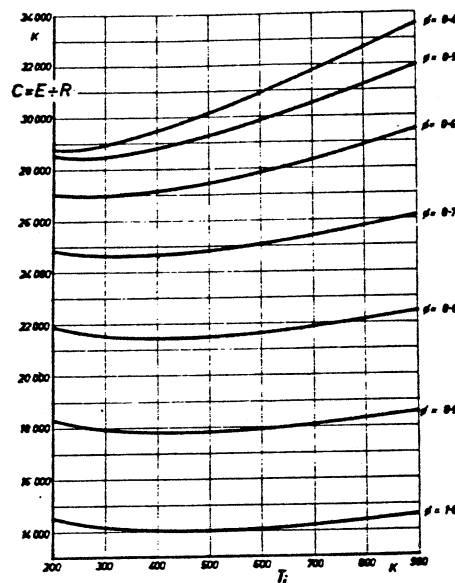


Fig 7.7 Variation of activation energy for methane

The exponent n varies from 1.3 to 2., and Kretschmer and Odgers(1973) have expressed it as a function of ϕ . However, $n=1.75$ and $f=1$ are widely accepted and a large number of data already exists correlating to these exponents and hence no attempt is made to review their value.

if ρ is the density at T , in the stirred reactor,

$$\text{mass} = \rho V$$

$$\text{O}_2 \text{ moles left over} = \frac{\rho V X_{\text{Oxi}}}{\text{Mol Wt}}$$

$$= \left(\frac{P}{RT} \right) V X_{\text{Oxi}}$$

$$\text{O}_2 \text{ moles consumed} = \left(\frac{P}{RT} \right) \frac{V X_{\text{Oxi}} \eta}{(1-\eta)} \quad \dots(7.27)$$

if t_K is the reaction time

$$\text{O}_2 \text{ consumption rate} = \left(\frac{P}{RT} \right) \frac{V X_{\text{Oxi}} \eta}{(1-\eta) t_K} \quad \dots(7.28)$$

equating (7.22) and (7.28)

$$t_K = \frac{\eta \exp(E/RT)}{\left(\frac{P}{RT} \right)^{n-1} k \sqrt{T} X_{\text{comb}}^f X_{\text{Oxi}}^{n-f-1} (1-\eta)} \quad \dots(7.29)$$

Assuming

$$n = 1.75$$

$$f = 1.0$$

$$E = 88 \text{ Mj/kg mole}$$

$$R = 8314.3 \text{ Mj/kg mole K}$$

$$= 0.08206 \text{ lit atm/g mole K}$$

$$k = \text{as given as eqn 7.26}$$

Kinetic times (τ_K) are evaluated for the Moonlight combustor and are presented for an AFR of 60 as below. The values for unvitiated air are reasonably in close agreement with the

values derived using eqn 7.20 of Odgers.

	T ₂	O ₂ %	t _k sec	η(expt)
M1	530	20.95	0.32480e-6	99.90
		18.50	0.52040e-6	99.51
		17.00	0.72924e-6	97.50
		16.00	0.94413e-6	94.10
		15.60	0.12035e-5	78.50
RLC1	990	12.40	0.3833e-6	99.99
		810	0.47789e-6	99.80
		730	0.52434e-6	99.30

Table 7.3 Kinetic times for Moonlight combustors

On a comparative basis, they appear to represent the efficiency degradation based on the kinetic reaction times. However, for similar drop in kinetics Leonard and Miller (1983) have reported only 2.5% increase in inefficiency, as against a drop of almost 20% in the efficiency in the present case. The evaluation of t_k here, has already assumed the knowledge of primary zone efficiency. The fidelity of the approach doesnot make it an easy predictive procedure, as originally indicated as Eqn 7.19. Also the data about the empirical constants such as k or E in the presence of excessive inerts is scarce. Hence this exercise is discontinued at this stage, leaving the empirical relation through modified θ parameter as representative of efficiency under vitiation.

7.3.3 STABILITY RELATION

The stirred reactor approach as explained in the preceding sections is the basis for stability calculations. The maximum loading parameter N/VP^n is chosen to represent the blow-off conditions. Here for a given inlet conditions, the efficiency is varied to get the maximum value of loading parameter from equation (7.22), which represents the blow-off condition at that equivalence ratio.

NOTE : In general, both rich and lean stability limits are required to complete the loop. However, the lean limit would be more important in instances like sudden throttling back when load is thrown off from the grid. Only bottom half of the loop upto stoichiometric ratio is considered, for all the cases.

Though qualitative, this method should bring out values for the maximum throughput as well as the lean blow off limit at

any power setting. The first being the maximum value of loading parameter at equivalence ratio one of the stability loop for the design point. The later from the appropriate stability curve against the loading parameter of the combustor at the operating condition. The flow and pressure values can be obtained from cycle considerations. The burning zone volume is again a matter of judgment. Water flow visualization also helps to locate the exact size of recirculation pattern and consequent combustion profile. However, as a first guess this could be made equal to the primary zone volume. Using this approach, the lean blow off limit is presented for the Moonlight's M1 combustor.

From the available measurements, the following are deduced

$$\begin{aligned} V_c &= 2.e^{-3} && \text{m}^3 \\ \dot{m}_{pz} &= 0.72 && \text{kg/s} \\ P &= 0.3 && \text{MPa} \end{aligned}$$

$$\frac{\dot{m}_{pz}}{(V_c P^{1.75})} = 9.37E-8 ; \log(9.37E-8) = -7.03$$

With $E/R = 16000 \text{ K}$, the results are as presented below.

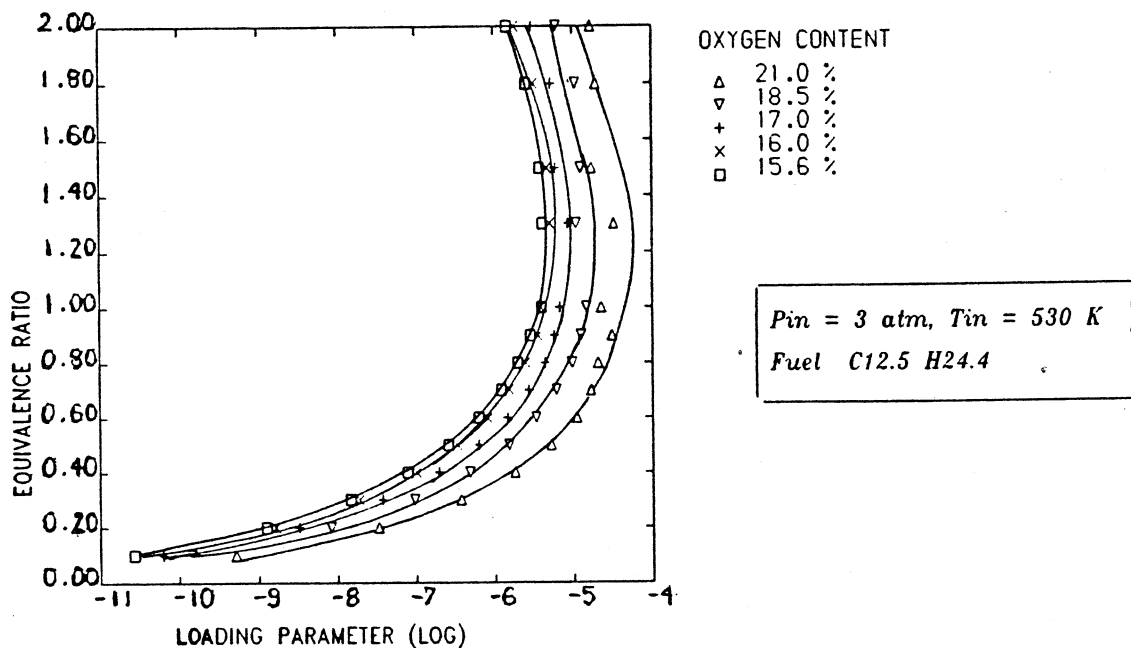


Fig 7.8 Stability Curves- Moonlight combustor

The same exercise is repeated with E/R as 20000 K. The stability curves move left giving more realistic picture for the vitiation, as shown below-

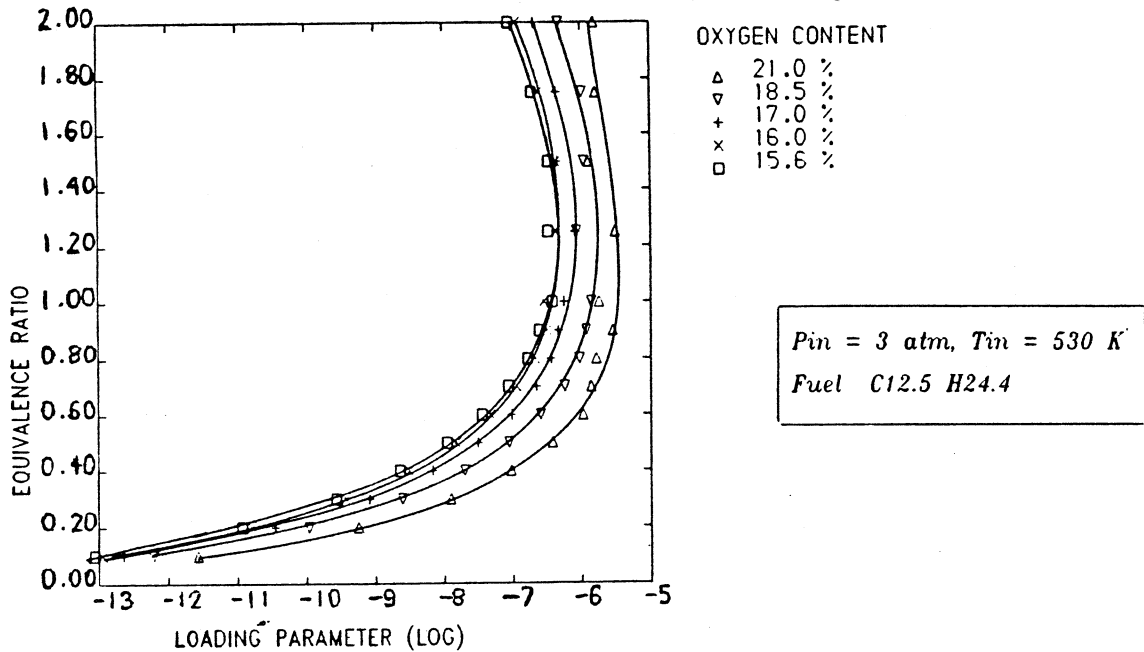


Fig 7.9 Stability Curves- Moonlight Combustor

One way of using them would be, knowing the given combustor operating loading parameter, pick out ϕ_{pz} for blowout.

$$\phi_{LBO} = \phi_{pz} \times \text{fraction of combustion air}$$

$$AFR_{LBO} = AFRS / \phi_{LBO}$$

For the present case, with different E/R values

O ₂ %	E/R	10584	16000	20000 K
20.9	AFR	693	284	156
15.6	Blow out	504	180	106

Table 7.4 Blow_out values for M1 combustor

The inference is:

From the experimental values, it appears that the value for E/R 10584 K, is more appropriate at O₂% for standard air. With Oxygen depletion, it increases to its maximum value

around 20000 K, as both the end values appear to reasonably represent the system. It appears logical to assume that as inerts increase, E/R value should increase. Inert content seems to be an additional variable to those represented in Fig 7.7. More experimental data may be required to confirm or improve this supposition. However, in the programme, user has choice to select this value, before undertaking stability calculations.

It may be highlighted, that so far the effects of mixing or evaporation on stability limits are not considered. A proven primary zone pattern or known blend of fuel can be used such that the above processes are insignificant. However, predictive capability is a must at preliminary design stage. Lefebvre's (1987) semi-empirical relation brings in the evaporative effects through the evaporation time constant

$$q_{LBO} = A \left[\frac{f_{pz}}{v_{pz}} \right] \left[\frac{\dot{m}_a}{P_2^{1.3} \exp(\tau_2/300)} \right] \left[\frac{d_0^2}{\lambda_{eff}^{LCV}} \right] \quad ..(7.30)$$

$$\text{where } \lambda_{eff} = \frac{8(\lambda/Cp)q}{\rho_1} \ln(1+B)(1+0.276Re^{1/2}Pr^{1/3}) \quad ..(7.31)$$

the terms are as explained in eqn (4.25), which is taken from Leonard and Mellor (1983)

It is worth noting that the pressure dependence has gone down from 1.75 to 1.3 may be due to the fact that the expression is just predicting the lean blow off limits. This equation could straightaway be used in the programme. However, it also has the fiddle factor in terms of its constant A, which requires to be experimentally evaluated. Our present requirement of using it under vitiated conditions can also be NOT satisfied.

To satisfy, the above requirement, a possible approach would be to treat the volume for combustion consisting of two parts, one where evaporation takes place and the rest acts like stirred reactor. Conceptually, it can be represented as

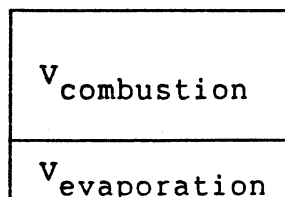


Fig 7.10 Conceptual representation of combustion volume

This would decrease the available stirred reactor volume, if the evaporation effects dominate, thus increasing the combustor operating loading point, more towards the critical point. A possible expression for the evaporation volume would be

$$V_e = f \left[\left\{ \dot{m}_{pz} / \rho_{pz} \right\} \left\{ d_0^2 / \lambda_{eff} \right\} \right] \quad \dots(7.32)$$

This can be explored, if suitable experimental data is available. In theory, this logic can be extended to the mixing as well. If mixing phenomenon can be quantified in terms of volume, the traditional loading parameter could well bring out the blow out values from the curves based on stirred reactors.

CHAPTER 8

EMISSIONS

8.1 SCOPE

The existing evaluation algorithm should extend from flow field calculations into realm of emission estimation. The growing importance of emission regulations necessitate this aspect, as in future, the choice of a combustor may well depend on these limits. Any design choice would obviously be made on a comprehensive performance basis, because there exists a need for optimization. As excessive cooling may reduce metal temperatures, but may produce deteriorated combustion efficiency. Similarly high primary equivalence ratio can result in better stability and heat release rates, but producing unacceptable amounts of NO_x. Hence information regarding trace species such as NO, NO₂, UHC (unburnt hydrocarbons), CO in the exhaust gases is needed from pollution as well as performance points of view.

The above statement cannot truly be implemented in the full sense in the present programme due to the following reasons. Out of the trace species of interest namely NO, NO₂, UHC and CO, the latter two namely UHC and CO which decide the combustion efficiency cannot truly be evaluated as gas temperatures are being estimated based on efficiency assumptions. This implicitly assumes the amount of UHC and CO concentrations. Till the flow field calculations are modified to account for the heat releases which again involve fuel chemistry and chemical kinetics (with or without simplifications), efficiencies will be assumed which in turn fix the amount of CO or UHC. Considering the modular structure of the programme, change should be a simple matter, if decided in the future. Approach based on the concentrations at the end of the primary zone and their subsequent history through characteristic times (Mellor(1984)) appear to be potentially a simple design tool. Alternatively, empirical formulations based on experimental data can be incorporated to predict the exhaust CO and UHC concentrations. Typical formulations are those proposed by Lefebvre (1984) of the form:

$$CO = \frac{86 \dot{m}_a T_{pz} \exp(-0.000345 T_{pz})}{\left(v_c - 0.55 \cdot 10^{-6} \frac{f_{pz} \dot{m}_a}{\rho_{pz}} \frac{D_0^2}{\lambda_{eff}} \right) \left(\frac{\Delta P_L}{P_2} \right)^{1.5}} \quad g/kg \quad \dots (8.1)$$

$$\text{UHC} = \frac{11,764 m_a T_{pz} \exp(-0.000345 T_{pz})}{\left(v_C - 0.55 \cdot 10^{-6} \frac{f_{pz} \dot{m}_a D_O^2}{\rho_{pz} \lambda_{eff}} \right) \left(\frac{\Delta P_L}{P_2} \right)^{P_2 2.5}} \quad \text{g/kg} \quad \dots(8.2)$$

However, for the present purpose these species are omitted.

There are a variety of ways of expressing the concentrations of trace species. The nomenclature and the relevant conversion factors are indicated as Appendix O. In the text mass fraction represented by { }, is adopted as the unit of measure. A detailed attempt is made to estimate the concentrations of NOx. The steps that would be followed are as follows :

8.2 NOx BURNING ZONE

- 1) Identify the NO formation rate mechanism. NO formation rates are strong functions of temperature and composition. The present analysis assumes a unique relation between equivalence ratio and the temperature. Hence specification of equivalence ratio decides species concentration and hence the temperature for a given fuel, oxidant media at a given inlet temperature and pressure. The final form of rate equation for changes in nitric oxide {NO} expressed as mass fraction, for a gas element at equivalence ratio ϕ is given by

$$\left. \frac{d\{\text{NO}\}}{dt} \right|_{\phi} = f [T, \text{composition}] \quad \dots(8.3)$$

$$\{\text{NO}\}_{t\phi} = \int_0^t \left. \frac{d\{\text{NO}\}}{dt} \right|_{\phi} dt \quad \dots(8.4)$$

- 2) However considering the complexities of phenomena in the burning zone, primary zone is best identified as a well stirred reactor.

NOTE : For easier understanding , author has schematically classified (fig 8.1) the different stirred reactors in terms of the distribution of the qualifying parameters namely, equivalence ratio and residence time through probability density functions. ϕ and τ are the respective mean values.

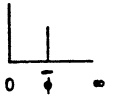
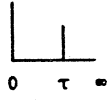


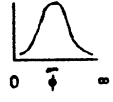
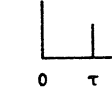
Reactor	Characteristic	Probability Density Functions	
		Equi. Ratio	Residence Time
Perfectly Stirred Reactor (PSR)	Mixing is complete. Uniform. Ideal.		
Well Stirred Reactor or Partially Stirred Reactor (WSR)	Mixing is complete at macro level. No inter-mixing between pockets. All fluid elements will have different speeds.		
Plug Flow Reactor (PFR)	A series of PSRs, with a distribution in mixing but having same residence time		

Fig 8.1 Schematic Representation of Stirred Reactors

For a WSR, both the distribution functions have to be considered.

3) Assuming a residence time distribution $\psi(t)$ as proposed by Beer and Lee (1965)

$$\psi(t) = \frac{1}{\tau} e^{-t/\tau} \quad \dots (8.5)$$

where

$$\tau = \text{mean residence time}$$

$$= \frac{\bar{\rho} V}{\dot{m}}$$

Integrating over the time distribution, the time average value of all gas elements with a given ϕ

$$\{NO\}_{\phi} = \int_0^{\infty} \{NO\}_{t\phi} \psi(t) dt$$

NOTE: A value of 50 times the mean (50τ) is assigned to the upper limit of residence time range which is considered sufficiently long to be treated as infinite.

4) A normal distribution characterised by a mean and standard deviation is assumed for the equivalence ratio, of the form:

$$f(\phi) = c \exp \left[-\frac{1}{2} \left(\frac{\phi - \bar{\phi}}{\sigma} \right)^2 \right] \quad \dots(8.6)$$

where c is a constant to ensure that the area under the PDF is unity and is defined as

$$c = \frac{1}{\int_0^{2\bar{\phi}} \exp \left[-\frac{1}{2} \left(\frac{\phi - \bar{\phi}}{\sigma} \right)^2 \right] d\phi}$$

σ = standard deviation

Note: The nature of the normal distribution function is that $f(\phi)d\phi$ tends to zero as ϕ tends to $\pm\infty$. Negative ϕ 's have no physical significance. However, All the possible combinations of fuel and air mixtures can be represented by equivalence ratio values between 0 or ∞ , the end values corresponding to neat air or neat fuel respectively. However, it is prohibitive in terms of calculating time, to consider such a vast range. Considering the above, a constraint is imposed upon the function that the limits are between 0 to $2\bar{\phi}$, thus retaining the symmetry about the mean value. For σ less than $\bar{\phi}/3$ it can be shown that the integral is greater than 99.7% of that over the range $\pm\infty$. Practically a range of σ from 0 to $\bar{\phi}/3$ will represent a wide range in distribution characteristics.

Here, a point of interest is if mixture fraction ξ defined as

$$\xi = \frac{1}{1 + AFR} \quad \dots(8.7)$$

is considered as opposed to equivalence ratio, the range will have finite limits of 0 to 1. The distribution could be represented by a beta function, as opposed to the present truncated Gaussian.

The mean nitric oxide mass fraction in the flow leaving the burning zone is given by

$$\bar{\{NO\}} = \int_0^{2\bar{\phi}} \{NO\}_\phi f(\phi) d\phi \quad \dots(8.8)$$

8.2.1 CHOICE OF KINETIC REACTION SCHEME

Nitric oxide is normally present in trace quantities and has negligible influence on the reactions associated with heat release, the thermodynamic state of the gas or the flow. It is generally accepted- at least under fuel lean and near stoichiometric conditions- that formation of NO is described by the extended Zeldovich mechanism :



In most combustion systems the NO concentrations will be well below their equilibrium levels and if a steady state approximation is then invoked for N atom concentration the instantaneous NO formation rate can be expressed. A variety of simplified representations are available.

1) Whitelaw (1981) :

$$\frac{d\{NO\}}{dt} = \rho K_f \frac{Mw_{NO}}{Mw_O Mw_{N_2}} \{O\} \{N_2\} \quad \dots(8.12)$$

where K_f is the forward rate constant for the reaction given by eqn (8.9).

2) Jones and Priddin (1978)

$$\frac{dn_{NO}}{dt} = 4.0917E13 T^{-0.0675} \exp(-67915/T) \rho^{1/2} n_{O_2}^{1/2} n_{N_2} \quad \dots(8.13)$$

where n is concentration in moles/unit mass

3) Hung (1975) expressing rate equation in ppm/ms

$$\frac{d X_{NO}}{dt} = P^{1/2} \left[\frac{a X_{N_2}^{1/2} X_{O_2}^2 - b X_{NO}^2 / X_{O_2}^{1/2}}{1 + c X_{NO} / X_{O_2}} \right] \quad \dots(8.14)$$

where X is the concentration in ppm/ms

P total pressure in atm

$$a = 4.6E18 T^{-1} \exp(-135000/RT)$$

$$b = 2.1E17 T^{-1} \exp(-92000/RT)$$

$$c = 8.5 \exp(74000/RT)$$

$$R = 1.98 \text{ cal/mol.K}$$

4) Fletcher and Heywood (1971) considering further reactions of N_2O

$$\frac{d\{NO\}}{dt} = \frac{2 M_w_{NO}}{\rho} (1 - \alpha)^2 \left[\frac{R_1}{1 + \alpha K_1} + \frac{R_6}{1 + K_2} \right] \quad \dots(8.15)$$

the explanation of individual terms follows.

Fletcher and Heywood (1971) model is chosen for the present programme as the reaction mechanism is exhaustive.

1)	$N + NO \rightleftharpoons N_2 + O$	$K_1 = 1.204 E10$
2)	$N + O_2 \rightleftharpoons NO + O$	$K_2 = 1.204 E10 \exp(-7100/RT)$
3)	$N + OH \rightleftharpoons NO + H$	$K_3 = 4.214 E10 \quad !$
4)	$H + N_2O \rightleftharpoons N_2 + OH$	$K_4 = 3.010 E10 \exp(-10800/RT)$
5)	$O + N_2O \rightleftharpoons N_2 + O_2$	$K_5 = 3.612 E10 \exp(-24000/RT)$
6)	$O + N_2O \rightleftharpoons NO + NO$	$K_6 = 4.816 E10 \exp(-24000/RT)$

Table 8.1 NOx Reaction Mechanism (Fletcher & Heywood (1971))

where K_1 to K_6 = one-way equilibrium reaction rate constants (m³/sec kg mole)

$$R = 1.98 \text{ cal/mol K}$$

! data is taken from Campbell (1968)
rest is adopted from Schofield (1967)

R_i is the one way equilibrium reaction rate for reaction i

$$\begin{aligned}
 R_1 &= K_1 [N]_e [NO]_e \\
 R_2 &= K_2 [N]_e [O_2]_e \\
 R_3 &= K_3 [N]_e [OH]_e \\
 R_4 &= K_4 [H]_e [N_2O]_e \\
 R_5 &= K_5 [O]_e [N_2O]_e \\
 R_6 &= K_6 [O]_e [N_2O]_e
 \end{aligned}$$

$$\begin{aligned}
 K_1 &= \frac{R_1}{R_2 + R_3} \\
 K_2 &= \frac{R_6}{R_4 + R_5} \quad \dots(8.16)
 \end{aligned}$$

$$\alpha = \frac{[NO]}{[NO]_e} \quad \dots(8.17)$$

where

{i} = mass fraction of ith species

[i] = concentration of the species kg mole/m³

$$= \{i\} \rho / Mw_i$$

Mw_i = molecular weight of ith species in kg/kg mole

ρ = density in kg/m³

The equilibrium concentrations for the operating conditions are taken using Gordon and McBride (1971) program. This obviously is a serious limitation of using the present programme on its own without having to depend on the external input. However at this stage, no effort is made to reduce the reaction mechanism to a simpler one where the existing species data can be made use of. Gaussian quadrature is used to integrate the above equations. The method is outlined as Appendix P.

The standard deviation σ , which is required to characterise the distribution of the equivalence ration (eqn 8.6), is represented by a mixing parameter S_0 , defined as

$$S_0 = \sigma / \bar{\phi} \quad \dots(8.18)$$

S_0 is also called "mixedness". This is a measure of non-uniformity of the burning zone. $S_0=0$ corresponds to perfect mixing.

The concentration at the end of burning zone appear to be reasonable, however, arbitration is involved in identifying the mixedness S_0 for the type of combustor and its power setting. However, a value of 0.2 at full power seem to correlate at least in two cases (chap 11). The following are

the burning zone end values for different mixedness for the two cases.

	Case 1	Case 2
P_{in}	1.14	1.76 Mpa
T_{in}	601	705 K
$\bar{\phi}_{in}$	0.852	0.65
τ	12.41	3.51 ms
S_0	NOx mass fraction $\times 10^6$	
0.05	1327.0	60.57
0.1	1218.0	102.30
0.2	989.2	252.50
0.3	631.8	365.70

Table 8.2 NOx mass fractions for different mixedness

8.3 NOx MIXING ZONE

Following Fletcher and Heywood (1971) model, the rest of combustor is treated as one mixing zone. The flow is assumed to be one-dimensional with gases uniformly mixed across each cross-section. Only the mean equivalence ratio is required to be considered and this only changes as the remaining air is added in. Hence, the nitric oxide mass fraction changes through chemical reaction and through dilution as additional air is mixed with the bulk liner flow according to

$$\frac{d\{NO\}}{dx} = \frac{1}{U} \frac{d\{NO\}}{dt} + \frac{\{NO\}}{\bar{\phi}} \frac{d\bar{\phi}}{dx} \quad \dots(8.19)$$

where U is the flow velocity

A more rigorous analysis could be incorporated considering the mixing of cooling and mixing air, however it is superfluous in the light of constant property assumptions at each axial plane. When the flow field calculations are altered to accommodate radial distribution, a detailed NOx analysis would be justified.

CHAPTER 9

DOUBLE COMBUSTOR

9.1 WHY REHEAT ?

"Optimizing Efforts" is always a primary design goal. Maximum output, efficiency, life etc, or minimum losses, size, weight, cost etc are a series of options which a designer constantly endeavours to compromise. The energy crisis will remain a constant driving factor for better performance gas turbines irrespective of aviation or industrial applications.

Material developments have consistently offered the scope to improve the output as well as thermal efficiency in a gas turbine by enabling higher cycle pressures and temperatures. Better liner materials to improve the metal temperature limits or improved technology to maximise the returns from the available materials are still very much desired. However, the power output and/ or thermal efficiencies can be greatly improved by shifting simple gas turbine cycle to combined cycle using reheat, regeneration, intercooling and steam cycles independently or collectively.

9.2 STATE OF ART

The reheat gas turbine cycle itself is well known and received attention in years gone by- particularly in Europe USSR (Uvarov et al (1974)) and more recently in Japan (Mori, Takeya (1981)).

It is well established that reheat will increase power output by 35 to 40 percent but without the complication of regeneration and intercooling the cycle efficiency is degraded over the simple cycle. Another example of the reheat gas turbine cycle presently being employed is the afterburner of the jet engine for aircraft use- particularly for the military and, to a limited extent, for commercial planes, namely Concorde SST. The jet reheat cycle has been developed to give reliable service where augmented output is required for a short or limited time. The greatly increased thrust comes at the expense of markedly increased fuel consumption. Commercial applications, because of the fuel consumption, have gone to efficient high bypass ratio fan jets for subsonic flights which in turn has made available the second generation high-ratio, high-firing temperature gas generators for industrial applications.

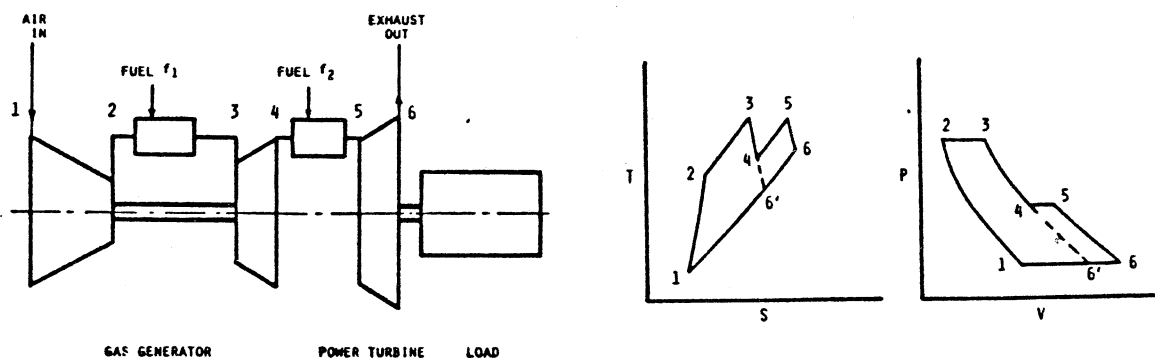
Perhaps it has been thought that the degradation in efficiency of the reheat cycle would not offer an advantage to combined cycle power plants. Attention has not been given to the cycle because of the gas turbine's increased fuel

consumption. Another explanation could be, that the extra complication and cost of more controls, another burner, compatibility of nozzle area, start-up procedures etc., would offset any advantage offered in terms of specific power output (reduction in physical size), particularly at a higher fuel consumption. Conventional Industrial (heavy duty) gas turbines are mostly single shaft units for power generation and do not readily lend themselves to the addition of reheat burners, unlike the aircraft derivative gas turbines which offer an advantage in potential physical arrangement for the reheat cycle such that a reheat combustor can be readily added between the gas generator and power turbine.

With the advent of the increasing number of high-temperature /high pressure-ratio gas turbines which lend themselves to reheat cycles, it is appropriate to consider the concept of second combustor in the traditional simple gas turbine cycle. The term double combustor may be used as a synonym to the traditional reheat combustor.

Cogeneration and combined cycles have already shown applications in this respect, the latest being the MOONLIGHT PROJECT undertaken by the "Engineering Research Association for Advanced Gas Turbines" of Japan. The Phase III results concerning the progress of this project had been recently presented by Takeya et. al. (1987). More information about reheat cycles, cooling systems, or component arrangements can be obtained from Rice (1979,1981), El-Masri (1985).

9.2.1 ANALYSIS



a) Layout

b) Cycle

Fig 9.1 Reheat Gas Turbine Schematic Diagram

The cycle analysis is the same whether it is a gutter or a double combustor. Fig 9.1 schematically represents a reheat gas turbine cycle. Comparison of reheat cycle with or without intercooling, regeneration and steam cycle with a simple cycle and the consequent relative merits can be obtained from any standard reference, such as Cohen et al (1981). Hence it requires no mention here, except for some conclusive comparisons.

9.2.2 CONCLUSIONS

- 1) The reheat cycle gas turbine efficiency is degraded over the simple cycle for equal TIT (Turbine Inlet Temperature).
- 2) The reheat cycle gas turbine output is increased significantly.
- 3) The reheat gas turbine cycle optimum pressure ratios run higher than for the simple cycle by significant amounts and both the optimum output and efficiency points take place simultaneously at this elevated pressure level.
- 4) The combined cycle incorporating the reheat gas turbine offers significant cycle efficiency improvements for equal TITs.

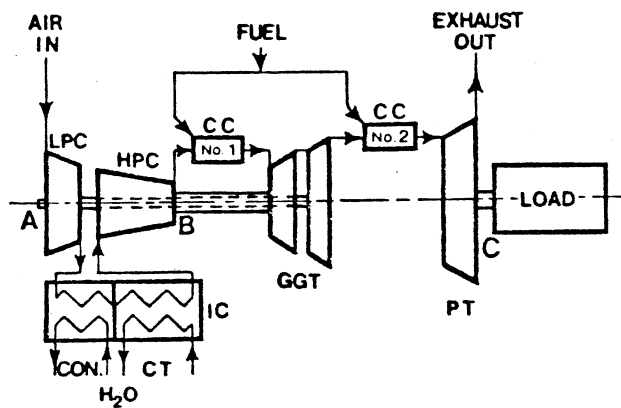


Fig 9.2 Intercooled Reheat Gas Turbine Schematic Diagram

- 5) If intercooling (Fig 9.2) is used, it can greatly

enhance the cooling potential in the first combustor.

- 6) Intercooling adds mechanical complexity and increases cost, but the combined-cycle output is also increased to offset the added cost.

9.2.3 RELEVANT COMBUSTOR FEATURES

- 1) Inlet pressures to the first combustor would be high, making the radiation problems of concern. Maximum pressure ratios would typically be 50.
- 2) The TIT for the first turbine would be accordingly higher to achieve the maximum cycle efficiency. Effective cooling would be required to avoid high metal temperatures. Better materials will always be an alternate solution.
- 3) If intercooling is used, the inlet temperatures would be low so that cooling potential of the first combustor is enhanced, partially counteracting the problems of high pressures.
- 4) The second or double combustor would be required to operate in a vitiated medium, containing as low as 11% of O_2 as opposed to 21% of O_2 in standard air medium.
- 5) For the operating pressures (generally equal to a simple cycle) of the second combustor, the inlet temperatures would be high, again causing a review of cooling techniques, due to the decreased cooling potential of the medium. Typical maximum values would be around 10 atmospheres of pressure and a 1000 K of inlet temperature. However, typically this inlet temperature would be lower if the same pressure levels were to be achieved through compression alone.

9.3 DESIGN CONCEPTS OF SECOND COMBUSTOR

The possible areas of conceptual understanding and design problems are listed below.

AREA	PROBLEM/CONCEPT
PROPERTIES	Composition Thermodynamic & Transport
COMBUSTION	AFRS Adiabatic Flame Temperature Combustion Efficiency Stability-Flammability Limits
HEAT TRANSFER	Evaluation procedure Emissivity, Absorptivity
NOx	Generation
DESIGN CRITERIA	Sizing
ASSOCIATED	Starting Controls for double fuel Thermal Stability of Fuel Auto ignition Cooling of fuel delivery lines

Table 9.1 Concepts - Double Combustors

9.3.1 PROPERTIES

The generalized method described as Chapter 5, which is based on the constituent concentration is adequate to evaluate the thermodynamic and transport properties.

9.3.2 COMBUSTION

The available 21% of O₂ in the standard air medium would be consumed partly in the first combustor, but will be sufficient for a subsequent combustion. This vitiation due to precombustion can be degraded by water/steam injection. This further depletion is purely by the fact that the relative O₂ content in the total flow is reduced. The addition could be for NO_x emission reduction. The water could also be introduced if evaporative intercooler is introduced into the cycle. However to gain insight into the order of magnitude of reduction in Oxygen content when only water is added, fig 9.3 is included.

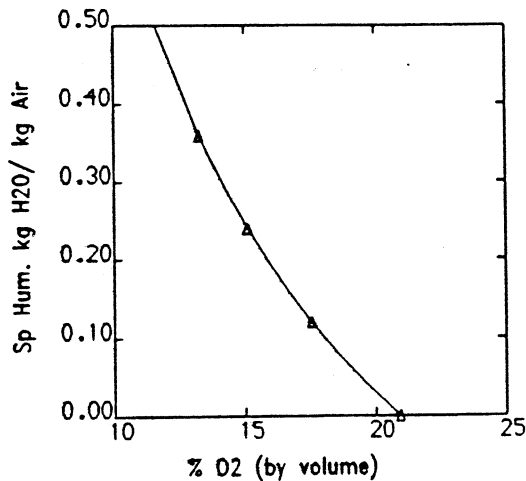


Fig 9.3 Specific Humidity versus Vitiation

9.3.2.1 AFRS

It can be safely guessed that vitiation would cause the AFRS to go up and adiabatic flame temperature to come down. Calculations are performed using methods developed in this program (Appendix A and C), to demonstrate this variation shown as Fig 9.4.

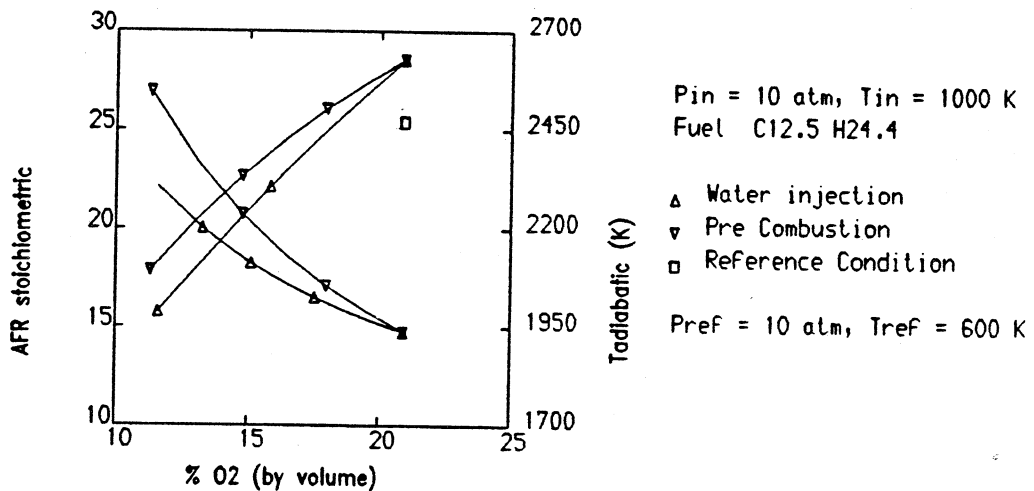


Fig 9.4 AFRS and Tadiabatic under vitiation

9.3.2.2 ADIABATIC FLAME TEMPERATURE

Similarly the maximum temperature attainable is also shown in Fig 9.4. Roughly for one % of O₂ depletion, the adiabatic flame temperature drops approximately by 50 K.

This means that in case of heavy air vitiation in the high temperature reheat combustor, the flame temperature will be lower than that of the conventional combustor. Also deteriorated combustibility, less NO_x generation and less wall temperature rise would be expected. However, this does not necessarily mean lower wall temperature because of the higher inlet air temperature. In order to keep this adiabatic flame temperature constant, if the inlet temperatures are raised by about 110-120 K (approximately double the temperature reduction due to O₂ depletion) the cooling potential would be lost.

9.3.2.3 COMBUSTION EFFICIENCY : A combustor designed for maximum efficiency, if made to operate under vitiated condition, the efficiency is expected to drop considering the drop in reaction kinetics. The equation (7.18), derived earlier, indicates the loss in η , considering the vitiation under moderate inlet temperatures. However the inlet temperature of any typical double combustor would be much higher. Thus a reheat combustor designed to operate at maximum efficiency, the deterioration due to O₂ depletion would not be as serious as in a normal combustor.

9.3.2.4 FLAMMABILITY LIMITS : Drop in reaction kinetics due to vitiation narrow the flammability limits. The relative drop can be seen for the main combustor of Moonlight project Fig 7.9. Similarly, Fig 9.5 represents the stability limits

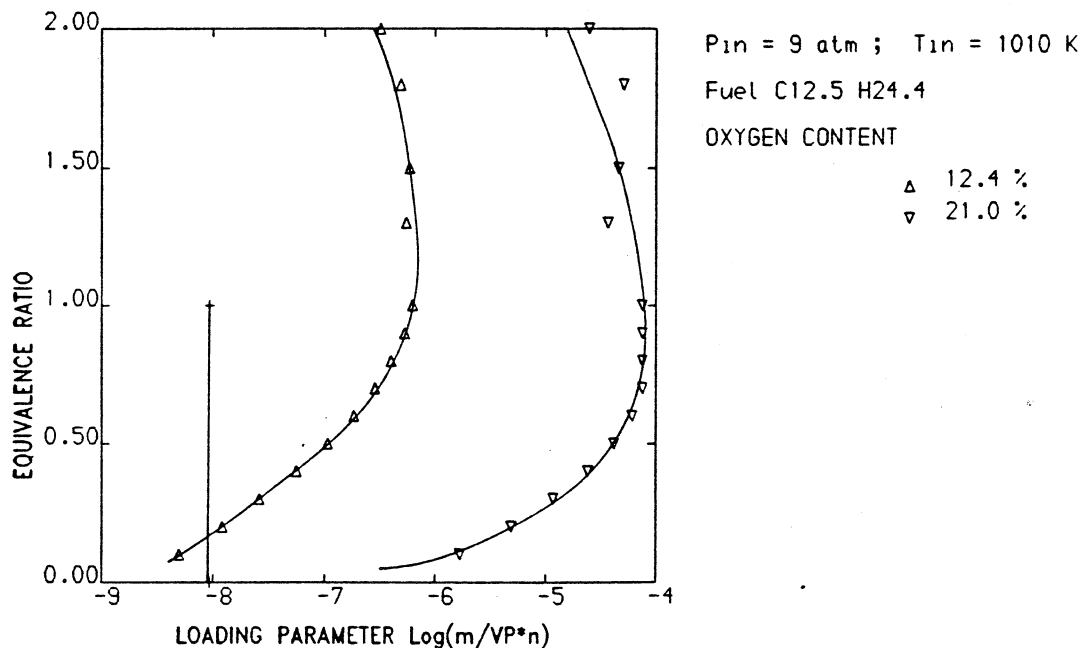


Fig 9.5 Effect of vitiation on Weak extinction in a double combustor

of a Reheat combustor designed by DEPTH, based on the operating conditions of those of the Moonlight's project (rest of the results are presented as Case 4 in Chapter 11).

9.3.3 HEAT TRANSFER

The operating environment has low pressure, but relatively higher temperature with depleted oxygen content. However the processes of heat transfer viz., radiation and convection are the same. No new procedure is suggested, as it is felt logical to assume that the earlier procedure (Chap. 6) is adequate. The change in medium is accounted for through composition and corresponding thermodynamic and transport properties. Considering the fact that the bulk is still nitrogen, there will not be appreciable change in transport properties due to composition, but the temperature at which these are evaluated will be higher in the annulus and possibly be lower in the liner due to lower gas temperatures due to vitiation. As regards to radiation, no simple procedure is available to estimate the emissivity or absorptivity if O₂ is reduced. However following the correlations which are temperature and pressure dependent, these should adequately represent the medium, until more experimental data is available. Non-luminous radiation should be more than what it would be for the same operating conditions considering higher concentrations of CO₂ and H₂O. Lower pressures and higher inlet temperatures would again conflict to increase the emissivities. Mean beam lengths should generally be higher as compared to the first due to possible higher flows (addition of first turbine coolant flows) and also due to the need for higher combustion air flows from the total available due to increased AFRS values because of vitiation. Hence the non-luminous emissivities cannot be expected to be lower in any case. The luminous part due to soot can be expected to be the same as otherwise obtained for the same injector, primary zone aerodynamics and pressure level. Pressure levels would generally be low, not promoting soot production. But as AFRS is higher and flame temperatures are lower, in order to achieve high heat release rates, tendency would be to run the primary zone richer than usual. But this effect would be mitigated if fuel distribution through proper selection of the injector is made. The method of heat transfer evaluation of Chapter 6 should represent the double combustor also. Applicability of correlations, which are experimentally derived, however, dubious, are the best available. The comparative results (Case 4 in Chapter 11) exhibit that the method is generally valid.

9.3.4 NO_x

As NO_x formation is directly dependent on the flame temperature, vitiation should produce reduced NO_x levels.

Following the existing method of evaluation, NO_x variation with vitiation is as shown.

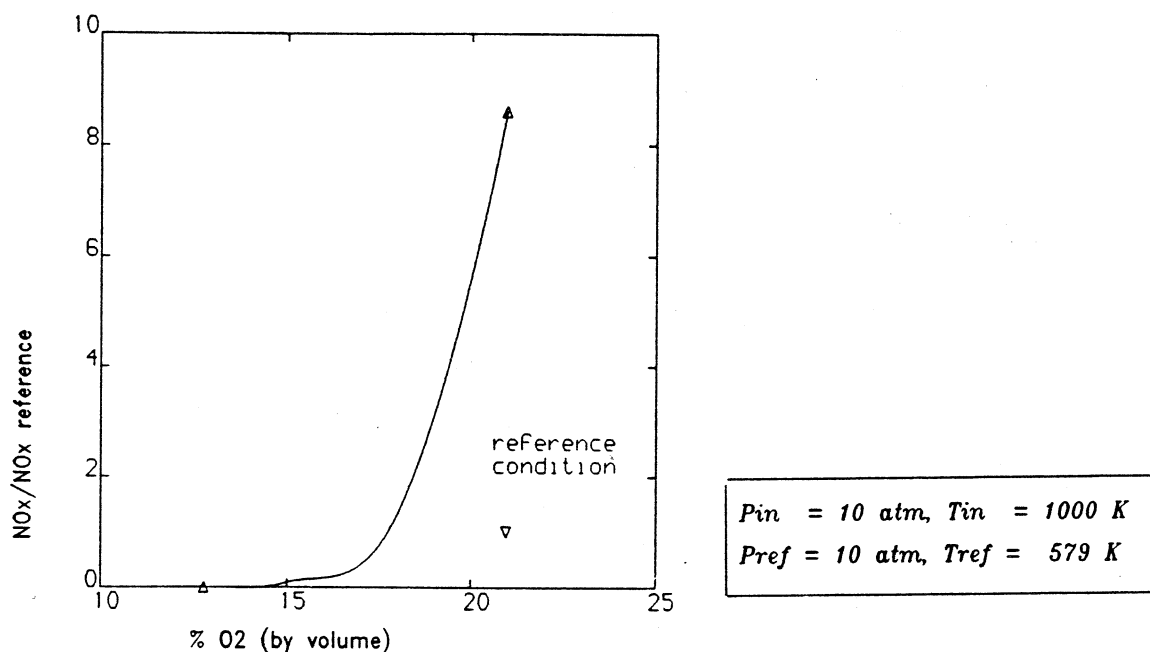


Fig 9.6 NO_x under Vitiation

The data pertains to what is generated in the primary zone only. For reference they are compared with a standard 10 atm condition, which would correspond to 579 K inlet temperature. At 20.95% of O₂, (which corresponds to standard dry air), the high increase in NO_x generation is obviously due to the increase in inlet temperature. But subsequent reduction for lower O₂% is due to the reduction in flame temperature due to vitiation. The level of NO_x produced at around 15% can be seen to be much less than what is even considered as a future limit at the exit of a combustor.

The inlet vitiated medium for the second combustor will carry trace species that are generated in the first combustor, the level of which will depend on the way fuel/oxidant are added in the first combustor. However, this total amount would be split between the burning and dilution zones of the second, shown schematically as fig 9.7. Considering higher AFRS, the amount of air for the burning zone would be above 25%. Mcvey et al. (1983), used vitiated medium to test conventional combustors, along with corrections for the trace species generated due to precombustion. According to them it is probable that the 25% of NO_x delivered to the burning zone is largely destroyed

and the balance of 75% NO_x in the dilution air passes through the combustor to exit as the total emissions of the system. However no experimental validation is offered. Similar suppositions are offered by Moreno et al (1987) in their article about a double combustor which is under investigation. No test results are offered yet. Incidentally this is the second design other than Moonlight project relating to reheat combustor concept under trial.

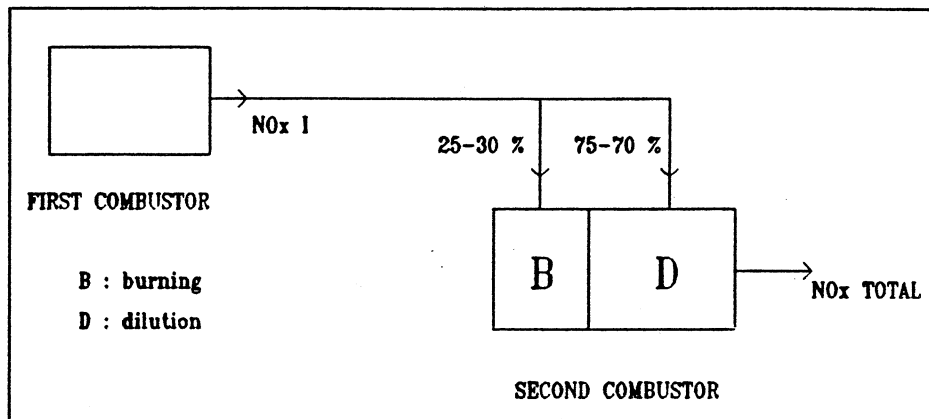


Fig 9.7 Schematic representation of NO_x production in a system with a double combustor

The assumptions regarding the destruction of NO_x (due to the first combustor) in the second combustor burning zone, will make the double combustor concept extremely attractive as regards to NO_x emissions. However, this assumption does not appear to be plausible and it would not be correct to presume the same without validation. Hence this supposition is disregarded. However, it is possible to maintain a very low NO_x generation level in the second combustor, by maintaining low peak temperatures in the primary zone due to high vitiation of the oxidant medium. This is clearly demonstrated by Case 4 in Chapter 11. Thus, the sum total is marginally higher than what has entered the burning zone. Hence the overall NO_x level of the system, i.e. including the first combustor, should at most be marginally higher than the first combustor alone.

However the NO_x generated for unit power output should be superior in a two combustor situation partly due to higher output at higher thermal efficiency and partly due to the lower NO_x generation level of second combustor as a result of vitiation. This, if confirmed experimentally, could well be a major incentive to go for a double combustor

arrangement for future applications.

Another interesting argument would be as to what is the right design philosophy for the level of primary zone equivalence ratios in the double combustor configuration. The possible four combinations of RICH-RICH, RICH-LEAN, LEAN-RICH AND LEAN-LEAN for the two combustors seem to be in a decreasing order of NOx generation levels. Here RICH may be viewed for equivalence ratios around stoichiometric, ie. anywhere above 0.9. RICH-RICH would be selected considering the thermal efficiency point of view and LEAN-RICH appears to be an optimum from NOx and durability considerations. However, more rigorous cycle analysis may be needed to confirm this.

9.3.5 SIZING CRITERIA

Considering the above, it can be seen that overall sizing can be done in the same lines as the conventional combustor, but cooling technique has to be considered.

9.3.6 STARTING

In the case of reheat Gas Turbine, the first stage power turbine nozzle area should be designed for the greater volume at the elevated temperature- the area varying directly with absolute temperature to maintain proper velocity. This situation leads to two possibilities (1) Variable first stage nozzles or (2) start up with both burners operating under a programmed control temperature rise. The second option appears to be practical and economical.

CHAPTER 10

PROGRAMME DESCRIPTION

10.1 FOREWORD

The complete description of the programme is intended to be compiled in three parts 1) Users' Guide 2) Users' Manual and 3) Programme Listing. The first deals with the execution of the programme containing information about Input/Output (I/O) devices and format, error messages along with typical examples. The second part contains brief design philosophy, description of modules/ subroutines, listing of variables, common blocks, and flow charts. The third part is the programme itself on a hard copy. A brief description of the I/O information is only included here for completeness sake. Attached as Appendix Q are four flow charts describing DEPTH's MAIN module and its INPUT/OUTPUT flow.

10.2 INPUT

It is aimed to make the programme a highly interactive one, so that no prior knowledge programming is required. The range of values the programme is expecting as well as the units are prompted so that the user can very easily follow the design procedure. The programme structure enables the user to choose one of the following options

1. Interactive Design
2. New Design
3. Continue from last termination

10.2.1 INTERACTIVE DESIGN

The user can carry out a design fully interactively, following the messages and inputting on to the screen directly, making suitable judgments as and when necessary.

10.2.2 NEW DESIGN

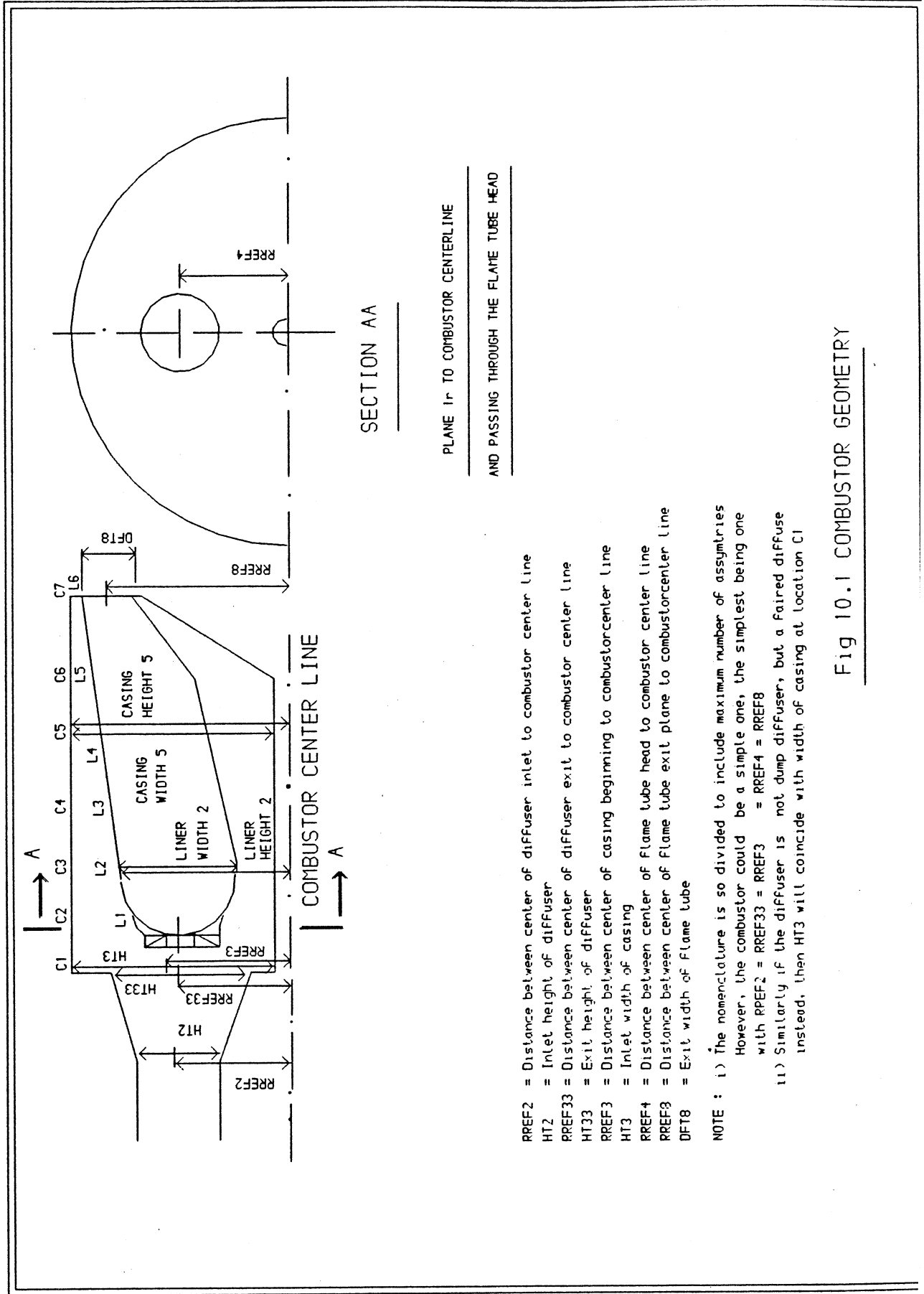
However, to hasten the session, the same input can be done through files appropriate for preliminary design and performance evaluation. These require to be created before running the programme. File name is of the format DESIGN.DAT or INPUT.FOR, containing not more than 12 characters in its specification. The data is required to be entered in block fashion, the title signifying the nature of the data. Care should be taken for order and the units of data in each block. The values are of free format. Whenever, the data is insufficient, the entire block can be omitted. The block information as input for preliminary design is given as Table 10.1 and that for the flow evaluation as 10.2.

Table 10.1 Input for Preliminary Design

FILE NAME : of the format DESIGN.DAT or INPUT.FOR , containing not more than 12 characters.

PARAMETER	UNITSE	OPTION
'SPEC'		
. Mass flow	kg/s	
. Total Pressure inlet	N/m ²	
. Total temperature inlet	degree K	
. Total temperature outlet	degree K	
. Overall Pressure loss	%	
. Pressure loss factor	R	
'GEOM'		
. Reference radius	m	refer fig 10.1
. Inlet Height	m	
'TYPE'		
. Type of Combustion Chamber	I	1 Annular 2 Tubular 3 Turboannular
. Type of Fuel	I	1 AVTUR 2 AVGAS 3 JP4 4 JP5 5 DIESEL 6 FUEL OF YOUR CHOICE
. Carbon Number	R	
. Hydrogen Number	R	
. Nitrogen Number	R	
. Oxygen number		
. Type of Diffuser	I	1 Faired 2 Dump
. Type of Atomiser	I	1 Pressure Atomiser 2 Air Blast atomiser 3 Air assist atomiser 4 Vaporiser
. Type of Operation	I	5 Atomiser of your choice 1 Industrial 2 Airborne < 30 K 3 Airborne > 30 K

NOTE : @ I : integer number
R : real number
'C' : character with colons either side
or units as indicated.



- RREF2 = Distance between center of diffuser inlet to combustor center line
- HT2 = Inlet height of diffuser
- RREF33 = Distance between center of diffuser exit to combustor center line
- HT33 = Exit height of diffuser
- RREF3 = Distance between center of casing beginning to combustor center line
- HT3 = Inlet width of casing
- RREF4 = Distance between center of flame tube head to combustor center line
- RREF9 = Distance between center of flame tube exit plane to combustor center line
- DFT8 = Exit width of flame tube

NOTE : i) The nomenclature is so divided to include maximum number of asymmetries. However, the combustor could be a simple one, the simplest being one with RREF2 = RREF33 = RREF3 = RREF4 = RREF8. ii) Similarly if the diffuser is not dump diffuser, but a faired diffuser instead, then HT3 will coincide with width of casing at location C1.

Fig 10.1 COMBUSTOR GEOMETRY

Table 10.2 Input for Performance Evaluation

FILE NAME : of the format PERFORM.DAT or INPUT.FOR , containing not more than 12 characters.

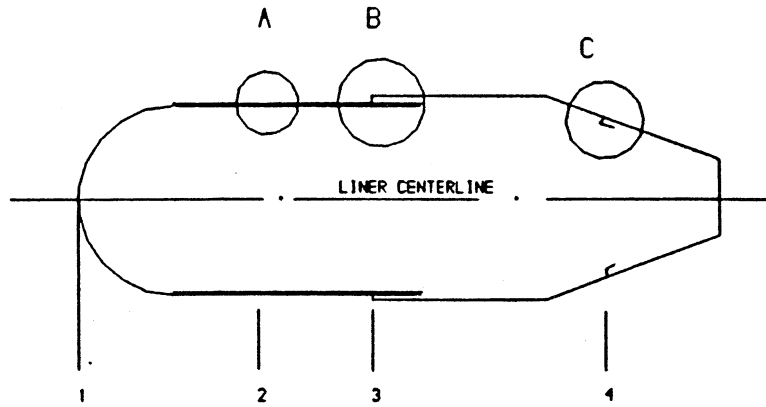
PARAMETER	UNIT [ⓐ]	OPTION
'MATRL'		
. Liner Material	I	1 Aluminium Alloy 2 Nimonic 90 3 Hastalloy 235 4 Inconel 700 5 Material of your choice
. Casing Material	I	Same as above
. Liner wall thickness	m	
. Casing wall thickness	m	
. Coating choice	'C'	'Y' YES 'N' NO
. Coating material	I	1 Alumina Al2O3 2 Zirconium Oxide 3 Beryllium Oxide 4 Silicon Nitride 5 Material of your choice
. Coating thickness	m	
'GUESS'		
. Slot selection	I	1 slots predicted
. Liner temperature limit	degree K	1 Outer radius constant 2 Inner radius constant 3 Axi symmetrical
. Nozzle option	I	
OR		
'GIVEN'		
. Slot selection	I	0 slots provided
. No of slots	I	
. No of evaluation routines	I	3 Annular 2 Other types
'SLOTS'		
. Slot position from dome head	m	
. Slot type	'C'	'M' Mixing Hole 'C' Cooling Slot 'D' Dome Hole 'A' Area Change 'N' change from tuboannular to annular
. Slot Choice	I	1 wiggle strip 2 unobstructed gap 3 splash cooled 4 impingement cooling 5 yet to be incorporated 6 plain circular holes 7 plunged circular holes 8 oval holes 9 yet to be incorporated
. Slot sign	'c'	'+' slot steeped up eg. machined ring '-' slot is stepped down eg. skirt welded to the liner
. Slot station Numbers	I	No of stations the slot is described refer fig 10.2
FOR EACH STATION :		
. Station position	m	with respect to the beginning of the slot
OUTER FOLLOWED BY INNER		
. Slot height	m	
. Slot major diameter	m	
. Slot minor diameter	m	
. No of holes	I	
. Discharge coefficient	R	
'VALUE'		
. Fraction of total massflow to annulus flow at the liner end	kg/s	Default value : 0.5E-3
. Control volume length	m	Default value : 0.001
. Iterations	I	Default value : 15
'END'		

NOTE :

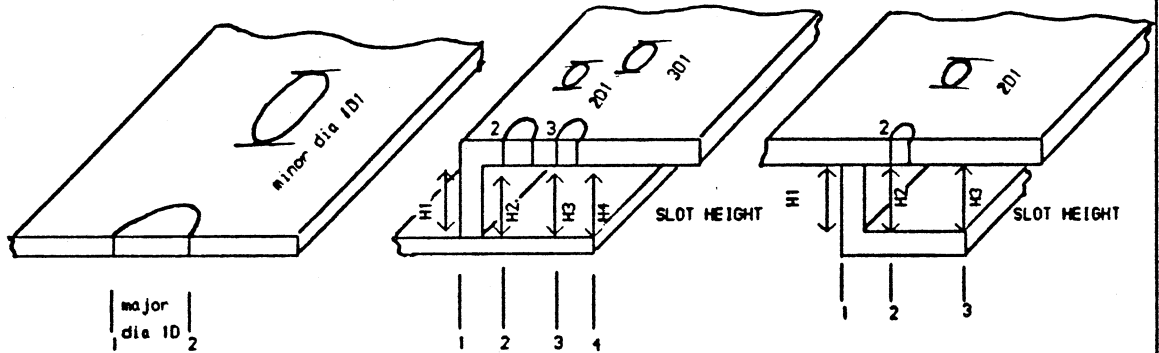
ⓐ I : integer number
R : real number
'C' : character with colons on either side or units as indicated.

* the first location is always as distance 0.000 m and is for dome head, whether dome holes are present or not.

NOTE : Usually modelling techniques adopt a two stage strategy in which gridding and evaluation are independent and are executed in the same order. But, as preliminary design is also coupled with the evaluation in the present work, prior gridding is not possible. In order to circumvent the problem, this new strategy of developing grid as well in a marching fashion is adopted. The grid is developed from the zonal exit points which form the reference in a new design. Linear interpolation is done between them to arrive at the complete picture of the combustor. However if cooling slots or mixing holes are incorporated subsequently, the starting of their location will also be included as the reference points. These features are called SLOTS, which are of six types (D,M,C,A,N,E)- D to signify the dome head, M for a mixing hole, C for a cooling slot, A for a curvature change like a nozzle or dome joining the straight portion of liner or N for tuboannular converting into annular section i.e. a common discharge or E for the end of the combustor. Reference is taken as the distance from dome head to the feature/slot. Again each slot is divided into STATIONS, to include the characteristics of the slot. Each station is described with reference to the beginning of the slot. Thus a mixing hole may require one station to signify the beginning, where as a cooling slot requires at least three to signify say beginning of slot, beginning of air entry passage, and end of lip. A curvature change can be described by one station only. The lip configuration can be broadly classified either as a step or a skirt. In the former the entire liner diameter grows at the step or beginning of the cooling configuration, where as in the later case an additional piece is joined keeping the liner diameter constant. These are differentiated by a sign convention of '+' or '-' respectively in the input. Fig 10.2 should amplify these above comments. It is reminded that in practical combustors, it may be hard to find such sharp bound geometries, however, approximations are necessary for evaluation. All these slots and station reference points along with the zonal points form the basis on which linear interpolation is done to develop the grid. Logically any complicated dome shape can be accounted for by assuming sufficiently large number of slots to account for the curvature. Major and minor axes are introduced to account for elliptical holes or rectangular holes. Effort is made to account for the cross section when it is circular or approximately rectangular. The later is a feature found in tubo annular combustors, when the nozzle joins the common discharge.



SLOT POSITION	12	13	14
SLOT TYPE	'H'	'C'	'C'
SLOT CHOICE	6	4	3
SLOT SIGN	-	'+'	'-'
SLOT STATION NO	1	4	3



	A	B				C		
STATION POSITION	11	11	12	13	14	11	12	13
SLOT HEIGHT	0.0	H1	H2	H3	H4	H1	H2	H3
SLOT MAJOR DIA	ID	0.0	2D	3D	0.0	0.0	2D	0.0
SLOT MINOR DIA	ID1	0.0	2D1	3D1	0.0	0.0	2D1	0.0
NO OF HOLES	N1	0	N2	N3	0	0	N2	0
DISCHARGE COEFFICIENT	0.0 #	0.0	0.7	0.6	0.0	0.0	0.0	0.0

if 0.0, program generates CD
! user specified CD.

Fig 10.2 Slot Specification

10.2.3 CONTINUE FROM LAST TERMINATION

This facility uses the I/O file which is created at the end of each session. Advantage lies in the fact that performance evaluation can be done without the need to go through the preliminary design. This is true in the case, when an existing chamber needs to be evaluated for performance.

10.3 OUTPUT

The output generated by the programme is tabular as well as graphical.

10.3.1 TABULAR

The results of each session are stored in a new I/O FILE, whose name can be inputted by the user. This, too is of the format RESULTS.DAT or OUTPUT.FOR, containing not more than 12 characters in the file name.

10.3.2 GRAPHICAL

The programme can generate the following graphs

1. Flow Evaluation:

- 1) Combustor geometry
- 2) Liner temperature variation
- 3) Mass flow splits
- 4) Radiative Coefficient Variation
- 5) Convective Coefficient Variation
- 6) Any one of the following variables by choice

- a) Pressure
- b) Mach No
- c) Velocity
- d) Emissivity
- e) Absorptivity
- f) Cooling Effectiveness

2. Stability Data

3. NOx Data

User can view the graphs on appropriate terminals, interactively while running the programme before opting to store

them. If opted, the programme stores the output in a file called PLOT.SAV. This can be viewed on any appropriate terminal and/or can be obtained as hard copy prints at any time.

Facility is provided to store flow evaluation and heat transfer data for upto four cases, so that ready comparison can be done for the heat transfer data interactively.

10.4 PC ADAPTABILITY

The boom in the desktop PC (Personal Computer) market by the end of 1986, had caused a review in the philosophy, that the programme should be able to be run on a PC. This obviously increases the transportability and stand alone capability of the programme. The immediate changes to the program was to size the VAX FORTRAN 77 to a PC version. Here, Microsoft's FORTRAN 77, which can be adopted by any IBM PC or its compatibles, is made use of. Typical discrepancies such as problems with double precision, format handlers, input output devices were eventually ironed out. External library dependence had to be avoided if PC usage has to be effective. The NAG (Numerical Algorithm Group) library used for non-linear equation solution in the heat transfer calculations had to be replaced by author's own algorithm. This completed the revision for the basic programme to be able to be run on desktop PC. However, the GINO libraries are not compatible with the PC. No attempt is made to establish suitable PC graphics package due to time constraints.

The programme was tested on an IBM AT as well as on AMSTRAD PC 1512 using Microsoft's FORTRAN 77 compiler version 3.3. The CPU time is roughly 3 to 4.5 times more than VAX, which was less than 30 sec for one iteration of flow evaluation along with a heat transfer calculation. However, being interactive and short overall duration for one iteration (of the order of 15 to 30 minutes) this point has no real significance. With the available compiler, as double precision can be used, the accuracy of the results have not suffered.

CHAPTER 11

CASE STUDIES AND DISCUSSION

11.1 VALIDATION

The combustor technology and the computing intricacies, both have assumed equal importance during the development of the present work. Before validating the programme as a whole, the sub-models such as property evaluation (Chapter 5) and flame temperature evaluation (Appendix C) were verified. The programme is validated against two existing combustors and the results are found to be quite realistic and encouraging. The proprietary nature of the information concerning the two combustors prohibits further identification of the combustors. However, the programme has been used on several cases. The discussion of the results of selected cases as examples is intended to indicate the strengths as well as the weaknesses of the programme, and also scope for the future work.

11.2 DISCUSSION

For the purpose of study, DEPTH is used on the following combustors

- 1) A tuboannular combustor for a Gas turbine for Industrial application.
- 2) A tuboannular combustor for an Aeroderived Gas turbine for Industrial application.
- 3) An annular combustor for a Gas turbine intended for airborne application
- 4) A reheat/double combustor

For Case 1 and 3 Performance Evaluation and for Case 2 and 4 Preliminary Design as well as Performance Evaluation are carried out. The results are included as Appendix R with the following comments.

CASE 1

This is a typical medium capacity (15 MW) industrial engine-a traditional design and hence little constraints on the size. Additional features that are incorporated are double walled cooling, the nozzle or the transition duct is a common annulus into which all the tubes discharge (in other words the tuboannular becomes an annular design). Programme's routine also had to be modified to suit the

peculiarity that the primary plunged holes go through the impingement cooling lip. The flow proportions and metal temperatures are reasonable. The impingement cooling relations (eqn 6.43) appear to be yielding sensible results. However, improvements, as described in Chapter 6, are needed to evaluate the leading portion of the cooling slot. The lean, but nearer stoichiometric primary zone coupled with the very large residence times are a source for the high NOx emissions.

CASE 2

As the engine is an aeroderivative, specific power is higher. Consequently the operating pressure and the turbine inlet temperature are higher. Hence the cooling requirement goes up. The programme has designed a liner which compares well with the available similar combustors in the field. The metal temperatures, level of NOx and lean blow off limits are within acceptable limits.

CASE 3

This engine was intended to be a design exercise upto the finished product, for a batch of students from one of the noted Technical Institutes. In order to match their water flow analysis and initial combustion tests, the combustor is analyzed for both cold as well as hot flows. Using the cold flow option in the programme, the mass flow splits obtained are as represented below.

% MASS FLOW SPLITS							BLOCK: 6
		(sec)		(dil)			
		16.82	47.39				
64.20		0.00	0.00	8.46	13.63	3.14	
25.23	MIXING	v	v	v	v	v	
		----- (kg/s/tube)					
		R	P	S	D	Z	
10.52	10.52(1SWRL) [x]						
	0.00(-1ATOM)	2.26	0.66	0.25	0.24		
	0.00(-1DOME) [x]		equivalence ratio				
0.00	COOLING						
		//	//	//	//	//	
99.96		0.00	0.00	0.00	0.00	0.00	

Fig 11.1 Mass Flow Splits - Case 3

It can be clearly seen that the flow proportions are mismatched to the traditional burning and mixing zones. The highly over rich primary zone and near stoichiometric condition in the secondary zone indicate that actual burning will be in the secondary zone. The highly over rich primary

zone will lead to starting problems, which was also observed by the team during the rig tests.

Though it is difficult to exactly locate the size of the burning zone and consequently where in the secondary zone the peak temperature would occur. It is reasonable to assume that this is likely to happen more towards the secondary zone exit. This is again based on a simple assumption that the peak temperature occurs at stoichiometric equivalence ratio. In this case a linear interpolation between 2.3 and 0.68, which are the exit values of equivalence ratios at primary and secondary zones respectively, leads to a stoichiometric plane more towards the secondary zone exit. This procedure is defaulted into the programme and comes into play when the primary zone is run over rich (the default limit is set as 1.1, PHI is 0.995 at an efficiency of 90%). Case 3B represents the output of assuming the temperature profile as indicated above.

The programme has the flexibility of varying the location of these peaks and review of the results. Here, a variation is tried in that the peak plane is assumed to occur immediately after the primary holes (as original design is intended to have the burning zone within the primary zone). Case 3C represents the consequent metal temperatures.

The programmes default logic appears to be reasonable as the the temperature profile (Case 3B) is not too far from the thermal paint exercise as explained subsequently.

The liner, after half an hour of running, is as displayed as Plate R-1 (Candelier et al (1987)). The darker regions near dilution holes indicate location of maximum temperature (>1073 K). Red indicates the coolest region, closer to the inlet temperature (~455 K). Case 3D is a run with operating conditions exactly matching with those of the above test conditions (the test is done with roughly half the mass flow and correspondingly lower inlet pressures)

Water flow visualisation has indicated a separation in the inner annulus entry region shown as Plate R-2 (Candelier et al (1987)), due to abrupt change in cross section due to the blunt liner head. The secondary holes on the inner liner, are in reality lying in the wake of the separated region. This causes deficiency in the secondary hole flow from the inner liner. This phenomenon cannot be predicted by DEPTH, however, it can be simulated by artificially lowering the effective flow area of secondary holes by inputting a lower discharge coefficient, (in this case a value of 0.01 appear to be more appropriate).

Thus, these variable options such as profile shifting or artificially adjusting mass flow rates through the slots, enable the programme to be used effectively supplementing the information provided by tests such as cold flow or thermal paint exercise.

CASE 4

The design is attempted at the inlet operating conditions as specified by the MOONLIGHT Project (Mori et al (1983)). The inlet oxidant medium is deduced based on the first combustor's inlet and overall flow proportions. As no information regarding the inlet or outlet geometry of the combustor is given, a simple traditional design is carried out.

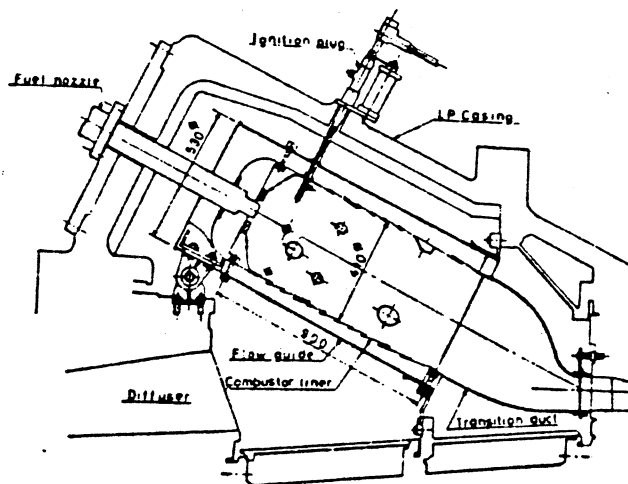


Fig 11.2 Basic configuration of Reheat Combustor
(Mori (1983))

The overall geometry specified by the programme is not very far behind the figures quoted in Fig 11.2. The reference diameter being 0.5m as opposed to their 0.53m. Though the combustor is depicted as canted (Fig 11.2) and also the additional overall length reduction due to the diffusers location, no attempt is made to adjust these or any other geometrical feature. Continuing with the Programmes generated values, a liner of 1.12m (this includes the transition duct of length 0.21m) length is evolved, which is of similar proportions to that of the MOONLIGHT project.

Considering the large size and also the possible high cooling flow requirements, a low dilution flow can be expected. But this may be adequate considering the fact that

the dilution and nozzle lengths are fairly large to ensure adequate mixing and hence reasonable pattern factor at the end of the combustor. Hence an initial flow of 20% is assumed as the dilution flow for the preliminary design sizing.

The mixing and cooling configurations are estimated following an interactive exercise in Performance Evaluation. The design limit for the permissible maximum wall temperature is taken as 1125 K. However, the cooling margin is not very much as the inlet temperature is 1010 K. Wiggle strips are chosen as the cooling configuration for the dome and impingement cooling with two rows of jets for the rest of the combustor. The total number of cooling slots are also convincingly closer. Thus, a design is successfully carried out with the metal temperature limit of 1125 K. However, the heat transfer analysis shows an exception at the location just before the secondary mixing hole, where the temperature is close to 1200 K. One of the reasons for the departure (ignoring the simplified empirical approach) is, though the initial selections of cooling slots is based on temperature limit of 1125 K, the flow proportions are not quite correct at that time. The remedy now is to reposition the cooling slots on either side of the problem area and/or change the conditions (say hole size or number etc) to promote higher cooling potential. The convection coefficient graph provides a rough measure, as to which is a better choice. This change will not only change the cooling configurations at that point but will also affect the overall flow proportions. This can, however, be quickly viewed through the programme. This fact can be considered as one of the strengths of the present programme in examining the effect of one such change on the overall performance. For comparison the extract of massflow splits is reproduced here.

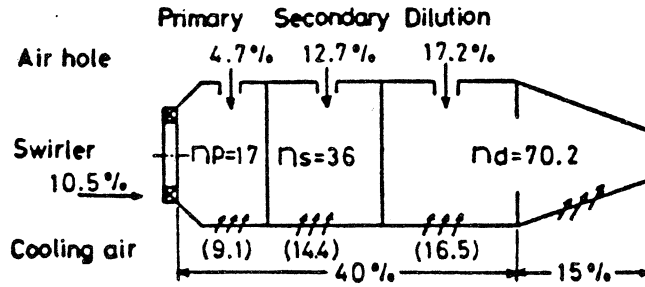


Fig 11.3 Air Distribution of RC (MORI (1983))

% MASS FLOW SPLITS		(sec)					(dil)					BLOCK: 6
39.88		0.00	0.00	21.39	0.00	0.00	18.50	0.00	0.00	0.00		
0.00	MIXING	∇	∇	∇	∇	∇	∇	∇	∇	∇		
10.77	10.77 (1SWRL) [x]	R	P	S	D	Z	A = 17.200					
10.77	0.00 (-1ATOM) [x]		1.00	0.58	0.33	0.31	F = 0.216					
	0.00 (-1DOME) [x]			equivalence ratio								
49.30	COOLING	//	//	//	//	//						
99.96		2.43	12.85	5.68	20.92	7.42						

Fig 11.4 Air Distribution of RC by DEPTH

The general level of agreement appears reasonable, despite the fact that the exact dimensions are not known. The flow splits for the individual cooling configurations are given in Appendix R. If the turbine entry temperature is further hoped to be increased, more air will be required for combustion and consequently better cooling techniques using reduced flows will be required. Once evolved they can be added to the existing cooling configurations.

Though the vitiation is considerable in that O₂ by volume drops to 12.15 from 20.95 of standard air, the tendency of reduced efficiency and stability is offset by the very high inlet temperature. Using the modified Theta parameter concept developed (eqn 7.14), the combustor is examined for its range of efficiency.

$$\begin{aligned}
 R_{ref} &= 1.0 \text{ (m)} & P_2 &= 911930.0 \text{ (N/m}^2\text{)} \\
 D_{ref} &= 0.5 \text{ (m)} & T_2 &= 1010 \text{ (K)} \\
 A_{ref} &= 3.142 \text{ (m}^2\text{)} & \dot{m}_2 &= 206.4 \text{ (kg/s)}
 \end{aligned}$$

$$\begin{aligned}
 C_1 &= 0.3491446 & C_2 &= 585.4 \\
 \phi_{pz} &= 0.99 & \Theta_{mod} &= 4.77 \text{ E8}
 \end{aligned}$$

from eqn 7.14 $\eta = 99.99\%$

The stability curve also shows reasonable margin. Here E/R is taken as 20000 K as explained in 7.3.3. The lean blow out value at this power condition is 442 AFR.

The NOx is evaluated using the mean equivalence ratio of primary zone as 0.996 and a mixedness of 0.2. This gives a NOx mass fraction of $0.6\text{E-}5$ in the primary zone, which ultimately results in 2.3 ppmw at the exit of the combustor. This apparently is the best value for any combustor. Parametric study, by changing the mixedness, has yielded, 2.3 and 3.0 ppmw for 0.3 and 0.1 respectively. All are exceptionally good, if the combustor can demonstrate this in practice.

Though the trend is as expected and explained in chapter 9, the extremely low figures for the NOx can be a cause for skepticism. However, it appears logical to expect very low figures in the present case as the inlet medium is at a reduced energy level after an expansion and is vitiated to around 12% of oxygen due to precombustion as well as water addition through the intercooler, with a consequent lower peak temperatures. The peak temperatures in the burning zone are kept below 2100 K.

This value for the second combustor, when added to what has been delivered by the first combustor, should make the entire system attractive on the basis of NOx. The magnitude of the values are realistic when compared with the limited experimental data of Moonlight Project. However the conclusions drawn are not definite till proved experimentally.

With suitable formulation this could bring about a convenient correlation for NO emissions, provided data is available. Similar empiricism can be found in expressions such as Eqn 2.29 given by Lefebvre (1987). However, there is a scope for refinement considering vitiation.

For the double combustor designed the programme demonstrates the increase in metal temperatures and consequent increase in cooling flow requirement to restrict them and a possible deterioration in the traverse quality due to lower diluting flow. It also indicates the attraction due to low levels of NOx generation, at the same time the change in stability limits. (reproduced as Fig 9.5)

Case 4B and 4C demonstrate the advantage of using coating (here Alumina of 0.5 mm thickness with a surface roughness value of $6\mu\text{m}$ is tried) on the metal surface. The reduction in wall temperature is of low order due to low heat fluxes resulted because of the high metal temperatures. However, the primary zone value can be seen to be higher than those in dilution zone. The high metal temperatures are also the cause for both the cases to yield more or less similar values. This is because at those high temperatures the value given by the polynomial in Case 4C approaches the constant emissivity assumed in the former Case.

11.3 CLOSURE

The programme works well within the assumptions made. The reason for the preliminary design resulting in geometries being very similar to the actual ones is obviously due to the traditional approach of zoning the combustors. The evaluation routines assume constants which are very close to reality. Hence figures concerning NO_x or stability are invariably true, at least in the sense of order of magnitude. One positive inference is that the programme cuts short the time required for tedious and repetitive calculations needed at a preliminary design stage and the scope of visualising the combustion chamber as a whole.

The one dimensional approach with a constant property assumption is a major simplification in analysing the combustor field, though at times grossly misrepresents the actual and also lacks resolution or complete information. Hence a caution or judgment is required in extending the results. For example, the empiricism incorporated in evaluating the amount of recirculation into the burning zone (Chapter 4.8.6) may appear logical, but cannot be a universal truth. In such cases, the option of changing the equivalence ratio may be used to judge what could have been the correct value, as the mean equivalence ratio decides the peak temperature in that zone. Similar argument holds for say NO_x or stability evaluation. For example the statistical parameters such as variance or distribution functions in NO_x estimation or the dependence exponents (1.75 or 1.3 for the pressure) in stability calculations may require judgment. However, following such philosophy for evaluation is justified. Similarly it can be argued as to which is the right way to size the combustor. Pressure loss, altitude relight or ignition characteristics can all be related to the operating conditions and geometry. Thus knowing the operating conditions and the parameter, the size can be evaluated. But the point to be noted is that there is a matter of judgment as to what would be the parameter and or operating conditions at that time. Hence guessing the PLF

for pressure loss approach is as uncertain as to guess the mass flow, the pressure and the temperature conditions at the relight conditions at the altitude. These indirectly make the designer fall back on experience and logically extend the limits or choose size. However, one pessimistic approach would be to guess the parameters as ones experience permits and choose the maximum size from all the concepts. The above comments may well apply for any design routine or equation chosen in the programme.

It could be seen that simplification routines developed to evaluate parameters such as stoichiometric air fuel ratio, flame temperature for any equivalence ratio at any efficiency, combustion product composition and transport and thermodynamic properties for any fuel, oxidant media should prove to be valuable at a preliminary design stage.

Refinement can be attempted. But the reminder to "kitchen sink theory" (para 2.3) should leave the programme to be content with the accuracy. Also refinement of one process may not necessarily lead to better results. Leaving the pessimistic hint behind this statement (if taken, there is a danger of remaining static taking cover under the contented statement that this is the maximum possible, marginal benefits are not worthwhile), every individual process in the programme can be better represented and better coupled. First one should be injector- its spray characteristics and consequent evaporation and mixing requires to be included. Higher cooling flows do indicate less dilution flow availability, but this information cannot be used to represent the loss in traverse quality. This can be achieved through 2 or 3D codes or simple juxtaposition of several 1D flows with suitable interaction between them. There is a need to incorporate this for a comprehensive analysis of combustor and its impact on the hot end components.

CHAPTER 12

CONCLUSIONS

DEPTH (Design, and Evaluation of Pressure, Temperature and Heat Transfer in Combustors), an interactive computer program in FORTRAN 77 has been produced with the following characteristics.

- 1) The programme is essentially one-dimensional, making use of the best correlations in the available literature.
- 2) It can carry out a preliminary design of a straight flow combustor of annular, tubular or tubo-annular type, and then execute a performance analysis in terms of estimation of flow proportions, heat transfer characteristics, stability and NOx emission parameters. The design has the feature of estimating the cooling configuration requirement based on a given metal temperature limit.
- 3) It can also carry out simply the performance analysis for an existing combustor, whose geometry is already defined.
- 4) It should prove to be an effective design tool, in reviewing the impact on performance by varying any of the variables, such as geometry or operating conditions, environment in terms of fuel or oxidant medium or hardware of the combustion chamber (injector or type of cooling slots etc).
- 5) Metal temperature calculations include both single wall as well as double wall configurations along with impingement or splash cooling.
- 6) It is a comprehensive study aid, drawing the benefits from its interactive nature.
- 7) Structured programming with modular concept should enhance modifiability for future needs.

An evaluation procedure is developed to calculate the combustion products concentration, their properties and temperature due to combustion of any generalised fuel and oxidant media. The results are within the accuracy, the programme is intended to be. NOx and stability based on stirred reactor theory, though requiring judgment in choosing some of the correlating constants, provide a comprehensive picture of the combustor. Accuracy is limited to the assumptions made in choosing the correlations.

However, the options that are offered and the flexibility for the user to change the assumptions or equations used should prove to be a definite advantage.

The need for and concepts of a double or reheat combustor are reviewed in the light of achieving very high thermal efficiencies. DEPTH is used to develop the understanding of these concepts and finally to design a double combustor. The low NOx generation levels in the second combustor could be an incentive to go for such a feature in conjunction with a combined cycle or cogeneration. The lower cooling potential of the medium for the second combustor may demand attention to the cooling technology if the cycle temperatures are high.

DEPTH is validated against two existing combustors and the overall agreement of flow proportions, metal temperatures, NOx levels and stability limits is quite realistic.

A version of DEPTH, using the VAX FMS (Forms Management System) is also produced for an effective interactive usage. Also the programme is sized to be able to be run on an IBM PC or its compatibles. So far the PC version of the DEPTH has been successfully tried on an AMSTRAD PC 1512. Stand-alone capability and portability should outweigh the increase in run time.

REFERENCES

- ** ADKINS RC (1978) : The Effect of compressor exit flow distribution on air placement in annular combustors, Engineering for Power, vol 100, No 3, July 1978, pp 444-451
- ** ADKINS RC, GUEROUI D (1986) : An improved method for accurate prediction of mass flows through combustor liner holes, ASME Paper No. 86-GT-149
- ** AGARD CP-275 (1980): Combustor Modelling
- ** AGARD CPP-422 (1987): Combustion and Fuels in Gas Turbine Engines
- ** AGRAWAL RK, YUNIS M (1981): A Generalised Mathematical Model to Estimate Gas Turbine Characteristics, ASME Paper No. 81-GT-202
- ** AL DABBAGH NA, ANDREWS GE (1981): The Influence of Premixed Combustion Flame Stabiliser Geometry on Flame Stability and Emissions, ASME Paper No. 81-GT-26
- ** BALLAL DR, LEFEBVRE AH (1972): A proposed method for calculating film cooled wall temperatures in gas turbine combustion chambers ASME 72-WA/HT-24
- ** BARR J, MULLINS BP (1947): Combustion in vitiated atmospheres IV- Performance of a typical Combustion Chamber, pp 225-229, Fuel
- ** BECKO Y (1976): Turbine blade cooling- impingement cooling review, Von Karman Institute for fluid dynamics, Jan 12-16.
- ** BEER JM, CHIGIER NA (1972): Combustion Aerodynamics, Applied Science, London
- ** BEER JM, LEE KB (1965): The effect of the residence time distribution on the performance and efficiency of combustors, 10th symposium on combustion, pp 1187-1202
- ** BENJAMIN GAL-OR (1984): New fighter engines, Int Jou of Turbo and jet Engines, Vol 1 No3
- ** BERGQUIST P, GUSAFSSON A (1975): Kanslighetsanalys av ett datorprogram for gasturbin-brannkammare och studier av filmkylningseffektivitet, STAL-LAVAL E-254, 1975-08.
- ** BERNARD L.KOFF (1984): Designing for durability in fighter engines Int. Jou. of Turbo and jet Engines, Vol1 No3.
- ** BOWMAN CT (1975): Kinetics of Pollutant Formation and Destruction in Combustion, Prog. Energy Combust. Science, Vol 1, No 1, pp33-45
- ** BOYSAN F, AYERS WH, SWITENBANK J, PAN Z (1982): Three-Dimensional Model of Spray Combustion in Gas Turbine Combustors, AIAA Paper No. 81-0324R, J.Energy, Vol 6, Nov-Dec 1982, pp 368-375.

- ** BRAGG SL (1953): Application of Reaction Rate Theory to Combustion Chamber Analysis, ARC 16170, Aeronautical Research Council, England.
- ** CAMPBELL IM, THRUSH BA (1968): Reactivity of Hydrogen to atomic nitrogen and atomic oxygen, Trans. Faraday Society, vol64, Part 5, pp 1265-1274
- ** CANDELIER P, FOULON JP (1987): Investigation of the performance of the combustion chamber of the MPT 01 jet engine, ENSICA, Toulouse, France.
- ** CARETTO LS (1976): Mathematical Modelling of Pollutant Formation, Prog. Energy Combust Science, Vol 1, No 2/3, pp 47-71, 1976
- ** CIFONE AJ, KRUEGER EL (1985): Combustion Technology, A Navy perspective, AIAA-85-1400
- ** CLARKE AE, ODGERS J, RYAN P (1962): Further studies of combustion phenomena in a spherical combustor, Eighth Symposium on combustion The Combustion Institute 1962, pp 982-994
- ** CLAUS RW, NEELY GM, HUMENIK FM (1984): Flame radiation & liner heat transfer in a tubular can combustor, AIAA-84-0443
- ** CLAYTON RM (1979): A Partial Oxidation Staging Concept for Gas Turbines Using Broadened Specification Fuels, ASME Paper No. 79-GT-169
- ** COHEN H, ROGERS GFC, SARAVANMUTTOO HIH (1982): Gas Turbine Theory, Longman
- ** COX GB (1975): An analytical model for predicting exit temperature profile from gas turbine engine annular combustors. AIAA paper No 75-1307
- ** COX GB, TILLER AR, LeTOURNEAU JJ (1981): Pattern Factor Improvement in the F-100 Primary Combustion System, ASME Paper No. 81-GT-25
- ** DOUGLAS IE (1986): Development of a Generalised computer program for Gas Turbine Performance Simulation; PhD thesis, SME, Cranfield Institute of Technology, England.
- ** DRYER FL, GLASSMAN I (1973): High temperature oxidation of CO and CH₄, 14th International symposium on Combustion
- ** DRYER FL, WESTBROOK CK (1979): A comprehensive mechanism for methanol oxidation, Comb Science & Tech. Vol 20, No 3-4, pp 125-140
- ** DOUGLAS IE (1986): Development of a generalised computer program for Gas Turbine performance simulation; Ph D thesis SME, CIT, Cranfield, England
- ** EDLEMAN RB, FORTUNE OF (1969): A quasi global chemical kinetic

model for the finite rate combustion of hydrocarbon fuels with application to turbulent burning & mixing in hypersonic engines and nozzles, AIAA Paper No 69-86.

- ** EDLEMAN RB, HARSHA PT (1978): Laminar and Turbulent Gas Dynamics in Combustors- current Status, Prog. Energy Combust. Sci. Vol 4, No 1, pp 1-62
- ** EL MASRI MA (1985): On thermodynamics of gas cycles: Part 3: Thermodynamic Potential & limitations of cooled reheat gas-turbine cycles, ASME Paper NO 85-GT-131
- ** EL SHANAWANY MSMR, LEFEBVRE AH (1980): Airblast atomisation- The effect of linear scale on mean drop size, J. Energy vol 4, NO 4, pp 184-189.
- ✓ ** ERCEGOVIC DB, WALKER CL, NORNGREN CT (1984): Ceramic composite liner material for gas turbine combustors, AIAA-84-0363.
- ** ESSENHIGH RH (1972): An introduction to stirred reactor theory applied to design of combustion chamber, Combustion technology, some more developmens, Academic Press
- ** EWAN BCR, BOYSAN F, SWITENBANK J (1984) : Closing the Gap between Finite Difference and Stirred Reactor Combustor Modelling Procedures, 20th Symposium on Combustion, The Combustion Institute 1984, pp 541-547
- ** FENIMORE CP (1971): Formation of Nitric Oxide in premixed hydrocarbon flames, 13th symposium on combustion, pp 373-380.
- ** FISHENDEN CR, STEVENS SJ (1977): The performance of annular combustor dump diffuser, Jou. Aircraft, vol 14, pp 60-67.
- ** FLETCHER RS, HEYWOOD JB (1971): A Model for Nitric Oxide Emissions from Aircraft Gas Turbine Engines, AIAA Paper No 71-123.
- ** FLORSCHUETZ LW, TRUMAN CR, METZGER (1981): Streamwise flow and heat transfer distributions for jet array impingement with crossflow, ASME paper No. 81-GT-77
- ** FREEMAN BC (1965): Discharge Coefficients of Combustion chamber dilution holes, College of Aeronautics M.Sc thesis, Cranfield, England
- ** FRISTROM. RM, and WESTENBERG. AA (1965): Flame Structure. Mcgraw-Hill Book Company.
- ** GARDON R, AKFIRAT JC (1966): Heat-transfer characteristics of impinging two dimensional air jets , ASME paper No 65-HT-20
- ** GARDON R, COBONPUE J (1962): Heat transfer between a flat plate and jets of air impinging on it, I.D.H.T., 61 Part II-ASME paper 53, pp 454-460.

- ** GORDON S, and McBRIDE. BJ (1971): Computer program for calculation of complex chemical equilibrium compositions, rocket performance incident and reflected shocks, and Chapman-Jouguet detonations. NASA SP-273.
- ** GREENHOUGH VW, LEFEBVRE AH (1957): Some applications of combustion theory to gas turbine development, Sixth Symposium on Combustion Reinhold, Newyork, 1957, pp 858-869
- ** GULDER OL (1986): Flame Temperature Estimation of Conventional and Future Jet Fuels, Jour Engg for Gas Turbines and Power, Vol 108, Apr 86, pp376-380
- ** HAMMOND DC, MELLOR AM (1970): A Preliminary Investigation of Gas Turbine Combustor Modelling, Combustion Science and Technology pp 67-80, Vol 2, 1970
- ✓ ** HAMMOND DC, MELLOR AM (1971): Analytical Calculations for the Performance and Pollutant Emissions of Gas Turbine Combustors, Combustion Science and Technology, pp 101-112, Vol 4, 1971
- ✓ ** HARSHA PT (1981): Combustion modelling for practical applications, Proceedings of turbulent reactive flows in practical systems, The Fluids Engg Conference
- ** HAYNES BS, WAGNER HGG (1981): Soot formation, Prog. Energy Combst. Science, Vol 7, pp 229-273.
- ** HERBERT MV (1962): A theroretical analysis of reaction rate controlled systems: Part II, Eighth Symposium on Combustion, The Combustion Institute 1962, pp 970-982
- ** HEYWOOD JB, FAY JA, LINDEN LH (1971): Jet Aircraft Pollutant Production and Dispersion, AIAA Paper No 70-115.
- ** HIRSCHFELDER. JO, CURTIS. CF, and BIRD. RB (1967): Molecular Theory of Gas and Liquids. Wiley and Sons.
- ** HOLDEMAN JD, COLEMAN EB, WHITE CD (1985): Experiments in Dilution jet mixing-Effects of multiple Rows and Non-circular Orifices AIAA-85-1104
- ** HOLLWORTH BR, DAGAN L (1980): Arrays of Impinging jets with Spent Fluid Removal through Vent Holes on the Target Surface, ASME Paper No. 80-GT-42
- ** HORI A, TAKEYA K (1981): Outline of plan for advanced Reheat Gas Turbine, ASME paper No. 81-GT-28
- ** HOTTEL HC, COHEN ES (1958): Radiant heat exchange in a gas filled enclosure, Allowancde for non-uniformity of gas temperature, AI.Ch.E journal, March, vol 4, pp 3-14

- ** . HOTTEL HC, WILLIAMS GC, BANDEL AH (1958): Application of Well-Stirred Reactor Theory to the Prediction of Combustor Performance, Combustion and Flame, pp 13-34 Vol 2, 1958
- ** . HOWARD CHILDS J, GRAVES CC (1957): Correlation of turbine-engine combustion efficiency with theoretical equations, Sixth Symposium on Combustion, The Combustion Institute, 1957, pp 869-878
- ** . HUNG WSY (1974): Accurate Method of Predicting the Effect of Humidity or Injected Water on NOx Emissions from Industrial Gas Turbines, ASME Paper No. 74-WA/GT-6
- ** . HUNG WSY (1975): An Experimentally Verified NOx Emission Model for Gas Turbine Combustors, ASME Paper No. 75-GT-71
- ** . HUNG WSY (1975b): A diffusion limited model that accurately predicts the NOx emissions from GT combustors including the use of Nitrogen containing fuels, ASME paper 75-PWR-11.
- ** . HUNYADI L, ANDERSSON L (1971): Heat transfer in Industrial Combustion chambers, CIMAC Conference, Stockholm
- ** . JEFFS RA (1962): The Flame stability and heat release rates of some can-type combustion chambers, Eighth Symposium on combustion, The Combustion Institute 1962, pp 1014-1027
- ** . JOHNSON TR, BEER JM (1973): The zone method analysis of radiant heat transfer, a model for luminous radiation; Jou. of the Inst. Fuel, Sept, pp 301-309
- ** . JONES RE (1978): Gas Turbine Engine Emissions, Problems, Progress & Future, Progress in Energy and Combustion Science, pp 73-113 Vol 4, No 2, 1978
- ** . JONES WP (1979): Models for turbulent flows with variable density and combustion, Von Karman Institute, Lecture series 1979 - 2.
- ** . JONES WP, PRIDDIN CH (1978): Predictions of the flow field and local gas composition in gas turbine combustors, 17 th symposium on combustion
- ** . JONES WP, WHITELOW JH (1981): Calculation methods for reacting turbulent flows, Proceedings of turbulent reactive flows in practical systems, The Fluids Engg Conference
- ** . KADDAH KS (1964): Discharge coefficients and jet deflection angles for combustor liner air entry holes, Coleege of Aeronautics, M.Sc thesis, Cranfield England.
- ** . KAYS WM (1966): Convective Heat and Mass Transfer, McGraw-Hill Book Company
- ** . KENWORTHY MJ, BURRUS DL (1984): Internal flow field calculations for annular combustor configurations (stairstep boundaries) AIAA-84-1168

- ** KERR NM, FRASER D (1965): Swirl effect on axi-symmetrical turbulent jets, J. Inst. of Fuel, vol 38, pp 519-526
- ** KHALIL EE (1984): Heat transfer in combustors, AIAA-84-1495
- ** KNIGHT MA, WALKER RB (1957): The component pressure losses in combustion chambers, Aeronautical Research Council RM 2987, England
- ** KOHLER J, BEER H (1985): Calculation of the disturbance to combustion chamber film cooling due to air injection through a row of jets, Zeitschrift fur flugwissen-schaften und weltraumforschung, Vol 9, Jan/Feb.
- ** KREITH F (1976): Principles of Heat Transfer, Harper and Row Publishers
- ** KRETSCHMER D, ODGERS J (1972): Modelling of Gas Turbine Combustors- A Convenient Reaction Rate Equation, ASME Paper No 71-WA/GT-5
- ** KRETSCHMER D, ODGERS J (1978): A simple method for the prediction of wall temperature in gas turbines, ASME 78-GT-90
- ** LAUNDER BE, SPALDING DB (1972): Mathematical Models of Turbulence, Academic Press, London
- ** LEFEBVRE AH (1966): Theoretical Aspects of Gas Turbine Combustion Performance, Co A Note Aero No. 163, Cranfield, August 1966
- ** LEFEBVRE AH (1969): Radiation from Flames in Gas Turbines and Rocket Engines, pp 1247-1253, Twelfth Symposium on Combustion
- ** LEFEBVRE AH (1983): Gas Turbine Combustion, McGraw-Hill
- ** LEFEBVRE AH (1984): Fuel Effects on Gas Turbine Combustion- Liner temperature, Pattern Factor and Pollutant Emissions, Jou. of Aircraft, vol21
- ** LEFEBVRE AH (1984b): Flame radiation in Gas turbine Combustion Chambers, Inst Jou. of Heat and Mass Transfer, Vol 27, pp 1493-1510.
- ** LEFEBVRE AH (1987): Atomization of alternative fuels, AGARD CPP-422
- ** LEFEBVRE AH, HERBERT MV(1960): Heat-transfer processes in gas turbine combustion chambers, Proceedings of Inst of Mech. Engg., vol 174, No 12
- ** LEFEBVRE AH, NORSTER ER (1969): The design of tubular gas turbine combustion chambers for optimum mixing performance, Technical advances in gas turbine design, Pt 3N, Proc. Inst. Mech. Engg.
- ** LEONARD PA, MELLOR AM (1983) : Correlation of Gas Turbine Efficiency, J.Energy Vol 7, No.6, Nov-Dec 1983, pp 596-602

- ** LIBBY PA, WILLIAMS FA (1980): Turbulent Reacting Flows, Springer
- ** LIEW SK, BRAY KNC, MOSS JB (1981): A Flamelet Model of Turbulent Non-Premixed Combustion, Comb. Sc. and Tech. 27, 69.
- ** LIEW SK, MOSS JB, BRAY KNC (1984): Predicted Structure of Stretched and Unstretched Methane-Air Diffusion Flames, Prog. in Astronautics and Aeronautics Vol 95.
- ** LILLEY DG (1977): Swirl Flows in Combustion: A Review, AIAA Journal 15, pp 1063-1078, 1977.
- ** LILLEY DG (1979): Flow field modelling in practical combustors: A review, J. Energy, July-aug, vol 3, No 4
- ** LILLEY DG, STILLWATER (1985): Swirling Flows in typical combustor geometries, AIAA-85-0184
- ** LOCKWOOD FC, NAGUIB AS (1975): The prediction of the fluctuations in the properties of free, round-jet, turbulent diffusion flames, Combustion and Flame 24, pp 109-124.
- ** LONGWELL JP, WEISS MA (1955): High temperature reaction rates in hydrocarbon combustion, Industrial and Engineering Chemistry, Vol 47, No 8, 1955, PP 1634-1643
- ** MARSLAND J, ODGERS J, WINTER J (1969): The Effects of Flame Radiation on Flame Tube Metal Temperatures, Twelfth Symposium on Combustion, pp 1265-1276
- ** MASON, E.A. and SAXENA, S.C (1958): Phys. Fluids,1: 361
- ** MASSEY BS (1975): Mechanics of fluids, Van Nostrad Reinhold Comp Ltd.
- ** McVEY JB, KENNEDY JB, SEDERQUIST RA, ANGELLO LA (1983): Testing of a full-scale staged combustor operating with a synthetic liquid fuel ASME 83-GT-27.
- ** MELLOR AM (1976): Gas Turbine Engine Pollution, Progress in Energy and Combustion Science, pp 111-133, Vol 1, 1976
- ** MELLOR AM (1977) : Characteristic Time Emissions Correlations: The T-63 Helicopter Gas Turbine Combustor J. Energy, Vol 1, July-Aug, pp 257-262.
- ** MELLOR AM (1978): Turbulent-Combustion Interaction Models for Practical High Intensity Combustors, 17th Symposium on Combustion, pp 377-386, The Combustion Institute , Pittsburgh, 1978
- ** MENGUC.MP, CUMMINGS WG, VISKANTA R (1985): Radiative Transfer in a Gas Turbine combustor, AIAA-85-1072

- ** METZGER DE, KORSTAD RJ (1972): Effects of Crossflow on Impingement Heat Transfer, Journal of Engg. for Power Jan 72, p 35-42
- ** MEYERS G, VAN DER GEEST J, SANBORN J, DAVIS F (1985): Comparison of advanced cooling concepts using color thermography, AIAA-85-1289
- ** MITCHELL R, SAROFIM A, CLOMBURG L (1980): Experimental and Numerical Investigation of Confined Laminar Diffusion Flames, Comb and Flame 37,377.
- ** MORENO FE, DIVIRGILO PJ (1987): A reheat gas turbine oil field cogeneration system fueled with heavy oil, which produces very low NOx emissions; Turbomachinery International July/Aug
- ** MORI K, KITAJIMA J, KIMURA T, MIKI S (1981): Preliminary Study on Reheat Combustors for Advanced Gas Turbines, ASME paper No. 81-GT-29
- ** MORI K, KITAJIMA J, KAJITA S, SONE H (1977): Development of the Can-Type Gas Turbine Combustors, 1977 Tokyo Joint Gas Turbine Congress
- ** MORI K, KITAJIMA J, KIMURA T, ENZAKI Y (1983): Research and Development on Combustors for Advanced Reheat Gas Turbine, 83-TOKYO-IGTC-21
- ** MORI K, KITAJIMA J, KIMURA T, NAKAMURA T (1986): Research on High Temperature Combustor for Advanced Reheat Gas Turbine, ASME paper No. 86-GT-281
- ** MOSIER SA, ROBERT R, HENDERSON RE (1973): Development and verification of analytical model for predicting emissions from gas turbine combustor during low power operation, AGARD CP 125
- ** MULLINS J, SIMMONS B, WILLIAMS A (1987): Rates of formation of soot from hydrocarbon flames and its destruction, AGARD CPP-422
- ** NAJJAR YSH (1986): Jou. Inst. Energy, pp 148, sep.
- ** NAJJAR YSH, GOODGER EM (1983): Radiation and smoke from the gas turbine combustor using heavy fuels, Jou. of Heat Transfer, vol 105, pp 82-88.
- ** NATIONAL ENGINEERING LABORATORIES (1972): Thermal Conductivity of gases in Metric units, Edinburgh, HMSO
- ** NATIONAL ENGINEERING LABORATORIES (1973): Viscosity of gases in Metric units, Edinburgh, HMSO
- ** NATIONAL ENGINEERING LABORATORIES (1979): Transport properties of fluids and fluid mixtures, Symposium 10-11 Apr, Glasgow.
- ** NEIDEL.W, SONTAG.R, FROSCH.B (1985): Mathematical model for the

- calculation of Heat Transfer in combustion chambers, Archivum Combustions, Vol 5, No 1, pp 99-111
- ** NEALY DA, REIDER SB, MONGIA HC (1985): Alternate Cooling configurations for Gas Turbine Combustion Systems, AGARD 65th meeting, NORWAY, 6-10 May.
 - ** NORGREN CT, RIDDLEBURGH SM (1985): Advanced liner-cooling techniques for gas turbine combustors, AIAA-85-1290
 - ** NORSTER ER (1964): Jet penetration and mixing studies, unpublished work at Cranfield Institute, England.
 - ** NORSTER ER, LEFEBVRE AH (1972): The influence of fuel preparation and operating conditions on flame radiation in a gas turbine combustor, ASME 72-WA/HT-26
 - ** NORTHERN RESEARCH ENGINEERING (1974): Computer Program for the Analysis of Annular Combustors, NASA CR 72374, NASA CR 72375
 - ** ODGERS J (1975): Current Theories of Combustion Within Gas Turbine Chambers, 15th Symposium on combustion, pp 1321-1338, The Combustion Institute, Pittsburgh, 1975.
 - ** ODGERS J (1980): Combustor Modelling, AGARD CP 275, Feb 1980
 - ** ODGERS J, CARRIER C (1973): Modelling of Gas Turbine Combustors; Considerations of Combustion Efficiency and Stability, ASME paper NO 72-WA/GT-1.
 - ** ODGERS J, COBAN A (1975): Film cooling: the effect of velocity variation in the slot, ASME 75-WA/GT-20
 - ** ODGERS J, KRETSCHMER D (1980): Consideration of the use of vitiated preheat, J. Energy, Vol 4, Nov-Dec, pp 260-265
 - ** PATANKAR SV (1980): Numerical heat transfer and fluid flow, Hemisphere Publishing Corporation.
 - ** PIERI G, SAROFIM AF, HOTTEL (1973): Radiant heat transfer in enclosures, extension of Hottel-Cohen zone method to allow for concentration gradients, J. of Inst. Fuel, Sep, PP 321-330
 - ** PITZ WJ, WESTBROOK CK, PROSCIA WM, DRYER FL (1984): A comprehensive chemical kinetic reaction mechanism for the oxidation of n-butane, 20th symposium on combustion, pp 831-843.
 - ** POWELL ES (1985): An improved procedure for calculating the Aero-thermodynamic properties of a vitiated air test medium, AIAA-85-0913
 - ** REEVES D (1956): Flame radiation in an industrial gas turbine combustion chamber, NGTE memo M285, England

- ** REID. RC, DAUSNITZ. JM and SHERWOOD. TK (1977): The Properties of gases and liquids, 3rd Ed., McGraw-Hill Book Company.
- ** REKLAITIS GV, SCHNEIDER D (1983): Introduction to material and energy balances, John Wiley and sons Inc.
- ** RICE IG (1979): The combined Reheat Gas Turbine/Steam Turbine Cycle Part I, ASME paper No 79-GT-7
- ** RICE IG (1979): The combined Reheat Gas Turbine/Steam Turbine Cycle Part II, ASME paper No 79-GT-8
- ** RICE IG (1981): The Reheat Gas Turbine With Steam-blade cooling- A Means of increasing Reheat Pressure, Output, and Combined Cycle Efficiency, ASME paper No. 81-GT-30
- ** RICE IG, JENKINS PE, (1981): Comparison of the HTTT Reheat Gas Turbine Combined Cycle With the HTTT Nonreheat Gas Turbine Combined Cycle, ASME paper No. 81-GT-69
- ** RIDDLEBURGH SM, NORGREN CT (1985): Small gas turbine combustor study-Fuel injector performance in a transpiration-cooled liner AIAA-85-1312
- ** RUSSELL PL, REILLY RS (1984): A design approach for a practical turbojet engine combustor diffuser system, ASME Paper No. 84-GT-104
- ** SABLA PE, TAYLOR JR, GAUNTNER DJ (1981): Design and Development of the Combustor Diffuser for NASA/GE Energy Efficient Engine, ASME Paper NO 81-GT-129
- ** SAROFIM AF, RICHARD CF (1976): NO_x Control for Stationary Combustion Sources, Prog. Energy Combust. Sci. Vol2, pp 1-25.
- ** SCHOFIELD K (1967): An evaluation of kinetic data for reactions of neutrals of atmospheric interest, Planet. Space Sciences, Vol 15, pp 643-670
- ** SCHOFIELD PR, MOORE A (1963): A comparison of film cooling correlations using various experimental data, BSE ltd, Report No. GN-6124.
- ** SCOTT. JN, HANKEY WL (1983): Numerical Solution of cold flow in an axi-symmetric centerbody combustor, AIAA-83-1741
- ** SEBAN RA (1960): Heat Transfer and effectiveness for a turbulent boundary layer with tangential fluid injection, Journal of heat transfer, Nov.
- ** SHAPIRO AH (1953): The Dynamics and Thermodynamics of Compressible Fluid Flow Vol 1, Roland Press, 1953

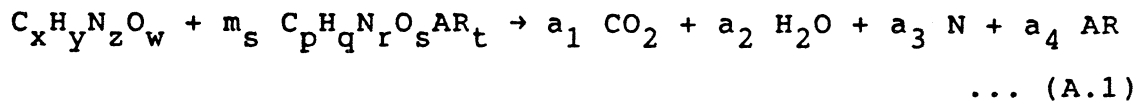
- ** SIDDALL RG (1972): Flux methods for the analysis of radiant heat transfer, presented at 4th sympo. on Flames and Industry, London.
- ** SIEGEL- HOWELL (1981): Thermal Radiation Heat Transfer, McGraw_Hill, Newyork.
- ** SINGH R (1972): Private communication
- ** SJOBLOM B (1984): Combined film-and convection-cooling in a gas turbine combustors, Int Jou of Turbo and jet Engines, Vol 1, No2.
- ** SLOAN DG, SMITH PJ, SMOOT LD (1986): Modeling of Swirl in Turbulent Flow Systems, Prog. Energy Combust. Sci. Vol.12, No 3, pp 163-250
- ** SOOD VM, SHEKLETON JR (1979): Ongoing Development of a Low Emission Industrial Gas Turbine Combustion Chamber, ASME Paper No.79-GT-203
- ** SOUTHERAN A (1983): The Rolls-Royce Annular vaporiser combustor ASME 83-GT-49
- ** SOVRAN G, KLOMP ED (1967): Experimentally determined optimum geometries for rectilinear diffusers with rectangular, conical or annular cross section, Fluid Mechanics of Internal Flow, pp 270-319
- ** STARK P.A (1970): Introduction to Numerical Methods, The Macmillan Company ✓
- ** STOLLERY JL, EL EHWANY AAM (1965): A note on the use of a boundary-layer model for correlating film-cooling data, Int. J. Heat Mass Transfer, Vol 8 pp 55-65.
- ** STULL. DR and PROPHET. H (1971): JANAF Thermochemical Tables, 2nd Ed., NSRDS-NBS 37, US Dept. of Commerce, Washington, D.C.
- ** STURGESS GJ (1979): Account of Film Turbulence for Predicting Film Cooling Effectiveness in Gas Turbine Combustors, ASME Paper No. 79-GT-200
- ** STURGESS GJ (1980): Gas turbine combustor design challenges for 1980's, AIAA-80-1285.
- ** SULLIVAN DA (1974) : Gas turbine Combustor analysis ASME 74-WA/GT-2
- ** SWITENBANK J, POLL I, VINCENT MW (1973): Combustion Design Fundamentals, 14 th Symposium on Combustion pp 627-638, The Combustion Institute, Pittsburgh, 1973
- ** SWITENBANK J, TURAN A, FELTON PG (1980): Three-Dimensional Two-Phase Mathematical Modelling of Gas Turbine Combustors, pp249-314, A Project Squid Workshop, Gas Turbine Combustor Design Problems, McGraw-Hill,1980

- ** SYED SA, STURGESS GJ (1980): Validation Studies of Turbulence and Combustion Models for Aircraft Gas Turbine Combustors, Proceedings of the ASME Symposium on Momentum and Heat Transfer Processes in Recirculation Flows, HTD, Vol 13, Nov 1980, pp 71-89.
- ** TAKEYA K, IMAI T, TESHIMA K, YASUI H (1987): Results of test operation of the advanced reheat gas turbines and an evaluation of their performance, CIMAC conference, Warsaw.
- ** TAM. LT (1981): The theory of turbulent flow with complex chemical kinetics. Ph. d. Thesis, University of London.
- ** TAYLOR JR, WIDENER SK (1986): Altitude Ignition/Lean Deceleration Study, AIAA-86-1530
- ** TOURIN RH (1966): Spectroscopic Gas Temperature Measurements (edited by BEER), Elsevier, Amsterdam
- ** TYLER RA, WILLIAMSON RG (1967): Diffuser performance with distorted inflow., Proc. Inst. Mech. Eng., Vol 182, Pt 3D, PP 115-125
- ** UBHI GS (1987): Emissivity measurement of Gas turbine combustor ceramic coatings and its influence on combustor design; Ph.D Thesis, SME, Cranfield Inst. of Technology, Cranfield, UK.
- ** UVAROV VV, BEKNEV VS, MANUSHIN EA (1974): 100s and 1000s MW Open and semi-closed Cycle Gas Turbines for Base and Peak Operation ASME Paper No. 74-GT-160
- ** VISKANTA R (1984): Radiative Heat Transfer, " Fortschritte der verfahrenstechnik", vol 22, section A, pp 51-81
- ** WAGNER HGG (1987): The influence of pressure on soot formation, AGARD CPP 422.
- ** WASSELL AB, BHANGU JK (1980): The development and application of improved combustor wall cooling techniques, ASME 80-GT-66
- ** WASSILJEWA, A. (1904): Physik. Z., 5: 737
- ** WESTBROOK CK, DRYER FL (1981): Applied Chemical Kinetics in practical combustion systems, Proceedings of turbulent reactive flows in practical systems, The Fluids Engg Conference
- ** WILD PN, Boysan F, Swithenbank J, LU X (1987): 3 Dimensional Gas Turbine Combustion Modelling, AGARD CPP-422.
- ** WOODWARD EC (1957): Simulated study of idealised combustors, Sixth Symposium on Combustion Reinhold, Newyork, 1957 pp 849-857

APPENDIX A

STOICHIOMETRIC AIR-FUEL RATIO EVALUATION :

Considering any general fuel and oxidant reaction, for stoichiometric proportions



C, H, O atom balances yield

$$m_s = \frac{4x + y + 0z - 2w}{2s - 4p - q + 0r + 0t} \quad \dots (A.2)$$

$$AFRS = \frac{m_s \{p[C] + q[H] + r[N] + s[O] + t[AR]\}}{\{x[C] + y[H] + z[N] + w[O]\}} \quad \dots (A.3)$$

Rewriting in terms of oxidation potentials

ATOM	C	H	N	O	AR
OXI. POT.	+4	+1	+0	-2	+0
ATOM. WT.	12.01115	1.00797	14.0067	15.9994	39.9480

$$AFRS = \frac{\left[\begin{array}{c} NS \\ \sum_i Oxi_i Atom_i \end{array} \right]_{fuel} Mw_{oxidant}}{\left[\begin{array}{c} NS \\ - \sum_i Oxi_i Atom_i \end{array} \right]_{oxidant} Mw_{fuel}} \quad \dots (A.4)$$

where

AFRS = Air_fuel ratio stoichiometric

Oxi_i = oxidation potential of individual species

Atom_i = no of atoms of each specie i

(x,y,z,w for fuel, p,q,r,s,t for oxidant)

Mw = molecular weight

[] = atomic weight of the species

NS = number of species

m_s, a₁, a₂, a₃, a₄ balancing coefficients

APPENDIX B

REFERENCE AREA EVALUATION

The reference area is the maximum cross sectional area of the casing in the absence of a liner. This is calculated based on the operating conditions and the two nondimensional parameters Overall Pressure Loss (OPL) and Pressure Loss Factor (PLF).

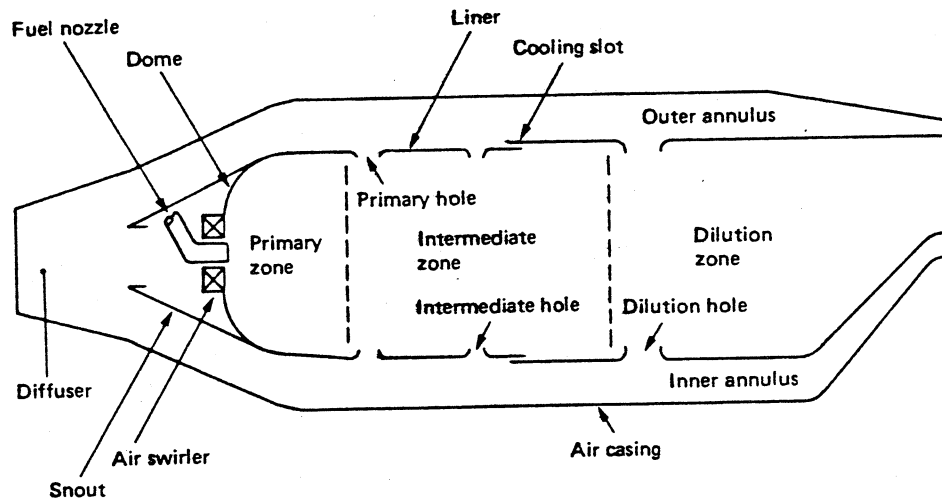


Fig B.1 Combustor Geometry

$$\text{OPL} = \frac{P_3 - P_4}{P_3} \quad \dots \text{ (B.1)}$$

$$\text{PLF} = \frac{P_3 - P_4}{Q_{\text{ref}}} \quad \dots \text{ (B.2)}$$

$$\dot{m}_3 = \rho_3 A_3 U_3 \quad \dots \text{ (B.3)}$$

$$= \rho_3 A_{\text{ref}} U_{\text{ref}} \quad \dots \text{ (B.4)}$$

$$Q_{\text{ref}} = \frac{1}{2} \rho_3 U_{\text{ref}}^2 \quad \dots \text{ (B.5)}$$

$$P_3 = \rho_3 R_a t_3 \quad \dots \text{ (B.6)}$$

using (B.1) and (B.2)

$$\frac{\text{OPL}}{\text{PLF}} = \frac{Q_{\text{ref}}}{P_3}$$

using (B.4) and (B.6)

$$\frac{OPL}{PLF} = \frac{1}{2} \frac{m_3^2 R_a t_3}{P_3 A_{ref}^2 \rho_3}$$

using Isentropic relations

$$T/t = \left(1 + \frac{\gamma - 1}{2} Mn^2 \right)$$

$$P/p = \left[1 + \frac{\gamma - 1}{2} Mn^2 \right]^{\gamma/(\gamma-1)}$$

$$\frac{OPL}{PLF} = \frac{R_a}{2} \left[\frac{m_3^2 T_3}{P_3^2 A_{ref}^2} \right] \left[1 + \frac{\gamma - 1}{2} Mn_3^2 \right]^{1/(\gamma-1)}$$

$$A_{ref} = \left[\frac{R_a}{2} \left[\frac{m_3^2 T_3}{P_3^2 A_{ref}^2} \right] \left[1 + \frac{\gamma - 1}{2} Mn_3^2 \right]^{1/(\gamma-1)} \right]^{1/2}$$

..(B.7)

form (B.3) and (B.4)

$$\text{Area Ratio} = AR = A_{ref} / A_3 = U_3 / U_{ref}$$

$$= \left[\frac{1}{2} \frac{\gamma Mn_3^2}{OPL} \frac{PLF}{1} \frac{1}{\left[1 + \frac{\gamma-1}{2} Mn_3^2 \right]^{\gamma/(\gamma-1)}} \right]^{1/2}$$

..(B.8)

APPENDIX C

A SIMPLE METHOD TO EVALUATE FLAME TEMPERATURE

Reiterating the guidelines concluded in Chapter 4.

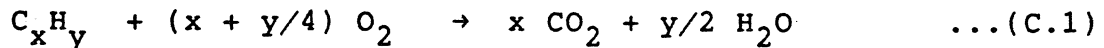
The strategy should be :

- 1) a simple method in terms of coding complexity and computing time, at the same time within reasonable accuracy.
- 2) fairly general that it accounts for any inlet conditions interms of medium (oxidant or fuel), or conditions such as temperature or pressure.
- 3) account for completeness of reaction and heat loss.
- 4) able to provide flame temperature along with the concentrations of combustion products.

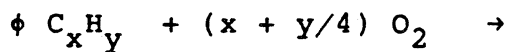
PROCEDURE:

Falling back on basic reaction of any fuel of the type C_xH_y reacting with O_2 , the only oxidant of the inlet oxidant medium.

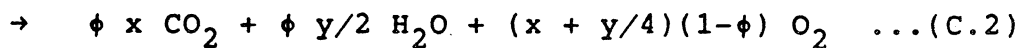
for stoichiometric equilibrium combustion



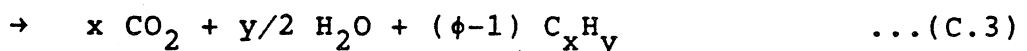
for any equivalence ratio ϕ , assuming excess O_2 or excess fuel will be left over as $\phi \leq 1$ or $\phi > 1$ respectively:



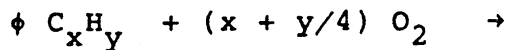
For $\phi \leq 1.0$:



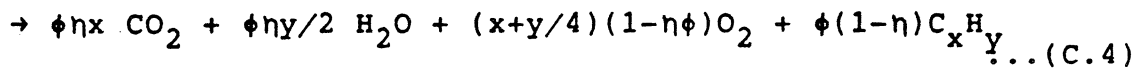
For $\phi > 1.0$:



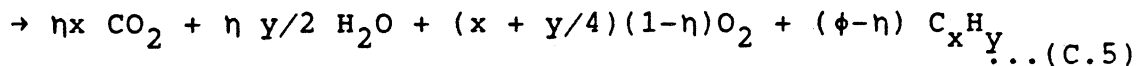
If the combustion efficiency η or extent of reaction is superimposed



For $\phi \leq 1.0$:



For $\phi > 1.0$:

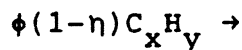


Further assumptions are made thus:

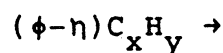
1) CO correction for low ϕ : When too much excess air is present, CO normally does not exist below a minimum equivalence ratios. The value is around 0.5 to 0.6. Here it is assumed to be 0.6. Hence, below this value all CO except that formed due to inefficiency oxidises to CO_2 . Correspondingly O_2 molecules are reduced.

2) Excess fuel correction : The excess fuel which is present cannot logically exist in the form of original $C_x H_y$. Hence this term in the right hand side of the equation is converted thus:

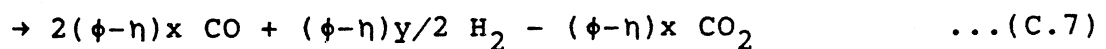
for $\phi \leq 1$



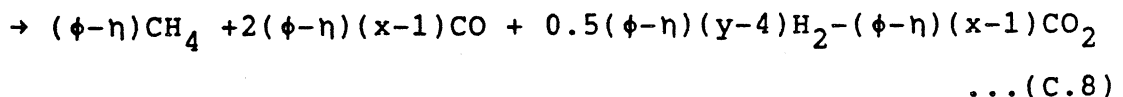
for $\phi > 1$



for $1 < \phi \leq 1.2$ $C_x H_y$ is converted into CO and H_2



for $\phi > 1.2$ $C_x H_y$ will exist in its intermediate forms say from a simple methane CH_4 to any complicated chain of higher order combinations. However, here they are approximated and grouped under one average formula. Methane CH_4 is chosen to represent all the intermediaries.



Heat Balance :

Steady flow thermal balance between energy released and absorbed gives rise to

$$\begin{aligned}
 s-f Q_{p \text{ ad}} &= (\Delta H_{T_{p \text{ ad}}} + \Delta H_{f^{\circ}})_P - (\Delta H_{T_I} + \Delta H_{f^{\circ}})_R \\
 &= \sum n_j (\Delta H^*)_j - \sum n_i (\Delta H^*)_i \\
 &= \text{zero} \qquad \dots \text{(C.9)}
 \end{aligned}$$

where

ΔH^* = net enthalpy change from 298.15 k to the temperature T

$T_{p \text{ ad}}$ = Adiabatic temperature of products

T_I = initial temperature of reactants

$H_{f^{\circ}}$ = formation enthalpy at 298.15 K

n = number of moles; P,j = products, R,i=reactants

Once the mole numbers of species are obtained based on the equivalence ratio and the empirical assumptions as mentioned in the earlier paragraphs, adiabatic temperature is evaluated knowing ΔH^* from thermodynamic data of individual species as given by eqn 5.5 & 5.6. A Newton Raphson's method is used to ensure a rapid convergence.

Correction for Radiation Loss :

The heat lost due to radiation is accounted for by estimating empirically the loss, as explained in chapter 6.

Now the heat balance becomes

$$\begin{aligned}
 s-f Q_p &= s-f Q_{p \text{ ad}} - (Q_{\text{radiation}}) \\
 &= \text{zero} \qquad \dots \text{(C.10)}
 \end{aligned}$$

 $Q_{\text{radiation}}$:

Radiation and so is the loss largely depends on the fuel type, air_fuel ratio, mixing, atomisation, operating conditions (pressure, temp etc.). This would be maximum in the burning zone and gradually reducing towards the exit of the combustor. Aromatic content, hydrogen concentration,

carbon hydrogen mass ratio have all been assessed as a correlating parameter for the effect of fuel type on radiation. C/H mass ratio is taken as the basis, through luminosity factor, as explained in Chapter 6. Air blast atomisers are known to yield lesser radiation (Lefebvre (1983)). Though the peak value shifts more towards the dome. The axial distribution of the loss also depends on power setting. The following is adopted, though qualitative, to represent the radiation loss.

It is assumed that $Q_{\text{radiation}}$ can be expressed as a fraction of net enthalpy of products, as

$$Q_{\text{radiation}} = Q_{\text{crad}} * \sum n_j (\Delta H^*)_j$$

where Q_{crad} is a function of all the qualifying parameters which influence the radiation loss as indicated. As it is difficult to interpret this in absolute terms, the following form is assumed.

$$Q_{\text{crad}} = Q_{\text{crad}_0} (T_g/T_{g_0})^4 C_{\text{inje}} (\text{RLC}/\text{RLC}_0)$$

Where

C_{inje} is a coefficient to account for the injector.

The following are arbitrarily chosen for the injectors available in the programme

- 1.0 Pressure atomiser
- 0.85 airblast atomiser
- 0.9 air_assist atomiser
- 0.8 vapouriser
- 1.01 user choice (pessimistic value)

RLC = a coefficient akin to emissivity (E_g)
 = f(C/H, ϕ , P_2 , T_2 , Injector, Combustor dia)

This should represent the fuel and operating conditions, which when used in conjunction with an appropriate base or reference value should yield a good qualitative picture.

0 signifies a base condition. Here, a pressure atomiser with kerosine is chosen as the base.

T_{g_0} = 2150 K (These data produced by Menguc (1985) based on experimental values of Najjar and Goodger (1985))
 RLC_0 = 0.602

Radiative flux = 557 W/m²

From the available data of Menguc (1985), the coefficient is estimated as following.

$$Q_{\text{crad}0} = 0.0152$$

Hence the LHS (left hand side) of eqn. (C.10) becomes

$$\text{LHS} = (1 - Q_{\text{crad}}) \sum n_j (\Delta H^*)_j - \sum n_i (\Delta H^*)_i$$

Thus, the percentage of loss due to radiation is calculated for the burning zone and this is dropped in the ratio of mean temperature of the zone raised to a power of four (following the quartic nature of radiation)

DISSOCIATION :

As near stoichiometric ratios, dissociation of CO_2 and H_2O intervenes, reducing the temperature. Following Douglas (1986), it is assumed that T_{disc} is the temperature above which dissociation occurs.

$$T_{\text{disc}} = 1666.67 + 101.1 \log (P_{\text{atm}}) \text{ K} \quad \dots (\text{C.11})$$

The dissociation equations are represented thus:



$$\frac{p_{\text{CO}_2}}{p_{\text{CO}} [p_{\text{O}_2}]^{1/2}} = k_{\text{CO}_2} = \frac{n_{\text{CO}_2}}{n_{\text{CO}} [P n_{\text{O}_2} / n_{\text{T}}]^{1/2}}$$

$$\frac{p_{\text{H}_2\text{O}}}{p_{\text{H}_2} [p_{\text{O}_2}]^{1/2}} = k_{\text{H}_2\text{O}} = \frac{n_{\text{H}_2\text{O}}}{n_{\text{H}_2} [P n_{\text{O}_2} / n_{\text{T}}]^{1/2}}$$

where

p partial pressure

P total pressure in atmospheres

n number of moles

n_{T} total number of moles

It is again involving if iterative methods using reaction rate constants or minimisation of free energy method is employed to evaluate the temperature. It is best to fall back on empirical approach.

For emissivity calculations, the partial pressures of CO_2 and H_2O are empirically evaluated.

Upto the region near stoichiometric, where dissociation intervenes, this variation was correlated by Lefebvre and Herbert (1960) to a close approximation by the expression

$$\frac{p}{P} = \frac{2.1 \text{ FAR}}{1 + 1.05 \text{ FAR}}$$

More general approach by Kunitomo and Kodama (1974) leading to

$$\frac{P_{\text{CO}}}{P} = 2.2 (1.0 - \Omega)(\phi - 1.2)^2 \quad \text{for } \phi \leq 1.2$$

$$= 0.0 \quad \text{for } \phi > 1.2$$

$$\frac{P_{\text{CO}_2}}{P} = 0.175 - 0.075\phi + 0.033 \Omega \quad \text{for } \phi > 1.1$$

$$= 0.092 + 0.038\Omega - 2.619(1.01 - \Omega)(\phi - 1.05)^2 \quad \text{for } \phi \leq 1.1$$

$$\frac{P_{\text{H}_2\text{O}}}{P} = 0.259 - 0.068\phi - 0.0783 \Omega \quad \text{for } \phi \geq 1.05$$

$$= 0.126 - 0.72[\phi + 0.887\Omega - 1.724 - 1.42(\Omega - 0.805)^2]^2$$

for $\phi < 1.05$

where Ω is the specific gravity of the fuel at 293 K.

ϕ is the excess air factor = 1/equivalence ratio

However, their utility for general inlet medium fuel or oxidant and varied inlet conditions such as pressure and temperature are again doubtful. However, accepting the approach it is decided to develop an empirical formula for $n_{\text{CO}}/n_{\text{CO}_2}$ directly.

A general review of results for variety of a AFRS and inlet media, yielded the author to correlate the molar ratio of CO and CO_2 (for a reference condition of 10atm, 600 K, AFRS 14.7247) as

$$(n_{CO}/n_{CO_2})_{ref} = 1.3495477 - 3.9479001 \phi + 2.8372667 \phi^2 \quad \dots(C.14)$$

The accuracy of the final result can be improved if the range of ϕ is still narrowed and split into different bands. However, no attempt is made at this stage as the accuracy of the temperature is within 3% of the result from the equilibrium programme of Gordon and McBride (1969).

The dissociation would be a function of inlet temperature, pressure and the ratio of oxygen to total moles of reactants (taking the reaction rate constant equations). The last term can be indirectly correlated to the stoichiometric air fuel ratio. Hence the final relation when all correction terms are applied is of the form

$$\frac{n_{CO}}{n_{CO_2}} = (n_{CO}/n_{CO_2})_{ref} C_T C_P C_A \quad \dots(C.15)$$

where C_T , C_P , C_A are the correction terms for the temperature, pressure and air fuel ratio, which in turn are of the following form.

$$C_v = (\text{const } v) \quad a + b \phi + c \phi^2$$

where v could be temperature, pressure or AFRS

Inlet Temperature Correction:

$$(T_2/600)^{xx} \quad \text{where } xx = a_1 + b_1 \phi + c_1 \phi^2$$

Pressure Correction:

$$(101325.0/PT_2)^{yy} \quad \text{where } yy = a_2 + b_2 \phi + c_2 \phi^2$$

The coefficients are evaluated for two inlet temperature ranges, $T_2 < 600$ K and ≥ 600 K, giving rise to a table of values as shown below.

	<600 K	≥ 600 K
a_1	8.4130688	13.4470283
b_1	-10.642003	-19.7610165
c_1	3.119978	7.3304683
a_2	1.17195244	0.6585379
b_2	-0.60457671	-0.0772085
c_2	-0.30561864	-0.3686883

AFRS Correction :

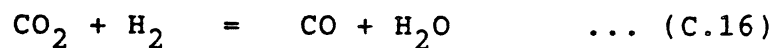
$$C_1 (\text{AFRS}/14.7247)^{zz} \quad \text{where } zz = a_3 + b_3 \phi + c_3 \phi^2$$

	< 14.72447	≤ 14.72447
a ₃	0.7951688	14.825443
b ₃	-0.6670292	-87.841416
c ₃	0.7322894	62.344971

and C_1 = 5.0 for $\phi = 1.0$ and $\text{AFRS} \geq 17.5$
 = 1.0 for $\phi > 1.0$
 = 1.2 otherwise

H₂O - H₂ exchange:

Once $n_{\text{CO}}/n_{\text{CO}_2}$ is obtained, then $n_{\text{H}_2}/n_{\text{H}_2\text{O}}$ is obtained through water gas reaction. Combining eqns C.12 and C.13



$$\frac{p_{\text{CO}} p_{\text{H}_2\text{O}}}{p_{\text{CO}_2} p_{\text{H}_2}} = k_{\text{WG}} = \frac{n_{\text{CO}} n_{\text{H}_2\text{O}}}{n_{\text{CO}_2} n_{\text{H}_2}}$$

which is a sole function of temperature. In the temperature range of interest the value for k_{WG} varies between 4.2 and 6. Correlating the inverse of this value:

$$k_{\text{WG}}^{-1} = 1/k_{\text{WG}} \\ = 1.32294323 - 8.57404542\text{E-}4 T + 1.569414583\text{E-}7 T^2$$

Hence,

$$\frac{n_{\text{H}_2}}{n_{\text{H}_2\text{O}}} = \frac{n_{\text{CO}}}{n_{\text{CO}_2}} k_{\text{WG}}^{-1} \quad \dots (\text{C.17})$$

DISSOCIATION CORRECTION :

$n_{\text{CO}}/n_{\text{CO}_2}$ is evaluated as per eqn (C.15), for a given equivalence ratio, AFRS, inlet temperature and pressure conditions.

CO₂ and CO mole numbers, evaluated from eqns. C.1 and C.8 are adjusted down to the ratio nCO/nCO₂ and correspondingly O₂ molecules are changed. Similar approach is followed for H₂O and H₂ using equations C.17 and C.13.

CORRECTION FOR RADICALS :

The amount of free radicals such as H, O, OH, NO is usually small and is not accounted for simplicity. However, near stoichiometric regions the amount of OH and NO radicals is quite substantial that their contribution is worth considering. Hence falling back on empiricism,

OH Radical

nOH/nH₂O is empirically correlated as

$$(nOH/nH_2O)_{ref} = -0.00488037 + 0.1152274 AFRS \quad \dots(C.18)$$

Again, similar temperature and pressure corrections are applied for, of the form given as eqn C.15.

$$\frac{nOH}{nH_2O} = (nOH/nH_2O)_{ref} (T_2/600)^{xx} (101325/PT_2)^{yy}$$

The coefficients for exponents xx and yy are as follows.

	< 600 K	≥ 600 K
a ₁	9.88377120	11.1303894
b ₁	-19.3447130	-21.2841742
c ₁	10.4204711	11.3074406
a ₂	1.1817425	1.1194420
b ₂	-2.5275913	-2.2915515
c ₂	1.5993100	1.3744739

H₂O mole numbers calculated in previous steps are further reduced in the above ratio



Correspondingly H₂ mole number is also changed. This will however change the ratio nH₂/nH₂O evaluated previously. However, no iterative approach is resorted to correct this.

NO Radical

Similarly n_{NO}/n_{N_2} are empirically correlated as :

$$(n_{NO}/n_{N_2})_{ref} = -0.0242110082 + 0.076380045 \phi - 0.04582283 \phi^2$$

As this is strongly dependent on the inlet temperature, the coefficients for temperature are evaluated as:

$$\frac{n_{NO}}{n_{N_2}} = (n_{NO}/n_{N_2})_{ref} (T/T_2/600)^{xx} \quad \dots(C.20)$$

	< 600 K	≥ 600 K
a ₁	8.1501203	8.6575719
b ₁	-18.3672682	-19.027442
c ₁	11.0291039	11.335452

N_2 mole numbers calculated in previous steps are further reduced in the above ratio



Correspondingly O_2 mole number is also reduced.

Heat balance is now performed, with the corrected concentrations of the species based on above dissociation assumptions.

COMPARISION :

For comparison three typical inlet conditions are chosen.

Case (a) with moderate pressures for a typical simple gas turbine combustor ($P_2=15$ atm, $T_2=650$ K).

Case (b) with very high pressures accompanied by water injection, say due to intercooling or for NOx control prior to entry into combustor, representing the current combustor philosophy for any combined cycle powerplant ($P_2=50$ atm, $T_2=950$ K, sp. humidity=0.1).

Case (c) with moderate pressures with burnt products, say from the first combustor as the oxidant medium, representing a reheat combustor ($P_2=10$ atm, $T_2=1000K$, vitiated air). The composition of the vitiated inlet medium in mass fractions is as indicated.

N ₂	0.74538
O ₂	0.18272
AR	0.01266
CO ₂	0.04248
H ₂ O	0.01676

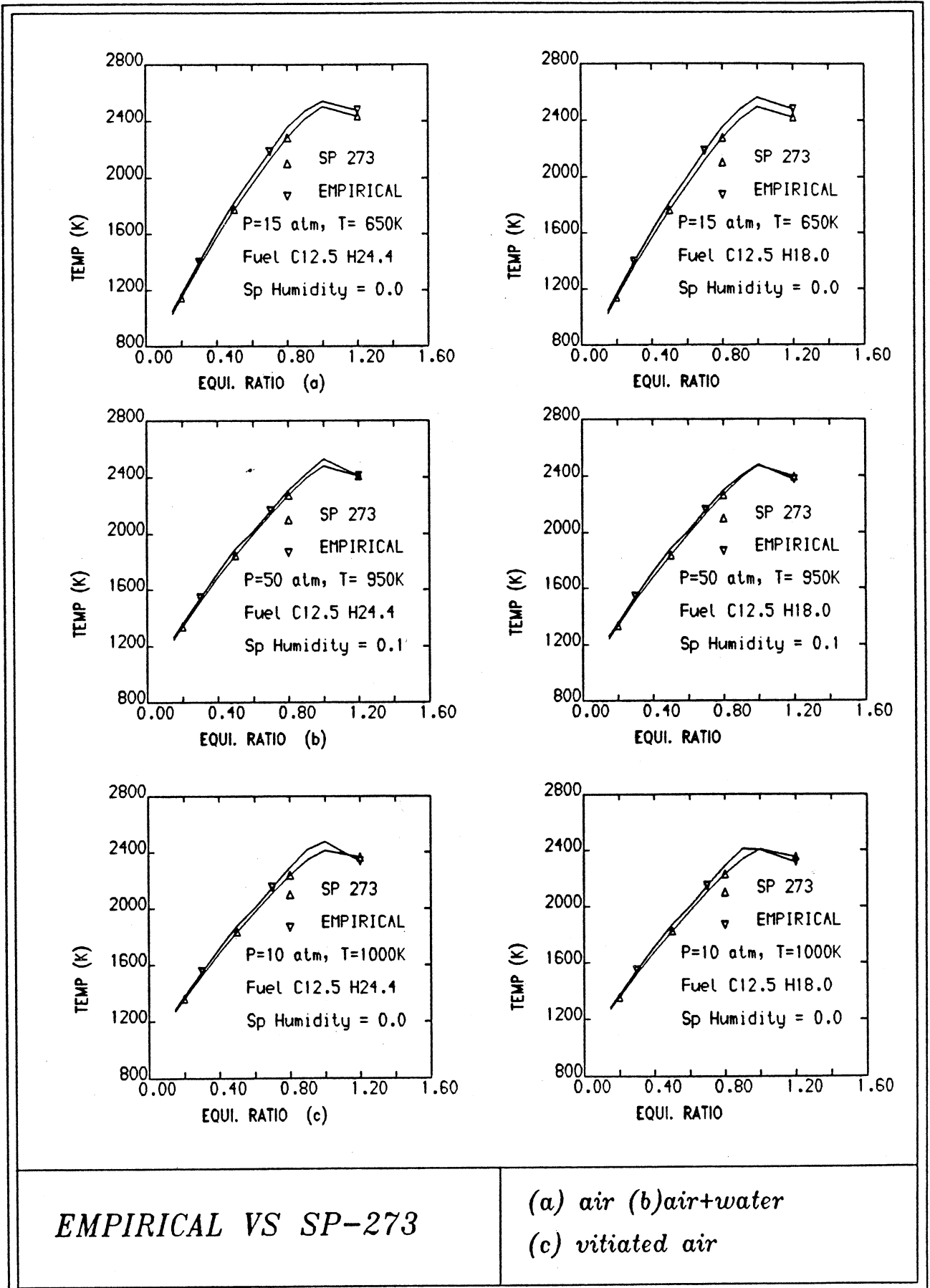
All the three cases are run with two types of fuels.

- (1) Standard kerosine represented by the formula $C_{12.5} H_{24.0}$
- (2) High aromatic content typical of fuels expected in the future represented by the formula $C_{12.5} H_{18.0}$.

The results are compared using Gordon and McBride's (1969) computer program. The flame temperatures between the equivalence ratios of 0.15 to 1.2 are shown as Fig C.1. The maximum error is less than 3%. It is always on the +ve side in the region of interest ie. between 0.6 to 1.0 equivalence ratio. The reasons are obviously due to the assumptions and the empirical correlations and the absence of other radicals. However in terms of the assumptions for the strategy, this error is justified. Hence one direct consequence of these high temperatures in the primary and secondary zones would be higher metal temperatures.

The molar percentages of major individual species are also reasonable and so their utility in calculation of transport properties should be with reasonable confidence.

FIG C.1 Adiabatic Flame Temperature Comparison



APPENDIX D

PROCEDURE TO ESTIMATE NUMBER OF INJECTORS

Experience plays a major part in selecting the number of fuel nozzles needed for a type of combustor geometry, type of fuel and other operating conditions. However, it is tried to relate some of the above parameters with simple geometrical variables. Though it is approximate, it should provide the user a reasonable starting point for an initial guess.

Assumptions

- 1) It is assumed that nozzles are considered as discrete points distributed equally around the centerline of the dome head.
- 2) From each point the fuel is sprayed with cone angle equal to 110 degrees. (this value, in reality, for certain type of injectors, could be as low as 45°, when the actual chamber pressures are considered).
- 3) The positioning of the nozzles is such that the cones meet at around the end of recirculation zone which is assumed to be half the length of the primary zone. The geometry is solved to find the distance between the nozzles and hence the total number of nozzles.

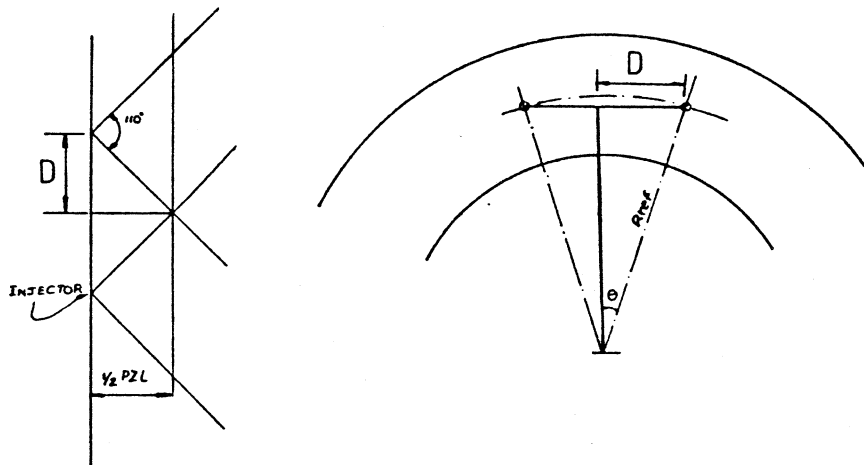


Fig D.1 Schematic of fuel spray pattern

$$D = 1/2 \text{ PZL } \tan (55^\circ) \quad \dots(\text{D.1})$$

$$\sin \theta = D/R_{\text{ref}} \quad \dots(\text{D.2})$$

$$\text{Number of Injectors} = \pi/\theta \quad \dots(\text{D.3})$$

APPENDIX E

COEFFICIENTS FOR THERMODYNAMIC PROPERTIES

The constant pressure heat capacities, and enthalpies of chemical species have been expressed as polynomials (eqn. 5.2 & 5.3). There are 14 coefficients for each species, represented by the matrix $Z(K,J,I)$, $J=1,7$, $K=1,2$, $I=1,NS$, $K=1$ corresponds to temperature 1000 to 5000 K and $K=2$ corresponds to 300 to 1000 K.

N2

1	0.28963194E+01,	0.15154866E-02,	-0.57235277E-06,
2	0.99807393E-10,	-0.65223555E-14,	-0.90586184E+03,
	0.61615148E+01,		
3	0.36748261E+01,	-0.12081500E-02,	0.23240102E-05,
4	-0.63217559E-09,	-0.22577253E-12,	-0.10611588E+04,
	0.23580424E01/		

O2

1	0.36219535E+01,	0.73618264E-03,	-0.19652228E-06,
2	0.36201558E-10,	-0.28945627E-14,	-0.12019825E+04,
	0.36150960E+01,		
3	0.36255985E+01,	-0.18782184E-02,	0.70554544E-05,
4	-0.67635137E-08,	0.21555993E-11,	-0.10475226E+04,
	0.43052778E01/		

AR

1	0.25000000E+01,	0.	, 0.
2	0.	, 0.	, -0.74537502E+03,
	0.43660006E+01,		
3	0.25000000E+01,	0.	, 0.
4	0.	, 0.	, -0.74537498E+03,
	0.43660006E+01/		

CO

1	0.29840696E+01,	0.14891390E-02,	-0.57899684E-06,
2	0.10364577E-09,	-0.69353550E-14,	-0.14245228E+05,
	0.63479156E+01,		
3	0.37100928E+01,	-0.16190964E-02,	0.36923594E-05,
4	-0.20319674E-08,	0.23953344E-12,	-0.14356310E+05,
	0.29555351E+01/		

H2O

1	0.27167633E+01,	0.29451374E-02,	-0.80224374E-06,
2	0.10226682E-09,	-0.48472145E-14,	-0.29905826E+05,
	0.66305671E+01,		
3	0.40701275E+01,	-0.11084499E-02,	0.41521180E-05,
4	-0.29637404E-08,	0.80702103E-12,	-0.30279722E+05,
	-0.32270046E+00/		

CH4

1	0.15027072E+01,	0.10416798E-01,	-0.39181522E-05,
2	0.67777899E-09,	-0.44283706E-13,	-0.99787078E+04,
	0.10707143E+02/		
3	0.38261932E+01,	-0.39794581E-02,	0.24558340E-04,
4	-0.22732926E-07,	0.69626957E-11,	-0.10144950E+05,
	0.86690073E+00/		

CO2

1	0.44608041E+01,	0.30981719E-02,	-0.12392571E-05,
2	0.22741325E-09,	-0.15525954E-13,	-0.48961442E+05,
	-0.98635982E+00,		
4	0.24007797E+01,	0.87350957E-02,	-0.66070878E-05,
5	0.20021861E-08,	0.63274039E-15,	-0.48377527E+05,
	0.96951457E+01/		

H2

1	0.31001901E+01,	0.51119464E-03,	0.52644210E-07,
2	-0.34909973E-10,	0.36945345E-14,	-0.87738042E+03,
	-0.19629421E+01,		
3	0.30574451E+01,	0.26765200E-02,	-0.58099162E-05,
4	0.55210391E-08,	-0.18122739E-11,	-0.98890474E+03,
	-0.22997056E+01/		

OH

1	0.29131230E+01,	0.95418248E-03,	-0.19084325E-06,
2	0.12730795E-10,	0.24803941E-15,	0.39647060E+04,
	0.54288735E+01/		
3	0.38365518E+01,	-0.10702014E-02,	0.94849757E-06,
4	0.20843575E-09,	-0.23384265E-12,	0.36715807E+04,
	0.49805456E+00/		

NO

1	0.31890000E+01,	0.13382281E-02,	-0.52899318E-06,
2	0.95919332E-10,	-0.64847932E-14,	0.98283290E+04,
	0.67458126E+01/		
3	0.40459521E+01,	-0.34181783E-02,	0.79819190E-05,
4	-0.61139316E-08,	0.15919076E-11,	0.97453934E+04,
	0.29974988E+01/		

APPENDIX F

TABLE F.1 COLLISION DIAMETERS AND LENNARD-JONES POTENTIAL PARAMETERS @

SPECIES	σ (A)	ϵ/K (K)	SPECIES	σ (A)	ϵ/K (K)
N2	3.798	71.4	CH4	3.758	148.6
O2	3.467	106.7	CO2	3.941	195.2
AR	3.542	93.3	H2	2.827	59.7
CO	3.690	91.7	OH	3.110	91.8
H2O	2.641	809.1	NO	3.470	119.0

@ data is taken from Reid et al. (1977)

TABLE F.2 VALUES OF KT/ϵ and $\Omega(2,2)^*$ †

KT/ϵ	$\Omega(2,2)^*$	KT/ϵ	$\Omega(2,2)^*$	KT/ϵ	$\Omega(2,2)^*$
1.90	1.197	3.3	1.014	4.8	0.9343
1.95	1.186	3.4	1.007	4.9	0.9305
2.00	1.175	3.5	0.9999	5.0	0.9269
2.10	1.156	3.6	0.9932	6.0	0.8963
2.20	1.138	3.7	0.9870	7.0	0.8727
2.30	1.122	3.8	0.9811	8.0	0.8538
2.40	1.107	3.9	0.9755	9.0	0.8379
2.50	1.093	4.0	0.9700	10.0	0.8242
2.60	1.081	4.1	0.9649	20.0	0.7432
2.70	1.069	4.2	0.9600	30.0	0.7005
2.80	1.058	4.3	0.9553	40.0	0.6718
2.90	1.048	4.4	0.9507	50.0	0.6504
3.00	1.039	4.5	0.9464	60.0	0.6335
3.10	1.030	4.6	0.9422	70.0	0.6194
3.20	1.022	4.7	0.9382	80.0	0.6076

† data taken from Hirschfelder et al. (1954)

APPENDIX G

COEFFICIENTS FOR SPECIES VISCOSITY DATA

Using least square fit analysis the temperature dependent viscosity of individual species generated using Kinetic theory are reduced to AT^B form. It is further divided into three ranges 300-800, 800-1300, 1300-2500 K. The matrix represents $VISCOF(K,J,I)$, $J=1,2$, $K=1,3$, $I=1,NS$, where K corresponds to the three temperature range, $J=1$ for the constant of multiplication A and $J=2$ for the power B .

N2	1	4.4249720E-07,	0.6511479	,
	2	8.1864022E-07,	0.5569940	,
	3	1.2107138E-07,	0.8218453	/
O2	1	3.0519510E-07,	0.7376035	,
	2	9.7767452E-07,	0.5644143	,
	3	6.2705396E-07,	0.6236016	/
AR	1	3.8466644E-07,	0.7162670	,
	2	1.2953406E-06,	0.5348911	,
	3	3.7022056E-07,	0.7058824	/
CO	1	3.0429968E-07,	0.7128531	,
	2	1.0134340E-06,	0.5329965	,
	3	2.6192052E-07,	0.7179117	/
H2O	1	2.2769083E-08,	1.067423	,
	2	3.5005293E-08,	1.003473	,
	3	4.7415284E-07,	0.6430891	/
CH4	1	1.5467951E-07,	0.7524964	,
	2	2.6708437E-07,	0.6722450	,
	3	7.1924870E-07,	0.5345844	/
CO2	1	2.4367341E-07,	0.7349151	,
	2	2.3944531E-07,	0.7385539	,
	3	7.2368522E-07,	0.5860700	/
H2	1	2.9646156E-07,	0.6031408	,
	2	2.2000563E-07,	0.6441427	,
	3	1.1770304E-07,	0.7349934	/
OH	1	3.2337837E-07,	0.7171631	,
	2	1.0864258E-06,	0.5361540	,
	3	3.1926515E-07,	0.7032359	/
NO	1	2.6910473E-07,	0.7481864	,
	2	7.4073671E-07,	0.5980423	,
	3	8.8341119E-07,	0.5718754	/

APPENDIX H

ISENTROPIC PROPERTY EVALUATION

In the flow at any given location, the unknown state parameters are evaluated assuming isentropic flow relations.

$$\frac{T}{t} = 1 + \frac{\gamma - 1}{2} \text{Mn}^2 \quad \dots(\text{H.1})$$

$$\frac{P}{p} = \left[1 + \frac{\gamma - 1}{2} \text{Mn}^2 \right]^{\gamma/(\gamma-1)} \quad \dots(\text{H.2})$$

$$\frac{\dot{m}}{A} = \frac{P}{\sqrt{\frac{\gamma}{RT}}} \frac{\text{Mn}}{\left[1 + \frac{\gamma - 1}{2} \text{Mn}^2 \right]^{0.5(\gamma+1)/(\gamma-1)}} \quad \dots(\text{H.3})$$

$$p = \frac{\rho R_t t}{\text{Mw}} \quad \dots(\text{H.4})$$

$$\text{Mn} = \frac{U}{\sqrt{\gamma R t}} \quad \dots(\text{H.5})$$

As an example, the evaluation of mach number is as shown: Equation (H.3) is rewritten as

$$\text{Mn} = \frac{\dot{m}}{AP} \sqrt{\frac{RT}{\gamma}} \left[1 + \frac{\gamma - 1}{2} \text{Mn}^2 \right]^{0.5(\gamma+1)/(\gamma-1)} \quad \dots(\text{H.6})$$

- 1) Guess initial mach number
- 2) Knowing the rest of the terms RHS of eqn (H.6) evaluated
- 3) The value $\text{abs}[(\text{Mn}-\text{Guess})/\text{Guess}]$ should be less than 0.0001.
- 4) If condition 3 is not satisfied steps 2 and 3 are repeated with the estimated mach number.

Convergence is usually quite rapid as initial guess is quite close to the actual one considering the low mach number in the combustor.

APPENDIX I

RAYLEIGH EQUATION SOLUTION

A process involving changes in the stagnation enthalpy or stagnation temperature of a gas stream which flows at constant area and without friction effects is termed as simple T-change (Shapiro (1953)). This is signified by Rayleigh Line as shown

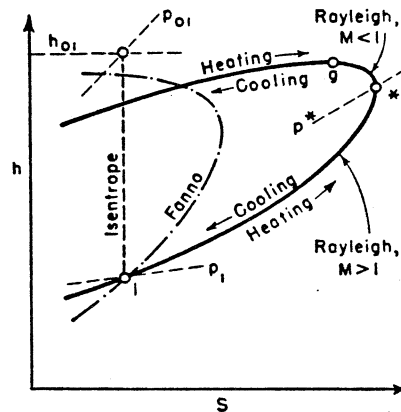


Fig I.1 Rayleigh Curve for simple T change

The normalised relation is given as

$$\frac{T}{T^*} = \frac{2(\gamma+1)Mn^2}{(1+\gamma Mn^2)^2} \left(1 + \frac{\gamma-1}{2} Mn^2 \right) \quad \dots(I.1)$$

- 1) Knowing state 1 before combustion, normalised temperature ratio T_1/T^* is evaluated using eqn (I.1)
- 2) Assuming the temperature rise, T_2/T_1 is evaluated
- 3) $T_2/T^* = T_2/T_1 \times T_1/T^*$
- 4) Using eqn (I.1) Mn_2 is evaluated in an iterative manner. Knowing Mn_2 and T_2 , the rest of the state is fully described using isentropic relations.

APPENDIX J

ONE-DIMENSIONAL STEADY FLOW SOLUTION

The procedure is as outlined by Shapiro (1953).

Consider the flow in a duct between two sections an infinitesimal distance dx apart (Fig J.1). In this element of duct length, gas is injected into the stream at the mass flow rate of dm_g , liquid evaporates into the stream at the mass flow rate of dm_L , heat in the amount dQ is exchanged with external sources, and shaft work, shearing work, or electrical work is delivered by the stream to external bodies in the amount dW_x .

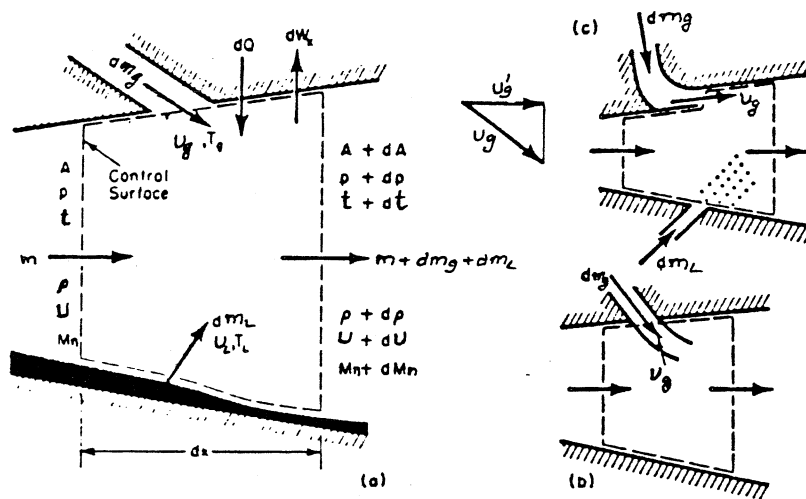


Fig J.1 Control surfaces defined for several methods of gas injection and liquid evaporation.

Equation of State

$$p = \rho R t / M_w \quad \dots (J.1)$$

$$\frac{dp}{p} = \frac{d\rho}{\rho} + \frac{dt}{t} + \frac{dM_w}{M_w} \quad \dots (J.2)$$

Mach Number

$$M_n^2 = U^2 M_w / \gamma R t \quad \dots (J.3)$$

$$\frac{dM_n^2}{M_n^2} = \frac{dU^2}{U^2} + \frac{dM_w}{M_w} - \frac{d\gamma}{\gamma} - \frac{dt}{t} \quad \dots (J.4)$$

Continuity

$$m = \rho AU \quad \dots(\text{J.5})$$

$$\frac{dm}{m} = \frac{d\rho}{\rho} + \frac{dA}{A} + \frac{dU}{U} \quad \dots(\text{J.6})$$

$$\text{where } dm = dm_L + dm_g$$

Energy

Neglecting gravity effects, the final form of energy balance appears as:

$$dQ - dW_x = dh + d \left[\frac{U^2}{2} + \left[h_{gt} - h_g + \frac{U^2 - U_g^2}{2} \right] \frac{dm_g}{m} \right. \\ \left. + \left[h_V - h_L + \frac{U^2 - U_L^2}{2} \right] \frac{dm_L}{m} \right] \quad \dots(\text{J.7})$$

The enthalpy change of the main stream, dh , is the sum of the changes due to chemical reaction and due to temperature change. Thus

$$dh = -dh_{pr} + C_p dt$$

where dh_{pr} , the enthalpy increase at the temperature t and pressure p for a change from products to reactants. h_{gt} and h_g denote the enthalpy at temperature t and at t_g at which gas enters respectively. The symbol h_V denotes the enthalpy of evaporated liquid dm_L at temperature t , and h_L the enthalpy of liquid entering the control volume. The eqn (J.7) is finally rearranged as

$$\frac{dQ - dW_x + dH}{C_p t} = \frac{dt}{t} + \frac{\gamma - 1}{2} Mn^2 \frac{dU^2}{U^2} \quad \dots(\text{J.8})$$

where

$$dH = dh_{pr} - [C_{p_g}(t - T_g) + U^2/2] \frac{dm_g}{m} \\ - \left[h_V - h_L + \frac{U^2 - U_L^2}{2} \right] \frac{dm_L}{m} \quad \dots(\text{J.9})$$

Momentum

$$\begin{aligned}
 pA + pdA - (p+dp)(A+dA) - \tau_w dA_w - dX \\
 = (m + dm_g + dm_L)(U + dU) - U_g' dm_g - U_L' dm_L - mU \quad \dots(J.10)
 \end{aligned}$$

Wall shear stress is related to the coefficient of friction f

$$\tau_w = f\rho U^2/2$$

dX is the sum of

- 1) the drag of stationary bodies immersed in the stream within the control surface boundaries.
- 2) the drag of liquid droplets and filaments travelling more slowly than the main gas stream.
- 3) the component of body or gravity forces acting on the material within the control surface in the direction opposite to that of the velocity vector.

$$\frac{dA_w}{A} = \frac{4dx}{D} \quad \text{where } D \text{ is the hydraulic diameter}$$

After substitution and rearrangement, eqn. (J.10) leads to

$$\begin{aligned}
 \frac{dp}{p} + \frac{\gamma Mn^2}{2} \frac{dU^2}{U^2} + \frac{\gamma Mn^2}{2} \left[4f \frac{dx}{D} + \frac{dx}{1/2 \gamma p A Mn^2} \right] + \gamma Mn^2 (1-y) \frac{dm}{m} = 0 \\
 \dots(J.11)
 \end{aligned}$$

where
$$y \frac{dm}{m} = y_g \frac{dm_g}{m} + y_L \frac{dm_L}{m}$$

$$y_g = U_g'/U \quad \text{and} \quad y_L = U_L'/U$$

The following are the six independent variables and the four unknowns from the above equations J.2, J.4, J.6, J.8, J.11.

$$\begin{array}{ll}
 dA/A & dMn^2/Mn^2 \\
 (dQ - dWx + dH)/Cp t & dU^2/U^2 \\
 4f \frac{dx}{D} + \frac{dX}{1/2\gamma p A Mn^2} - 2\gamma \frac{dm}{m} & dp/p \\
 dm/m & d\rho/\rho \\
 dMw/Mw & \\
 d\gamma/\gamma &
 \end{array}$$

The dependent variable dMn^2/Mn^2 is expressed in them, by solving the above system of simultaneous, linear, algebraic equations :

$$\begin{aligned}
 \frac{dMn^2}{Mn^2} = & - \frac{2[1+1/2(\gamma-1)Mn^2]}{1-Mn^2} \frac{dA}{A} + \frac{1+\gamma Mn^2}{1-Mn^2} \frac{dQ - dWx + dH}{Cp t} \\
 & + \frac{\gamma Mn^2(1+1/2(\gamma-1)Mn^2)}{1-Mn^2} \left[4f \frac{dx}{D} + \frac{dX}{1/2\gamma p A Mn^2} - 2\gamma \frac{dm}{m} \right] \\
 & + \frac{2(1+Mn^2)[1+1/2(\gamma-1)Mn^2]}{1-Mn^2} \frac{dm}{m} - \frac{1+\gamma Mn^2}{1-Mn^2} \frac{dMw}{Mw} - \frac{d\gamma}{\gamma} \\
 & \dots(J.12)
 \end{aligned}$$

The coefficients of the independent variables are called the influence coefficients. The dependent variables of interest viz., dMn^2/Mn^2 , and dp/p are better expressed in a tabular form in terms of their influence coefficients as Table J.1.

Variable	dMn^2/Mn^2	dp/p
dA/A	$-\frac{2[1+1/2(\gamma-1)Mn^2]}{1-Mn^2}$	$\frac{\gamma Mn^2}{1-Mn^2}$
$(dQ - dW_x + dH)/Cp t$	$\frac{1+\gamma Mn^2}{1-Mn^2}$	$-\frac{\gamma Mn^2}{1-Mn^2}$
$4f \frac{dx}{D} + \frac{dX}{1/2\gamma P A Mn^2} - 2y \frac{dm}{m}$	$\frac{\gamma Mn^2(1+1/2(\gamma-1)Mn^2)}{1-Mn^2}$	$-\frac{\gamma Mn^2(1+(\gamma-1)Mn^2)}{2(1-Mn^2)}$
dm/m	$\frac{2(1+Mn^2)[1+1/2(\gamma-1)Mn^2]}{1-Mn^2}$	$\frac{2\gamma Mn^2(1+1/2(\gamma-1)Mn^2)}{1-Mn^2}$
dMw/Mw	$-\frac{1+\gamma Mn^2}{1-Mn^2}$	$\frac{\gamma Mn^2}{1-Mn^2}$
$d\gamma/\gamma$	-1	0

Table J.1 Influence Coefficients

The equation (J.12) is solved, by transforming the differentials to finite differences through the average values across the control volume, by the following steps:

- 1) Compute the average flow properties over the increment

$$T_{ave} = 1/2 (T_2 + T_1)$$

$$A_{ave} = 1/2 (A_2 + A_1)$$

$$HD_{ave} = 1/2 (D_2 + D_1)$$

$$Mw_{ave} = 1/2 (Mw_2 + Mw_1)$$

$$m_{ave} = 1/2 (m_2 + m_1)$$

$$Mn_{ave} = 1/2 (Mn_2 + Mn_1)$$

$$\gamma_{ave} = 1/2 (\gamma_2 + \gamma_1)$$

$$\mu_{ave} = 1/2 (\mu_2 + \mu_1)$$

2) Differentials are put to finite difference

$$d\gamma/\gamma = F_\gamma = (\gamma_2 - \gamma_1)/\gamma_{ave}$$

$$dA/A = F_A = (A_2 - A_1)/A_{ave}$$

$$dT/T = F_T = (T_2 - T_1)/T_{ave}$$

$$dMw/Mw = F_{Mw} = (Mw_2 - Mw_1)/Mw_{ave}$$

$$dm/m = F_m = (m_2 - m_1)/m_{ave}$$

$$F_F = 4f \frac{dx}{Hd_{ave}} + \frac{dx}{1/2 \gamma p A m n^2} - 2yF_m$$

where

$$\cdot dx = 0.0$$

$$\cdot \text{Reynolds Number } Re = \frac{\rho U H d_{ave}}{\mu_{ave}}$$

\cdot friction factor f (Massey(1975))

$$16/Re \quad \text{for } Re < 2100$$

$$0.079/Re^{0.25} \quad \text{for } Re \geq 2100^e$$

@ Blasius suggested this approximate formula and this was found to correlate well for Re from 3000 to 10000. However its simplicity and range of applicability for ducts or annuli with rough surfaces makes it automatic choice in relation to any other complicated expression. It is felt adequate to assume it even for the transition region upto 3000.

$$\cdot y = U_g' / U$$

U_g' is the tangential velocity component of the dilutant or coolant flow.

$$U_g' = 0 \quad \text{for mixing hole}$$

$$U_g' = U_g \quad \text{for cooling slot}$$

3) It is also assumed that the independent variable

$$(dQ - dW_x + dH)/c_p T = \left(1 + \frac{\gamma - 1}{2} M_n^2\right) \frac{dT}{T}$$

METHOD OF SOLUTION

1) Guess the outlet mach number Mn_2 . Reasonable estimate can be obtained using

$$Mn_2 = Mn_1 \times (1 + F_m - F_A)^{0.5}$$

2) $Mn_{ave} = 0.5(Mn_2 + Mn_1)$

3) if Eqn J.12 is represented as

$$\frac{Mn_2^2 - Mn_1^2}{Mn_{ave}^2} = \text{LHS (left hand side)}$$

$$Mn_2^2 = Mn_1^2 + \text{LHS} (Mn_{ave}^2)$$

new estimate of Mn_2 can be obtained.

4) If the abs $[(Mn_2 - \text{Guess})/\text{Guess}]$ is greater than 0.0005, calculations are repeated from step 2 with the estimated Mn_2 .

5) If convergence is not obtained within 40 iterations option is given to try another 40 iterations, with a suitable initial guess. However in normal circumstances convergence is rapid.

6) Static pressure is then evaluated by integrating the corresponding dp/p influence coefficient terms, after Mn_2 is evaluated.

APPENDIX K

C05NCF - NAG FORTRAN Library Routine Document

NOTE: before using this routine, please read the appropriate implementation document to check the interpretation of *bold italicised* terms and other implementation-dependent details. The routine name may be precision-dependent.

1. Purpose

C05NCF is a comprehensive routine to find a zero of a system of N nonlinear functions in N variables by a modification of the Powell hybrid method.

2. Specification

```

SUBROUTINE C05NCF (FCN, N, X, FVEC, XTOL, MAXFEV, ML, MU,
1 EPSFCN, DIAG, MODE, FACTOR, NPRINT, NFEV, FJAC, LDFJAC,
2 R, LR, QTF, W, IFAIL)
C INTEGER N, MAXFEV, ML, MU, MODE, NPRINT, NFEV, LDFJAC, LR,
C 1 IFAIL
C real X(N), FVEC(N), XTOL, EPSFCN, DIAG(N), FACTOR,
C 1 FJAC(LDFJAC,N), R(LR), QTF(N), W(N,4)
C EXTERNAL FCN

```

3. Description

C05NCF is based upon the MINPACK routine HYBRD. It chooses the correction at each step as a convex combination of the Newton and scaled gradient directions. Under reasonable conditions this guarantees global convergence for starting points far from the solution and a fast rate of convergence. The Jacobian is updated by the rank-1 method of Broyden. At the starting point the Jacobian is approximated by forward differences, but these are not used again until the rank-1 method fails to produce satisfactory progress.

4. References

- [1] POWELL, M.J.D.
A hybrid method for nonlinear algebraic equations. In 'Numerical Methods for Nonlinear Algebraic Equations', Ed. Rabinowitz, P., Gordon and Breach, 1970.
- [2] MORE, J.J., GARBOW, B.S. and HILLSTROM, K.E.
User Guide for MINPACK-1.
ANL-80-74, Argonne National Laboratory.

5. Parameters

FCN - SUBROUTINE, supplied by the user.

FCN must calculate the values of the functions at X and return these in the vector FVEC.

Its specification is:-

```

SUBROUTINE FCN(N, X, FVEC, IFLAG)
INTEGER N, IFLAG
real X(N), FVEC(N)

```

N - INTEGER.

On entry, N contains the number of equations. The value of N must not be changed by FCN.

X - real array of DIMENSION (N).

On entry, X contains the point at which the functions are to be evaluated. The values in X must not be changed by FCN.

FVEC - real array of DIMENSION (N).

On exit, unless IFLAG was zero on entry or IFLAG is reset to a negative number, FVEC(i) must contain the value of the i (th) function evaluated at X .

IFLAG - INTEGER.

If, on entry, IFLAG is zero, then X and FVEC are available for printing. See NPRINT below.

In general IFLAG should not be reset by FCN. If, however, the user wishes to terminate execution (perhaps because some illegal point X has been reached) then IFLAG should be set to a negative integer. This value will be returned through IFAIL.

FCN must be declared as EXTERNAL in the (sub)program from which C05NCF is called.

N - INTEGER.

On entry, N must specify the number of equations. $N > 0$.

Unchanged on exit.

X - real array of DIMENSION at least (N).

Before entry, X(j) must be set to a guess at the j(th) component of the solution ($j = 1, 2, \dots, N$).

On exit, X contains the final estimate of the solution vector.

FVEC - real array of DIMENSION at least (N).

On exit, FVEC contains the function values at the final point, X.

XTOL - real.

On entry, XTOL must specify the accuracy in X to which the solution is required. $XTOL \geq 0.0$. If XTOL is less than machine precision (see NAG FORTRAN Library routine X02AAF) then machine precision is used. See Section 10. The recommended value is the square root of machine precision.

Unchanged on exit.

MAXFEV - INTEGER.

On entry, MAXFEV must specify the maximum number of calls to FCN with IFLAG $\neq 0$. COSNCF will exit with IFAIL = 2, if, at the end of an iteration, the number of calls to FCN exceeds MAXFEV. A suitable choice of MAXFEV is $200 \times (N+1)$. $MAXFEV > 0$.

Unchanged on exit.

ML - INTEGER.

On entry, ML must specify the number of subdiagonals within the band of the Jacobian matrix. (If the Jacobian is not banded, or you are unsure, set $ML = N-1$.) $ML \geq 0$.

Unchanged on exit.

MU - INTEGER.

On entry, MU must specify the number of superdiagonals within the band of the Jacobian matrix. (If the Jacobian is not banded, or you are unsure, set $MU = N-1$.) $MU \geq 0$.

Unchanged on exit.

EPSFCN - real.

On entry, EPSFCN must specify the order of the largest relative error in the functions. If EPSFCN is less than machine precision (see NAG FORTRAN Library routine X02AAF) then machine precision is used. Consequently a value of 0.0 will often be suitable.

Unchanged on exit.

DIAG - real array of DIMENSION at least (N).

Before entry, if $MODE = 2$ (see below), DIAG must contain positive entries that serve as multiplicative scale factors for the variables. If $MODE \neq 2$, then DIAG is set internally.

MODE - INTEGER.

On entry, MODE must specify whether or not the user has provided scaling factors in DIAG. If $MODE = 2$ the scaling must have been specified in DIAG. Otherwise, the variables will be scaled internally.

Unchanged on exit.

FACTOR - real.

On entry, FACTOR must specify a quantity to be used in determining the initial step bound. In most cases $0.1 \leq FACTOR \leq 100.0$, and $FACTOR = 100.0$ is generally suitable. (The step bound is $FACTOR \times ||DIAG \times X||_2$ if this is non-zero; otherwise the bound is $FACTOR$.) $FACTOR > 0.0$.

Unchanged on exit.

NPRINT - INTEGER.

On entry, NPRINT must specify whether special calls to FCN, with IFLAG set to 0, are to be made for printing purposes.

If $NPRINT \leq 0$ then no calls are made. If $NPRINT > 0$, then FCN is called at the beginning of the first iteration, every NPRINT iterations thereafter and immediately prior to the return from COSNCF. In this case, FCN should usually be coded to print both X and FVEC (see FCN above).

Unchanged on exit.

NFEV - INTEGER.

On exit, NFEV specifies the number of calls made to FCN.

FJAC - real array of DIMENSION (LDFJAC,p), where $p \geq N$.

On exit, FJAC contains the orthogonal matrix Q produced by the QR factorisation of the final approximate Jacobian.

LDFJAC - INTEGER.

On entry, LDFJAC must specify the first dimension of FJAC as declared in the calling (sub)program. $LDFJAC \geq N$.

Unchanged on exit.

R - real array of DIMENSION at least (LR).

On exit, R contains the upper triangular matrix R produced by the QR factorisation of the final approximate Jacobian, stored row-wise.

LR - INTEGER.

On entry, LR must specify the dimension of R as declared in the calling (sub)program.
 $LR \geq \frac{1}{4}N \times (N+1)$.

Unchanged on exit.

QTF - real array of DIMENSION (N).

On exit, QTF contains the vector $Q^T \times FVEC$.

W - real array of DIMENSION (N,q),

where $q \geq 4$.

Used as workspace.

IFAIL - INTEGER.

Before entry, IFAIL must be assigned a value. For users not familiar with this parameter (described in Chapter P01) the recommended value is 0.

Unless the routine detects an error (see next section), IFAIL contains 0 on exit.

6. Error Indicators and Warnings

Errors detected by the routine:-

IFAIL < 0

This indicates an exit from C05NCF because the user has set IFLAG negative in FCN. The value of IFAIL will be the same as the user's setting of IFLAG.

IFAIL = 1

On entry, $N \leq 0$, $XTOL < 0.0$, $MAXFEV \leq 0$, $ML < 0$, $MU < 0$, $FACTOR \leq 0.0$, $LDFJAC < N$, $LR < \frac{1}{4}N \times (N+1)$ or $MODE = 2$ and $DIAG(i) \leq 0.0$, $i = 1, 2, \dots, N$.

IFAIL = 2

There have been at least MAXFEV evaluations of FCN. Consider restarting the calculation from the final point held in X.

IFAIL = 3

No further improvement in the approximate solution X is possible; XTOL is too small.

IFAIL = 4

The iteration is not making good progress, as measured by the improvement from the last 5 Jacobian evaluations.

IFAIL = 5

The iteration is not making good progress, as measured by the improvement from the last 10 iterations.

The values IFAIL = 4 and IFAIL = 5 may indicate that the system does not have a zero. Otherwise, rerunning C05NCF from a different starting point may avoid the region of difficulty.

7. Auxiliary Routines

Details are distributed to sites in machine-readable form.

8. Timing

The time required by C05NCF to solve a given problem depends on N, the behaviour of the functions, the accuracy requested and the starting point. The number of arithmetic operations executed by C05NCF to process each call of FCN is about $11.5 \times N^2$. Unless FCN can be evaluated quickly, the timing of C05NCF will be strongly influenced by the time spent in FCN.

9. Storage

There are no internally declared arrays.

10. Accuracy

If D denotes the diagonal matrix whose entries are defined by the array DIAG, then C05NCF tries to ensure that

$$\| |D \times (X - XSOL) | \|_2 \leq XTOL \times \| |D \times XSOL | \|_2.$$

If this condition is satisfied with $XTOL = 10^{-k}$ then the larger components of $D \times X$ have k significant decimal digits. There is a danger that the smaller components of $D \times X$ may have large relative errors, but the fast rate of convergence of C05NCF usually avoids this possibility.

The test assumes that the functions are reasonably well behaved. If this condition is not satisfied, then C05NCF may incorrectly indicate convergence. The validity of the answer can be checked for example, by rerunning C05NCF with a tighter tolerance.

11. Further Comments

Ideally the problem should be scaled so that, at the solution the function values are of comparable magnitude.

12. Keywords

Equations, nonlinear algebraic; Powell hybrid method.

APPENDIX L

NON-LINEAR HEAT TRANSFER EQUATION SOLVER

In order to evaluate the metal temperatures, heat balance specified as equation (6.7), is required to be performed. The final form when all the terms are considered yields a set of non-linear equations. The non-linearity is due to RR1 the radiation term which is a function of the temperature to its fourth power. The number of simultaneous equations depends on the number of skins and cooling channel configuration (Fig 6.3). FVEC in the foregoing discussion represents the residue which should be zero for the exact solution. AREA1 to AREA6 are the respective surface areas of the skins.

SINGLE SKIN

$$FVEC(1) = (RR1+CC1)AREA1 - KK12 \quad \dots (L.1)$$

$$FVEC(2) = (RR2+CC2)AREA2 - KK12 \quad \dots (L.2)$$

SINGLE WALL

$$FVEC(1) = (RR1+CC1)AREA1 - KK12$$

$$FVEC(2) = (RR2+CC2)AREA2 - KK42$$

$$FVEC(3) = (RR3+CC3)AREA3 - KK12$$

$$FVEC(4) = (RR3-CC4)AREA4 - KK42$$

$$FVEC(5) = (CC4)AREA4+(CC3)AREA3 - MCPA(TL(5) - TL(6))$$

TL(1)to TL(4): respective skin temperatures T_{w1} to T_{w4}

TL(5)& TL(6): coolant temperature inside the slot

$$MCPA = (m Cp)_c$$

DOUBLE WALL

$$\begin{aligned}
\text{FVEC}(1) &= (\text{RR1} + \text{CC1})\text{AREA1} - \text{KK12} \\
\text{FVEC}(2) &= (\text{RR2} + \text{CC2})\text{AREA2} - \text{KK62} \\
\text{FVEC}(3) &= (\text{RR3} + \text{CC3})\text{AREA3} - \text{KK12} \\
\text{FVEC}(4) &= (\text{RR3} - \text{CC4})\text{AREA4} - \text{KK42} \\
\text{FVEC}(5) &= (\text{RR5} + \text{CC5})\text{AREA5} - \text{KK42} \\
\text{FVEC}(6) &= (\text{RR5} - \text{CC6})\text{AREA6} - \text{KK62} \\
\text{FVEC}(7) &= (\text{CC4})\text{AREA4} + (\text{CC3})\text{AREA3} - \text{MCPA}(\text{TL}(7) - \text{TL}(9)) \\
\text{FVEC}(8) &= (\text{CC5})\text{AREA5} + (\text{CC6})\text{AREA6} - \text{MCPA}(\text{TL}(8) - \text{TL}(10))
\end{aligned}$$

TL(1) to TL(6) : respective skin temperatures T_{w1} to T_{w4}
 TL(7) to TL(10): coolant temperature inside the slots

The coefficients are evaluated as per the procedure outlined in Chapter 6.

$$\begin{aligned}
\text{RR1} &= A_1 T_g^4 - A_2 T_{w1}^4 \\
\text{RR2} &= A_3 (T_{w2}^4 - T_{in}^4) \\
\text{CC1} &= A_4 (T_{wad} - T_{w1}) \\
\text{CC2} &= A_5 (T_{w2} - T_{in}) \\
\text{KK12} &= f(T_{w1}, T_{w2}, \lambda, \text{geometry})
\end{aligned}$$

The RR1 term consists of two parts, wherein A_1 is a function of gas emissivity which in turn depends on gas temperature, whereas A_2 is a function absorptivity which is evaluated based on the wall temperature T_{w1} . Thus all coefficients, except A_2 are constants for a given condition. A_2 however, is a function of T_{w1} and therefore needs to be estimated. By assuming an initial value of T_{w1} , which estimates an initial value of A_2 , leaving as many unknowns as there are equations.

NEWTON-RAPHSON'S TECHNIQUE

Rewriting equations (L.1) and (L.2)

$$f_1(x, y) = 0 \quad \text{where} \quad x \rightarrow T_{w1}$$

$$f_2(x, y) = 0 \quad \quad \quad y \rightarrow T_{w2}$$

expanding in Taylor's series and neglecting the higher order terms

$$0 = f_1(x_i, y_i) + \frac{\partial f_1}{\partial x}(x_{i+1} - x_i) + \frac{\partial f_1}{\partial y}(y_{i+1} - y_i)$$

$$0 = f_2(x_i, y_i) + \frac{\partial f_2}{\partial x}(x_{i+1} - x_i) + \frac{\partial f_2}{\partial y}(y_{i+1} - y_i)$$

$$\text{if} \quad x_{i+1} - x_i = h$$

$$y_{i+1} - y_i = k$$

$$\frac{\partial f_1}{\partial x} h + \frac{\partial f_1}{\partial y} k = - f_1(x_i, y_i)$$

$$\frac{\partial f_2}{\partial x} h + \frac{\partial f_2}{\partial y} k = - f_2(x_i, y_i)$$

These simultaneous equations can easily be solved for h and k. For this Gaussian Elimination technique is used.

GAUSSIAN ELIMINATION TECHNIQUE

As this is also a fairly standard technique no detailed explanation is needed. However for completeness sake, the methodology is indicated.

If we have n equations with n unknowns

$$\begin{aligned} a_{11}x_1 + a_{12}x_2 + a_{13}x_3 + \dots + a_{1n}x_n &= Y_1 \\ a_{21}x_1 + a_{22}x_2 + a_{23}x_3 + \dots + a_{2n}x_n &= Y_2 \\ a_{31}x_1 + a_{32}x_2 + a_{33}x_3 + \dots + a_{3n}x_n &= Y_3 \\ \cdot & \cdot \\ \cdot & \cdot \\ a_{n1}x_1 + a_{n2}x_2 + a_{n3}x_3 + \dots + a_{nn}x_n &= Y_n \end{aligned}$$

To evaluate we form the augmented matrix

$$\begin{bmatrix} a_{11} & a_{12} & a_{13} & \cdots & a_{1n} & Y_1 \\ a_{21} & a_{22} & a_{23} & \cdots & a_{2n} & Y_2 \\ a_{31} & a_{32} & a_{33} & \cdots & a_{3n} & Y_3 \\ \cdot & & & & \cdot & \cdot \\ \cdot & & & & \cdot & \cdot \\ a_{n1} & a_{n2} & a_{n3} & \cdots & a_{nn} & Y_n \end{bmatrix}$$

After triangularisation we have the new matrix

$$\begin{bmatrix} a_{11} & a_{12} & a_{13} & \cdots & a_{1n} & Y_1 \\ 0 & a'_{22} & a'_{23} & \cdots & a'_{2n} & Y_2 \\ 0 & 0 & a''_{33} & \cdots & a''_{3n} & Y_3 \\ \cdot & & & & \cdot & \cdot \\ \cdot & & & & (n-1) & (n-1) \\ 0 & 0 & 0 & \cdots & a_{nn} & Y_n \end{bmatrix}$$

Finally we perform the back substitution to know the unknowns x_1 to x_n

Once h and k are evaluated, we then use

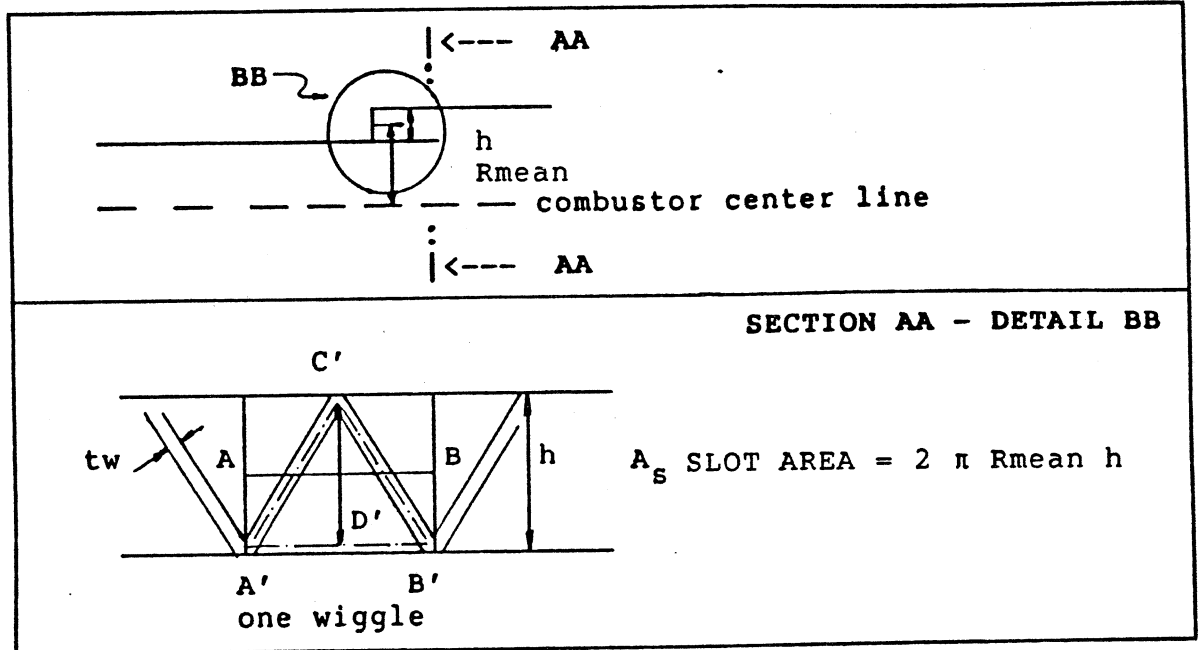
$$x_{i+1} = x_i + h$$

$$Y_{i+1} = Y_i + k$$

to get the next approximation and repeat. This procedure is extended to the single wall and double wall cases where the numbers of equations would increase to 5 and 8 respectively.

It has been found when the programme is run with double precision, the results are as accurate as that of NAG library. Rarely it requires as high as 6 iterations for the final solution, mainly because the initial guess is very close to the solution. Thus the need of external libraries is eliminated.

APPENDIX M
FLOW AREA - WIGGLE STRIP



if N is the number of wiggles

$$\begin{aligned} \text{slot area per wiggler} &= A_s / N \\ &= AB h \end{aligned}$$

$$\text{hence, } AB = A_s / Nh$$

if each wiggler is approximated to the triangle $A'B'C'$

$$\text{wiggler height } C'D' = (h - tw) \text{ where } tw \text{ wiggler thickness}$$

$$\text{wiggler base } A'B' = C_f * AB$$

(C_f is introduced considering the curvature effects, a more detailed geometrical relation can be incorporated, however C_f can be approximated to 0.9)

$$\text{wiggler length } A'C' = \sqrt{(A'B'/2)^2 + C'D'^2}$$

$$\text{wiggler area } A_w = 2 (A'C') tw$$

$$\text{wiggler blockage} = A_w N / A_s$$

$$\text{Flow area fraction} = 1 - \text{wiggler blockage}$$

APPENDIX N
MATERIAL PROPERTIES

Sl No	Material	Thermal Condt. (W/m K)	Emissivity -
Liner/ Casing Material			
1	Alluminium alloy	80	0.4
2	Nimonic 90	25	0.7
3	Hastalloy 275	22	0.7
4	Inconel 700	17	0.7
Coating Material			
1	Allumina	2.74	0.45
2	Zirconia	0.6	0.4
3	Beryllium oxide	25.13	0.5
4	Silicon Nitride	18.84	0.3

Table N.1 Representative properties of typical materials

ALUMINA , (X(i,j),j=1,2,i=1,4)	
0.5204662050532104,	2.165653971160257
-0.0787224302793582,	-1.215433485988361
0.0180849436871110,	0.516784558750829
0.0086515266491387,	0.39252800808 298
C = 0.9039389681214779	
ZIRCONIA , (X(i,j),j=1,2,i=1,4)	
0.4198776679325266,	3.151012812469279
-0.0554946809863555,	-1.050571553314007
0.0563636506469235,	0.969195702938641
-0.0304724552006618,	-0.802167723362267
C = 0.7897476451189523	

Table N.2 Coefficients for Temperature dependent Emissivity (Ubhi (1987))

APPENDIX O

CONVERSIONS FOR TRACE CONCENTRATIONS

Concentrations of trace species in a multicomponent gaseous mixture can be expressed in a variety of ways.

Volumetric

1. mole fraction = $\frac{\text{no of moles of trace species}}{\text{total moles of the mixture}}$
2. 1 ppmv = $\frac{1 \text{ volume of trace species}}{10^6 \text{ volumes of gaseous mixture}}$
(1ppm = one part per million)
3. 1 ppmv = mole fraction $\times 10^6$

Gravimetric

1. mass fraction = $\frac{\text{mass of trace species}}{\text{total mass of the mixture}}$
= mole fraction $\frac{\text{mol. wt. of species}}{\text{mean mol. wt. of mixture}}$
2. 1 ppmw = mass fraction $\times 10^6$
= ppmv $\frac{\text{mol. wt. of species}}{\text{mean mol. wt. of mixture}}$
3. mg/m^3 = ppmw \times density $\times 10^{-12}$
where density in Kg/m^3
4. Kg/hr = ppmw \times (air+fuel) $\times 0.0036$
where (air+fuel) in Kg/s
5. Emission Index = g trace species/ Kg of fuel
6. g/MW = g of trace species/ energy output in MW

CORRECTIONS

The measured content normally is corrected to a reference condition so that comparison is standardised.

1. 15% Oxygen

$$\text{NOx}_{\text{obs}} = \text{NOx}_{\text{meas}} \frac{(20.95-15.0)}{(20.95-\text{O2}_{\text{meas}})}$$

where O2_{meas} = O2 % volume measured in the exhaust

2. Reference conditions as per EPA, USA standards

$$\text{NOx}_{\text{corr}} = \text{NOx}_{\text{obs}} \left(\frac{P_{\text{ref}}}{P_{\text{obs}}} \right)^{0.5} \exp[19 \cdot (H_{\text{obs}} - H_{\text{ref}})] \cdot \left(\frac{T_{\text{ref}}}{T_{\text{amb}}} \right)^{1.53}$$

where $P_{\text{ref}} = 101.32$ kpa

$T_{\text{ref}} = 288$ °K

$H_{\text{ref}} = 0.00633$ Kg H₂O/Kg dry air

others are correspondingly as observed

APPENDIX P

INTEGRATION TECHNIQUE FOR NO_x EQUATIONS

The integration over the time and equivalence ratio is carried out using Gaussian quadrature. Computing time and accuracy had to be optimized, while considering the number of points or terms in the quadrature formula. After comparing the results of various combinations, using 6, 10 and 20 point formulae, the optimum method was found as to divide the entire integration region into suitable intervals and performing integrating with Gaussian Quadrature using 6 point formula for each interval. The term suitable interval is used depending on the mean values for time and equivalence ratio.

Residence Time

$$0 \leq t/\tau \leq 3 \quad \Delta t/\tau = 0.25$$

$$3 < t/\tau \leq 39 \quad \Delta t/\tau = 3$$

$$39 < t/\tau \leq 50 \quad \Delta t/\tau = 11 \quad \dots(P.1)$$

Equivalence Ratio

Coefficient of variation $S_0 = \sigma/\phi_{\text{mean}}$
(the typical values being around 0.2 or lower)

$$\sigma > 0.15$$

$$0 \leq \phi \leq \phi_{\text{mean}} \quad \Delta\phi = \sigma \text{ or } (\phi_{\text{mean}} - \phi) \text{ whichever is lower}$$

$$\phi_{\text{mean}} < \phi \leq 2\phi_{\text{mean}} \quad \Delta\phi = - " -$$

$$\sigma \leq 1.5$$

$$0 \leq \phi \leq \phi_{\text{mean}} - 3S_0 \quad \Delta\phi = \phi_{\text{mean}} - 3S_0$$

$$\phi_{\text{mean}} - 3S_0 < \phi \leq \phi_{\text{mean}} \quad \Delta\phi = \sigma \text{ or } (\phi_{\text{mean}} - \phi) \text{ whichever is lower}$$

$$\phi_{\text{mean}} < \phi \leq \phi_{\text{mean}} + 3S_0 \quad \Delta\phi = - " -$$

$$\phi_{\text{mean}} + 3S_0 < \phi \leq 2\phi_{\text{mean}} \quad \Delta\phi = \phi_{\text{mean}} - 3S_0 \quad \dots(P.2)$$

The limits of the function is transformed to

$$\int_0^{\infty} f(y) dy = \int_{-1}^{+1} f(x) dx \quad \dots(P.3)$$

using quadrature formula

$$\int_{-1}^{+1} f(x) dx = \sum_{k=1}^n W_k f(x_k) \quad \dots(P.4)$$

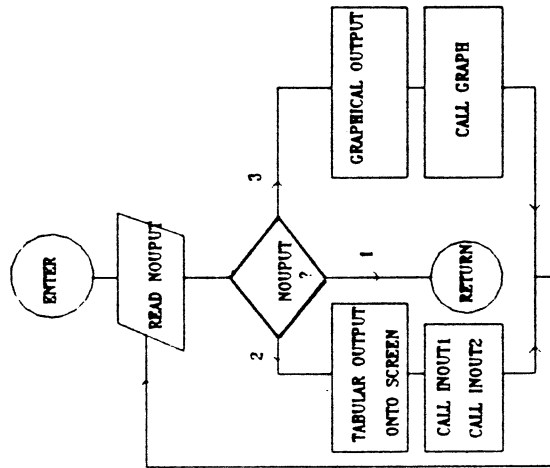
where n is the number of points, here it is 6

the x_k (abscissa) and W_k (weight factors) values are as follows.

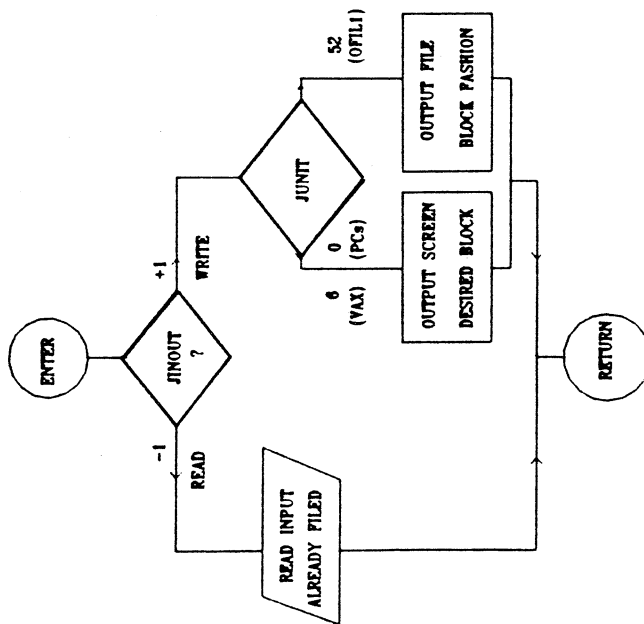
x_k	W_k
-0.9324695142	0.1713244924
-0.6612093865	0.3607615730
-0.2386191861	0.4679139346
0.2386191861	0.4679139346
0.6612093865	0.3607615730
0.9324695142	0.1713244924

Table P.1 Values for 6 Point Formula

SUBROUTINE INOUT3



SUBROUTINE INOUT2



APPENDIX R
CASE RESULTS

1) CASE 1 : Turboannular Industrial Gas Turbine Combustor (evaluation).	233
2) CASE 2 : Turboannular aeroderived gas turbine combustor (design & evaluation).	255
3) CASE 3 : Annular aero Gas Turbine combustor (evaluation)- cold flow analysis	270
CASE 3B: Flow analysis with combustion.	273
CASE 3C: CASE 3B with shifted temperature profile	283
CASE 3D: CASE 3B with test rig operating conditions	284
4) CASE 4 : Double/ Reheat combustor (design & evaluation)	287
CASE 4B: CASE 4 with coating with constant emissivity	303
CASE 4C: CASE 4B with temperature and coating characteristic dependent emissivity	304

CASE 1

INPUT FOR PRELIMINARY DESIGN

(refer Table 10.1 for nomenclature)

```
'SPEC'  
83.3  
1136866.5  
601.  
1073.  
4.55  
65  
'GEOM'  
0.365  
0.05  
'TYPE'  
3  
1  
12.5  
22.4  
0.  
0.  
1  
1  
1  
'END'
```

CASE 1 (contd)

INPUT FOR PERFORMANCE EVALUATION
(refer Table 10.2 for nomenclature)

```

'MATRL'
2,1,0.002,0.002
'NOZZL'
3
'COAT'
'N',5,0.0
'GIVEN'
0,23,2
'SLOTS'
0.000,'D',6,'C',+,1
0.0.0.00.0.0.0.0.0
0.0118,'C',3,'C',+,3
0.0.0.00.0.00.0.00.0.0
0.002,0.0025,0.003,0.003,97,0.0
0.0085,0.004,0.00.0.0.0.0
0.0242,'C',3,'C',+,3
0.0.0.00.0.0.0.0.0
0.002,0.0026,0.003,0.003,112,0.0
0.022,0.004,0.00.0.0.0.0
0.0337,'A',0,'C',+,1
0.0.0.00.0.0.0.0.0
0.0383,'C',4,'C',+,4
0.0.0.00.0.00.0.00.0.0
0.0005,0.001,0.003,.003,124,0.0
0.004,0.0025,0.003,.003,124,0.0
0.0235,0.0044,0.00.0.0.0.0
0.0542,'C',4,'C',+,4
0.0.0.00.0.00.0.00.0.0
0.0005,0.001,0.003,.003,137,0.0
0.004,0.0018,0.003,.003,137,0.0
0.024,0.004,0.00.0.0.0.0
0.0706,'C',3,'C',+,3
0.0.0.00.0.00.0.00.0.0
0.0023,0.0018,0.003,.003,149,0.0
0.0227,0.0038,0.00.00.0.0.0
0.0892,'C',3,'C',+,3
0.0.0.00.0.00.0.00.0.0
0.0042,0.0018,0.003,.003,159,0.0
0.0196,0.003,0.00.00.0.0.0
0.1166,'A',0,'C',+,1
0.0.0.00.0.00.0.00.0.0
0.1256,'C',4,'C',-,17
0.0.0.00.0.00.0.00.0.0
0.0316,0.0114,0.002,.002,65,0.0
0.0526,0.0114,0.002,.002,65,0.0
0.0736,0.0114,0.002,.002,65,0.0
0.0900,0.0114,0.002,.002,64,0.0
0.1106,0.0114,0.002,.002,80,0.0
0.1256,0.0114,0.002,.002,90,0.0
0.1406,0.0114,0.002,.002,90,0.0

```

0.1546,0.0114,0.002,.002,100,0.0
0.1686,0.0114,0.002,.002,100,0.0
0.1806,0.0114,0.002,.002,110,0.0
0.1926,0.0114,0.002,.002,110,0.0
0.2046,0.0114,0.002,.002,110,0.0
0.2156,0.0114,0.002,.002,120,0.0
0.2266,0.0114,0.002,.002,120,0.0
0.2376,0.0114,0.002,.002,120,0.0
0.2517,0.0114,0.00,0.0,0.0
0.2192,'M',7,'C',+,1
0.00,0.00,0.012,.012,16,0.0
0.4776,'M',8,'C',+,1
0.00,0.00,0.07,.028,6,0.0
0.6231,'A',0,'C',+,1
0.0,0.00,0.00,0.00,0.0
0.6379,'C',3,'C',-,3
0.0,0.00,0.00,0.00,0.0
0.006,0.003,0.002,.002,120,0.0
0.0260,0.003,0.00,0.0,0.0
0.7721,'C',3,'C',-,3
0.0,0.00,0.00,0.00,0.0
0.006,0.003,0.002,.002,120,0.0
0.0260,0.003,0.00,0.0,0.0
0.8514,'A',0,'C',+,1
0.0,0.00,0.00,0.00,0.0
0.9291,'A',0,'C',+,1
0.0,0.00,0.00,0.00,0.0
0.9929,'A',0,'C',+,1
0.0,0.00,0.00,0.00,0.0
1.0169,'M',0,'C',+,1
0.0,0.00,0.00,0.00,0.0
1.0179,'M',6,'C',+,1
0.0,0.00,0.004,0.004,42,0.0
1.2071,'A',0,'C',+,1
0.0,0.00,0.00,0.00,0.0
1.2221,'A',0,'C',+,1
0.0,0.00,0.00,0.00,0.0
1.2436,'A',0,'C',+,1
0.0,0.00,0.00,0.00,0.0

```
'GEOM'  
23  
0.75350 0.43200 0.62480 0.16950 0.16950  
0.76300 0.44400 0.65000 0.22000 0.22000  
0.77300 0.46500 0.66880 0.25760 0.25760  
0.78000 0.47600 0.67950 0.27900 0.27900  
0.78000 0.48000 0.68500 0.29000 0.29000  
0.78000 0.48000 0.70050 0.32100 0.32100  
0.78000 0.48000 0.71450 0.34900 0.34900  
0.78100 0.48100 0.72630 0.37260 0.37260  
0.78400 0.48300 0.74500 0.41000 0.41000  
0.78400 0.48300 0.75450 0.42900 0.42900  
0.78400 0.48300 0.75450 0.42900 0.42900  
0.78400 0.48300 0.75450 0.42900 0.42900  
0.78400 0.48300 0.74900 0.41800 0.41800  
0.78400 0.48300 0.70550 0.33100 0.33100  
0.78400 0.48300 0.68000 0.28000 0.28000  
0.78400 0.48300 0.68000 0.28000 0.28000  
0.76400 0.41600 0.69200 0.30400 0.30400  
0.72000 0.37650 0.70000 0.33600 0.33600  
0.56300 0.19300 0.49580 0.08800 0.08800  
0.54800 0.17500 0.48250 0.07150 0.07150  
0.53900 0.14500 0.47500 0.05930 0.05930  
'END'
```

OUTPUT

Case No : 1 DATE : 24-JAN-88

Run By : USER TIME : 16:23:39

BLOCK NUMBER AT LAST TERMINATION = 13

BLOCK: 2			
TYPE	1	2	3
SINO	1	2	3
CHAMBER		DIFFUSER	INJECTOR
3 TUBOANNULAR		2 DUMP	1 PRESSURE ATOMISER
APPLICATION			1 GROUND

BLOCK: 2	
5) FUEL:	6) OXIDANT: (mole fractions)
1) I AVTUR	Molecular Wt : 28.9640
2) C	1) Sp Humidity: 0.0000
12.50000 24.40000	(fraction of inlet air)
0.00000 0.00000	
3) L C V	N2
46.4000 (MJ/kg)	2) O2
4) AFRS	3) AR
14.7170	4) CO
5) Fuel temp TTF	5) H2O
300.0000 K	6) CH4
6) Enthalpy fuel	7) CO2
-266.1000 (kJ/mole)	8) H2
at TTF	
Molecular Wt	
174.7300	
Sp. Gravity	
0.8000	

BLOCK: 3	
DESIGN SPECIFICATIONS	
1) Mass Flow W2 = 83.300 (kg/s)	4) O P L = 4.550 (\$)
2) Tot. Press PT2 = 1136900.0 (N/m2)	5) P L F = 65.000 (-)
3) Tot. Temp TT2 = 601.0 (K)	6) Tot. Temp TT8 = 1073.0 (K)
COMBUSTOR INLET PLANE	COMBUSTOR EXIT PLANE
7) Ref Rad RREF2 = 0.36500 (m)	Ref Rad RREF8 = 0.44535 (m)
8) Channel Ht HT2 = 0.05000 (m)	Channel Ht HT8 = 0.05930 (m)
Inlet Area A2 = .11467E+00 (m2)	9) Exit Area A8 = .11615E+01 (m2)
Inlet Mach No MN2 = 0.2337 (-)	10) Exit Mach No MN8 = 0.2269 (-)

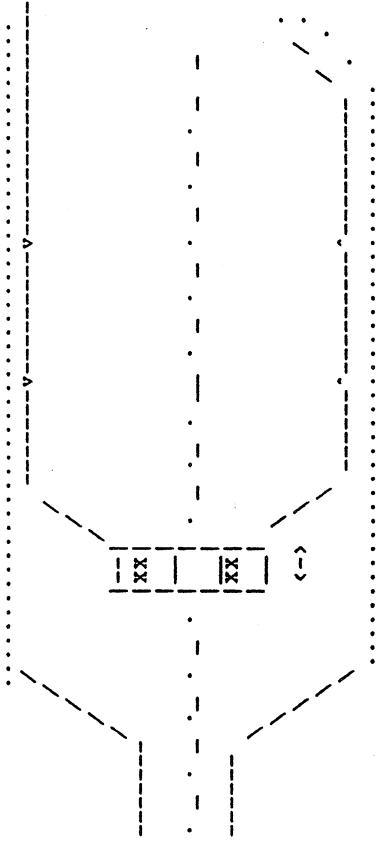
BLOCK: 4

REFERENCE AREA					
SLMO->	RRF	HT	AR	A	DL
PLANE	1	2	3	4	6
1	0.36500	0.05000	1.0000	.11467E+00	0.00000
2	0.40875	0.06750	1.5118	.17336E+00	0.10000
3	0.49800	0.13994	3.8185	.43786E+00	0.17300
4	0.55750	0.24500	7.4843	.85820E+00	0.16000
5	0.54000	0.29510	8.7317	.10013E+01	0.00000

BLOCK: 5

COMBUSTOR SIZING	
1) FLAMETUBE WIDTH	DFT= 0.40789(m)
2) DIFFUSER LENGTH	DL = 0.43300(m)
3) DIFFUSER TO DOME LENGTH	DDL= 0.04810(m)
4) DOME LENGTH	DML= 0.06700(m)
5) PRIMARY ZONE LENGTH	PZL= 0.18100(m)
6) SECONDARY ZONE LENGTH	SZL= 0.22200(m)
7) DILUTION ZONE LENGTH	DZL= 0.44800(m)
8) NOZZLE LENGTH	ZNL= 0.11000(m)
9) COMBUSTOR LENGTH	CCL= 1.44210(m)
10) FLAME TUBE EXIT WIDTH	DFT8= 0.05930(m)
11) NUMBER OF TUBES	NTUBE= 7

COMBUSTOR GEOMETRY (not to scale)



DL	DDL	PZL	SZL	DZL	ZNL
0.43300	0.04810	0.18100	0.22200	0.44800	0.11000

% MASS FLOW SPLITS		BLOCK: 6									
47.46		(sec)	(dil)								
		6.62	40.84								
0.23	MIXING	0.00	0.00	0.00	0.00	0.00	0.23				
18.49	18.49 (1SWRL) [K]	R	P	S	D	Z	A = 11.900				
	0.00 (-1ATOM)	0.92	0.33	0.18	0.17	F = 0.152					
	0.00 (-1DOME) [K]			equivalence ratio							
33.65	COOLING										
99.83		19.58	0.00	11.95	0.00	2.13					
MASS FLOW SPLITS											
5.647		(sec)	(dil)								
		0.788	4.859								
0.028	MIXING	0.000	0.000	0.000	0.000	0.028					
2.200	2.200 (1SWRL) [K]	R	P	S	D	Z	A = 11.900				
	0.000 (-1ATOM)	0.92	0.33	0.18	0.17	F = 0.152					
	0.000 (-1DOME) [K]			equivalence ratio							
4.005	COOLING										
11.880		2.330	0.000	1.422	0.000	0.253					
MASS FLOW SPLITS											
		PZL	SZL	DZL	ZNL						
		I	EFF(1)	EFF(2)	EFF(3)	EFF(4)	I				
		I	PHI(1)	PHI(2)	PHI(3)	PHI(4)	I				
		TT(1)	TT(2)	TT(3)	TT(4)	TT(5)	TT(6)				
		LL(1)	LL(2)	LL(3)	LL(4)	LL(5)	LL(6)				
1)	LINER LGTH :	0.00000	0.11660	0.21920	0.47760	0.62310	1.24360				
2)	ZONE LGTH :	0.18100	0.22200	0.44800	0.11000						
3)	EFFICIENCY :	0.9000	0.9900	0.9950	0.9990						
4)	EQ. RATIO :	0.9187	0.3329	0.1759	0.1721						
5)	TEMPERATURE:	601.0	2372.3	1999.5	1241.2	1157.1	1073.0				

SWID		BLOCK: 7	
1)DSW	= 0.12000(m)	4)No of Vanes	= 10
2)DHUB	= 0.04000(m)	5)Vane Angle	= 60.0
3)Swirler Length	= 0.01400(m)	6)Swirler Area	= .10053E-01(m2)
7)No. Injectors	= 7	1 PRESSURE ATOMISER	
8)DATM1	= 0.00000(m)	10)Atomiser area	= .00000E+00(m2)
9)DATM2	= 0.00000(m)	11)CD atomiser	= 0.00000

GENERAL DATA :

GEOMETRY : (3 23)

SL NO ->	(1)	(2)	(3)	(4)	(5)
SLOT NO	CASING HGT	CASING WPTH	LINER HGT	LINER WIDTH	LINER WPTH HOR
1	0.00000	0.43200	0.62480	0.16950	0.16950
2	0.01180	0.44400	0.65000	0.22000	0.22000
3	0.02420	0.46500	0.66880	0.25760	0.25760
4	0.03370	0.47600	0.67950	0.27900	0.27900
5	0.03830	0.48000	0.68500	0.29000	0.29000
6	0.05420	0.48000	0.70050	0.32100	0.32100
7	0.07060	0.48000	0.71450	0.34900	0.34900
8	0.08920	0.48100	0.72630	0.37260	0.37260
9	0.11660	0.48300	0.74500	0.41000	0.41000
10	0.12560	0.48300	0.75450	0.42900	0.42900
11	0.21920	0.48300	0.75450	0.42900	0.42900
12	0.47760	0.48300	0.75450	0.42900	0.42900
13	0.62310	0.48300	0.75450	0.42900	0.42900
14	0.63790	0.48300	0.74900	0.41800	0.41800
15	0.77210	0.48300	0.70550	0.33100	0.33100
16	0.85140	0.48300	0.68000	0.28000	0.28000
17	0.92910	0.48300	0.68000	0.28000	0.28000
18	0.99290	0.41600	0.69200	0.30400	0.30400
19	1.01690	0.37650	0.70000	0.33600	0.33600
20	1.01790	0.72000	0.70000	0.33600	0.33600
21	1.20710	0.56300	0.49580	0.08800	0.08800
22	1.22210	0.54800	0.48250	0.07150	0.07150
23	1.24360	0.53900	0.47500	0.05930	0.05930

SLOT DETAILS : (0 23 2)

SLOT NO	POSTI (m)	TYPE	SIGN +/-	STATIONS	RES. TIME. (sec)
1	0.00000	D 6C	*	1	0.0000E+00
2	0.01180	C 3C	+	3	0.6894E-03
3	0.02420	C 3C	+	3	0.1534E-02
4	0.03370	A 0C	*	1	0.2193E-02
5	0.03830	C 4C	+	4	0.2514E-02
6	0.05420	C 4C	+	4	0.3645E-02
7	0.07060	C 3C	+	3	0.4706E-02
8	0.08920	C 3C	+	3	0.5716E-02
9	0.11660	A 0C	*	1	0.7007E-02
10	0.12560	C 4C	*	17	0.7436E-02
11	0.21920	M 7C	*	1	0.1198E-01
12	0.47760	M 8C	*	1	0.2590E-01
13	0.62310	A 0C	*	1	0.3234E-01
14	0.63790	C 3C	-	3	0.3293E-01
15	0.77210	C 3C	-	3	0.3708E-01
16	0.85140	A 0C	*	1	0.3870E-01
17	0.92910	A 0C	*	1	0.4006E-01
18	0.99290	A 0C	*	1	0.4129E-01
19	1.01690	N 0C	*	1	0.4185E-01
20	1.01790	M 6C	*	1	0.4190E-01
21	1.20710	A 0C	*	1	0.4713E-01
22	1.22210	A 0C	*	1	0.4727E-01
23	1.24360	E 0C	*	1	0.4743E-01

SLOT FLOWS : (0 23 2)

SLT NO	OI I2	POSTI (m)	HT (m)	DIA (m)	DIA2 (m)	NO	AREA (m2)	FRACTION	CD	EFF. AREA (m2)	FLOW (kg/s)	% FLOW	Ymax/Dft	PHI deg
1	1	0.00000	0.00000	0.00000	0.00000	0	.00000E+00	0.0000	0.0000	.00000E+00	0.0000	0.0000	0.00000	0.00
2	1	0.00000	0.00000	0.00000	0.00000	0	.00000E+00	0.0000	0.0000	.00000E+00	0.0000	0.0000	0.00000	0.00
2	1	0.00200	0.00250	0.00300	0.00300	97	.18461E-02	0.3714	0.6000	.41139E-03	0.2168	1.8215	0.00000	0.00
2	1	0.00850	0.00400	0.00000	0.00000	0	.29673E-02	0.0000	0.0000	.00000E+00	0.2168	1.8215	0.00000	0.00
3	1	0.00000	0.00000	0.00000	0.00000	0	.00000E+00	0.0000	0.0000	.00000E+00	0.0000	0.0000	0.00000	0.00
3	1	0.00200	0.00260	0.00300	0.00300	112	.21904E-02	0.3614	0.6000	.47501E-03	0.2505	2.1049	0.00000	0.00
3	1	0.02200	0.00400	0.00000	0.00000	0	.37536E-02	0.0000	0.0000	.00000E+00	0.2505	2.1049	0.00000	0.00
4	1	0.00000	0.00000	0.00000	0.00000	0	.00000E+00	1.0000	0.0000	.00000E+00	0.0000	0.0000	0.00000	0.00
5	1	0.00000	0.00000	0.00000	0.00000	0	.49035E-02	0.0000	0.0000	.00000E+00	0.0000	0.0000	0.00000	0.00
5	1	0.00500	0.00100	0.00300	0.00300	124	.93916E-03	0.9333	0.6000	.52590E-03	0.2770	2.3278	0.00000	0.00
5	1	0.00400	0.00250	0.00300	0.00300	124	.23828E-02	0.3678	0.6000	.52590E-03	0.2771	2.3285	0.00000	0.00
5	1	0.02350	0.00440	0.00000	0.00000	0	.45253E-02	0.0000	0.0000	.00000E+00	0.5541	4.6563	0.00000	0.00
6	1	0.00000	0.00000	0.00000	0.00000	0	.55866E-02	0.0000	0.0000	.00000E+00	0.0000	0.0000	0.00000	0.00
6	1	0.00500	0.00100	0.00300	0.00300	137	.10340E-02	0.9366	0.6000	.58104E-03	0.3066	2.5763	0.00000	0.00
6	1	0.00400	0.00180	0.00300	0.00300	137	.18856E-02	0.5136	0.6000	.58104E-03	0.3066	2.5769	0.00000	0.00
6	1	0.02400	0.00400	0.00000	0.00000	0	.44497E-02	0.0000	0.0000	.00000E+00	0.6132	5.1532	0.00000	0.00
7	1	0.00000	0.00000	0.00000	0.00000	0	.55542E-02	0.0000	0.0000	.00000E+00	0.0000	0.0000	0.00000	0.00
7	1	0.00230	0.00180	0.00300	0.00300	149	.20176E-02	0.5220	0.6000	.63193E-03	0.3349	2.8143	0.00000	0.00
7	1	0.02270	0.00380	0.00000	0.00000	0	.43892E-02	0.0000	0.0000	.00000E+00	0.3349	2.8143	0.00000	0.00
8	1	0.00000	0.00000	0.00000	0.00000	0	.61879E-02	0.0000	0.0000	.00000E+00	0.0000	0.0000	0.00000	0.00
8	1	0.00420	0.00180	0.00300	0.00300	159	.21691E-02	0.5181	0.6000	.67434E-03	0.3602	3.0266	0.00000	0.00
8	1	0.01960	0.00300	0.00000	0.00000	0	.37076E-02	0.0000	0.0000	.00000E+00	0.3602	3.0266	0.00000	0.00
9	1	0.00000	0.00000	0.00000	0.00000	0	.00000E+00	1.0000	0.0000	.00000E+00	0.0000	0.0000	0.00000	0.00
10	1	0.00000	0.00000	0.00000	0.00000	0	.00000E+00	0.0000	0.0000	.00000E+00	0.0000	0.0000	0.00000	0.00
10	1	0.03160	0.01140	0.00200	0.00200	65	.14956E-01	0.0137	0.6000	.12252E-03	0.0655	0.5508	0.00000	0.00
10	1	0.05260	0.01140	0.00200	0.00200	65	.14956E-01	0.0137	0.6000	.12252E-03	0.0655	0.5505	0.00000	0.00
10	1	0.07360	0.01140	0.00200	0.00200	65	.14956E-01	0.0137	0.6000	.12252E-03	0.0655	0.5501	0.00000	0.00
10	1	0.09000	0.01140	0.00200	0.00200	64	.14956E-01	0.0134	0.6000	.12064E-03	0.0644	0.5414	0.00000	0.00
10	1	0.11060	0.01140	0.00200	0.00200	80	.14956E-01	0.0168	0.6000	.15080E-03	0.0809	0.6800	0.00000	0.00
10	1	0.12560	0.01140	0.00200	0.00200	90	.14956E-01	0.0189	0.6000	.16965E-03	0.0910	0.7646	0.00000	0.00
10	1	0.14060	0.01140	0.00200	0.00200	90	.14956E-01	0.0189	0.6000	.16965E-03	0.0910	0.7643	0.00000	0.00
10	1	0.15460	0.01140	0.00200	0.00200	100	.14956E-01	0.0210	0.6000	.18850E-03	0.1010	0.8488	0.00000	0.00
10	1	0.16860	0.01140	0.00200	0.00200	100	.14956E-01	0.0210	0.6000	.18850E-03	0.1010	0.8485	0.00000	0.00
10	1	0.18060	0.01140	0.00200	0.00200	110	.14956E-01	0.0231	0.6000	.20735E-03	0.1110	0.9330	0.00000	0.00
10	1	0.19260	0.01140	0.00200	0.00200	110	.14956E-01	0.0231	0.6000	.20735E-03	0.1110	0.9326	0.00000	0.00

10	1	0.20460	0.01140	0.00200	0.00200	0.00200	110	.14956E-01	0.0231	0.6000	.20735E-03	0.1109	0.9323	0.00000	0.00
10	1	0.21560	0.01140	0.00200	0.00200	0.00200	120	.14956E-01	0.0252	0.6000	.22619E-03	0.1210	1.0167	0.00000	0.00
10	1	0.22660	0.01140	0.00200	0.00200	0.00200	120	.14956E-01	0.0252	0.6000	.22619E-03	0.1209	1.0163	0.00000	0.00
10	1	0.23760	0.01140	0.00200	0.00200	0.00200	120	.14956E-01	0.0252	0.6000	.22619E-03	0.1209	1.0160	0.00000	0.00
10	1	0.25170	0.01140	0.00000	0.00000	0.00000	0	.14956E-01	0.0000	0.0000	.00000E+00	1.4216	11.9460	0.00000	0.00
11	1	0.00000	0.00000	0.01200	0.01200	0.01200	16	.18096E-02	1.0000	0.8153	.14754E-02	0.7879	6.6209	0.21697	81.29
12	1	0.00000	0.00000	0.07000	0.02800	0.02800	6	.10751E-01	1.0000	0.8442	.90757E-02	4.8595	40.8364	0.86298	83.71
13	1	0.00000	0.00000	0.00000	0.00000	0.00000	0	.00000E+00	1.0000	0.0000	.00000E+00	0.0000	0.0000	0.00000	0.00
14	1	0.00000	0.00000	0.00000	0.00000	0.00000	0	.00000E+00	0.0000	0.0000	.00000E+00	0.0000	0.0000	0.00000	0.00
14	1	0.00600	0.00300	0.00200	0.00200	0.00200	120	.38624E-02	0.0976	0.6000	.22619E-03	0.1239	1.0413	0.00000	0.00
14	1	0.02600	0.00300	0.00000	0.00000	0.00000	0	.37524E-02	0.0000	0.0000	.00000E+00	0.1239	1.0413	0.00000	0.00
15	1	0.00000	0.00000	0.00000	0.00000	0.00000	0	.00000E+00	0.0000	0.0000	.00000E+00	0.0000	0.0000	0.00000	0.00
15	1	0.00600	0.00300	0.00200	0.00200	0.00200	120	.30428E-02	0.1239	0.6000	.22619E-03	0.1294	1.0873	0.00000	0.00
15	1	0.02600	0.00300	0.00000	0.00000	0.00000	0	.29337E-02	0.0000	0.0000	.00000E+00	0.1294	1.0873	0.00000	0.00
16	1	0.00000	0.00000	0.00000	0.00000	0.00000	0	.00000E+00	1.0000	0.0000	.00000E+00	0.0000	0.0000	0.00000	0.00
17	1	0.00000	0.00000	0.00000	0.00000	0.00000	0	.00000E+00	1.0000	0.0000	.00000E+00	0.0000	0.0000	0.00000	0.00
18	1	0.00000	0.00000	0.00000	0.00000	0.00000	0	.00000E+00	1.0000	0.0000	.00000E+00	0.0000	0.0000	0.00000	0.00
19	1	0.00000	0.00000	0.00000	0.00000	0.00000	0	.00000E+00	1.0000	0.0000	.00000E+00	0.0000	0.0000	0.00000	0.00
20	1	0.00000	0.00000	0.00400	0.00400	0.00400	42	.52779E-03	1.0000	0.6250	.32986E-03	0.1942	1.6316	0.06731	89.73
21	1	0.00000	0.00000	0.00000	0.00000	0.00000	0	.00000E+00	1.0000	0.0000	.00000E+00	0.0000	0.0000	0.00000	0.00
22	1	0.00000	0.00000	0.00000	0.00000	0.00000	0	.00000E+00	1.0000	0.0000	.00000E+00	0.0000	0.0000	0.00000	0.00
23	1	0.00000	0.00000	0.00000	0.00000	0.00000	0	.00000E+00	1.0000	0.0000	.00000E+00	0.0000	0.0000	0.00000	0.00

TOTAL EFFECTIVE HOLE AREA = 0.23204E-01 (M2)

MATERIAL SPECIFICATIONS:

SL. NO.	LINER	CASING	COATING
	1	2	3
MATERIAL	2 NIMONIC 90	1 ALUMINIUM ALLOY	0 *****
EMISSIVITY	.70000E+00	.40000E+00	.00000E+00
CONDUCTIVITY	.25000E+02	.80000E+02	.00000E+00
THICKNESS	.20000E-02	.20000E-02	.00000E+00

ITERATION = 3	NO OF CONTROL VOLUMES = 1169
LINER = 84.225 (Kg/s)	ANNULUS = 0.142 (Kg/s)
OPL CALCULATED = 3.175 %	OPL EXPECTED = 4.550 %
PLF CALCULATED = 180.845	PLF EXPECTED = 65.000
PATTERN FACTOR = 0.025577	

EXIT PLANE COMPOSITION: (mole fractions)

Molecular Weight	: 28.9597
N2	: 0.7718
O2	: 0.1714
AR	: 0.0092
CO	: 0.0000
H2O	: 0.0233
CH4	: 0.0000
CO2	: 0.0242
H2	: 0.0000

STABILITY DATA

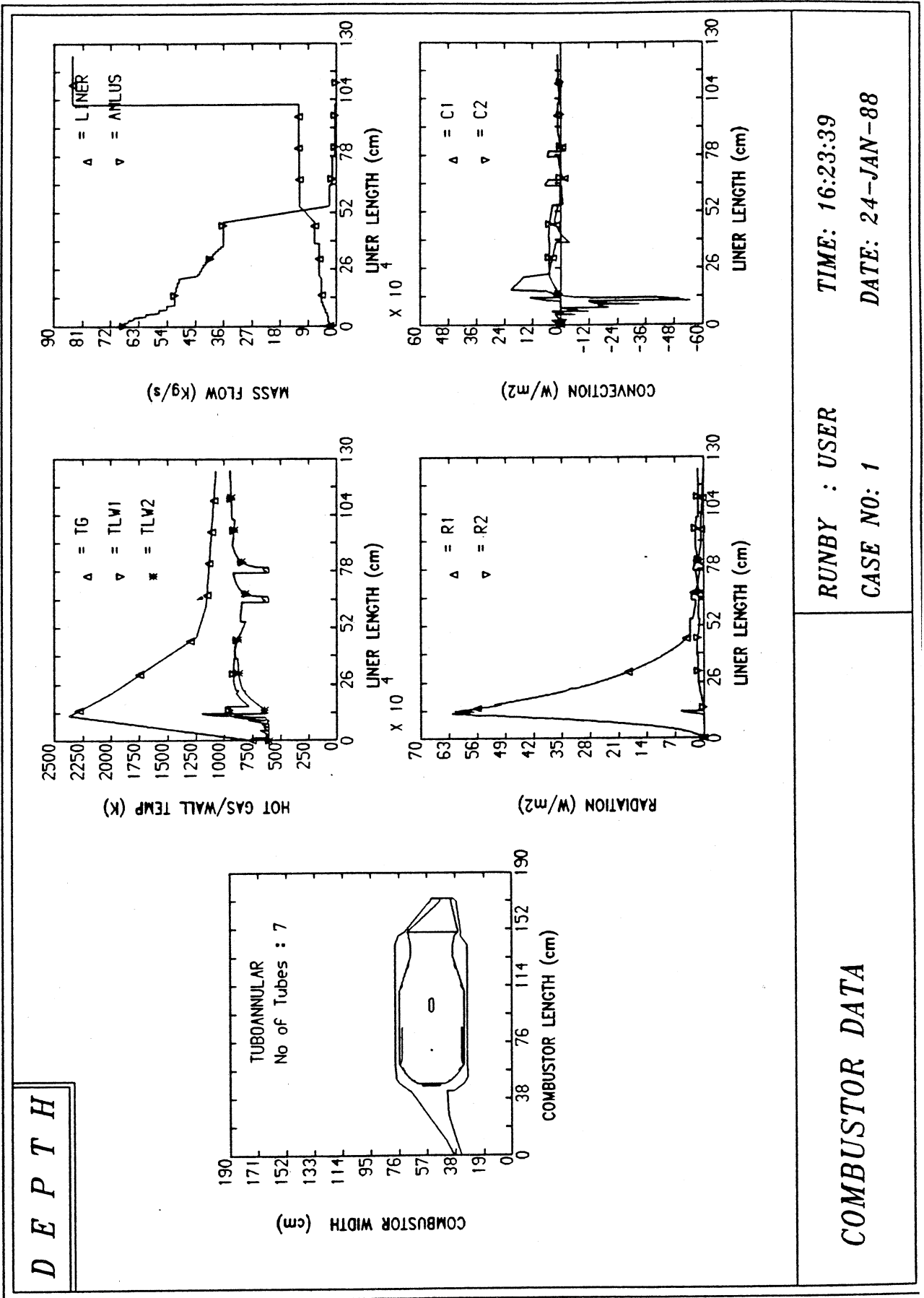
SL NO	Equ. Rat.	m/VP**n
1	0.1	0.23912E-08
2	0.2	0.79763E-07
3	0.3	0.67164E-06
4	0.4	0.27303E-05
5	0.5	0.71905E-05
6	0.6	0.14631E-04
7	0.7	0.22263E-04
8	0.8	0.27539E-04
9	0.9	0.39524E-04
10	1.0	0.29799E-04
11	1.3	0.41453E-04
12	1.5	0.27508E-04
13	1.8	0.30774E-04
14	2.0	0.24642E-04
Loading Parameter		0.22608E-08

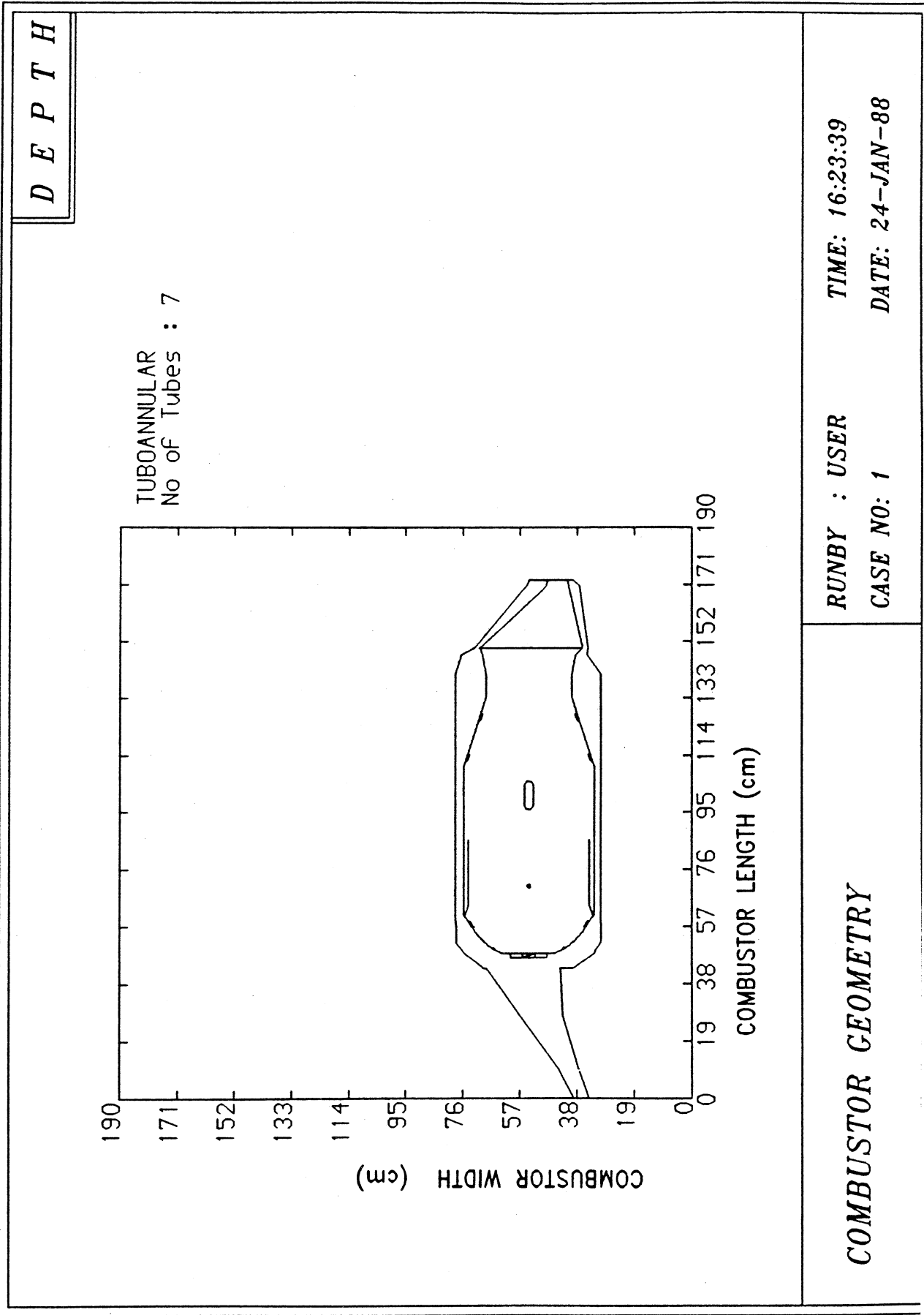
NOX DATA (mass fraction)						
Res. Time (sec)	Eq. Rat. (-)	Temp (K)	GENERATION (-)	DILUTION (-)	TOTAL (-)	TOTAL (-)
0.0000E+00	0.0000	0.010	0.0000E+00	0.0000E+00	0.0000E+00	0.0000E+00
0.11984E-01	0.9187	1999.510	0.98145E-03	0.0000E+00	0.98145E-03	0.98145E-03
0.25909E-01	0.3329	1241.210	0.10904E-02	-0.91875E-03	0.11531E-02	0.11531E-02
0.32359E-01	0.1759	1157.110	0.25855E-09	-0.71178E-03	0.44134E-03	0.44134E-03
0.32949E-01	0.1758	1155.110	0.21740E-15	-0.22698E-06	0.44111E-03	0.44111E-03
0.37109E-01	0.1750	1136.910	0.15210E-14	-0.20624E-05	0.43905E-03	0.43905E-03
0.38727E-01	0.1745	1126.210	0.58571E-15	-0.12175E-05	0.43783E-03	0.43783E-03
0.40091E-01	0.1740	1115.610	0.48941E-15	-0.11929E-05	0.43664E-03	0.43664E-03
0.41320E-01	0.1736	1107.010	0.43830E-15	-0.97929E-06	0.43566E-03	0.43566E-03
0.41879E-01	0.1735	1103.710	0.19845E-15	-0.36813E-06	0.43529E-03	0.43529E-03
0.41925E-01	0.1734	1103.610	0.16270E-16	-0.15332E-07	0.43528E-03	0.43528E-03
0.47159E-01	0.1723	1077.910	0.18377E-14	-0.29105E-05	0.43237E-03	0.43237E-03
0.47300E-01	0.1722	1075.910	0.48938E-16	-0.23004E-06	0.43214E-03	0.43214E-03
0.47463E-01	0.1721	1073.010	0.56715E-16	-0.32976E-06	0.43181E-03	0.43181E-03

NOX AT EXIT PLANE			
MASS FRACTION (Kg/Kg)	PPMw (weight)	PPMv (volume)	EMISSION INDEX (g/Kg fuel)
0.43181E-03	431.8	226.8	37.364

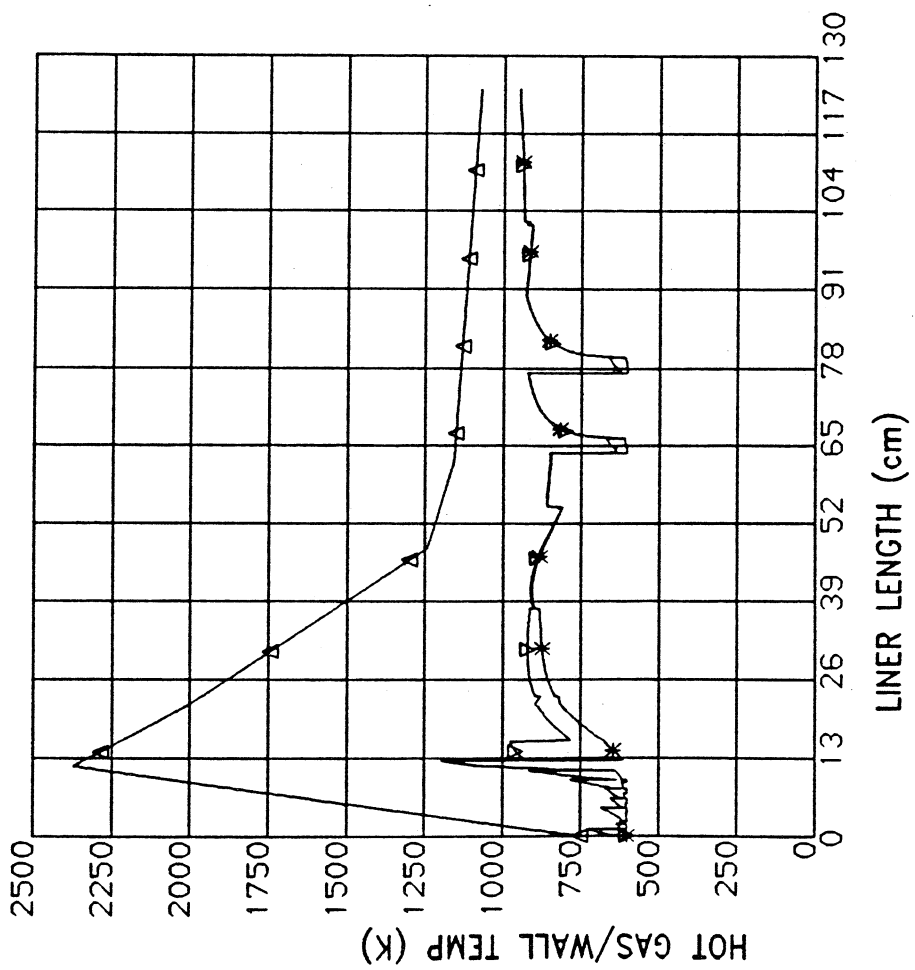
NOx EQUILIBRIUM DATA

EQ RAT (-)	DENSITY (Kg/m3)	TEMP (K)	k1 (-)	k2 (-)	R1 (see text for units)	R6 (see text for units)	[NO]eq ()
0.00000	0.00634	601.9	0.0000E+00	0.1333E+01	0.0000E+00	0.2317E-34	0.5287E-07
0.10000	0.00460	860.7	0.1951E-02	0.1321E+01	0.1260E-28	0.2065E-28	0.5880E-05
0.20000	0.00359	1102.1	0.1324E-01	0.1274E+01	0.2463E-21	0.7038E-19	0.8773E-04
0.30000	0.00298	1326.5	0.4332E-01	0.1179E+01	0.5614E-17	0.1373E-15	0.4328E-03
0.40000	0.00258	1536.2	0.9848E-01	0.1041E+01	0.4361E-14	0.2006E-13	0.1218E-02
0.50000	0.00228	1732.8	0.1794E+00	0.8771E+00	0.4847E-12	0.6516E-12	0.2457E-02
0.60000	0.00206	1917.3	0.2766E+00	0.7023E+00	0.1566E-10	0.7996E-11	0.3969E-02
0.70000	0.00189	2089.9	0.3632E+00	0.5290E+00	0.2143E-09	0.4869E-10	0.5395E-02
0.80000	0.00176	2248.0	0.4024E+00	0.3635E+00	0.1486E-08	0.1634E-09	0.6224E-02
0.90000	0.00165	2383.0	0.3740E+00	0.2115E+00	0.5283E-08	0.2839E-09	0.5826E-02
1.00000	0.00159	2470.9	0.2885E+00	0.8596E-01	0.7496E-08	0.1783E-09	0.3791E-02
1.10000	0.00157	2469.1	0.1860E+00	0.2001E-01	0.2685E-08	0.2381E-10	0.1408E-02
1.20000	0.00158	2402.4	0.1195E+00	0.4184E-02	0.4318E-09	0.1528E-11	0.4228E-03
1.30000	0.00161	2321.5	0.8278E-01	0.1035E-02	0.6205E-10	0.1017E-12	0.1353E-03
1.40000	0.00164	2239.7	0.6063E-01	0.2908E-03	0.8883E-11	0.7398E-14	0.4608E-04
1.50000	0.00167	2159.7	0.4611E-01	0.8848E-04	0.1260E-11	0.5650E-15	0.1626E-04
1.60000	0.00171	2082.1	0.3598E-01	0.2821E-04	0.1743E-12	0.4364E-16	0.5830E-05
1.70000	0.00174	2006.7	0.2857E-01	0.9209E-05	0.2312E-13	0.3303E-17	0.2091E-05
1.80000	0.00178	1933.6	0.2299E-01	0.3024E-05	0.2898E-14	0.2386E-18	0.7414E-06
1.90000	0.00182	1862.5	0.1864E-01	0.9841E-06	0.3378E-15	0.1604E-19	0.2570E-06
2.00000	0.00186	1793.2	0.1518E-01	0.3134E-06	0.3605E-16	0.9832E-21	0.8624E-07
2.10000	0.00191	1725.8	0.1238E-01	0.9670E-07	0.3479E-17	0.5381E-22	0.2776E-07
2.20000	0.00195	1659.9	0.1010E-01	0.2853E-07	0.2985E-18	0.2566E-23	0.8490E-08
2.30000	0.00201	1595.6	0.8220E-02	0.7968E-08	0.2238E-19	0.1042E-24	0.2440E-08
2.40000	0.00206	1532.6	0.6665E-02	0.2076E-08	0.1437E-20	0.3490E-26	0.6507E-09
2.50000	0.00212	1471.1	0.5378E-02	0.4973E-09	0.7753E-22	0.9384E-28	0.1589E-09
2.60000	0.00218	1411.4	0.4317E-02	0.1084E-09	0.3474E-23	0.1976E-29	0.3508E-10
2.70000	0.00225	1354.9	0.3468E-02	0.2185E-10	0.1377E-24	0.3455E-31	0.7136E-11
2.80000	0.00231	1307.0	0.2858E-02	0.4713E-11	0.6640E-26	0.7333E-33	0.1541E-11
2.90000	0.00236	1274.4	0.2500E-02	0.1420E-11	0.6716E-27	0.3723E-34	0.4610E-12
3.00000	0.00239	1255.5	0.2321E-02	0.6275E-12	0.1523E-27	0.5046E-35	0.2011E-12
3.10000	0.00241	1244.7	0.2237E-02	0.3562E-12	0.5816E-28	0.1295E-35	0.1122E-12
3.20000	0.00243	1238.6	0.2206E-02	0.2340E-12	0.3020E-28	0.4834E-36	0.7239E-13





DEPTH

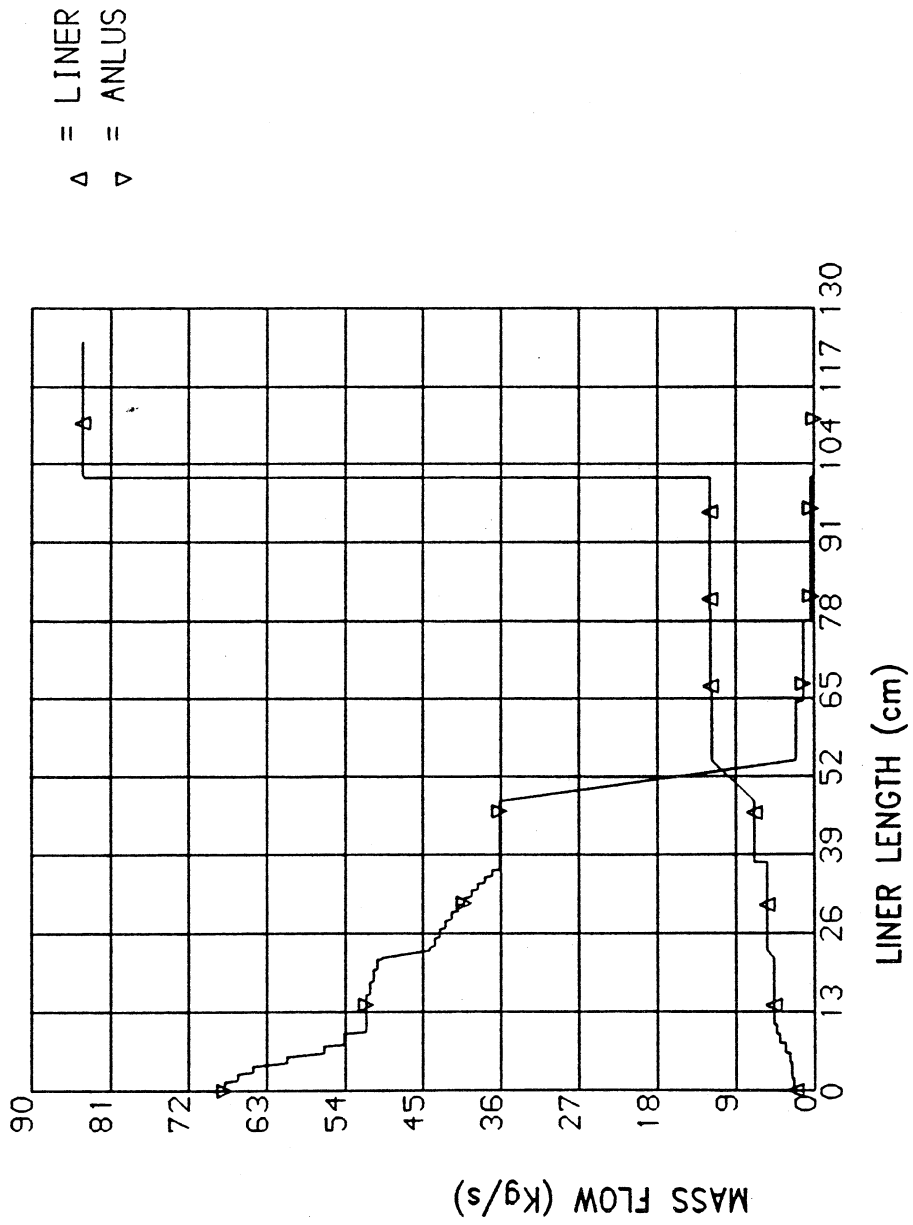


△ = TG
▽ = TLW1
* = TLW2

RUNBY : USER TIME: 16:23:39
CASE NO: 1 DATE: 24-JAN-88

TEMPERATURE VARIATION

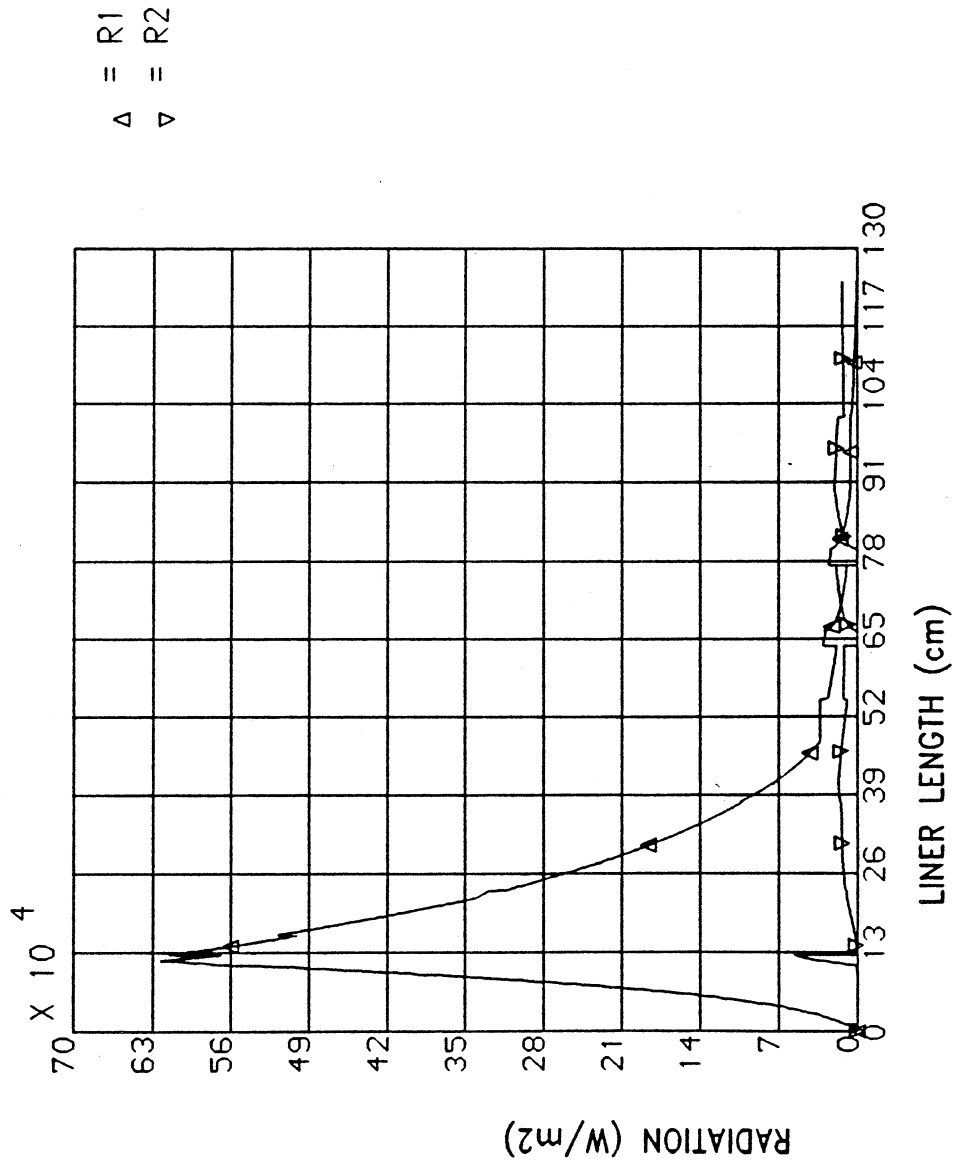
D E P T H



RUNBY : USER TIME: 16:23:39
 CASE NO: 1 DATE: 24-JAN-88

MASS FLOW VARIATION

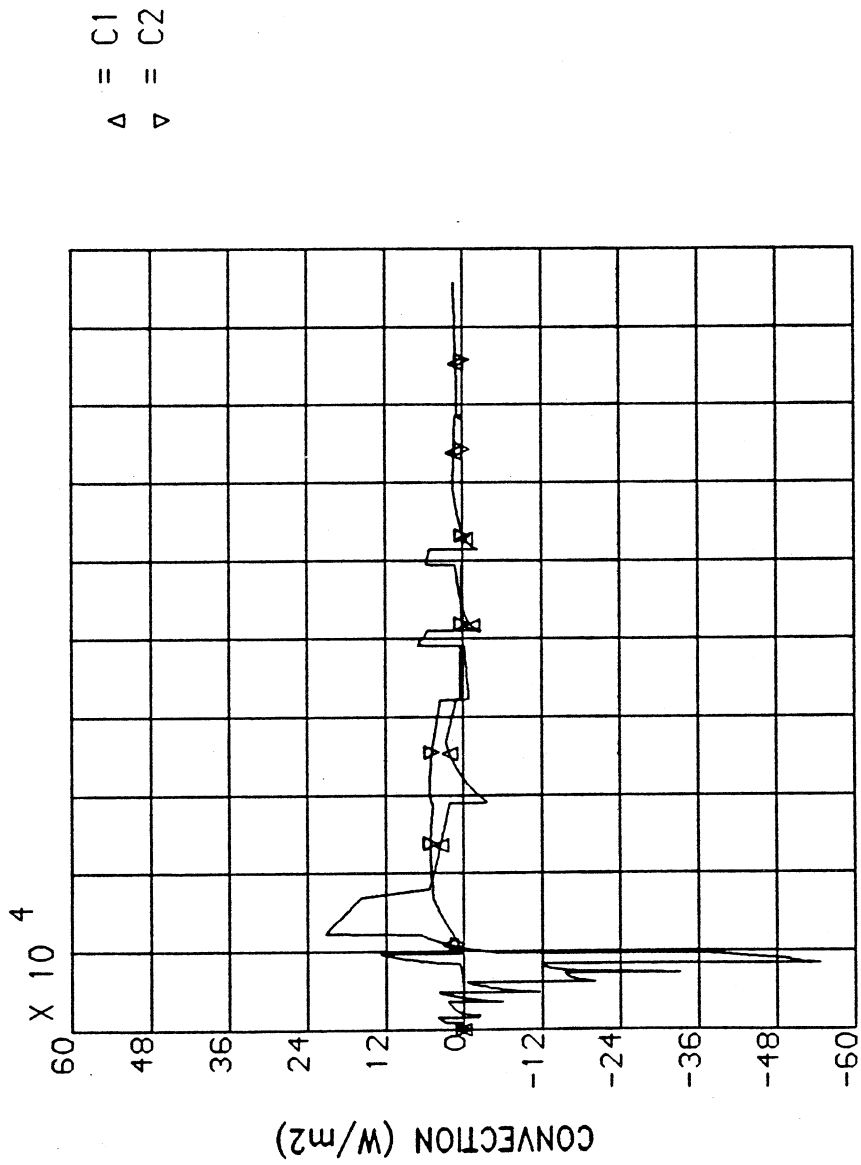
DEPTH



RUNBY : USER
 TIME: 16:23:39
 CASE NO: 1
 DATE: 24-JAN-88

RADIATION COEFFICIENT VARIATION

DEPTH



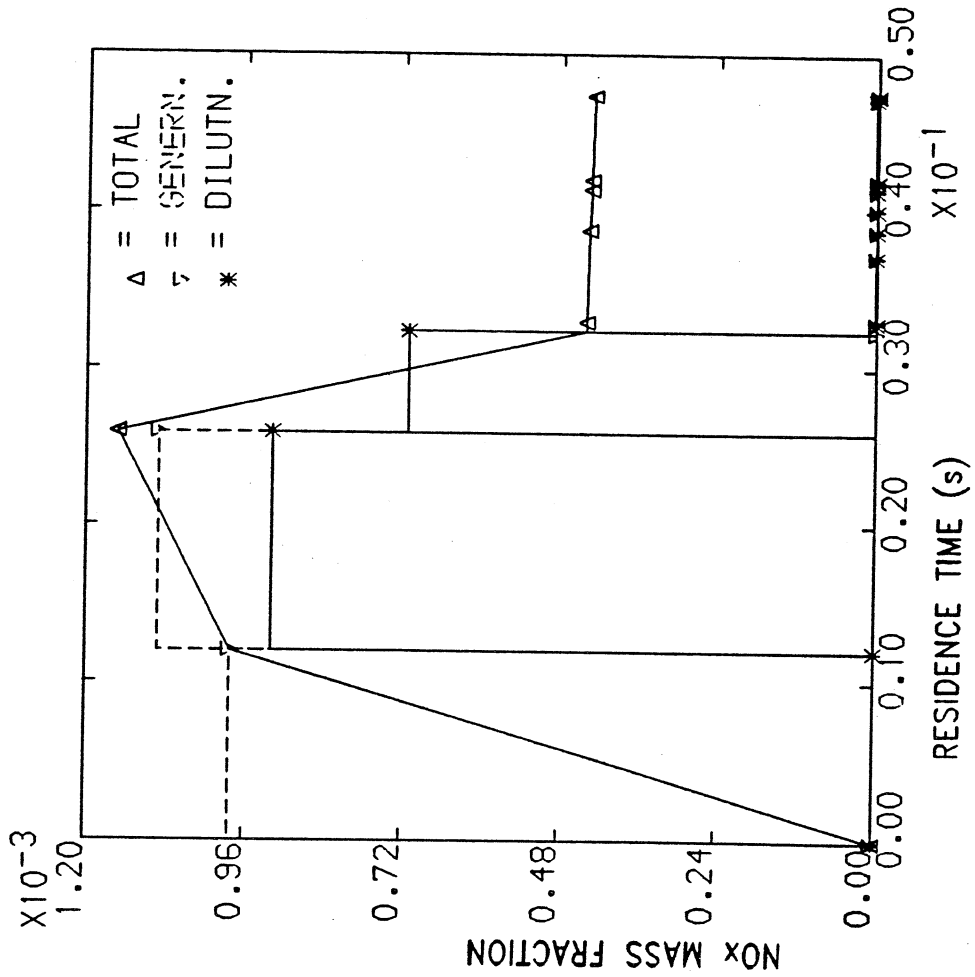
LINER LENGTH (cm)

RUNBY : USER
TIME: 16:23:39
CASE NO: 1
DATE: 24-JAN-88

CONVECTION COEFFICIENT VARIATION

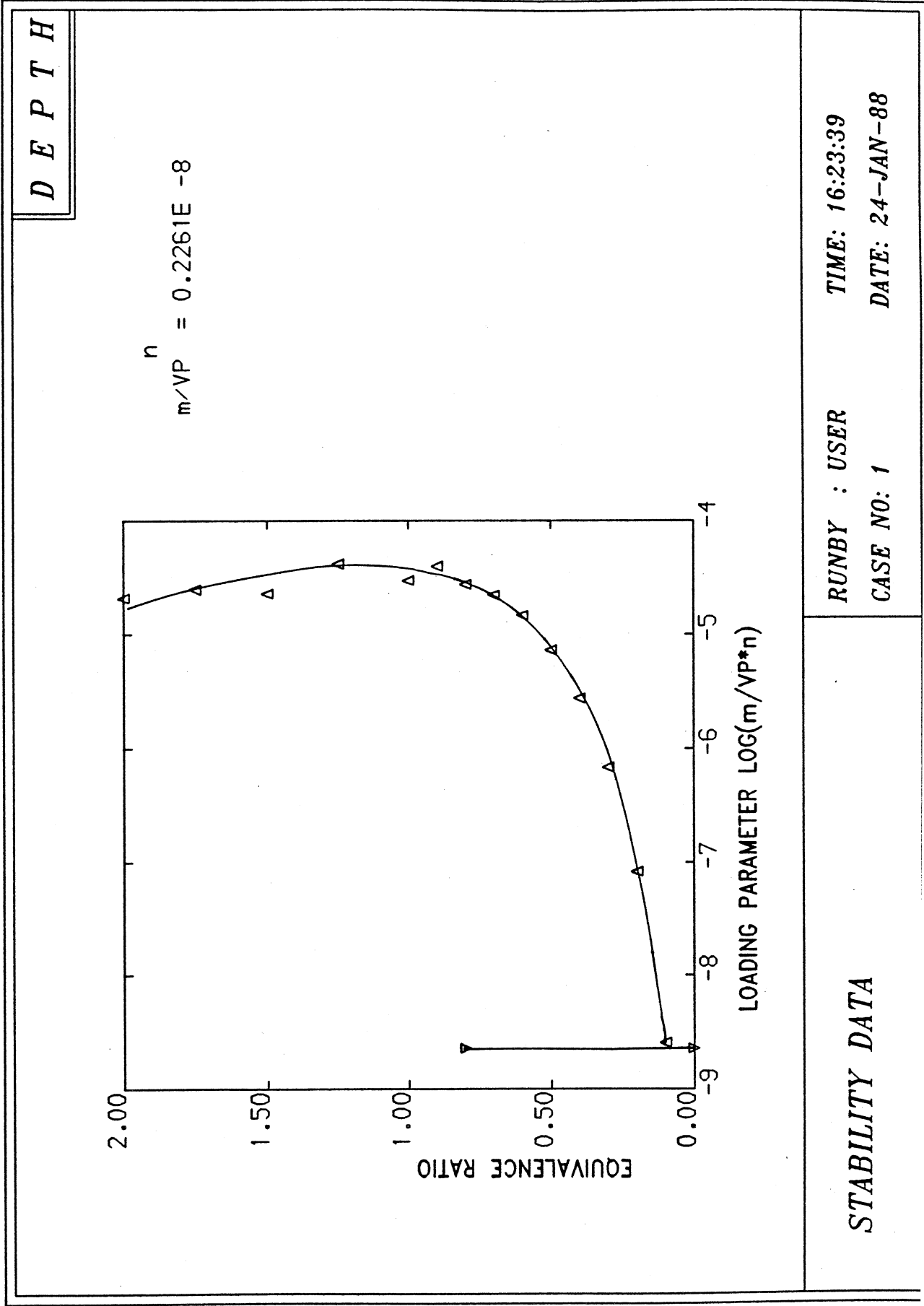
D E P T H

$\text{PHI}_{\text{mean}} = 0.92$, $\text{Pin} = 1.14 \text{ MPa}$
 $\text{MIXEDNES} = 0.20$, $\text{Tin} = 601.0 \text{ K}$
 $\text{EMI. INDEX} = 37.364 \text{ g/Kg Fuel}$
 $\text{NOx CONC.} = 431.8 \text{ PPMw}$
 $= 226.8 \text{ PPMv}$



NOx DATA

RUNBY : USER **TIME: 16:23:39**
CASE NO: 1 **DATE: 24-JAN-88**



INPUT FOR PRELIMINARY DESIGN

```
'SPEC'  
45.0  
1621200.0  
695.0  
1240.  
4.00  
20.0  
'GEOM'  
0.23  
0.0298  
'TYPE'  
3  
1  
12.864  
23.936  
0.  
0.  
1  
1  
1  
1  
'END'
```

OUTPUT

Case No : 2 DATE : 24-JAN-88

Run By : USER TIME : 19:31:56

BLOCK NUMBER AT LAST TERMINATION = 13

TYPE				BLOCK: 2		
SINO	1	2	3	4		
TYPE	CHAMBER	DIFFUSER	INJECTOR	APPLICATION		
	3	TUBOANNULAR	1	PRESSURE ATOMISER	1	GROUND
5) FUEL:						
6) OXIDANT: (mole fractions)						
1) 5 DIESEL	Molecular Wt : 28.9640					
2) C	1) Sp Humidity: 0.0000					
12.86400	23.93600	0.00000	0.00000	(fraction of inlet air)		
3) L C V	44.3000	(MJ/kg)	N2	0.7809		
4) AFRS	14.5870	-	2) O2	0.2095		
5) Fuel temp	300.0000	K	3) AR	0.0093		
6) Enthalpy Fuel	-300.0000	(kJ/mole)	4) CO	0.0000		
at TTF			5) H2O	0.0000		
Molecular Wt	178.6400		6) CH4	0.0000		
Sp. Gravity	0.8700		7) CO2	0.0003		
			8) H2	0.0000		
DESIGN SPECIFICATIONS						
BLOCK: 3						
1) Mass Flow	W2 = 45.000	(kg/s)	4) O P L	= 4.000 (%)		
2) Tot. Press	PT2 = 1621200.0	(N/m2)	5) P L F	= 20.000 (-)		
3) Tot. Temp	TT2 = 695.0	(K)	6) Tot. Temp	TT8 = 1240.0	(K)	
COMBUSTOR INLET PLANE						
COMBUSTOR EXIT PLANE						
7) Ref Rad	RREF2 = 0.23000	(m)	Ref Rad	RREF8 = 0.25972	(m)	
8) Channel Ht	HT2 = 0.02980	(m)	Channel Ht	HT8 = 0.04400	(m)	
Inlet Area	A2 = .43065E-01	(m2)	9) Exit Area	A8 = .61600E-01	(m2)	
Inlet Mach No	MN2 = 0.2561	(-)	10) Exit Mach No	MN8 = 0.2289	(-)	

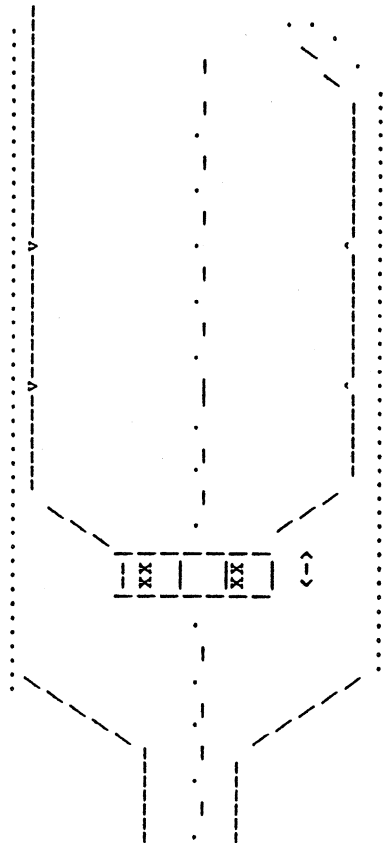
BLOCK: 4

REFERENCE AREA					
SLNO->	REF	HT	AR	A	DL
	1	2	3	4	6
1	0.23000	0.02980	1.0000	.43065E-01	0.00000
2	0.23000	0.13790	4.6275	.19928E+00	0.07000
3	0.23000	0.13790	4.6275	.19928E+00	0.00000
4	0.23000	0.13790	4.6275	.19928E+00	0.00000
5	0.23000	0.13790	4.6275	.19928E+00	0.00000

BLOCK: 5

COMBUSTOR SIZING	
1) FLAMETUBE WIDTH	DFT= 0.10343(m)
2) DIFFUSER LENGTH	DL = 0.07000(m)
3) DIFFUSER TO DOME LENGTH	DDL= 0.01379(m)
4) DOME LENGTH	DML= 0.03310(m)
5) PRIMARY ZONE LENGTH	PZL= 0.08274(m)
6) SECONDARY ZONE LENGTH	SZL= 0.04137(m)
7) DILUTION ZONE LENGTH	DZL= 0.14480(m)
8) NOZZLE LENGTH	ZNL= 0.06205(m)
9) COMBUSTOR LENGTH	CCL= 0.41475(m)
10) FLAME TUBE EXIT WIDTH	DFT8= 0.04400(m)
11) NUMBER OF TUBES	NTUBE= 10

COMBUSTOR GEOMETRY (not to scale)



DL	DDL	PZL	SZL	DZL	ZNL
<----->	<----->	<----->	<----->	<----->	<----->
0.07000	0.01379	0.08274	0.04137	0.14480	0.06205

SWID		BLOCK: 7	
1)DSW	= 0.02500(m)	4)No of Vanes	= 10
2)DHUB	= 0.01000(m)	5)Vane Angle	= 60.0
3)Swirler Length	= 0.01400(m)	6)Swirler Area	= .41233E-03(m2)
7)No. Injectors	= 10	1)PRESSURE ATOMISER	
8)DATM1	= 0.00000(m)	10)Atomiser area	= .00000E+00(m2)
9)DATM2	= 0.00000(m)	11)CD atomiser	= 0.00000

GENERAL DATA :

GEOMETRY : (1 15)

SL NO ->	(1)	(2)	(3)	(4)	(5)	
SLOT NO	DIST	CASING HGT	CASING WPTH	LINER HGT	LINER WIDTH	LINER WPTH HOR
1	0.00000	0.29895	0.13790	0.24250	0.02500	0.02500
2	0.00700	0.29895	0.13790	0.24954	0.03908	0.03908
3	0.02605	0.29895	0.13790	0.26971	0.07941	0.07941
4	0.03900	0.29895	0.13790	0.28172	0.10343	0.10343
5	0.04105	0.29895	0.13790	0.28172	0.10343	0.10343
6	0.05810	0.29895	0.13790	0.28319	0.10639	0.10639
7	0.08274	0.29895	0.13790	0.28172	0.10343	0.10343
8	0.09616	0.29895	0.13790	0.28172	0.10343	0.10343
9	0.12411	0.29895	0.13790	0.28172	0.10343	0.10343
10	0.15000	0.29895	0.13790	0.28172	0.10343	0.10343
11	0.19908	0.29895	0.13790	0.28172	0.10343	0.10343
12	0.22513	0.29895	0.13790	0.28328	0.10656	0.10656
13	0.26891	0.29895	0.13790	0.28172	0.10343	0.10343
14	0.29023	0.29895	0.13483	0.28172	0.08300	0.11600
15	0.33096	0.29895	0.12896	0.28172	0.04400	0.14000

SLOT DETAILS : (0 15 2)

SLOT NO	POSTI (m)	TYPE	SIGN +/-	STATIONS	RES. TIME (sec)
1	0.00000	D 6C	*	1	0.0000E+00
2	0.00700	C 1C	+	2	0.4179E-04
3	0.02605	C 1C	+	2	0.2856E-03
4	0.03900	A 0C	*	1	0.5408E-03
5	0.04105	C 1C	+	2	0.5850E-03
6	0.05810	C 1C	+	2	0.9358E-03
7	0.08274	M 6C	*	1	0.1388E-02
8	0.09616	C 3C	-	3	0.1573E-02
9	0.12411	M 6C	*	1	0.1918E-02
10	0.15000	C 4C	-	4	0.2174E-02
11	0.19908	C 3C	+	3	0.2549E-02
12	0.22513	C 3C	+	3	0.2762E-02
13	0.26891	A 0R	*	1	0.3232E-02
14	0.29023	C 3R	-	3	0.3443E-02
15	0.33096	E 3R	*	1	0.3753E-02

SLOT FLOWS : (0 15 2)

SLOT NO	NO	POSTI (m)	HT (m)	DIA (m)	DIA2 (m)	NO	AREA (m2)	FRACTION	CD	EFF. AREA (m2)	FLOW (kg/s)	% FLOW	Ymax/Dft	PHI deg
1	1	0.00000	0.00000	0.00550	0.00550	12	.28510E-03	0.0000	0.7000	.00000E+00	0.3193	7.0947	0.00000	0.00
2	1	0.00000	0.00100	0.00000	0.00000	120	.13533E-03	0.3235	0.7900	.34586E-04	0.0369	0.8192	0.00000	0.00
2	1	0.01000	0.00100	0.00000	0.00000	120	.19360E-03	0.0000	0.0000	.00000E+00	0.0369	0.8192	0.00000	0.00
3	1	0.00000	0.00100	0.00000	0.00000	120	.26204E-03	0.4235	0.7900	.87673E-04	0.0787	1.7490	0.00000	0.00
3	1	0.01000	0.00100	0.00000	0.00000	120	.30818E-03	0.0000	0.0000	.00000E+00	0.0787	1.7490	0.00000	0.00
4	1	0.00000	0.00000	0.00000	0.00000	120	.00000E+00	1.0000	0.0000	.00000E+00	0.0000	0.0000	0.00000	0.00
5	1	0.00000	0.00150	0.00000	0.00000	120	.50861E-03	0.5592	0.7900	.22467E-03	0.2008	4.4618	0.00000	0.00
5	1	0.01000	0.00150	0.00000	0.00000	120	.50021E-03	0.0000	0.0000	.00000E+00	0.2008	4.4618	0.00000	0.00
6	1	0.00000	0.00100	0.00000	0.00000	120	.34680E-03	0.4407	0.7900	.12075E-03	0.1103	2.4511	0.00000	0.00
6	1	0.01000	0.00100	0.00000	0.00000	120	.33665E-03	0.0000	0.0000	.00000E+00	0.1103	2.4511	0.00000	0.00
7	1	0.00000	0.00000	0.01200	0.01200	12	.13572E-02	1.0000	0.5886	.79883E-03	0.7403	16.4511	0.28204	70.57
8	1	0.00000	0.00100	0.00000	0.00000	0	.32179E-03	0.0000	0.0000	.00000E+00	0.0000	0.0000	0.00000	0.00
8	1	0.00500	0.00100	0.00180	0.00180	100	.32179E-03	0.7908	0.6000	.15268E-03	0.1534	3.4092	0.00000	0.00
8	1	0.02000	0.00100	0.00000	0.00000	0	.32179E-03	0.0000	0.0000	.00000E+00	0.1534	3.4092	0.00000	0.00

9	1	0.00000	0.00000	0.01800	0.01800	10	.25447E-02	1.0000	0.6069	.15443E-02	1.5193	33.7629	0.28989	76.56
10	1	0.00000	0.00100	0.00000	0.00000	0	.32179E-03	0.0000	0.0000	.00000E+00	0.0000	0.0000	0.00000	0.00
10	1	0.00500	0.00200	0.00180	0.00180	100	.63730E-03	0.3993	0.6000	.15268E-03	0.1850	4.1113	0.00000	0.00
10	1	0.01750	0.00200	0.00180	0.00180	120	.63730E-03	0.4791	0.6000	.18322E-03	0.2214	4.9205	0.00000	0.00
10	1	0.03000	0.00200	0.00000	0.00000	0	.63730E-03	0.0000	0.0000	.00000E+00	0.4064	9.0319	0.00000	0.00
11	1	0.00000	0.00100	0.00000	0.00000	0	.33750E-03	0.0000	0.0000	.00000E+00	0.0000	0.0000	0.00000	0.00
11	1	0.00500	0.00100	0.00180	0.00180	125	.33597E-03	0.9468	0.6000	.19085E-03	0.2328	5.1731	0.00000	0.00
11	1	0.01500	0.00100	0.00000	0.00000	0	.33412E-03	0.0000	0.0000	.00000E+00	0.2328	5.1731	0.00000	0.00
12	1	0.00000	0.00100	0.00000	0.00000	0	.34733E-03	0.0000	0.0000	.00000E+00	0.0000	0.0000	0.00000	0.00
12	1	0.00500	0.00100	0.00180	0.00180	100	.34337E-03	0.7411	0.6000	.15268E-03	0.1767	3.9279	0.00000	0.00
12	1	0.02000	0.00100	0.00000	0.00000	0	.33567E-03	0.0000	0.0000	.00000E+00	0.1767	3.9279	0.00000	0.00
13	1	0.00000	0.00000	0.00000	0.00000	0	.00000E+00	1.0000	0.0000	.00000E+00	0.0000	0.0000	0.00000	0.00
14	1	0.00000	0.00100	0.00000	0.00000	0	.25761E-03	0.0000	0.0000	.00000E+00	0.0000	0.0000	0.00000	0.00
14	1	0.00500	0.00100	0.00180	0.00180	100	.23716E-03	1.0730	0.6000	.15268E-03	0.1853	4.1181	0.00000	0.00
14	1	0.02000	0.00100	0.00000	0.00000	0	.19745E-03	0.0000	0.0000	.00000E+00	0.1853	4.1181	0.00000	0.00
15	1	0.00000	0.00000	0.00000	0.00000	0	.00000E+00	1.0000	0.0000	.00000E+00	0.0000	0.0000	0.00000	0.00

TOTAL EFFECTIVE HOLE AREA = 0.40074E-02 (m2)

MATERIAL SPECIFICATIONS:

SL. NO.	LINER	CASING	COATING	N
	1	2	3	
MATERIAL	2 NIMONIC 90	1 ALUMINIUM ALLOY	0 *****	
EMISSIVITY	.70000E+00	.40000E+00	.00000E+00	
CONDUCTIVITY	.25000E+02	.80000E+02	.00000E+00	
THICKNESS	.15000E-02	.20000E-02	.00000E+00	

ITERATION = 3	NO OF CONTROL VOLUMES = 325
LINER = 4.565 (Kg/s)	ANNULUS = 0.009 (Kg/s)
OPL CALCULATED = 5.741 %	OPL EXPECTED = 4.000 %
PLF CALCULATED = 28.715	PLF EXPECTED = 20.000
PATTERN FACTOR = 0.195604	

EXIT PLANE COMPOSITION: (mole fractions)

Molecular Weight	: 28.9760
N2	: 0.7697
O2	: 0.1615
AR	: 0.0092
CO	: 0.0000
H2O	: 0.0286
CH4	: 0.0000
CO2	: 0.0310
H2	: 0.0000

STABILITY DATA

SL NO	Equ. Rat.	m/VP**n
1	0.1	0.15699E-07
2	0.2	0.24007E-06
3	0.3	0.14162E-05
4	0.4	0.48036E-05
5	0.5	0.11520E-04
6	0.6	0.21791E-04
7	0.7	0.32869E-04
8	0.8	0.41052E-04
9	0.9	0.43857E-04
10	1.0	0.43857E-04
11	1.3	0.28367E-04
12	1.5	0.38742E-04
13	1.8	0.38634E-04
14	2.0	0.33274E-04
Loading Parameter		0.26350E-07

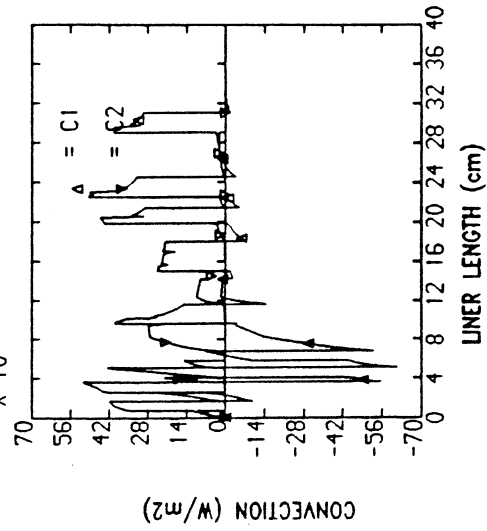
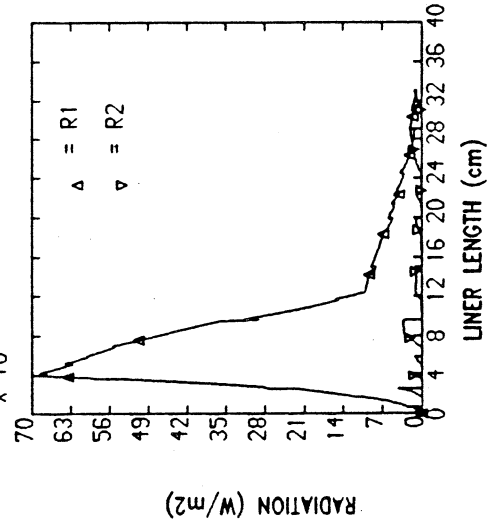
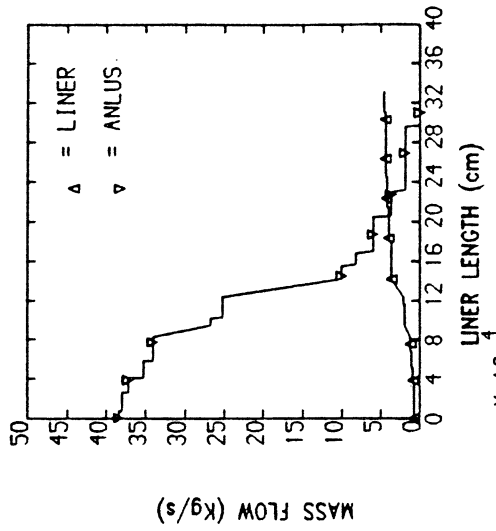
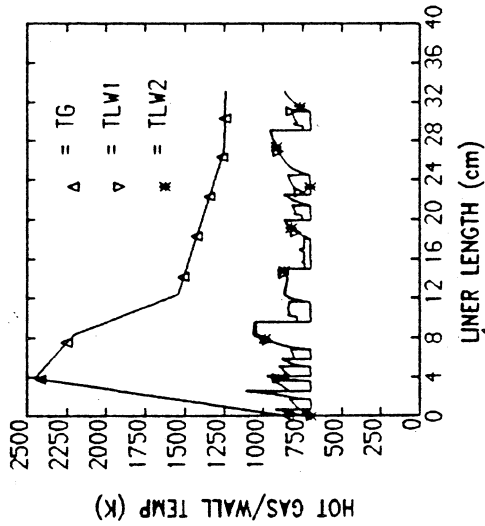
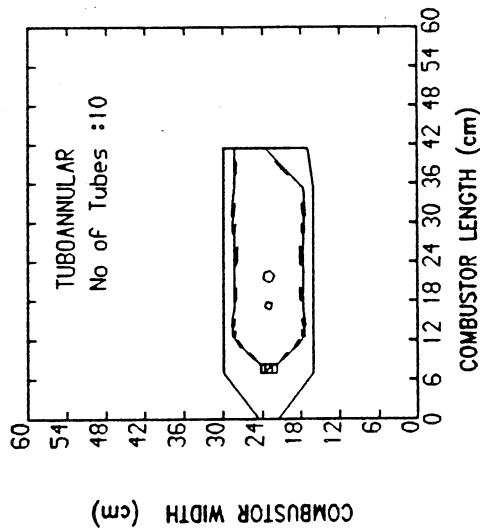
NOX DATA (mass fraction)						
Res. Time (sec)	Eq. Rat. (-)	Temp (K)	GENERATION (-)	DILUTION (-)	TOTAL (-)	TOTAL (-)
0.0000E+00	0.0000	0.0	0.0000E+00	0.0000E+00	0.0000E+00	0.0000E+00
0.13878E-02	0.9549	2231.0	0.39757E-03	0.0000E+00	0.39757E-03	0.39757E-03
0.15728E-02	0.8028	2007.2	0.74381E-04	-0.68812E-04	0.40314E-03	0.40314E-03
0.19184E-02	0.4858	1540.8	0.26640E-04	-0.19831E-03	0.23147E-03	0.23147E-03
0.21736E-02	0.4388	1488.6	0.22097E-07	-0.23536E-04	0.20795E-03	0.20795E-03
0.25490E-02	0.3497	1389.7	0.96764E-08	-0.47005E-04	0.16096E-03	0.16096E-03
0.27621E-02	0.3024	1337.2	0.16728E-09	-0.23350E-04	0.13761E-03	0.13761E-03
0.32319E-02	0.2229	1248.9	0.21588E-10	-0.41648E-04	0.95960E-04	0.95960E-04
0.34425E-02	0.2197	1245.9	0.10163E-11	-0.13682E-05	0.94591E-04	0.94591E-04
0.37530E-02	0.2137	1240.0	0.11672E-11	-0.26312E-05	0.91960E-04	0.91960E-04

NOX AT EXIT PLANE			
MASS FRACTION (Kg/Kg)	PPMw (weight)	PPMv (volume)	EMISSION INDEX (g/Kg fuel)
0.91960E-04	92.0	48.5	6.369

NOx EQUILIBRIUM DATA

EQ RAT (-)	DENSITY (Kg/m ³)	TEMP (K)	k1 (-)	k2 (-)	R1 (see text for units)	R6 (NO)eq
0.0000	0.00837	706.0	0.4985E-03	0.1332E+01	0.3068E-34	0.9089E-29
0.1000	0.00638	960.5	0.4705E-02	0.1314E+01	0.7267E-25	0.2229E-21
0.2000	0.00512	1196.3	0.2231E-01	0.1260E+01	0.5283E-19	0.6164E-17
0.3000	0.00433	1416.2	0.6135E-01	0.1164E+01	0.2478E-15	0.3602E-14
0.4000	0.00378	1621.9	0.1260E+00	0.1031E+01	0.7927E-11	0.2671E-12
0.5000	0.00338	1815.0	0.2144E+00	0.8750E+00	0.5094E-11	0.5701E-11
0.6000	0.00307	1996.4	0.3133E+00	0.7083E+00	0.1143E-09	0.5295E-10
0.7000	0.00283	2165.7	0.3944E+00	0.5401E+00	0.1209E-08	0.2644E-09
0.8000	0.00264	2320.2	0.4246E+00	0.3767E+00	0.6918E-08	0.7655E-09
0.9000	0.00249	2450.8	0.3901E+00	0.2239E+00	0.2135E-07	0.1201E-08
1.0000	0.00240	2535.0	0.3042E+00	0.9634E-01	0.2860E-07	0.7501E-09
1.1000	0.00237	2536.4	0.2028E+00	0.2537E-01	0.1149E-07	0.1211E-09
1.2000	0.00239	2473.5	0.1329E+00	0.5763E-02	0.2124E-08	0.9298E-11
1.3000	0.00242	2393.4	0.9273E-01	0.1489E-02	0.3367E-09	0.6938E-12
1.4000	0.00247	2311.3	0.6816E-01	0.4322E-03	0.5240E-10	0.5553E-13
1.5000	0.00251	2230.6	0.5201E-01	0.1355E-03	0.8062E-11	0.4645E-14
1.6000	0.00256	2152.1	0.4072E-01	0.4453E-04	0.1214E-11	0.3939E-15
1.7000	0.00261	2075.8	0.3248E-01	0.1501E-04	0.1759E-12	0.3286E-16
1.8000	0.00267	2001.7	0.2625E-01	0.5105E-05	0.2422E-13	0.2633E-17
1.9000	0.00273	1929.7	0.2139E-01	0.1725E-05	0.3121E-14	0.1981E-18
2.0000	0.00279	1859.5	0.1752E-01	0.5729E-06	0.3715E-15	0.1369E-19
2.1000	0.00286	1791.1	0.1440E-01	0.1846E-06	0.4032E-16	0.8525E-21
2.2000	0.00292	1724.3	0.1184E-01	0.5716E-07	0.3923E-17	0.4670E-22
2.3000	0.00300	1659.1	0.9713E-02	0.1679E-07	0.3369E-18	0.2199E-23
2.4000	0.00308	1595.3	0.7949E-02	0.4615E-08	0.2504E-19	0.8631E-25
2.5000	0.00316	1533.0	0.6481E-02	0.1169E-08	0.1580E-20	0.2739E-26
2.6000	0.00325	1472.5	0.5265E-02	0.2687E-09	0.8364E-22	0.6818E-28
2.7000	0.00334	1415.5	0.4287E-02	0.5674E-10	0.3921E-23	0.1395E-29
2.8000	0.00343	1367.9	0.3589E-02	0.1261E-10	0.2239E-24	0.3387E-31
2.9000	0.00350	1337.0	0.3201E-02	0.3904E-11	0.2704E-25	0.1961E-32
3.0000	0.00354	1320.7	0.3031E-02	0.1772E-11	0.7266E-26	0.3015E-33
3.1000	0.00357	1312.7	0.2975E-02	0.1029E-11	0.3215E-26	0.8621E-34
3.2000	0.00359	1309.1	0.2978E-02	0.6869E-12	0.1881E-26	0.3498E-34

DEPTH

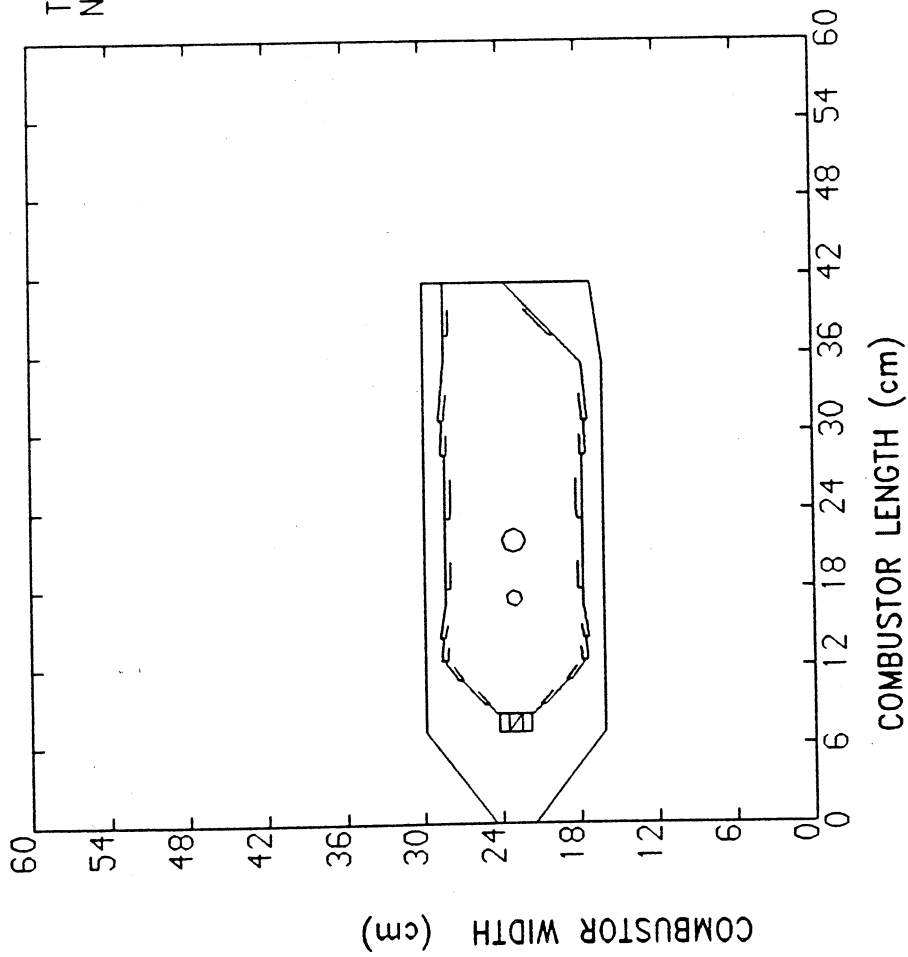


COMBUSTOR DATA

RUNBY : USER TIME: 19:31:56
 CASE NO: 2 DATE: 24-JAN-88

D E P T H

TUBOANNULAR
No of Tubes :10

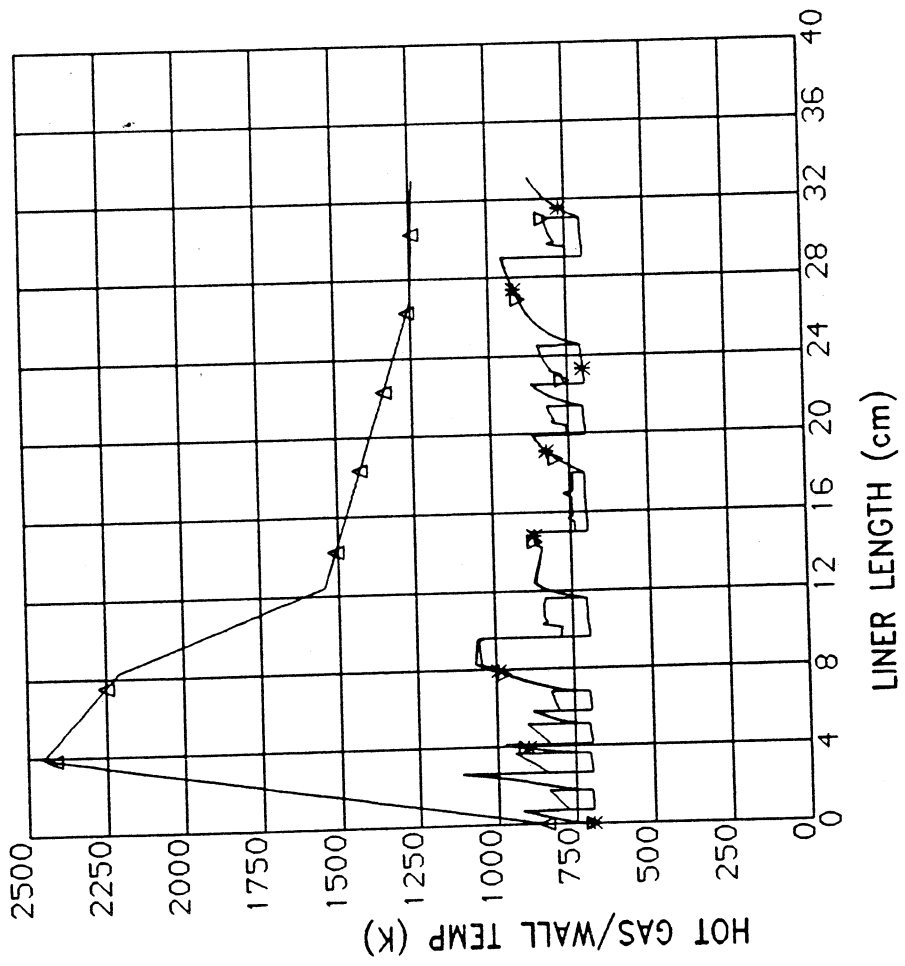


RUNBY : USER TIME: 19:31:56
CASE NO: 2 DATE: 24-JAN-88

COMBUSTOR GEOMETRY

D E P T H

Δ = TG
 ▽ = TLW1
 * = TLW2

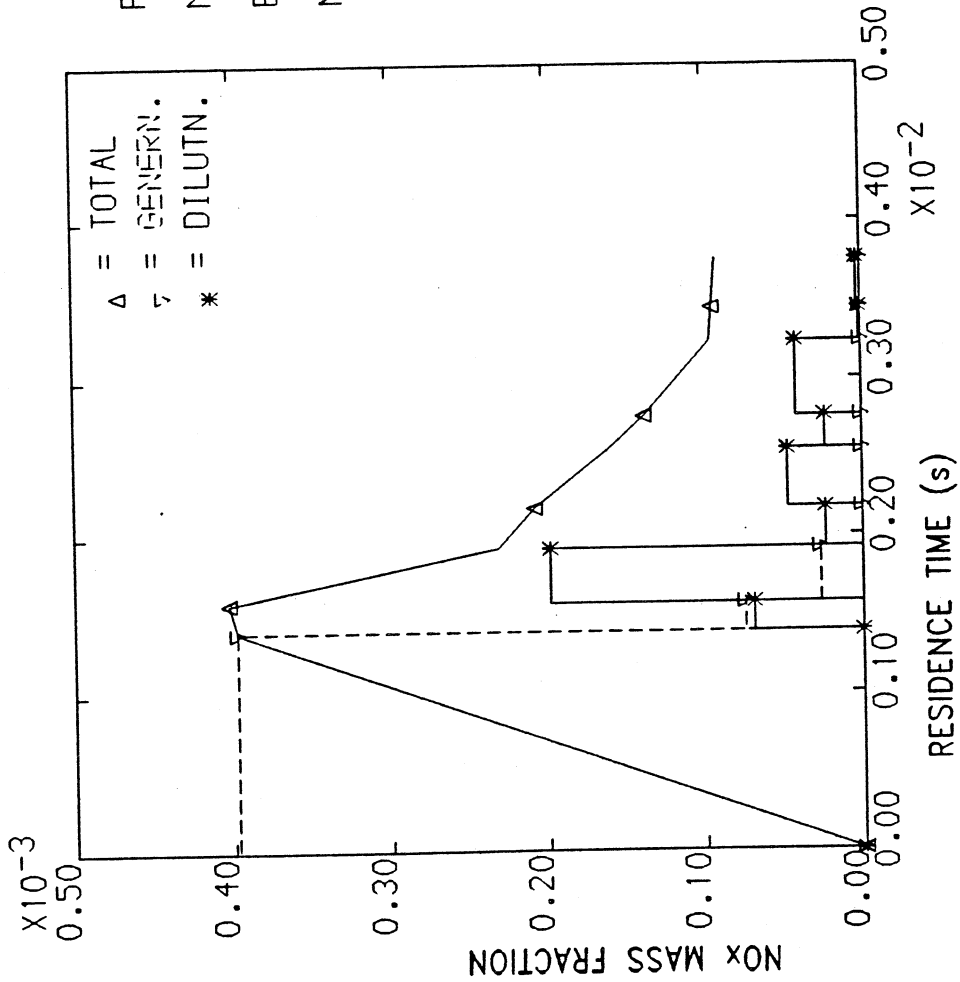


RUNBY : USER TIME: 19:31:56
 CASE NO: 2 DATE: 24-JAN-88

TEMPERATURE VARIATION

D E P T H

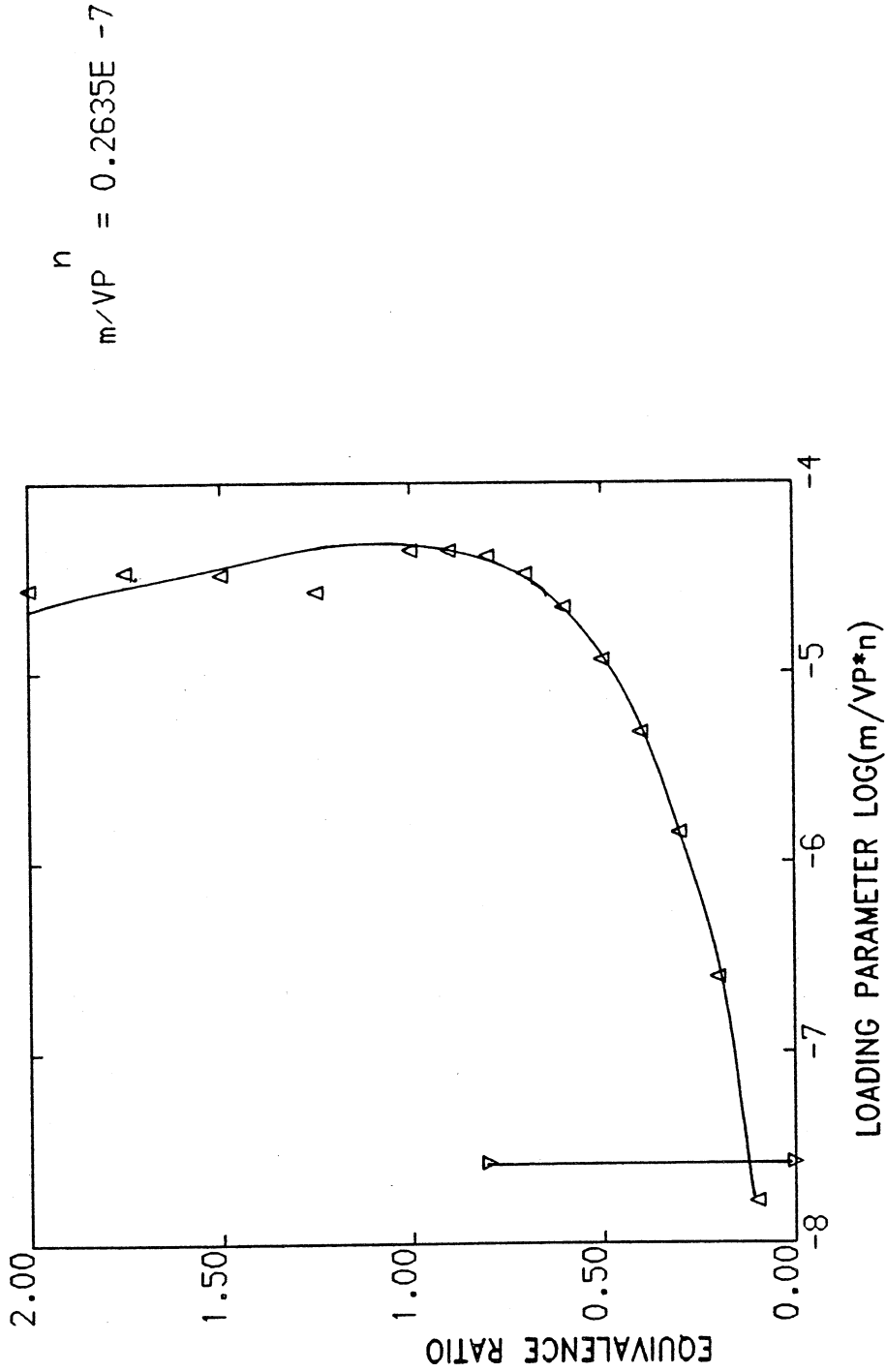
$\text{PHI}_{\text{mean}} = 0.95$, $P_{\text{in}} = 1.62 \text{ MPa}$
 $\text{MIXEDNES} = 0.20$, $T_{\text{in}} = 695.0 \text{ K}$
 $\text{EMI. INDEX} = 6.369 \text{ g/Kg fuel}$
 $\text{NOx CONC.} = 92.0 \text{ PPMw}$
 $= 48.5 \text{ PPMv}$



RUNBY : USER **TIME: 19:31:56**
CASE NO: 2 **DATE: 24-JAN-88**

NOx DATA

DEPTH



RUNBY : USER TIME: 19:31:56
CASE NO: 2 DATE: 24-JAN-88

STABILITY DATA

INPUT FOR PRELIMINARY DESIGN

```
'SPEC'  
2.0  
363700.0  
453.0  
1100.0  
8.5  
35.0  
'GEOM'  
0.0685  
0.013  
'TYPE'  
1  
1  
12.5  
24.4  
0  
0  
2  
1  
1  
1  
←  
'END'
```

INPUT FOR PERFORMANCE EVALUATION

```

'MATRL'
2,1,0.001,0.001
'COAT'
'N',1,0
'GIVEN'
0,13,3
'SLOTS'
0,'D',0,'C','*',1
0,0,0,0,0
0,0,0,0,0
0,0,0,0,0
0.01328,'A',1,'C','*',1
0,0,0,0,0
0,0,0,0,0
0.021,'M',7,'C','*',1
0,0,0.008,0.008,12,0
0,0,0.008,0.008,12,0
0.0515,'M',6,'C','*',1
0,0,0.003,0.003,26,0
0,0,0.003,0.003,26,0
0.0755,'M',6,'C','*',1
0,0,0.003,0.003,26,0
0,0,0.003,0.003,26,0
0.0935,'M',7,'C','*',1
0,0,0.013,0.013,12,0
0,0,0.013,0.013,12,0
0.1125,'M',6,'C','*',1
0,0,0.003,0.003,26,0
0,0,0.003,0.003,26,0
0.1245,'M',6,'C','*',1
0,0,0.003,0.003,26,0
0,0,0.003,0.003,26,0
0.1365,'M',6,'C','*',1
0,0,0.003,0.003,26,0
0,0,0.003,0.003,26,0
0.144,'A',0,'C','*',1
0,0,0,0,0
0,0,0,0,0
0.15125,'M',6,'C','*',1
0,0,0,0,0
0,0,0.0035,0.0035,26,0
0.1615,'A',0,'C','*',1
0,0,0.00,0.0,0
0.17000,'E',0,'C','*',1
0,0,0.00,0.0,0
0,0,0.00,0.0,0

```

```
'GEOM'  
13  
0.09900 0.06200 0.09050 0.04150 0.04150 0.04150  
0.09900 0.06700 0.09050 0.04150 0.04150 0.04150  
0.09900 0.06700 0.09050 0.04150 0.04150 0.04150  
0.09900 0.06700 0.09050 0.04150 0.04150 0.04150  
0.09900 0.06700 0.09050 0.04150 0.04150 0.04150  
0.09900 0.06700 0.09050 0.04150 0.04150 0.04150  
0.09900 0.06700 0.09050 0.04150 0.04150 0.04150  
0.09900 0.06700 0.09050 0.04150 0.04150 0.04150  
0.09900 0.06700 0.09050 0.04150 0.04150 0.04150  
0.09900 0.05100 0.08900 0.03500 0.03500 0.03500  
0.09900 0.05100 0.08650 0.02850 0.02850 0.02850  
0.09900 0.05100 0.08650 0.02850 0.02850 0.02850  
'END'
```

OUTPUT

Case No : 3B
 DATE : 24-JAN-88
 Run By : USER
 TIME : 19:08:37
 BLOCK NUMBER AT LAST TERMINATION = 12

BLOCK: 2			
TYPE	1	2	3
CHAMBER			
DIFFUSER			
INJECTOR			
APPLICATION			3 AIR <30K
1 ANNULAR		2 DUMP	1 PRESSURE ATOMISER

BLOCK: 2	
5) FUEL:	6) OXIDANT: (mole fractions)
1) 1 AVTUR	Molecular Wt : 28.9640
2) C	1) Sp Humidity: 0.0000
12.50000 24.40000 0.00000 0.00000	(fraction of inlet air)
3) L C V	N2 0.7809
4) AFRs	2) O2 0.2095
5) Fuel temp TTF	3) AR 0.0093
6) Enthalpy Fuel at TTF	4) CO 0.0000
Molecular Wt	5) H2O 0.0000
Sp. Gravity	6) CH4 0.0000
	7) CO2 0.0003
	8) H2 0.0000

BLOCK: 3			
DESIGN SPECIFICATIONS			
1) Mass Flow W2 = 2.000 (kg/s)	4) O P L = 8.500 (%)		
2) Tot. Press PT2 = 363700.0 (N/m2)	5) P L F = 35.000 (-)		
3) Tot. Temp TT2 = 453.0 (K)	6) Tot. Temp TT8 = 1100.0 (K)		
COMBUSTOR INLET PLANE		COMBUSTOR EXIT PLANE	
7) Ref Rad RREF2 = 0.06850 (m)	Ref Rad RREF8 = 0.07225 (m)		
8) Channel Ht HT2 = 0.01300 (m)	Channel Ht HT8 = 0.02850 (m)		
Inlet Area A2 = .55952E-02 (m2)	9) Exit Area A8 = .12938E-01 (m2)		
Inlet Mach No MN2 = 0.3192 (-)	10) Exit Mach No MN8 = 0.2435 (-)		

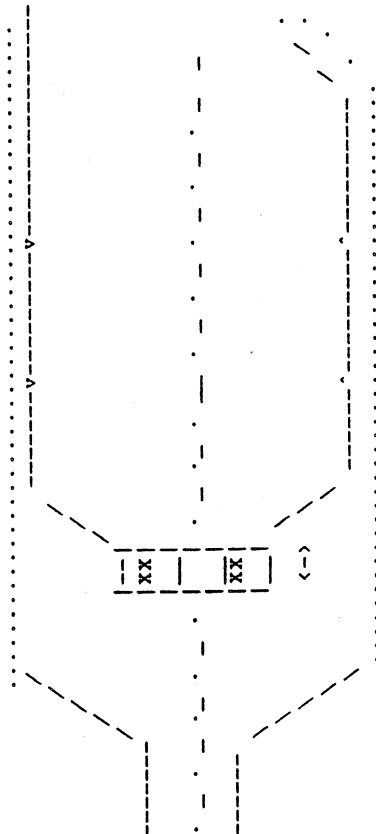
BLOCK: 4

REFERENCE AREA					
SLNO->	RRF	HT	AR	A	DL
	1	2	3	4	6
PLANE					
1	0.06850	0.01300	1.0000	.55952E-02	0.0000
2	0.06850	0.01900	1.4615	.81776E-02	0.02200
3	0.06850	0.02400	1.8462	.10330E-01	0.01600
4	0.06850	0.03050	2.3462	.13127E-01	0.00900
5	0.07200	0.05400	4.3661	.24429E-01	0.01700

BLOCK: 5

COMBUSTOR SIZING	
1) FLAMETUBE WIDTH	DFT= 0.04150(m)
2) DIFFUSER LENGTH	DL = 0.06400(m)
3) DIFFUSER TO DOME LENGTH	DDL= 0.02580(m)
4) DOME LENGTH	DML= 0.01328(m)
5) PRIMARY ZONE LENGTH	PZL= 0.02100(m)
6) SECONDARY ZONE LENGTH	SZL= 0.07250(m)
7) DILUTION ZONE LENGTH	DZL= 0.05050(m)
8) NOZZLE LENGTH	ZNL= 0.02600(m)
9) COMBUSTOR LENGTH	CCL= 0.25980(m)
10) FLAME TUBE EXIT WIDTH	DFTS= 0.02850(m)
11) NUMBER OF TUBES	NTUBE= 1

COMBUSTOR GEOMETRY (not to scale)



DL	DDL	PZL	SZL	DZL	ZNL
<----->	<----->	<----->	<----->	<----->	<----->
0.06400	0.02580	0.02100	0.07250	0.05050	0.02600

% MASS FLOW SPLITS		(sec)		(dil)		(kg/s/tube)	
62.87		16.08	46.79				
27.00	MIXING	0.00	8.40	15.05	3.55		
10.07	10.07(1SWRL) [x]						
	0.00(-1ATOM)	2.36	0.69	0.25	0.24	F = 0.032	
	0.00(-1DOME) [x]						
0.00	COOLING						
99.94		0.00	0.00	0.00	0.00		
MASS FLOW SPLITS							
1.257		0.322	0.936				
0.540	MIXING	0.00	0.168	0.301	0.071		
0.201	0.201(1SWRL) [x]						
	0.000(-1ATOM)	2.36	0.69	0.25	0.24	F = 0.032	
	0.000(-1DOME) [x]						
0.000	COOLING						
1.999		0.000	0.000	0.000	0.000		
MASS FLOW SPLITS							
	PZL	SZL	DZL	ZNL			
I	EFF(1)	EFF(2)	EFF(3)	EFF(4)	I		
I	PHI(1)	PHI(2)	PHI(3)	PHI(4)	I		
TT(1)TT(2)	TT(3)	TT(4)	TT(5)	TT(6)			
LL(1)LL(2)	LL(3)	LL(4)	LL(5)	LL(6)			
1) LINER LGTH :	0.00000	0.01328	0.02100	0.09350	0.14400	0.17000	
2) ZONE LGTH :	0.02100	0.07250	0.05050	0.02600			
3) EFFICIENCY :	0.6000	0.9000	0.9500	0.9500			
4) EQ. RATIO :	2.3584	0.6875	0.2464	0.2377			
5) TEMPERATURE:	453.0	1581.0	2006.9	1534.0	1317.0	1100.0	

SWID		BLOCK: 7	
1)DSW	= 0.02410(m)	4)No of Vanes	= 10
2)DHUB	= 0.02000(m)	5)Vane Angle	= 50.0
3)Swirler Length	= 0.01400(m)	6)Swirler Area	= .14201E-03(m2)
7)No. Injectors	= 6	1) PRESSURE ATOMISER	
8)DATM1	= 0.00000(m)	10)Atomiser area	= .00000E+00(m2)
9)DATM2	= 0.00000(m)	11)CD atomiser	= 0.00000

GENERAL DATA :

GEOMETRY : (0 13)

SL NO ->	(1)	(2)	(3)	(4)	(5)
SLOT NO	CASING HGT	CASING WPTH	LINER HGT	LINER WIDTH	LINER WPTH HOR
1	0.00000	0.09900	0.06200	0.09050	0.04150
2	0.01328	0.09900	0.06700	0.09050	0.04150
3	0.02100	0.09900	0.06700	0.09050	0.04150
4	0.05150	0.09900	0.06700	0.09050	0.04150
5	0.07550	0.09900	0.06700	0.09050	0.04150
6	0.09350	0.09900	0.06700	0.09050	0.04150
7	0.11250	0.09900	0.06700	0.09050	0.04150
8	0.12450	0.09900	0.06700	0.09050	0.04150
9	0.13650	0.09900	0.06700	0.09050	0.04150
10	0.14400	0.09900	0.06700	0.09050	0.04150
11	0.15125	0.09900	0.05100	0.08900	0.03500
12	0.16150	0.09900	0.05100	0.08650	0.02850
13	0.17000	0.09900	0.05100	0.08650	0.02850

SLOT DETAILS : (0 13 3)

SLOT NO	POSI (m)	TYPE	SIGN +/-	STATIONS	RES. TIME (sec)
1	0.00000	D 0C	*	1	0.0000E+00
2	0.01328	A 1C	*	1	0.9905E-03
3	0.02100	M 7C	*	1	0.1306E-02
4	0.05150	M 6C	*	1	0.1848E-02
5	0.07550	M 6C	*	1	0.2158E-02
6	0.09350	M 7C	*	1	0.2394E-02

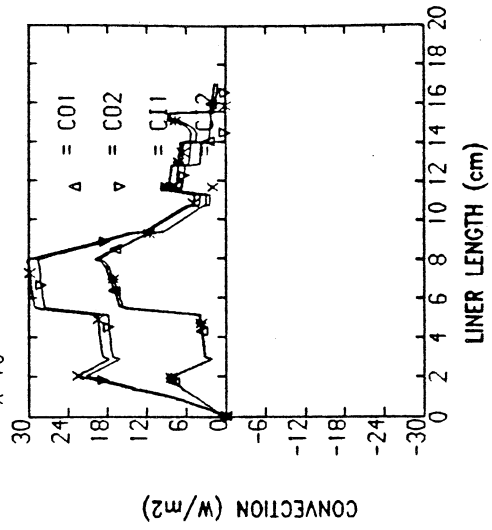
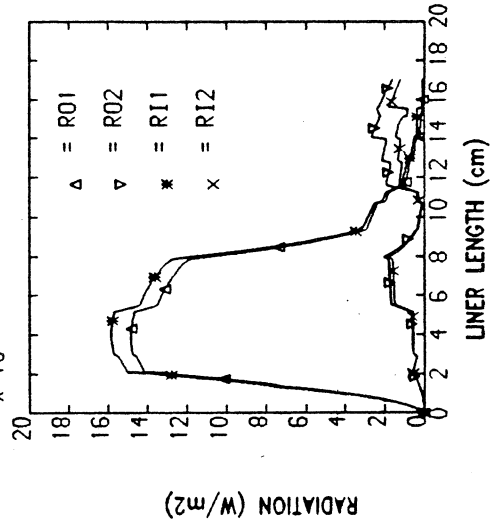
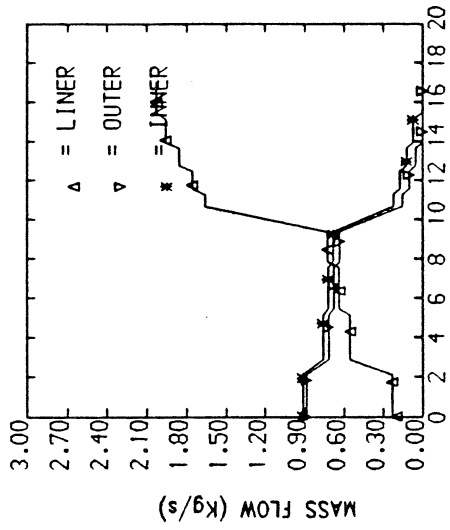
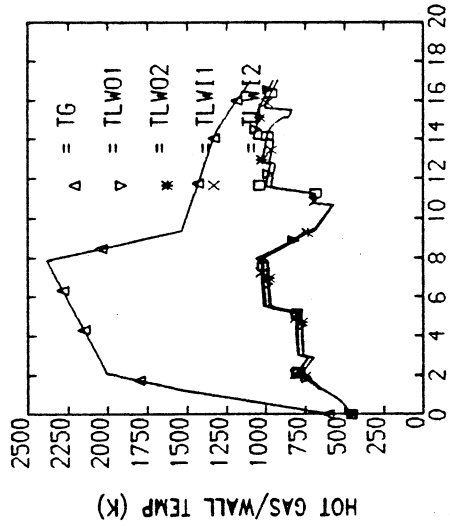
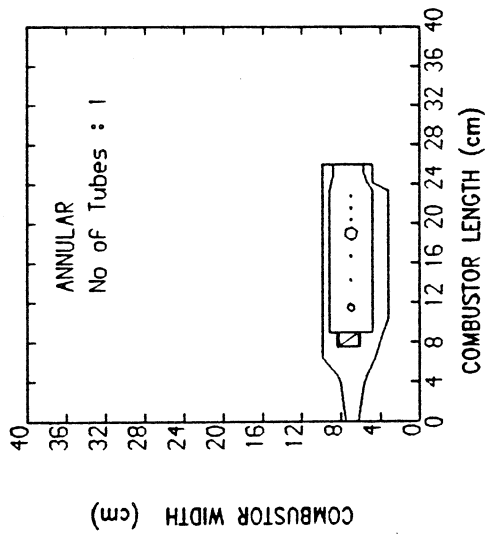
6	0.09350	M 7C	*	1	0.2394E-02
7	0.11250	M 6C	*	1	0.2591E-02
8	0.12450	M 6C	*	1	0.2688E-02
9	0.13650	M 6C	*	1	0.2782E-02
10	0.14400	A 0C	*	1	0.2840E-02
11	0.15125	M 6C	*	1	0.2893E-02
12	0.16150	A 0C	*	1	0.2958E-02
13	0.17000	E 0C	*	1	0.3010E-02

SLOT FLOWS : (0 1 3 3)

SLT NO	IOI I2	POSI (m)	HT (m)	DIA (m)	DIA2 (m)	NO	AREA (m ²)	FRACTION	CD	EFF. AREA (m ²)	FLOW (kg/s)	% FLOW	Ymax/Dft	PHI deg
1	1	0.00000	0.00000	0.00000	0.00000	0	.00000E+00	0.0000	0.0000	.00000E+00	0.0000	0.0000	0.00000	0.00
1	2	0.00000	0.00000	0.00000	0.00000	0	.00000E+00	0.0000	0.0000	.00000E+00	0.0000	0.0000	0.00000	0.00
2	1	0.00000	0.00000	0.00000	0.00000	0	.00000E+00	1.0000	0.0000	.00000E+00	0.0000	0.0000	0.00000	0.00
2	2	0.00000	0.00000	0.00000	0.00000	0	.00000E+00	1.0000	0.0000	.00000E+00	0.0000	0.0000	0.00000	0.00
3	1	0.00000	0.00000	0.00800	0.00800	12	.60319E-03	1.0000	0.6955	.41954E-03	0.1666	8.3309	1.68374	60.18
3	2	0.00000	0.00000	0.00800	0.00800	12	.60319E-03	1.0000	0.6490	.39149E-03	0.1550	7.7498	1.67421	54.86
4	1	0.00000	0.00000	0.00300	0.00300	26	.18378E-03	1.0000	0.5708	.10490E-03	0.0424	2.1190	0.36920	66.66
4	2	0.00000	0.00000	0.00300	0.00300	26	.18378E-03	1.0000	0.5474	.10061E-03	0.0406	2.0275	0.36255	61.94
5	1	0.00000	0.00000	0.00300	0.00300	26	.18378E-03	1.0000	0.5781	.10624E-03	0.0434	2.1682	0.31762	68.36
5	2	0.00000	0.00000	0.00300	0.00300	26	.18378E-03	1.0000	0.5574	.10244E-03	0.0418	2.0877	0.31274	63.88
6	1	0.00000	0.00000	0.01300	0.01300	12	.15928E-02	1.0000	0.7427	.11829E-02	0.4790	23.9487	1.09323	69.64
6	2	0.00000	0.00000	0.01300	0.01300	12	.15928E-02	1.0000	0.7088	.11290E-02	0.4568	22.8389	1.08897	65.32
7	1	0.00000	0.00000	0.00300	0.00300	26	.18378E-03	1.0000	0.6225	.11441E-03	0.0498	2.4897	0.17749	85.53
7	2	0.00000	0.00000	0.00300	0.00300	26	.18378E-03	1.0000	0.6188	.11373E-03	0.0491	2.4526	0.17565	82.68
8	1	0.00000	0.00000	0.00300	0.00300	26	.18378E-03	1.0000	0.6238	.11464E-03	0.0505	2.5258	0.17282	87.03
8	2	0.00000	0.00000	0.00300	0.00300	26	.18378E-03	1.0000	0.6212	.11416E-03	0.0499	2.4929	0.17117	84.38
9	1	0.00000	0.00000	0.00300	0.00300	26	.18378E-03	1.0000	0.6246	.11480E-03	0.0512	2.5598	0.16866	88.51
9	2	0.00000	0.00000	0.00300	0.00300	26	.18378E-03	1.0000	0.6230	.11449E-03	0.0506	2.5308	0.16718	86.06
10	1	0.00000	0.00000	0.00000	0.00000	0	.00000E+00	1.0000	0.0000	.00000E+00	0.0000	0.0000	0.00000	0.00
10	2	0.00000	0.00000	0.00000	0.00000	0	.00000E+00	1.0000	0.0000	.00000E+00	0.0000	0.0000	0.00000	0.00
11	1	0.00000	0.00000	0.00000	0.00000	0	.00000E+00	1.0000	0.0000	.00000E+00	0.0000	0.0000	0.00000	0.00
11	2	0.00000	0.00000	0.00350	0.00350	26	.25015E-03	1.0000	0.6197	.15503E-03	0.0710	3.5485	0.19972	84.37
12	1	0.00000	0.00000	0.00000	0.00000	0	.00000E+00	1.0000	0.0000	.00000E+00	0.0000	0.0000	0.00000	0.00
12	2	0.00000	0.00000	0.00000	0.00000	0	.00000E+00	1.0000	0.0000	.00000E+00	0.0000	0.0000	0.00000	0.00

STABILITY DATA		
SL NO	Equ. Rat.	m/VP**n
1	0.1	0.65700E-10
2	0.2	0.10621E-07
3	0.3	0.18187E-06
4	0.4	0.10869E-05
5	0.5	0.36136E-05
6	0.6	0.83292E-05
7	0.7	0.14983E-04
8	0.8	0.20652E-04
9	0.9	0.23436E-04
10	1.0	0.16426E-04
11	1.3	0.25392E-04
12	1.5	0.12592E-04
13	1.8	0.14958E-04
14	2.0	0.13339E-04
Loading Parameter		0.99205E-07

DEPTH

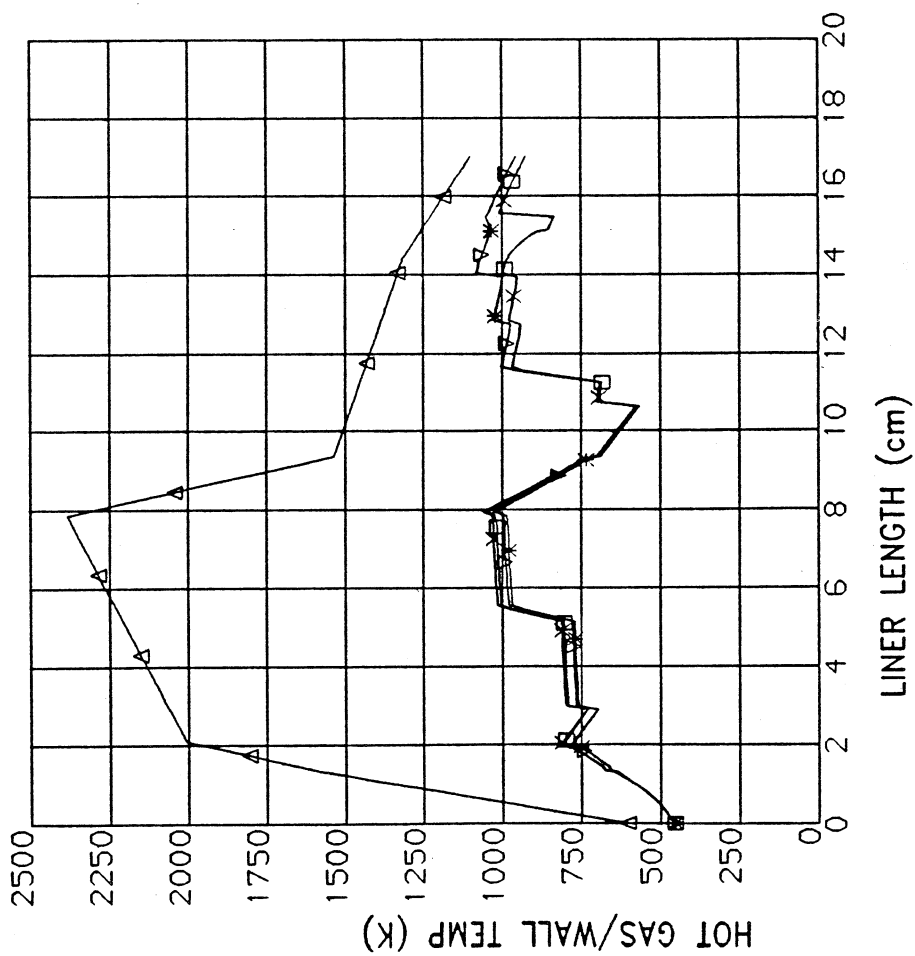


COMBUSTOR DATA

RUNBY : USER TIME: 19:08:37
 CASE NO: 3B DATE: 24-JAN-88

DEPTH

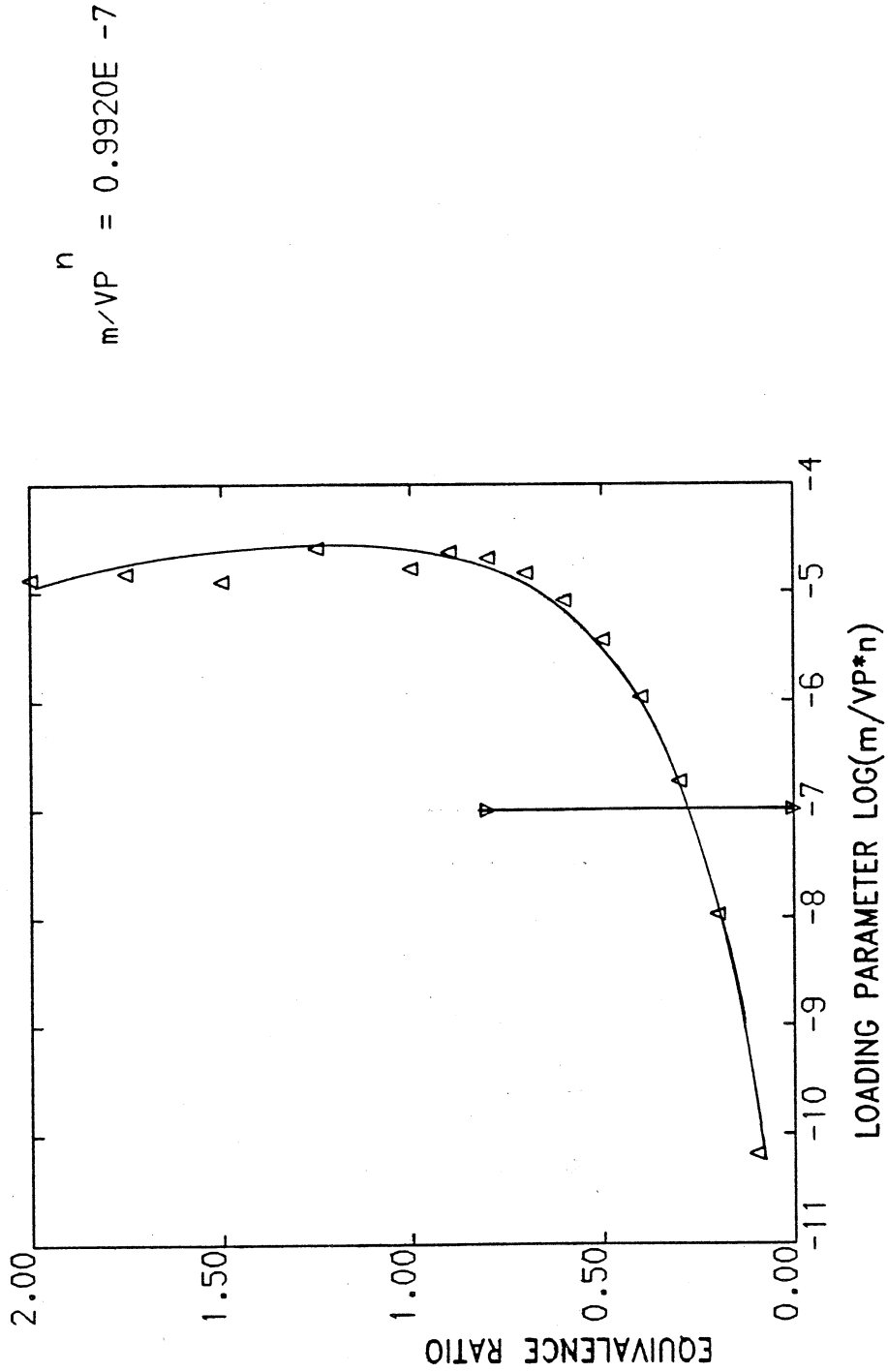
= TG
 = TLW01
 = TLW02
 = TLW11
 = TLW12
 Δ = TG
 ▽ = TLW01
 * = TLW02
 x = TLW11
 □ = TLW12



RUNBY : USER
 CASE NO: 3B
 TIME: 19:08:37
 DATE: 24-JAN-88

TEMPERATURE VARIATION

DEPTH

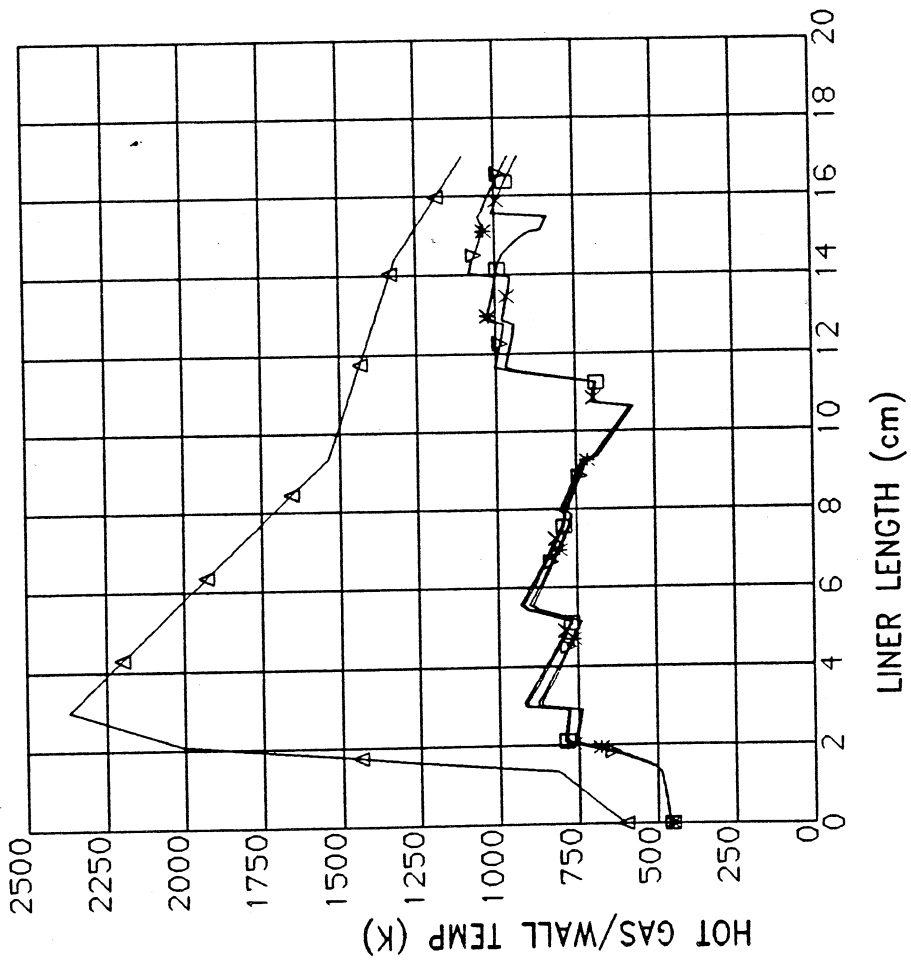


RUNBY : USER TIME: 19:08:37
CASE NO: 3B DATE: 24-JAN-88

STABILITY DATA

DEPTH

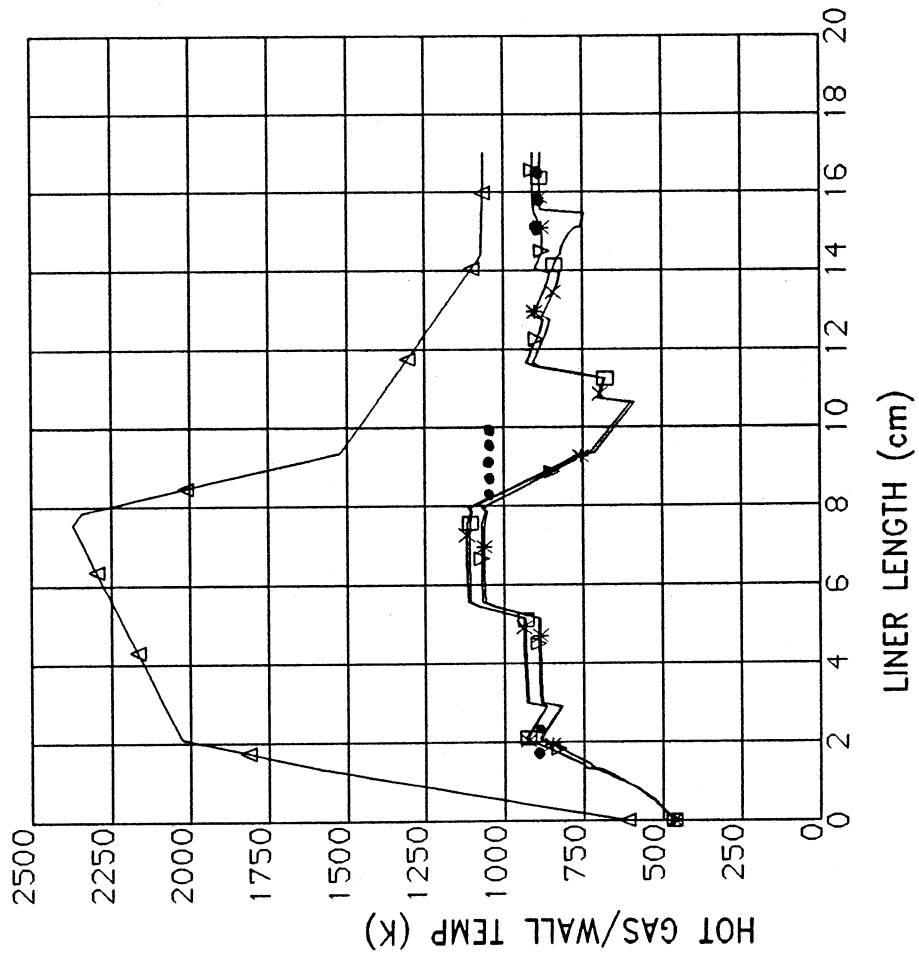
= TG
△ = TLW01
▽ = TLW02
* = TLWI1
x = TLWI2
□ = TLWI2



RUNBY : USER TIME: 19:17:13
CASE NO: 3C DATE: 24-JAN-88

TEMPERATURE VARIATION

DEPTH



RUNBY : USER TIME: 18:23:50
CASE NO: 3D DATE: 27-JAN-88

TEMPERATURE VARIATION

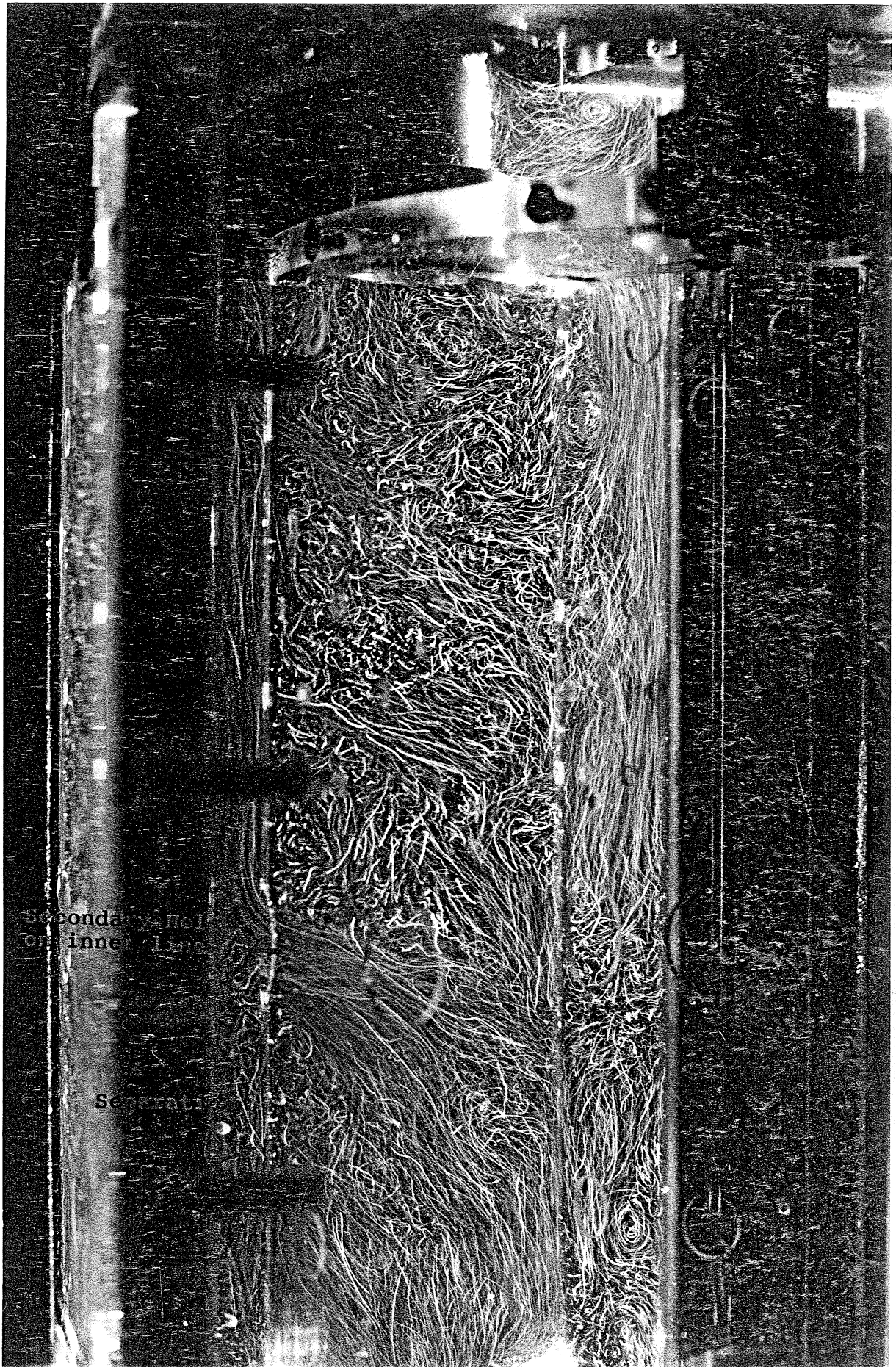
Plate 1: TEST LINER (CASE 3) - RUN WITH THERMAL PAINT



Original Colour: Red

683 K	Brown Grey
763 K	Yellow
848 K	Orange
1073 K	Green

Plate 2 : TEST LINER (CASE 3) - WATER FLOW VISUALISATION



INPUT FOR PRELIMINARY DESIGN

```
'SPEC'  
206.4  
911925.  
1010.  
1439.  
2.5  
19.7  
'GEOM'  
1.0  
0.1  
'TYPE'  
3  
1  
12.5,24.4,0.,0.  
2  
1  
1  
'END'
```

OUTPUT

Case No : 4 DATE : 24-JAN-88
 Run By : USER TIME : 17:04:57
 BLOCK NUMBER AT LAST TERMINATION = 8

BLOCK: 2			
TYPE	1	2	3
SINO	1		4
CHAMBER		DIFFUSER	INJECTOR
3 TUBOANNULAR	2 DUMP	1 PRESSURE ATOMISER	1 GROUND

BLOCK: 2	
5) FUEL:	6) OXIDANT: (mole fractions)
1) 1 AVTUR	Molecular Wt : 28.1000
2) C H N O	1) Sp Humidity: 0.0000
12.50000 24.40000 0.00000 0.00000	(fraction of inlet air)
3) L C V	N2
46.4000 (MJ/kg)	0.7027
4) AFRS	2) O2
24.6290 -	0.1215
5) Fuel temp TTF	3) AR
300.0000 K	0.0084
6) Enthalpy Fuel	4) CO
-300.0000 (kJ/mole)	0.0001
at TTF	5) H2O
174.7300	0.1221
Molecular Wt	6) CH4
0.8000	0.0000
	7) CO2
	8) H2
	0.0452
	0.0000

BLOCK: 3			
DESIGN SPECIFICATIONS			
1) Mass Flow W2 = 206.400 (kg/s)	4) O P L	= 2.500	(%)
2) Tot. Press PT2 = 911930.0 (N/m2)	5) P L F	= 19.700	(-)
3) Tot. Temp TT2 = 1010.0 (K)	6) Tot. Temp TT8	= 1439.0	(K)
COMBUSTOR INLET PLANE			
7) Ref Rad RREF2 = 1.00000 (m)	Ref Rad RREF8	= 0.93505	(m)
8) Channel Ht HT2 = 0.10000 (m)	Channel Ht HT8	= 0.22009	(m)
Inlet Area A2 = .62832E+00 (m2)	9) Exit Area A8	= .45653E+00	(m2)
Inlet Mach No MN2 = 0.1750 (-)	10) Exit Mach No MN8	= 0.3036	(-)

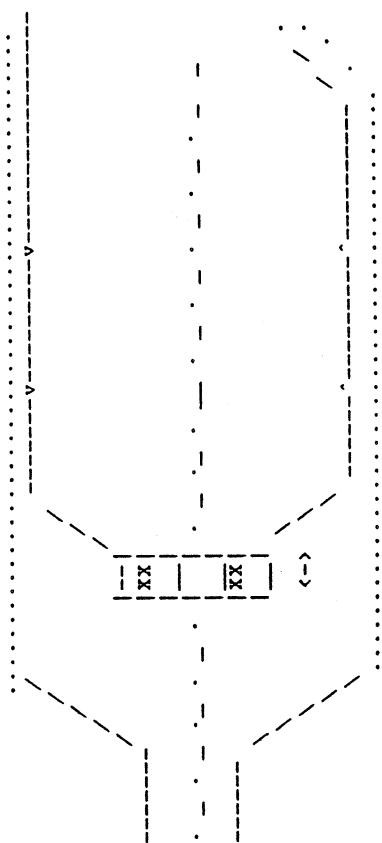
BLOCK: 4

REFERENCE AREA					
SLNO->	RRF	HT	AR	A	DL
	1	2	3	4	6
1	1.00000	0.10000	1.0000	.62832E+00	0.00 0.00000
2	1.00000	0.18000	1.8000	.11310E+01	20.00 0.10990
3	1.00000	0.50000	5.0000	.31416E+01	90.00 0.00000

BLOCK: 5

COMBUSTOR SIZING	
1) FLAMETUBE WIDTH	DFT= 0.35000 (m)
2) DIFFUSER LENGTH	DL = 0.10990 (m)
3) DIFFUSER TO DOME LENGTH	DDL= 0.05000 (m)
4) DOME LENGTH	DML= 0.11200 (m)
5) PRIMARY ZONE LENGTH	PZL= 0.28000 (m)
6) SECONDARY ZONE LENGTH	SZL= 0.14000 (m)
7) DILUTION ZONE LENGTH	DZL= 0.49000 (m)
8) NOZZLE LENGTH	ZNL= 0.21000 (m)
9) COMBUSTOR LENGTH	CCL= 1.27990 (m)
10) FLAME TUBE EXIT WIDTH	DFT8= 0.22009 (m)
11) NUMBER OF TUBES	NTUBE= 12

COMBUSTOR GEOMETRY (not to scale)



DL	DDL	PZL	SZL	DZL	ZNL
0.10990	0.05000	0.28000	0.14000	0.49000	0.21000

* MASS FLOW SPLITS										BLOCK: 6	
39.88				(sec)	(dil)						
				21.39	18.50						
0.00	MIXING	0.00	0.00	0.00	0.00	0.00	0.00	0.00	0.00		
10.77	10.77(1SWRL) [x]			R	P	S	D	Z	A = 17.200		
	0.00(-1ATOM)										
	0.00(-1DOME) [x]			1.00		0.58	0.33	0.31	F = 0.216		
						equivalence ratio					
49.30	COOLING										
99.96		2.43	12.85	5.68	20.92	7.42					
MASS FLOW SPLITS											
6.860				(sec)	(dil)						
				3.678	3.182						
0.000	MIXING	0.000	0.000	0.000	0.000	0.000	0.000	0.000			
1.853	1.853(1SWRL) [x]			R	P	S	D	Z	A = 17.200		
	0.000(-1ATOM)										
	0.000(-1DOME) [x]			1.00		0.58	0.33	0.31	F = 0.216		
						equivalence ratio					
8.480	COOLING										
17.193		0.418	2.210	0.977	3.598	1.276					
				PZL	SZL	DZL	ZNL				
				I	EFF(1)	EFF(2)	EFF(3)	EFF(4)			
				I	PHI(1)	PHI(2)	PHI(3)	PHI(4)			
				TT(1)	TT(2)	TT(3)	TT(4)	TT(5)	TT(6)		
				LL(1)	LL(2)	LL(3)	LL(4)	LL(5)	LL(6)		
1)	LINER LGTH :	0.00000	0.11200	0.28000	0.42000	0.91000	1.12000				
2)	ZONE LGTH :	0.28000	0.14000	0.49000	0.21000						
3)	EFFICIENCY :	0.9000	0.9900	0.9990	0.9990						
4)	EQ. RATIO :	0.9976	0.5818	0.3338	0.3091						
5)	TEMPERATURE:	1010.0	2083.5	1952.5	1594.0	1516.5	1439.0				

SWID		BLOCK: 7	
1)DSW	= 0.09780(m)	4)No of Vanes	= 10
2)DHUB	= 0.04135(m)	5)Vane Angle	= 60.0
3)Swirler Length	= 0.01400(m)	6)Swirler Area	= .61693E-02(m2)
7)No. Injectors	= 12	1 PRESSURE ATOMISER	
8)DATM1	= 0.00000(m)	10)Atomiser area	= .00000E+00(m2)
9)DATM2	= 0.00000(m)	11)CD atomiser	= 0.00000

GENERAL DATA :

GEOMETRY : (2 25)

SL NO ->	(1)	(2)	(3)	(4)	(5)
SLOT NO	CASING HGT	CASING WPTH	LINER HGT	LINER WIDTH	LINER WPTH HOR
1	0.00000	1.25000	0.50000	1.05090	0.10180
2	0.02800	1.25000	0.50000	1.08190	0.16385
3	0.07005	1.25000	0.50000	1.13030	0.26053
4	0.09810	1.25000	0.50000	1.16130	0.32267
5	0.11200	1.25000	0.50000	1.17500	0.35000
6	0.12315	1.25000	0.50000	1.17500	0.35007
7	0.15920	1.25000	0.50000	1.17700	0.35390
8	0.19525	1.25000	0.50000	1.17810	0.35625
9	0.23130	1.25000	0.50000	1.17820	0.35646
10	0.28000	1.25000	0.50000	1.17500	0.35000
11	0.31637	1.25000	0.50000	1.17500	0.35000
12	0.36142	1.25000	0.50000	1.17640	0.35283
13	0.42000	1.25000	0.50000	1.17500	0.35000
14	0.47073	1.25000	0.50000	1.17500	0.35000
15	0.53178	1.25000	0.50000	1.17720	0.35431
16	0.59383	1.25000	0.50000	1.17890	0.35778
17	0.65788	1.25000	0.50000	1.18010	0.36019
18	0.72493	1.25000	0.50000	1.18060	0.36115
19	0.79498	1.25000	0.50000	1.18000	0.36004
20	0.86903	1.25000	0.50000	1.17770	0.35536
21	0.91000	1.25000	0.50000	1.17500	0.35000
22	0.94705	1.21730	0.46726	1.15210	0.32708
23	1.01710	1.15530	0.40535	1.10880	0.28375
24	1.08620	1.09430	0.34433	1.06600	0.24103
25	1.12000	1.06440	0.31441	1.04510	0.22009

SLOT DETAILS : (0 25 2)

SLOT NO	POSTI (m)	TYPE	SIGN	STATIONS	RES. TIME (sec)
1	0.00000	D 0C	*	1	0.0000E+00
2	0.02800	C 1C	+	2	0.4246E-03
3	0.07005	C 1C	+	2	0.1694E-02
4	0.09810	C 1C	+	2	0.2941E-02
5	0.11200	A 1C	*	1	0.3630E-02
6	0.12315	C 4C	+	4	0.4182E-02
7	0.15920	C 4C	+	4	0.5849E-02
8	0.19525	C 4C	+	4	0.7327E-02
9	0.23130	C 4C	+	4	0.8650E-02
10	0.28000	M 1C	*	1	0.1022E-01
11	0.31637	C 4C	+	4	0.1103E-01
12	0.36142	C 4C	+	4	0.1184E-01
13	0.42000	M 7C	*	1	0.1291E-01
14	0.47073	C 4C	+	4	0.1369E-01
15	0.53178	C 4C	+	4	0.1453E-01
16	0.59383	C 4C	+	4	0.1537E-01
17	0.65788	C 4C	+	4	0.1623E-01
18	0.72493	C 4C	+	4	0.1711E-01
19	0.79498	C 4C	+	4	0.1800E-01
20	0.86903	C 4C	+	4	0.1890E-01
21	0.91000	A 3C	*	1	0.1937E-01
22	0.94705	C 4C	-	4	0.1976E-01
23	1.01710	C 4C	-	4	0.2035E-01
24	1.08620	C 4C	-	4	0.2077E-01
25	1.12000	E 3C	*	1	0.2092E-01

SLOT FLOWS : (0 25 2)

SLT NO	01	02	POSTI (m)	HT (m)	DIA (m)	DIA2 (m)	NO	AREA (m2)	FRACTION	CD	EFF. AREA (m2)	FLOW (kg/s)	% FLOW	Ymax/Dft	PHI deg
1	1		0.00000	0.00000	0.00000	0.00000	0	.00000E+00	0.0000	0.0000	.00000E+00	0.0000	0.0000	0.00000	0.00
2	1		0.00000	0.00200	0.00000	0.00000	120	.10609E-02	0.3403	0.7900	.28522E-03	0.1602	0.9312	0.00000	0.00
2	1		0.02000	0.00200	0.00000	0.00000	0	.13289E-02	0.3654	0.0000	.00000E+00	0.1602	0.9312	0.00000	0.00
3	1		0.00000	0.00200	0.00000	0.00000	120	.16684E-02	0.3534	0.7900	.46583E-03	0.2583	1.5017	0.00000	0.00
3	1		0.02000	0.00200	0.00000	0.00000	0	.19154E-02	0.0000	0.0000	.00000E+00	0.2583	1.5017	0.00000	0.00
4	1		0.00000	0.00200	0.00000	0.00000	120	.20588E-02	0.3565	0.7900	.57989E-03	0.3214	1.8683	0.00000	0.00
4	1		0.02000	0.00200	0.00000	0.00000	0	.21870E-02	0.0000	0.0000	.00000E+00	0.3214	1.8683	0.00000	0.00

MATERIAL SPECIFICATIONS:

SL. NO.	LINER 1	CASING 2	COATING N
MATERIAL	2 NIMONIC 90	1 ALUMINIUM ALLOY	0 *****
EMISSIVITY	.7000E+00	.4000E+00	.0000E+00
CONDUCTIVITY	.2500E+02	.8000E+02	.0000E+00
THICKNESS	.1500E-02	.2000E-02	.0000E+00

ITERATION = 3	NO OF CONTROL VOLUMES = 1073
LINER = 17.409 (Kg/s)	ANNULUS = 0.088 (Kg/s)
OPL CALCULATED = 7.300 %	OPL EXPECTED = 2.500 %
PLF CALCULATED = 92.697	PLF EXPECTED = 19.700
PATTERN FACTOR = 0.065201	

EXIT PLANE COMPOSITION: (mole fractions)	
Molecular Weight	: 28.1075
N2	: 0.6942
O2	: 0.0829
AR	: 0.0083
CO	: 0.0000
H2O	: 0.1449
CH4	: 0.0000
CO2	: 0.0697
H2	: 0.0000

STABILITY DATA		
SL NO	Equ. Rat.	m/VP**n
1	0.1	0.49492E-08
2	0.2	0.12044E-07
3	0.3	0.25955E-07
4	0.4	0.55563E-07
5	0.5	0.10595E-06
6	0.6	0.18282E-06
7	0.7	0.28424E-06
8	0.8	0.40210E-06

9	0.9	0.53285E-06
10	1.0	0.62852E-06
11	1.3	0.55053E-06
12	1.5	0.59057E-06
13	1.8	0.49177E-06
14	2.0	0.32234E-06
Loading Parameter		0.93329E-08

NOX DATA (mass fraction)

Res. Time (sec)	Eq. Rat. (-)	Temp (K)	GENERATION (-)	DILUTION (-)	TOTAL (-)
0.0000E+00	0.0000	0.010.0000E+00	0.0000E+00	0.0000E+00	0.0000E+00
0.10216E-01	0.9976	1952.510.59421E-05	0.0000E+00	0.0000E+00	0.59421E-05
0.11027E-01	0.8896	1859.310.97919E-06	-6.8027E-06	-6.8027E-06	0.62410E-05
0.11833E-01	0.7558	1744.010.50525E-06	-1.0151E-05	-1.0151E-05	0.57311E-05
0.12907E-01	0.5818	1594.010.11577E-06	-1.4911E-05	-1.4911E-05	0.43558E-05
0.13687E-01	0.5561	1586.010.59063E-08	-1.9653E-06	-1.9653E-06	0.41652E-05
0.14526E-01	0.5252	1576.310.40761E-08	-2.3799E-06	-2.3799E-06	0.39313E-05
0.15370E-01	0.4938	1566.510.18994E-08	-2.4226E-06	-2.4226E-06	0.36909E-05
0.16227E-01	0.4614	1556.410.78612E-09	-2.5047E-06	-2.5047E-06	0.34413E-05
0.17106E-01	0.4275	1545.810.48129E-09	-2.6270E-06	-2.6270E-06	0.31790E-05
0.17998E-01	0.3920	1534.710.19926E-09	-2.7501E-06	-2.7501E-06	0.29042E-05
0.18900E-01	0.3546	1523.010.59662E-10	-2.9152E-06	-2.9152E-06	0.26128E-05
0.19371E-01	0.3338	1516.510.18979E-10	-3.2362E-07	-3.2362E-07	0.24554E-05
0.19761E-01	0.3295	1502.810.11617E-10	-3.2362E-07	-3.2362E-07	0.24231E-05
0.20349E-01	0.3212	1477.010.14428E-10	-6.1554E-07	-6.1554E-07	0.23615E-05
0.20768E-01	0.3130	1451.510.75169E-11	-6.0709E-07	-6.0709E-07	0.23008E-05
0.20918E-01	0.3091	1439.010.19750E-11	-2.9497E-07	-2.9497E-07	0.22713E-05

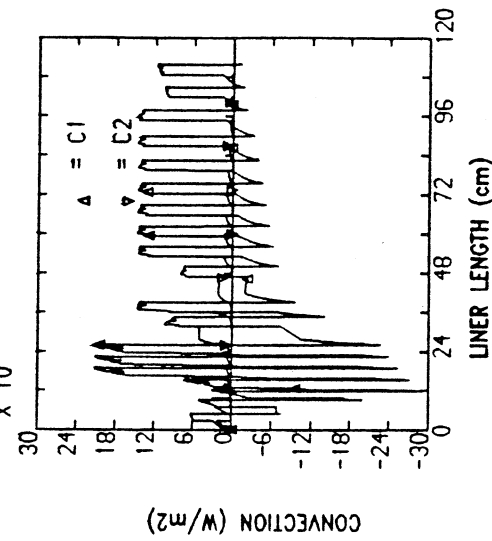
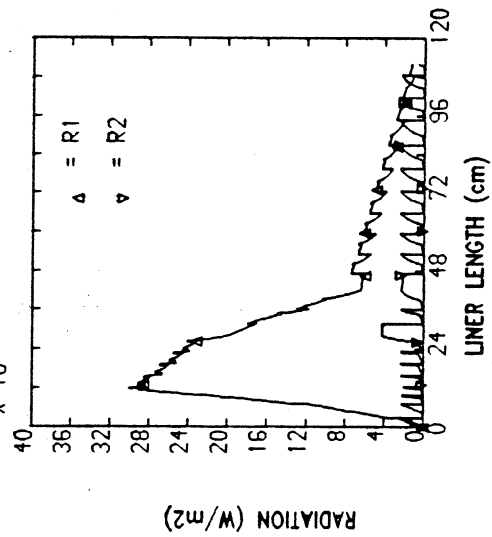
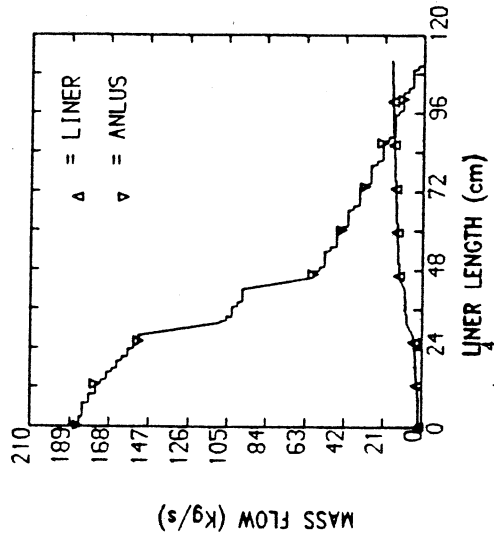
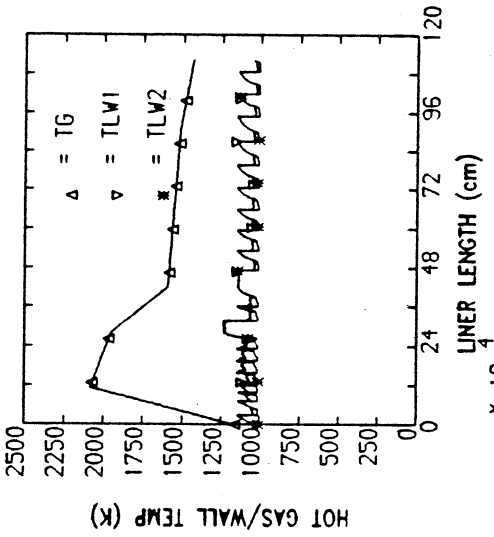
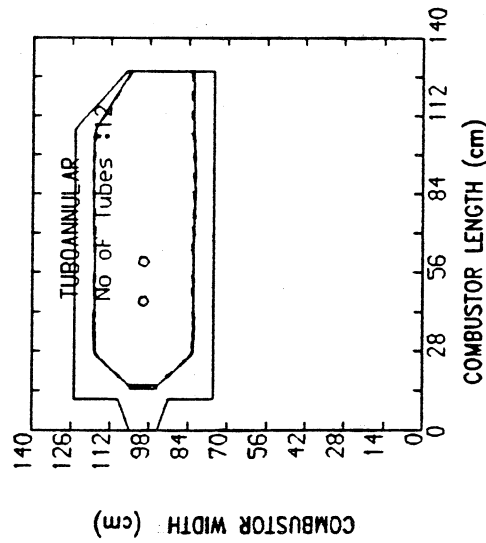
NOX AT EXIT PLANE

MASS FRACTION (Kg/Kg)	PPMV (weight)	PPMV (volume)	EMISSION INDEX (g/Kg fuel)
0.22713E-05	2.3	1.2	0.183

NO_x EQUILIBRIUM DATA FOR VITIATED MEDIUM

EQ RAT (-)	DENSITY (Kg/m ³)	TEMP (K)	k1 (-)	k2 (-)	R1 (see text for units)	R6 ([NO]eq)
0.00000	0.00301	1010.4	0.9332E-02	0.1205E+01	0.1368E-23	0.7618E-21
0.10000	0.00270	1142.3	0.1963E-01	0.1137E+01	0.1071E-20	0.1352E-18
0.20000	0.00243	1269.1	0.3936E-01	0.1031E+01	0.3204E-18	0.9750E-17
0.30000	0.00222	1391.1	0.6930E-01	0.9102E+00	0.2781E-16	0.2709E-15
0.40000	0.00204	1508.4	0.1111E+00	0.7827E+00	0.9955E-15	0.3776E-14
0.50000	0.00190	1621.5	0.1653E+00	0.6532E+00	0.1848E-13	0.8036E-03
0.60000	0.00178	1730.6	0.2302E+00	0.5257E+00	0.2060E-12	0.1712E-12
0.70000	0.00168	1836.0	0.2993E+00	0.4015E+00	0.1520E-11	0.6545E-12
0.80000	0.00159	1937.7	0.3578E+00	0.2798E+00	0.7800E-11	0.1756E-11
0.90000	0.00152	2034.6	0.3774E+00	0.1582E+00	0.2656E-10	0.2880E-11
1.00000	0.00146	2113.4	0.2812E+00	0.3586E-01	0.3224E-10	0.9921E-12
1.10000	0.00146	2090.5	0.1231E+00	0.2150E-02	0.3377E-11	0.1661E-13
1.20000	0.00148	2041.7	0.7836E-01	0.4343E-03	0.5237E-12	0.1010E-14
1.30000	0.00150	1993.0	0.5727E-01	0.1318E-03	0.1030E-12	0.1025E-15
1.40000	0.00152	1944.8	0.4428E-01	0.4674E-04	0.2162E-13	0.1240E-16
1.50000	0.00154	1898.0	0.3547E-01	0.1824E-04	0.4754E-14	0.1677E-17
1.60000	0.00156	1851.9	0.2901E-01	0.7473E-05	0.1047E-14	0.2356E-18
1.70000	0.00158	1807.2	0.2412E-01	0.3192E-05	0.2330E-15	0.3444E-19
1.80000	0.00160	1763.6	0.2028E-01	0.1391E-05	0.5117E-16	0.5057E-20
1.90000	0.00163	1720.5	0.1716E-01	0.6103E-06	0.1090E-16	0.7271E-21
2.00000	0.00165	1678.2	0.1459E-01	0.2680E-06	0.2247E-17	0.1017E-21
2.10000	0.00168	1636.5	0.1245E-01	0.1172E-06	0.4451E-18	0.1372E-22
2.20000	0.00170	1596.1	0.1067E-01	0.5149E-07	0.8632E-19	0.1824E-23
2.30000	0.00173	1555.8	0.9148E-02	0.2215E-07	0.1571E-19	0.2260E-24
2.40000	0.00176	1517.1	0.7871E-02	0.9580E-08	0.2823E-20	0.2783E-25
2.50000	0.00179	1478.1	0.6749E-02	0.3997E-08	0.4624E-21	0.3084E-26

D E P T H

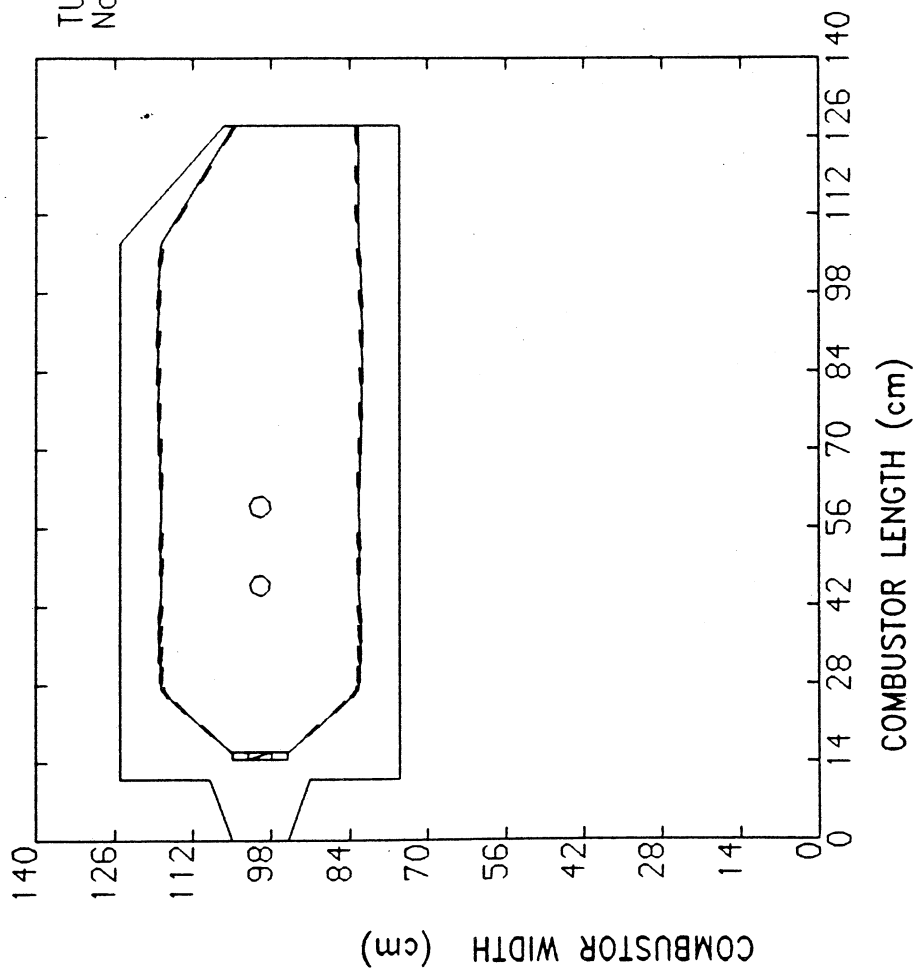


COMBUSTOR DATA

RUNBY : USER
 TIME: 17:04:57
 CASE NO: 4
 DATE: 24-JAN-88

D E P T H

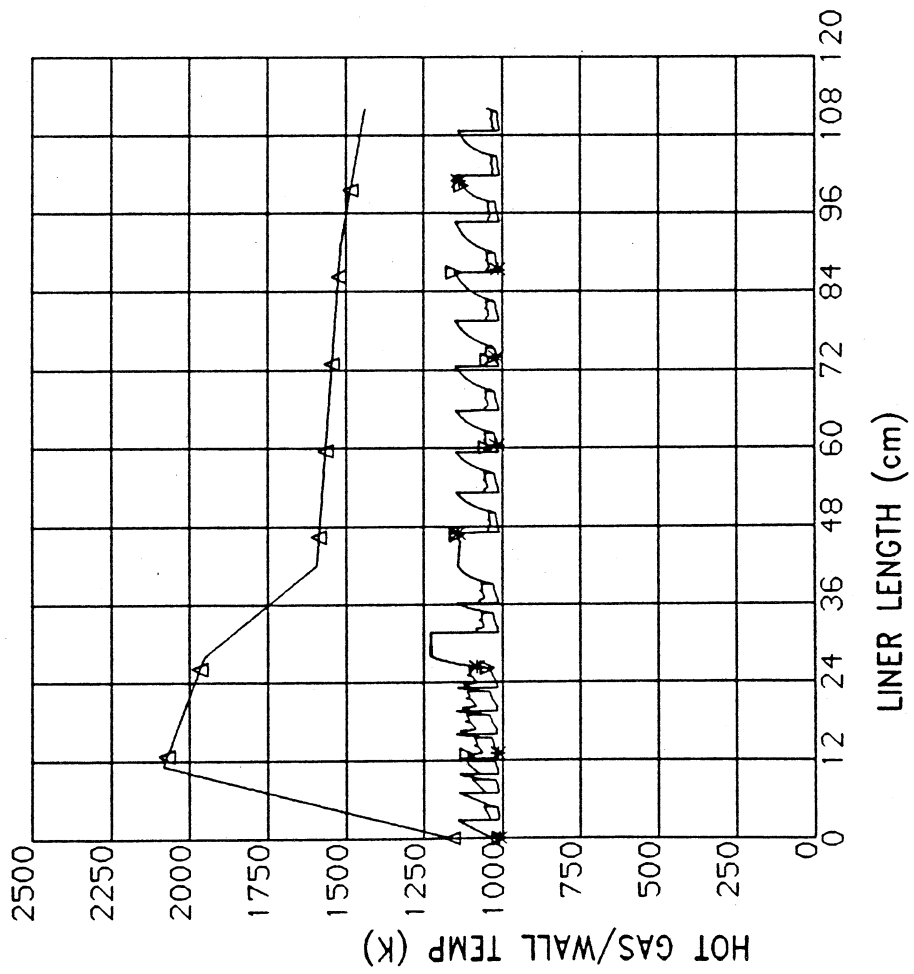
TUBOANNULAR
No of Tubes :12



RUNBY : USER TIME: 17:04:57
CASE NO: 4 DATE: 24-JAN-88

COMBUSTOR GEOMETRY

D E P T H

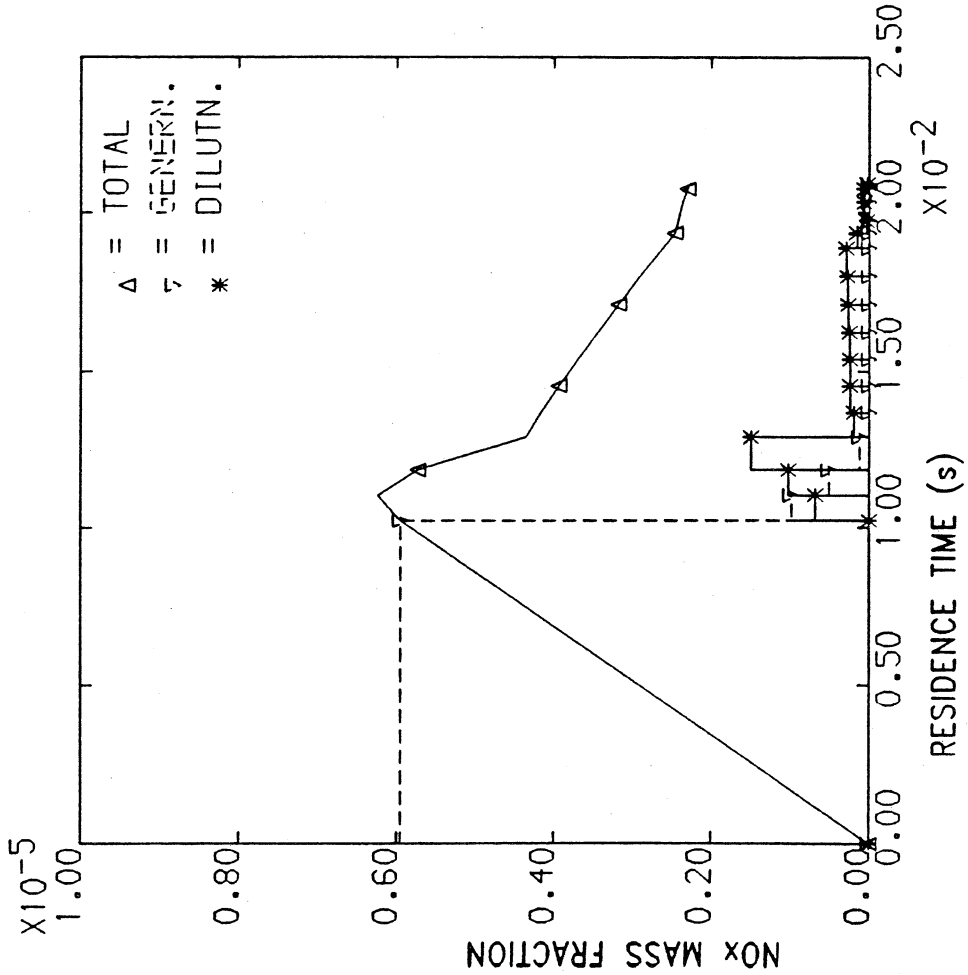


RUNBY : USER TIME: 17:04:57
CASE NO: 4 DATE: 24-JAN-88

TEMPERATURE VARIATION

D E P T H

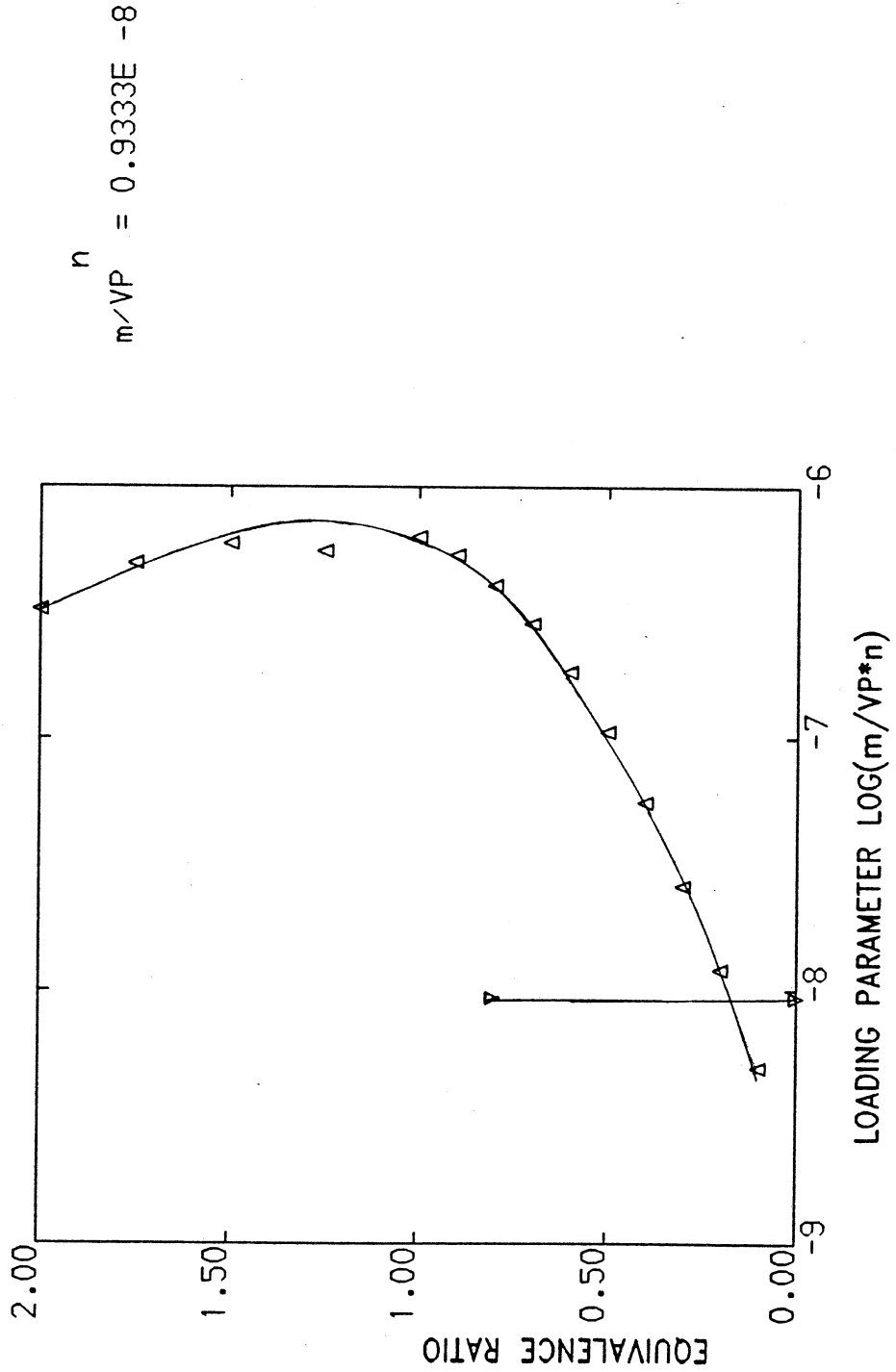
PHI_{mean} = 1.00, P_{in} = 0.91 MPa
 MIXEDNES = 0.20, T_{in} = 1010.0 K
 EMI. INDEX = 0.183 g/Kg Fuel
 NO_x CONC. = 2.3 PPM_w
 = 1.2 PPM_v



RUNBY : USER TIME: 17:04:57
 CASE NO: 4 DATE: 24-JAN-88

NO_x DATA

D E P T H



RUNBY : USER
CASE NO: 4
TIME: 17:04:57
DATE: 24-JAN-88

STABILITY DATA

